

Functional role of the overexpression of the myelin and lymphocyte protein MAL in Schwann cells

Inauguraldissertation

Zur Erlangung der Würde eines Doktors der Philosophie

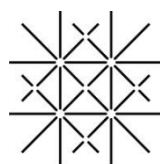
Vorgelegt der Philosophisch-Naturwissenschaftlichen Fakultät der Universität Basel

von

Daniela Schmid

aus Ramsen (SH)

Basel, 2013



UNI
BASEL

Genehmigt von der Philosophisch-Naturwissenschaftlichen Fakultät auf Antrag von:

Prof. M.A. Rüegg (Fakultätsverantwortlicher)

Prof. N. Schaeren-Wiemers (Dissertationsleiterin)

Prof. J. Kapfhammer (Korreferent)

Basel, den 18. Juni 2013

Prof. J. Schibler (Dekan)

To Michael

1. ACKNOWLEDGMENTS	6
2. ABBREVIATIONS.....	7
3. SUMMARY	10
4. INTRODUCTION.....	11
4.1. THE NERVOUS SYSTEM AND MYELIN SHEATH COMPOSITION	11
4.2. SCHWANN CELL ORIGIN AND LINEAGE	12
4.3. THE FUNCTIONAL ROLE OF THE BASAL LAMINA	14
4.3.1. <i>Cytoskeleton in Schwann cells.....</i>	15
4.4. SCHWANN CELL SIGNALING	16
4.4.1. <i>The Neuregulin 1/ ErbB system.....</i>	17
4.4.2. <i>Neurotrophins – TrkA, B, C / p75^{NTR} system.....</i>	18
4.4.3. <i>The cAMP signaling pathway.....</i>	19
4.4.4. <i>The PI3-kinase/ Akt signaling pathway.....</i>	21
4.4.5. <i>The MAP-kinase signal transduction pathway.....</i>	21
4.4.5.1. The ERK1/2 signaling cascade.....	22
4.4.5.2. The c-Jun N-terminal kinases (JNK) cascade	22
4.5. THE MYELIN AND LYMPHOCYTE PROTEIN MAL.....	23
4.5.1. <i>Characterization of MAL and its biochemical properties.....</i>	23
4.5.2. <i>Expression pattern of MAL in the nervous system.....</i>	23
4.5.3. <i>Putative functional role of MAL.....</i>	24
4.5.4. <i>Phenotype of MAL overexpression in the peripheral nervous system.....</i>	24
4.5.5. <i>Septin 6 is an interaction partner of MAL.....</i>	25
5. AIM OF THE WORK.....	26
6. MATERIAL AND METHODS.....	27
6.1. CELL CULTURE	27
6.1.1. <i>Primary Schwann cell cultures</i>	27
6.1.1.1. Primary mouse Schwann cell cultures.....	27
6.1.1.2. Stimulation assays of mouse Schwann cell cultures.....	27
6.1.1.3. Primary rat Schwann cell cultures	27
6.1.2. <i>Standard cell cultures.....</i>	29
6.2. IMMUNOHISTOCHEMISTRY	30
6.2.1. <i>Immunohistochemistry on cell cultures</i>	30
6.2.2. <i>Immunohistochemistry on fresh frozen mouse tissue.....</i>	30
6.2.3. <i>Antibodies</i>	30
6.3. EXPRESSION ANALYSIS.....	31
6.3.1. <i>RNA isolation of Schwann cells</i>	31
6.3.2. <i>RNA isolation of sciatic nerves.....</i>	31
6.3.3. <i>Reverse transcription reaction.....</i>	31
6.3.4. <i>Quantitative RT-PCR analysis.....</i>	32
6.3.4.1. Quantitative RT-PCR analysis.....	32
6.3.4.2. Primer pairs for quantitative RT-PCR.....	32
6.3.5. <i>Whole genome expression profiling.....</i>	33
6.4. GENERATION OF MCHERRY TAGGED MAL AND PMP22 CONSTRUCTS	33

6.4.1.	<i>Eliminating STOP sequence of the pMX-mCherry_{STOP} vector</i>	34
6.4.2.	<i>Cloning MAL into the pMX-mCherry vector</i>	34
6.4.3.	<i>Cloning PMP22 into the pMX-mCherry vector</i>	34
6.4.4.	<i>Primer pairs for cloning the retroviral constructs</i>	36
6.4.5.	<i>Production of retroviral stocks in Phoenix_{Eco} packaging cell line</i>	36
6.4.6.	<i>Retroviral infection</i>	37
6.5.	IN SITU HYBRIDIZATION.....	37
6.5.1.	<i>Cloning of the riboprobes</i>	37
6.5.2.	<i>DIG RNA labeling by in vitro transcription</i>	39
6.5.3.	<i>In situ hybridization</i>	39
6.5.4.	<i>Buffer composition for in situ hybridization</i>	40
7.	RESULTS	41
7.1.	MAL-DEPENDENT GENE REGULATION IN SCHWANN CELLS.....	41
7.1.1.	<i>Differential expression analysis on developing sciatic nerves</i>	41
7.1.2.	<i>Establishment of primary mouse Schwann cell cultures</i>	44
7.1.3.	<i>Investigation of Schwann cell differentiation in vitro</i>	44
7.1.3.1.	Stimulation with forskolin led to Schwann cell differentiation.....	45
7.1.3.2.	MAL-overexpressing Schwann cells manifest reduced P0 and p75 ^{NTR} expression.....	47
7.1.3.3.	Most transcription factors known to modulate P0 expression are unaffected by MAL overexpression.....	49
7.1.4.	<i>Investigation of other stimulation reagents</i>	50
7.1.4.1.	Neuregulin1 decreased forskolin-induced P0 expression.....	50
7.1.4.2.	Treatment with FGF1 did not improve P0 expression in MAL-overexpressing cells.....	51
7.1.4.3.	NGF treatment increased P0 expression levels.....	52
7.1.5.	<i>Differential gene expression analysis in MAL-overexpressing Schwann cells</i>	54
7.1.5.1.	Majority of known genes in Schwann cells is unaffected by MAL overexpression.....	55
7.1.5.2.	Several differentially expressed genes in MAL-overexpressing cells are associated with the extracellular matrix.....	57
7.1.5.3.	MAL-dependent differential gene expression in Schwann cells.....	57
7.1.5.4.	Hierarchical cluster analysis of differentially expressed genes.....	59
7.1.5.5.	Investigation of differentially expressed genes due to MAL overexpression in vivo.....	60
7.1.5.6.	Palmitoylation is an overrepresented annotation of genes reduced in MAL-overexpressing Schwann cells.....	62
7.2.	INVESTIGATION OF A DIRECT LINK BETWEEN MAL OVEREXPRESSION AND DOWNREGULATION OF P75 ^{NTR}	63
7.2.1.	<i>Immortalized S16 Schwann cell line</i>	63
7.2.1.1.	Morphological change and induction of Krox20 protein expression upon forskolin treatment.....	63
7.2.1.2.	Forskolin treatment did not lead to a robust induction of P0 and Krox20 mRNA.....	65
7.2.1.3.	S16 cells manifested a nonphysiological morphology.....	66
7.2.2.	<i>Proliferating Rat Schwann cell cultures</i>	68
7.2.2.1.	Forskolin induced P0 and Krox20 expression and reduced p75 ^{NTR} mRNA levels.....	68
7.2.2.2.	Retroviral infection of rat Schwann cell cultures to overexpress MAL.....	70
7.3.	TRANSCRIPTIONAL REGULATION INDUCED BY cAMP ELEVATION IN MOUSE SCHWANN CELLS.....	76
7.3.1.	<i>Forskolin-induced transcriptional regulation of genes involved in Schwann cell development</i>	76
7.3.2.	<i>General forskolin-induced transcriptional regulation in Schwann cells</i>	80
7.3.3.	<i>Olig1 expression in the peripheral nervous system</i>	82
7.3.4.	<i>Analysis of possible target regulators</i>	85
7.3.5.	<i>GO-annotation analysis in differentiated Schwann cells</i>	87
7.3.6.	<i>Pathway analysis implicated in Schwann cell differentiation</i>	89

7.3.7.	<i>Forskolin-induced regulation of components of the extracellular matrix</i>	90
7.3.8.	<i>Correlation analysis between in vivo and in vitro samples</i>	92
8.	DISCUSSION	94
8.1.	MAL-DEPENDENT GENE REGULATION IN SCHWANN CELLS	94
8.2.	TRANSCRIPTIONAL REGULATION INDUCED BY cAMP ELEVATION IN CULTURED MOUSE SCHWANN CELLS.....	102
9.	OUTLOOK	108
10.	REFERENCES	110
11.	APPENDIX I: DIFFERENTIALLY EXPRESSED TRANSCRIPTS	130
12.	APPENDIX II: CURRICULUM VITAE	135

1. Acknowledgments

This work was accomplished under the supervision of Prof. Nicole Schaeren-Wiemers in the laboratory of Neurobiology at the Department of Biomedicine, University Hospital in Basel. The project was supported by grants from the Swiss National Science Foundation.

First, I would like to thank Nicole for giving me the opportunity to perform my thesis in her lab. I appreciated her scientific and mentoring support during these years, and thank her for allowing me great scientific latitude. Further, I am much obliged for her critical reading of this manuscript.

Thanks go also to my faculty responsible Prof. Markus A. Rüegg and to my co-advisor Prof. Josef P. Kapfhammer.

Special thanks go to my parents Marlise and Engelbert and especially to my better half Michael, who were always appreciative of my time-consuming work and encouraged me through rough periods.

Further, I cordially thank Dr. Thomas Zeis for productive discussions, for performing the microarray study and for helping to analyze the data.

Many thanks go also to Melanie Gentner for technical support with the in situ hybridizations and to Monia Sobrio for the investigation of phosphorylation of Akt in MAL-overexpressing mice.

I would also like to thank former members of the lab, especially Dr. Andres M. Buser, Frances Kern and Beat Erne, who supported me at the beginning of my thesis.

Last but not least, I would like to thank all present and former colleagues of our lab as well as friends from neighboring labs for their support, the pleasant atmosphere in the lab and for helpful discussions.

2. Abbreviations

AC	Adenylyl cyclase
ADAMs	A disintegrin and metalloprotease
AP	Alkaline phosphatase
Aqp1	Aquaporin 1
AraC	Cytosine β -D-arabinofuranoside
Asgr1	Asialoglycoprotein receptor 1
BDNF	Brain-derived neurotrophin factor
BSA	Bovine serum albumin
cAMP	Cyclic adenosine monophosphate
Cdc42	Cell division control protein 42
CHO cell	Chinese hamster ovary cell
Clca4	Chloride channel calcium activated 4
CNPase	2'-3'-cyclic nucleotide 3' phosphodiesterase
CNS	Central nervous system
CREB	cAMP response element-binding protein
Dag1	Dystroglycan
DAVID	Database for Annotation, Visualization and Integrated Discovery
DAPI	4',6-diamidino-2-phenylindole
DGC	Dystrophin-glycoprotein complex
DIG	Digoxigenin
Diras1	DIRAS family, GTP-binding RAS-like 1
DMEM	Dulbecco's Modified Eagle Medium
DMSO	Dimethyl sulfoxide
dNTP	Deoxynucleotide triphosphate
DRG	Dorsal root ganglion
Dtna	α -dystrobrevin
DTT	Dithiothreitol
E17	Embryonic day 17
ECM	Extracellular matrix
EDTA	Ethylenediaminetetraacetic acid
EGF-like	Epidermal growth factor-like
EGFR	Epidermal growth factor receptor
EM	Electron microscopy
Entpd2	Ectonucleoside triphosphate diphosphohydrolase 2 (= NTPDase)
ERK	Extracellular signal-regulated kinase
FACS	Fluorescence-activated cell sorting
F-actin	filamentous actin

Fak	Focal adhesion kinase
FBS	Foetal bovine serum
FDR	False discovery rate
FGF1	Fibroblast growth factor
Gad2	Glutamic acid decarboxylase (=Gad65)
GFAP	Glial fibrillary acidic protein
Gpr126	G protein-coupled receptor 126
Gria1	Glutamate receptor, ionotropic, AMPA1 (alpha 1) (=Glur1)
GSK-3 β	Glycogen synthase kinase 3 beta
H ₂ O	Water
HBS	HEPES-buffered saline
IGF-I	Insulin-like growth factor I
Igsf10	Immunoglobulin superfamily, member 10
IPA	Ingenuity Pathway Analysis software
JNK	c-Jun N-terminal kinase
Krt23	Keratin 23
Ldb2	LIM domain binding 2
MAG	Myelin-associated glycoprotein
MAL	Myelin and lymphocyte protein
MAP2K	MAPK kinase
MAPK	Mitogen-activated protein kinase
MAP-kinase	Mitogen-activated protein kinase
MDCK	Madin-Darby canine kidney
MEFs	Mouse embryonic lung fibroblasts
MMLV	Murine leukemia virus
Moxd1	Monooxygenase, DBH-like 1
Mpz	Myelin protein zero (PO)
mRNA	messenger ribonucleic acid
MTC cells	Mammary nonmetastatic adenocarcinoma cell line
Nect4	Nectin-like protein 4
NF155	Neurofascin 155
NGF	Nerve growth factor
Ngfr	Nerve growth factor receptor = p75 ^{NTR}
NIH 3T3	Fibroblast cell line
NRG1	Neuregulin1
NT-3	Neurotrophin-3
NT-4	Neurotrophin-4
o.n.	Overnight

Osbp13	Oxysterol binding protein-like 3
P1	Postnatal 1
PBS	Phosphate buffered saline
PCA	Principal componen analysis
PDL	Poly-D-lysine
PFA	Paraformaldehyde
Pfkfb4	6-phosphofructo-2-kinase/fructose-2,6-biphosphatase 4
PI3-kinase	Phosphatidylinositol-3-kinase
PIP ₂	Phosphatidylinositol-3,4,-biphosphate
PIP ₃	Phosphatidylinositol-3,4,5,-triphosphate
PKA	Protein kinase A
PLP	Myelin proteolipid protein
PMP22	Peripheral myelin protein 22
PNS	Peripheral nervous system
PTEN	Phosphatase and tensin homologe
qRT-PCR	Quantitative reverse transcriptase-polymerase chain reaction
RhoU	Ras homolog family member U (= Wrch1)
ROCK	Rho-associated protein kinase
RT	Room temperature
RTK	Receptor tyrosine kinase
S100a4	Ca ²⁺ -binding protein A4 (=Mts1)
S16	Immortalized Schwann cell line
SC medium	Schwann cell medium
SCP	Schwann cell precursor
SCPM	Schwann cell proliferating medium
SLI	Schmidt-Lanterman incisure
Src2	Steroid receptor coactivator-2
SREBP	Sterol responsive element binding protein
SSC buffer	Saline Sodium Citrate Buffer
Sv2b	Synaptic vesicle glycoprotein 2 b
tgMAL	MAL-overexpressing mice
TGN	Trans-Golgi network
Tnik	TRAF2 and NCK interacting kinase
TrkB	Tropomyosin-related kinase B
Vat1l	Vesicle amine transport protein 1 homolog-like
Wnt16	Wingless-related MMTV integration site 16
wt	Wildtype

3. Summary

For fast propagation of action potentials in the nervous system, higher vertebrates have developed a specialized plasma membrane structure, the myelin, ensheathing nerve fibers. Myelin sheaths are formed by Schwann cells in the peripheral nervous system (PNS), whereas oligodendrocytes are the myelin-forming cells in the central nervous system (CNS). Impairment of the myelin sheath results in severe pathology as seen in multiple sclerosis in the CNS or polyneuropathies such as the Charcot-Marie-Tooth disease in the PNS. During development of peripheral nerves, a coordinated reciprocal signaling between Schwann cells and axons is crucial for accurate Schwann cell development, differentiation as well as maintenance of the myelin sheaths. In addition to orchestrated signal transduction, large amounts of lipids and membrane proteins are synthesized and have to be transported to distinct compartments for proper myelin formation. The transmembrane myelin and lymphocyte protein MAL is associated with lipid rafts, and is important for targeting proteins and lipids to distinct myelin membrane domains. In the PNS, MAL expression starts at around embryonic day 17, implicating a functional role in Schwann cell development. MAL overexpression retards the onset of peripheral myelination, and leads to reduced expression of p75^{NTR} and myelin protein zero (P0). Since accurate expression of p75^{NTR} is essential for proper initiation of myelination, it was suggested that altered p75^{NTR} expression in MAL-overexpressing mice might be the cause of delayed onset of myelination.

To elucidate a functional link between MAL overexpression and retarded myelination, primary mouse Schwann cell cultures were investigated. We could show that the induction of the CREB signaling pathway is functional, indicating that Schwann cells overexpressing MAL are not less responsive to axonal signals. Despite functional activation of the cAMP signaling pathway, significantly reduced mRNA expression levels of P0 and p75^{NTR} were detected in untreated Schwann cells overexpressing MAL. This study revealed that most transcription factors known to modulate P0 expression were not altered in Schwann cells overexpressing MAL. During development, Schwann cells depend on accurate levels of different growth factors. To determine whether the delayed onset of myelination might be caused by a deficient downstream signaling of a particular growth factor, Schwann cells were treated with neuregulin1, nerve growth factor or fibroblast growth factor 1. However, none of the investigated growth factors could ameliorate the reduced expression of P0 and p75^{NTR} in MAL-overexpressing Schwann cells.

MAL-overexpressing Schwann cells were further investigated using a whole genome expression analysis. Most transcripts of genes implicated in Schwann cell development, differentiation and maintenance were not affected by MAL-overexpression. However, we identified a number of genes associated with cytoskeleton organization and components of the basal lamina that are regulated in a MAL-dependent manner. Especially during development and differentiation of Schwann cells, major changes in cellular processes and architecture are crucial for accurate radial sorting and myelination, proposing them as novel candidates for influencing myelination.

4. Introduction

4.1. The nervous system and myelin sheath composition

The nervous system is one of the most complex structures in our body. It has highly specialized cell types, which are involved in the control of vital functions such as the respiration and the heartbeat. It is divided into the central nervous system (CNS) containing the brain and the spinal cord, and the peripheral nervous system (PNS), which consists of peripheral nerve fibers as well as sensory neurons. An appropriate interaction via electrical signals and growth factors between the central and the peripheral nervous system is essential to fulfill their functions. Fast transmission of electrical impulses in motor fibers is dependent on an insulating myelin sheath to increase the electrical velocity of action potentials. The myelin sheath is a unique multilamellar structure in vertebrates, which is vital for fast conduction of axon potential. In contrast to other plasma membranes, myelin membranes are characterized by a high content of lipids (75-80%) and a low content of proteins (20-25%). Characteristic glycosphingolipids of the myelin membrane are the galactosylceramide and sulfatide. In the CNS, the myelin sheaths are generated by oligodendrocytes, whereas Schwann cells are the myelin-forming cells in the PNS. The most obvious difference between these two cell types is the number of axons they associate with: Schwann cells form only one single internode, whereas oligodendrocytes myelinate multiple segments (Figure 1).

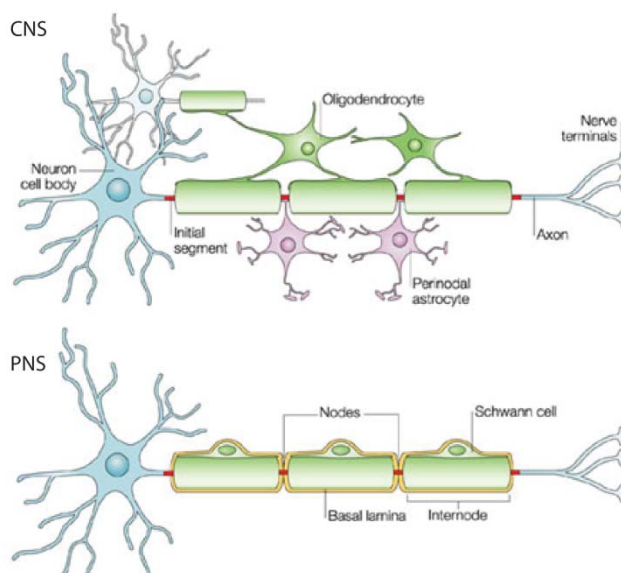


Figure 1: Differences between myelinating oligodendrocytes and Schwann cells. In contrast to oligodendrocytes, Schwann cells form only one single internode. Modified after Poliak and Peles, 2003.

4.2. Schwann cell origin and lineage

Schwann cells are derived from the neural crest cells (Figure 2). During embryonic development, they migrate as Schwann cell precursors (SCPs) in tight contact with the outgrowing axons to reach distal target tissue. SCPs are an intermediate precursor stage from neural crest stem cells to Schwann cells. At around embryonic day 17 (E17), Schwann cell precursors become immature Schwann cells ensheathing large axon bundles. This transition entails an orchestrated change in response to survival signals and growth factors. In contrast to Schwann cell precursors, which are dependent on survival signals from axons, immature Schwann cells ensure their own survival by an autocrine survival circuits (Meier et al., 1999, Weiner and Chun, 1999). The basal lamina is absent from both migrating crest cells and Schwann cell precursors, and is assembled in immature Schwann cells (reviewed in Jessen and Mirsky, 2005, Simons and Trotter, 2007).

Around birth in rodents, immature Schwann cells differentiate into either myelinating or nonmyelinating Schwann cells. The step from an immature Schwann cell to a mature myelinating Schwann cell, respectively mature nonmyelinating Schwann cell coincides with major changes in their cellular architecture.

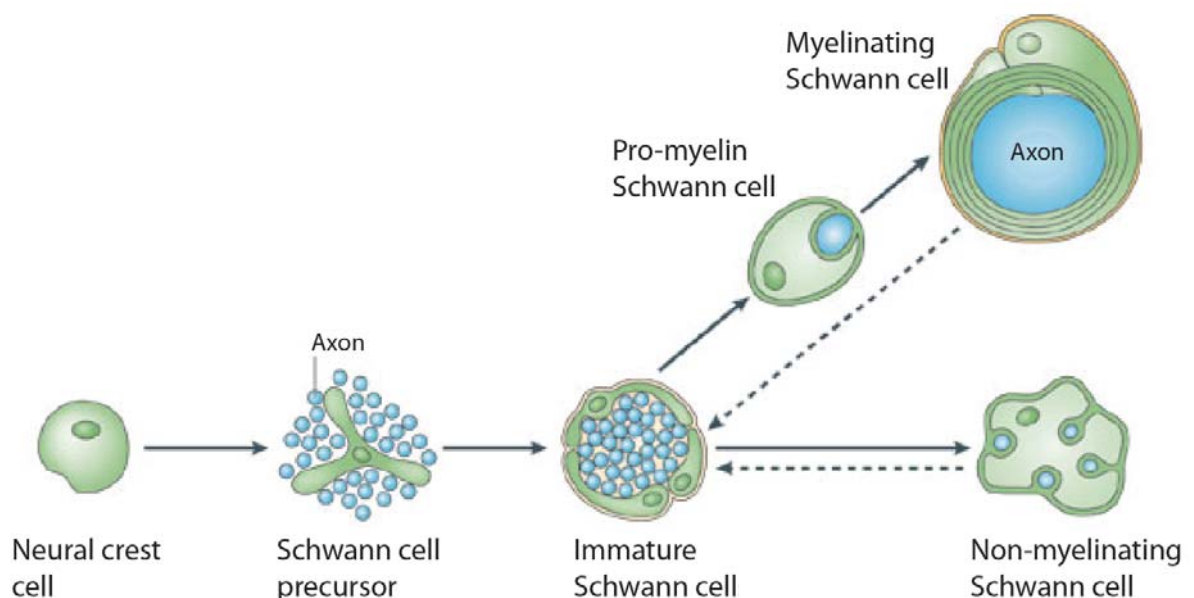


Figure 2: The Schwann cell origin. This schematic illustration comprises distinct stages of the Schwann cell lineage during peripheral nerve development. Modified after Jessen et al., 2005.

Differentiation into myelinating Schwann cells is characterized by the so-called radial sorting. This process implies the association of an individual Schwann cell with a single large diameter axon and the subsequent segregation from the axon bundle, resulting in a 1:1-relationship between Schwann cells and axons. An essential regulator for radial sorting is the accurate expression of proteins associated with the basal lamina, such as integrin $\beta 1$ and laminin (Webster, 1971, Webster et al., 1973, Bunge et al., 1986, Feltri et al., 2002, Pietri et al., 2004, Yu et al., 2005, Grove et al., 2007).

During the process of myelination, a single, modified plasma membrane extension wraps spirally around an axon. At future internodes, compact myelin is formed by close association of two adjacent membrane layers (Figure 3A). During compaction, any cytoplasm is extruded laterally into non-compact regions (Webster, 1971, Bunge et al., 1978). Not compacted myelin sheaths can be found at the paranodal region, the innermost and outermost cytoplasmic tongues, as well as at Schmidt-Lantermann incisures (Figure 3C, arrows). Schmidt-Lantermann incisures are common structures in the PNS, but are absent in the central myelin. These tubes of non-compact myelin are proposed to serve as a corridor between the Schwann cell body, and the axon and might be implicated in their nutrition and communication.

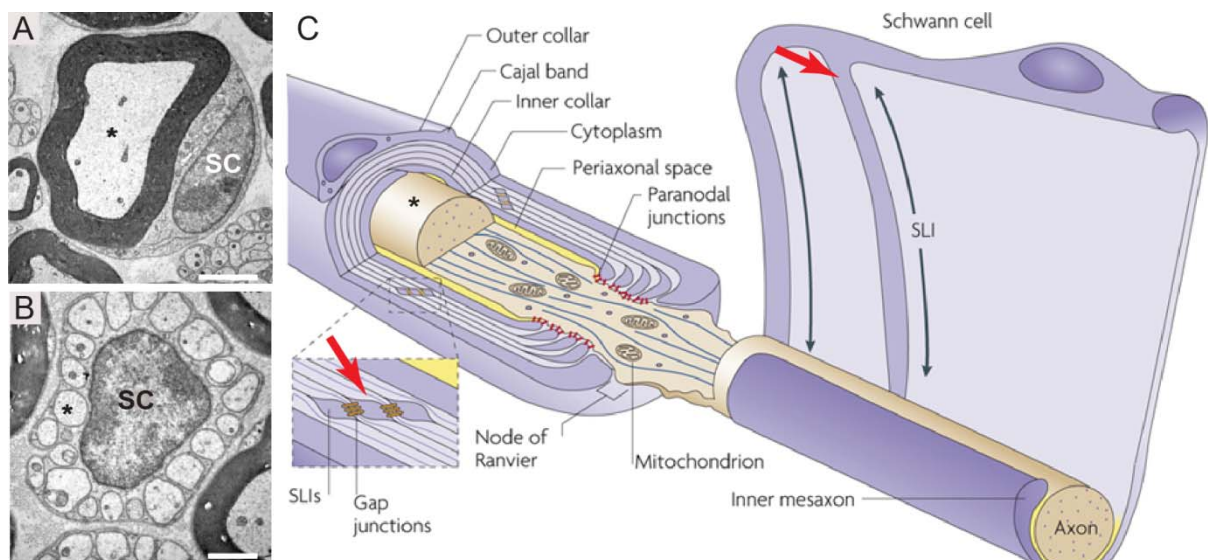


Figure 3: Myelinating cells in the peripheral nervous system. A mature myelinating (A) and nonmyelinating Schwann cell (B) are depicted by EM. (C) The different compartments of a myelinating Schwann cell are schematically illustrated. Arrows indicate Schmidt-Lanterman incisures. SC: Schwann cell, SLI: Schmidt-Lanterman incisures, asterisk: axon. Bars: 10 μ m (A), 1 μ m (B). Copied and modified from Schaeren-Wiemers et al., 2004 (A, B) and Nave, 2010 (C).

In contrast to myelinating Schwann cells, mature nonmyelinating Schwann cells ensheath several axons, forming the so-called Remak bundles (Figure 3B). Remak fibers are small diameter axons, including C-fiber nociceptors, postganglionic sympathetic fibers and some of the preganglionic sympathetic and parasympathetic fibers.

4.3. The functional role of the basal lamina

During development, the basal lamina is assembled earliest in immature Schwann cells. Components in the extracellular matrix of the basal lamina, mainly distinct laminin isoforms, modulate crucial aspects of the Schwann cell development such as ensheathment, radial sorting and myelination (Bunge et al., 1986, Bunge, 1993, Smyth et al., 1999, Feltri et al., 2002). Members of the extracellular matrix are commonly referred to basement membrane. The internal domain of the basement membrane is the basal lamina containing laminin, collagens, nidogen/entactin and the proteoglycans perlecan, agrin and bamacan. The composition of the basal lamina and the expression of ECM receptors are changing considerably during development, enabling orchestrated modulation of cellular processes and architecture (reviewed in Court et al., 2006). In Schwann cells, basal lamina-dependent initiation of cellular asymmetry and polarity is crucial for accurate development (reviewed in Simons and Trotter, 2007). For adhesion of Schwann cells to the axons, distinct expression of nectin-like 4 (Necl4, also known as Cadm4) and myelin-associated glycoprotein (MAG) and their localization along the axon-glia interface is crucial (Maurel et al., 2007, Spiegel et al., 2007, Kinter et al., 2013) (Figure 4). At the edge of the Schwann cell membrane forming the paranodal loops, higher expression of neurofascin 155 (NF155), gliomedin and TAG-1 (contactin2) is detected, which are important for axon-glia interactions at the node of Ranvier. These specialized compartments suggest that polarization of the plasma membrane into radial and longitudinal dimensions is crucial for Schwann cell myelination.

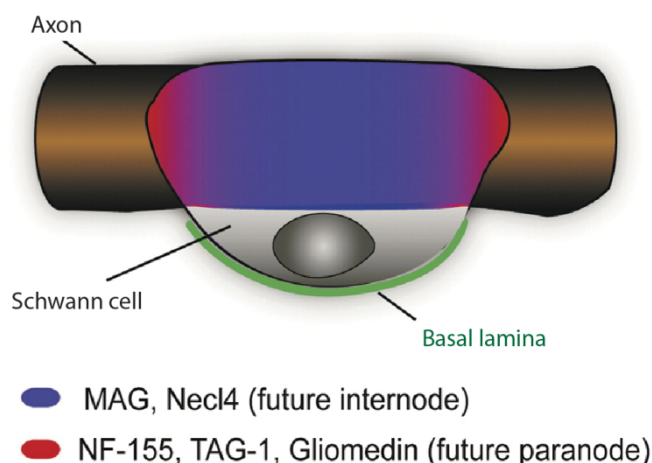


Figure 4: Schwann cell polarization during development: Basal lamina-dependent initiation of asymmetry is important for both radial and longitudinal polarization. Modified after Simons and Trotter, 2008.

During Schwann cell differentiation and axonal segregation, intracellular signaling cascades are activated by the interaction of basal lamina proteins and receptors. Laminin binds to integrin and dystroglycan on the abaxonal plasma membrane of Schwann cells and activates an autocrine signal transduction pathway for myelination. Both laminin and integrin are suggested to influence the PI3-kinase/Akt and Ras/MAP-kinase pathways as well as the focal adhesion kinase (FAK) (Cognato et al., 2002, Chen and Strickland, 2003, Previtali et al., 2003, Saito et al., 2003, Yang et al., 2005, Yu et al., 2005, Hoshina et al., 2007, Chernousov et al., 2008, Barros et al., 2009). Furthermore, laminin expression is essential for proper neuregulin signaling (Yu et al., 2005). Another implication of laminin is the activation of Fyn: Upon laminin binding, Fyn can activate members of the small Rho GTPases, such as Rac1 and Cdc42, and modulate process outgrowth by influencing actin cytoskeleton (Hoshina et al., 2007).

4.3.1. Cytoskeleton in Schwann cells

Radial sorting and myelination require tremendous changes in Schwann cell shape. These morphogenetic changes involve the remodeling of the actin cytoskeleton. In line, for protein and lipid transport, an accurate organization of the cytoskeleton is vital. The cytoskeleton contains three main filamentous systems: microfilaments, intermediate filaments and microtubules. The microfilaments are composed of polymers of actin subunit and are the thinnest filaments in the cytoskeleton. The system of intermediate filaments contains filaments made by keratin, vimentins and glial fibrillary acidic protein (GFAP) in glial cells. The third group is formed by polymers of α - and β -tubulin. Besides microfilaments, intermediate filaments and microtubules, a fourth filamentous system is known in Schwann cells, namely the family of septins (Buser et al., 2009a). Septins form higher-ordered filaments by heteromeric assembly, and can interact with components of cellular membranes, as well as with actin filaments and microtubules (reviewed in Saarikangas and Barral, 2011). Septins are involved in membrane compartmentalization and vesicle transport in polarized cells including Schwann cells.

In polarized Schwann cells, Golgi-derived vesicles are transported to distinct compartments such as the adaxonal or abaxonal membrane. There are several proteins described to regulate the cytoskeletal reorganization in developing and myelinating Schwann cells. Crucial modulators of microfilaments are the Rho GTPases Cdc42 and Rac1 that are activated by signals derived from the extracellular matrix or neuregulin1 (Chernousov et al., 2008, Feltri et al., 2008). Their deletion in mice was shown to impair myelin formation (Benninger et al., 2007, Nodari et al., 2007). Laminin mediated signal transduction at the basal lamina have been shown to be important regulator of the cytoskeleton (Cody and

Wicha, 1986, Colognato et al., 1999, Yu et al., 2009). Cofilin, which depolymerizes actin, was recently identified as a downstream target of the neuregulin1 signaling pathway, highlighting the impact of neuregulin1 on the cytoskeleton organization (Sparrow et al., 2012). Deficiency in cofilin impeded myelination, and resulted in a discontinuous basal lamina in Schwann cell cocultures (Sparrow et al., 2012). In addition, neural Wiskott-Aldrich syndrome protein (N-WASp) is an important actin cytoskeletal regulator. Like other family members, N-WASp mediates extracellular stimuli and actin polymerization (Wegner et al., 2008). It is upregulated in myelinating Schwann cells, and is vital in Schwann cell maturation (Jin et al., 2011). The Rho-associated protein kinase (ROCK), a major downstream effector of Rho, has a key role in the modulation of the cytoskeleton by regulating myosin light chain phosphorylation, which is transiently activated during early development. Inhibition of ROCK leads to loss of microvilli and stress fibers in cultured Schwann cells (Melendez-Vasquez et al., 2004). In Schwann cell/neuron cocultures, aberrant myelination was observed upon pharmacological inhibition of ROCK (Melendez-Vasquez et al., 2004). Interestingly, neither proliferation nor differentiation was affected (Melendez-Vasquez et al., 2004). Further, the cytoskeletal crosslinker protein dystonin is proposed to be a necessary component of the cytoskeleton in Schwann cells. In mice carrying mutations in dystonin, Schwann cells are arrested at the promyelinating stage, and hypomyelination can be observed (Bernier et al., 1998). This study also manifested that mutant Schwann cells are abnormally polarized and have an altered matrix attachment, as well as a disorganized cytoskeleton.

4.4.Schwann cell signaling

During development of peripheral nerves, Schwann cells are in tight contact with axons providing mutual trophic support. Accurate Schwann cell development and myelination is controlled and regulated by reciprocal axon-glia interaction (reviewed in Nave and Trapp, 2008). Although axonal signals crucial for development were recently identified, the process of differentiation and myelination is not yet entirely understood. The complexity is even increased, since many pathways can influence each other, resulting in a sophisticated system. For illustration, only the main pathways are disclosed (Figure 5).

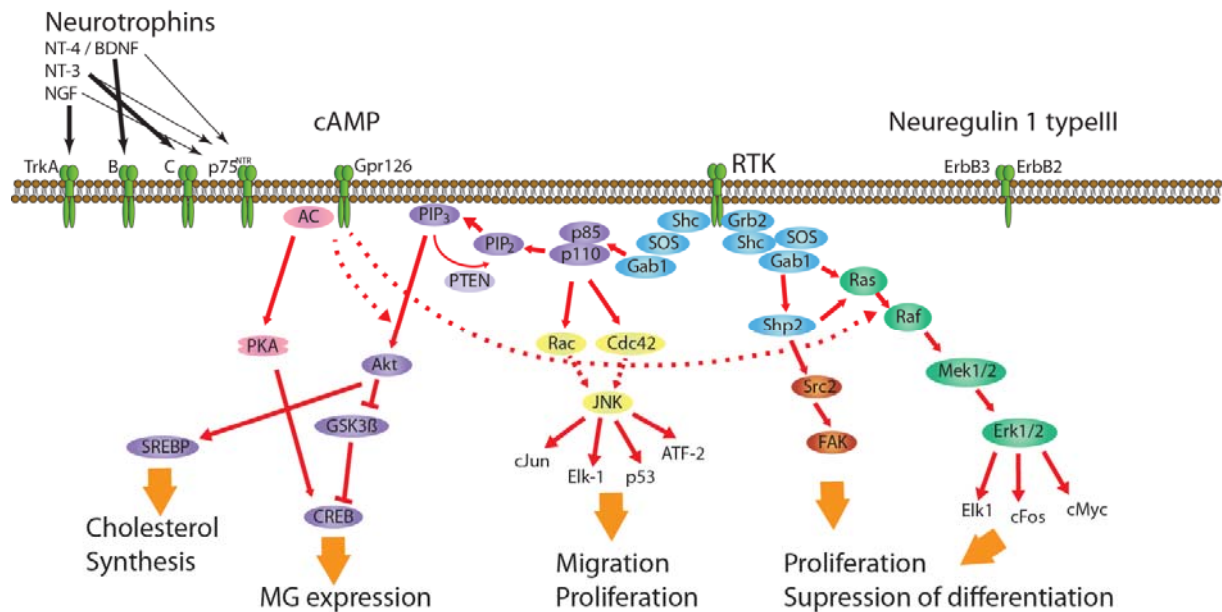


Figure 5: Simplified pathway of intracellular Schwann cell signaling. The main pathways in Schwann cells can be activated by receptor tyrosine kinases (RTK) and are important for either expression of myelin-related genes (MG), migration or proliferation. See respective chapter for details and abbreviations.

4.4.1. The Neuregulin 1/ ErbB system

One essential growth factor is the axonal neuregulin1 (NRG1), which signals via the ErbB receptor tyrosine kinases (Webster et al., 1973, Wood and Bunge, 1975, Holmes et al., 1992, Wen et al., 1992). In Schwann cells, NRG1 is a ligand for the high affinity receptor ErbB3. ErbB3 has no tyrosine kinase activity, and only ErbB2 in a heterodimer with ErbB3 contributes to downstream signaling such as MAP-kinase or PI3-kinase (Yarden and Sliwkowski, 2001).

By alternative splicing of transcripts, multiple isoforms of NRG1 are generated (reviewed in Falls, 2003, Birchmeier and Nave, 2008) (Figure 6). All of the isoforms have an EGF-like domain, but contain individual N-terminal domains. Further, the NRG1 type III contains an additional transmembrane domain, which is rich in cysteines (Buonanno and Fischbach, 2001). Proteolytic processes of the receptors NRG1 type I and III is executed by the metalloprotease ADAM, a disintegrin and metalloprotease (Montero et al., 2000, Shirakabe et al., 2001, Horiuchi et al., 2005). Further, the aspartyl protease BACE1 is implicated in cleavage of NRG1, whereas NRG1 type I and IV are released from the membrane, and serve as paracrine signaling molecules (Hu et al., 2006, Willem et al., 2006). Due to the second transmembrane domain, NRG1 type III remains attached to the plasma membrane, and acts as a juxtacrine signal (Nave and Salzer, 2006).

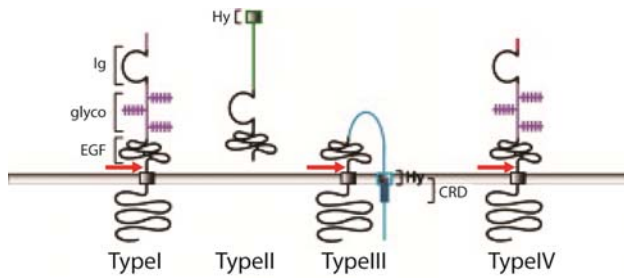


Figure 6: Isoforms of neuregulin1: Multiple isoforms of neuregulin1 are generated by alternative splicing. All isoforms share a common EGF-like domain, but have distinct N-terminal domains. Arrows indicate cleavage sites for proteases. CRD: cysteine rich domain, Hy: hydrophobic sequence, glyco: glycosylation site, Ig: Ig domain. Modified after Birchmeier and Nave, 2008.

In Schwann cell cultures, NRG1 promotes proliferation, as well as migration and survival (Dong et al., 1995, Maurel and Salzer, 2000, Vartanian et al., 2000, Meintanis et al., 2001, Ogata et al., 2004). In the PNS, NRG1 type III plays the most important role among the other neuregulin isoforms by mediating the entire Schwann cell lineage. The essential role of NRG1/ErbB signaling for survival and development of Schwann cells was confirmed *in vivo* by transgenic mice either deficient in functional NRG1 type III or ErbB2/3 (Riethmacher et al., 1997, Garratt et al., 2000a, Taveggia et al., 2005). NRG1 type III also determines the myelin thickness in Schwann cells. Heterozygous knockout mice for NRG1 type III show thinner myelin and decreased expression of myelin-related transcription factors, whereas NRG1 type III overexpression leads to hypermyelination (Garratt et al., 2000b, Michailov et al., 2004, Taveggia et al., 2005).

4.4.2. Neurotrophins – TrkA, B, C / p75^{NTR} system

The growth factors neurotrophins are secreted proteins that modulate survival, growth, differentiation and myelination in both PNS and CNS (Anton et al., 1994, Cosgaya et al., 2002, Yamauchi et al., 2003, Chan et al., 2004, Reichardt, 2006). The family of neurotrophins contains four structurally related members: Nerve growth factor (NGF), brain-derived neurotrophic factor (BDNF), neurotrophins-3 (NT-3) and neurotrophin-4 (NT-4). Neurotrophins are ligands for the tropomyosin-related kinase (Trk) family of receptor tyrosine kinases; NGF signals via TrkA, BDNF and NT-4 via TrkB and NT-3 via TrkC. Additionally, the neurotrophin receptor p75^{NTR} binds all neurotrophins, but with lower affinity. Activation upon ligand binding results in downstream signal transduction via a variety of pathways such as PI3-kinase and MAP kinase signaling pathways. Besides neuregulin1, neurotrophins are key regulators of peripheral myelination.

In Schwann cells, TrkC activation by binding of endogenous **NT-3** results in enhanced migration of promyelinating Schwann cells, mediated by the c-Jun N-terminal kinase (JNK) cascade (Yamauchi et al., 2003). Application of exogenous NT-3 to Schwann cell/dorsal root ganglia cocultures resulted in inhibition of myelination, whereas decreased endogenous NT-3 by using the NT-3 receptor TrkC-Fc fusion protein enhanced myelination in these cocultures (Chan et al., 2001). These findings were confirmed *in vivo* by injections of

exogenous NT-3 or TrkC-Fc fusion protein into developing sciatic nerves of P1 mice, resulting in suppressed or promoted myelination, respectively (Chan et al., 2001). These data indicate that TrkC-mediated signaling has a negative effect on peripheral myelination. In contrast to NT-3, **BDNF** promotes myelination in the peripheral nervous system. In Schwann cell/dorsal root ganglia cocultures, exogenous BDNF increased the expression of MAG and P0, whereas removal of endogenous BDNF by applying the TrkB-Fc fusion protein suppressed myelination (Chan et al., 2001). In line with *in vitro* observations, removal of BDNF by injection of TrkB-Fc fusion protein into developing sciatic nerves resulted in decreased myelination (Chan et al., 2001). Furthermore, injection of exogenous BDNF strongly increased P0 and MAG protein expression. In addition to induced protein expression, also an increased number of myelinated axons and increased thickness of myelin sheaths could be detected in BDNF-injected nerves by electron microscopy (Chan et al., 2001). Another study determined that the enhancement of myelination by endogenous BDNF is mediated by p75^{NTR}, pointing to its essential role during myelin formation (Cosgaya et al., 2002). In a recent study, BDNF was shown to activate the small GTPase Rac1 at the axon-glial interface at the onset of Schwann cell myelination, resulting in enhanced myelination (Tep et al., 2012).

The neurotrophin **NGF** was identified to modulate axonal signals that regulate myelination of TrkA-positive DRGs. Interestingly, its functional role on myelination is opposite in the central and the peripheral nervous system. NGF enhances myelination by Schwann cells, whereas it suppresses myelin-related gene expression in oligodendrocytes (Chan et al., 2004). In Schwann cell/DRG cocultures, addition of exogenous NGF resulted in robust myelination, and removal of endogenous NGF by TrkA-Fc fusion protein inhibited myelination by Schwann cells. In contrast, exogenous NGF in oligodendrocytes/DRG cocultures suppressed myelination, and its removal strongly enhances myelination (Chan et al., 2004). By using cultures derived from p75^{NTR}^{-/-} mice, Chan et al. demonstrated that the receptor p75^{NTR} is not required for NGF-dependent myelination, but the effect of NGF is mediated solely via TrkA. The finding of opposite effects of NGF-regulated signals in the central and peripheral nervous system highlights the complex and distinct regulation of myelination.

4.4.3. The cAMP signaling pathway

The cAMP signaling pathway is a G-protein-coupled receptor-triggered signaling cascade (Figure 7). Upon ligand binding, the intracellular heterotrimeric G protein complex activates the adenylyl cyclase (AC), which converts ATP into the second messenger cAMP (Hanoune and Defer, 2001). In the presence of cAMP, protein kinase A (PKA) is activated, which

subsequently stimulates the cAMP response element (CREB). In Schwann cells, elevation of intracellular cAMP has been shown to induce myelin-related gene expression *in vitro* (Lemke and Chao, 1988, Monuki et al., 1989, Morgan et al., 1991, Parkinson et al., 2003, Monje et al., 2009). However, mechanisms regulating cAMP levels *in vivo* have been unknown for a long time. In mutant zebrafish, a key role for the G protein-coupled receptor Gpr126 has been identified in peripheral myelination (Monk et al., 2009). In fish lacking *gpr126*, Schwann cells were arrested at a promyelinating state and expression of Oct6 and Krox20 was impaired. Treatment with cAMP analogues rescued myelination in *gpr126* mutants, indicating that *gpr126* drives Schwann cell differentiation by elevating cAMP levels and activating protein kinase A (Monk et al., 2009, Monk et al., 2011).

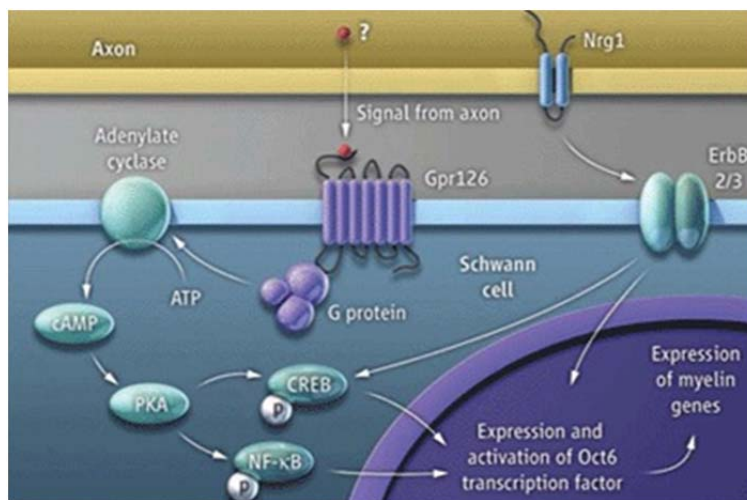


Figure 7: cAMP signaling pathways in Schwann cells. Schematic illustration of the cAMP signaling pathway, resulting in expression of myelin-related genes by CREB activation. Copied from Meijer, 2009.

The presence of a cross-talk between cAMP and other signaling pathways was proposed in several studies (Stewart et al., 1996, Kim et al., 1997, Cohen and Frame, 2001, Grimes and Jope, 2001, Ogata et al., 2004, Monje et al., 2006, Monje et al., 2010). It was shown that the IGF-I pathway requires cAMP signals to exert its differentiating effect on Schwann cells, which is supported by the finding that cAMP also increases IGF-I-induced PI3-kinase activities (Stewart et al., 1996, Ariga et al., 2000).

In addition to Schwann cell differentiation, elevation of cAMP was also shown to promote Schwann cell proliferation (Sobue et al., 1986, Lemke et al., 1990, Morgan et al., 1991, Jung-Testas et al., 1993, Arthur-Farraj et al., 2011). Investigation of the interaction between cAMP and neuregulin revealed that cAMP potentiates neuregulin-dependent proliferation and activation of both Erk and Akt signaling pathways, suggesting that cAMP might act early on neuregulin receptor-activated signaling cascade, e.g. upstream or at the level of Raf/Mek and Akt (Monje et al., 2006).

4.4.4. The PI3-kinase/ Akt signaling pathway

In Schwann cells, one of the key pathways activated by ErbB receptors is the phosphatidylinositol-3-kinase (PI3-kinase)/Akt pathway (Maurel and Salzer, 2000, Taveggia et al., 2005). Upon ligand binding, the regulatory subunit p85 of PI3-kinase becomes phosphorylated. Consequently, the catalytic subunit p110 catalyzes the transition of phosphatidylinositol-3,4-bisphosphate (PIP₂) to phosphatidylinositol-3,4,5-trisphosphate (PIP₃), which is hydrolyzed by the phosphatase and tensin homologue (PTEN). Recent data of PTEN knockout mice show that lack of PTEN causes hypermyelination in both CNS and PNS by elevation of PIP₃ level (Goebbels et al., 2010). PIP₃ recruits Akt to the plasma membrane, where it gets phosphorylated at threonine308 and serine473, and consequently affects a variety of downstream signaling. To further examine the Akt pathway, transgenic mice with constitutively active Akt were generated using the myelin proteolipid protein (PLP) promoter to drive the expression of constitutively active Akt1 (Flores et al., 2008). This form has aspartic acids at two sites, whose phosphorylation leads to full activation of Akt (Bellacosa et al., 1991). In the CNS, activation of the Akt pathway was shown to result in enhanced myelination (Flores et al., 2008). In contrast, no evident effect on PNS myelination could be detected in these mice, which might be explained by the fact that PLP is only weakly expressed in the PNS (Flores et al., 2008). It was also shown that selective activation of the PI3-kinase pathway in rat Schwann cell cultures by adenoviral vectors resulted in enhanced Schwann cell differentiation (Ogata et al., 2004). Activation of this pathway promoted myelination in Schwann cell/DRG cocultures *in vitro* and in nerve graft experiments *in vivo* (Ogata et al., 2004). A known target for phosphorylated Akt is the inhibition of the glycogen synthase kinase 3 β (GSK-3 β), which acts as a negative modulator for myelination. Phosphorylated Akt influences the expression of the sterol responsive element binding proteins (SREBPs) via mTOR, and consequently regulates cholesterol biosynthesis (Porstmann et al., 2005). Lack of mTOR in Schwann cells was shown to result in reduced axonal growth, and radial as well as longitudinal growth of myelinating Schwann cells, indicated by thinner myelin sheaths, shorter internodes and reduced axonal diameter (Sherman et al., 2012). These findings emphasize Akt as a positive regulator for myelination.

4.4.5. The MAP-kinase signal transduction pathway

Another well-known signaling pathway implicated in Schwann cell development is the mitogen-activated protein kinase (MAPK) pathway. So far, more than a dozen members of the MAPK family are identified. The best investigated genes are the extracellular signal-regulated kinase 1 and 2 (ERK1 and ERK2), cJun amino-terminal kinase (JNK) and p38 (Nishida and Gotoh, 1993, Robinson and Cobb, 1997, Davis, 2000, Kyriakis and Avruch, 2001,

Raman et al., 2007). Signaling via MAPK mediates proliferation, growth and survival in the nervous system, and is a negative modulator for peripheral myelination (reviewed in Nishimoto and Nishida, 2006).

4.4.5.1. The ERK1/2 signaling cascade

There are several signals or ligands activating receptor tyrosine kinases (RTK), which leads to ERK1/2 activation, including growth factors, serum, cytokines and microtubule depolarization (reviewed in Johnson and Lapadat, 2002, Yoon and Seger, 2006). Small G proteins of the Ras family bind to one isoform of the Raf family and activates it by phosphorylation. Raf itself phosphorylates the MAPK-kinases (MAP2K) MEK1 and MEK2, which are the upstream of the ERK1/2 kinases. Phosphorylation of tyrosine and threonine residues of ERK1/2 acts on several distinct targets, of which the best known is the activation of the transcription factors Elk1, c-Fos and c-Myc.

In Schwann cells, the Ras/Raf/Mek/Erk signaling cascade blocks differentiation, and drives dedifferentiation. Infections with adenoviral and retroviral vectors to selectively activate the Erk pathway suppressed Schwann cell differentiation *in vitro* (Harrisingh et al., 2004, Ogata et al., 2004). Further, activation of Raf signaling in differentiated Schwann cells resulted in decreased expression of differentiation markers within 48 h, indicating that Raf signaling promotes dedifferentiation in Schwann cells (Harrisingh et al., 2004). Inhibition of the Erk pathway by adding Mek inhibitor to Schwann cells had only a minor effect on P0 expression, indicating that inhibition of Erk pathway is not sufficient to induce Schwann cell differentiation (Harrisingh et al., 2004).

4.4.5.2. The c-Jun N-terminal kinases (JNK) cascade

The JNK is encoded by three genes, JNK1, JNK2 and JNK3, which contain highly identical protein sequences (Kyriakis and Avruch, 2001, Johnson and Lapadat, 2002). The pathway can be activated by growth factors, DNA synthesis inhibition and inflammatory cytokines (Kyriakis and Avruch, 2001). The main downstream effect of JNK is the activation of transcription factors such as c-Jun, p53, Elk-1 and ATF-2. In Schwann cells, the JNK/c-Jun pathway is activated by both neuregulin1 and TGF β , and was shown to be implicated in proliferation, NT-3/TrkC-induced migration and cell death (Yamauchi et al., 2003, Parkinson et al., 2004). Further, it can be suppressed by Krox20 expression, suggesting an important regulatory activity during Schwann cell development (Parkinson et al., 2004).

4.5. The myelin and lymphocyte protein MAL

4.5.1. Characterization of MAL and its biochemical properties

In 1987, a human cDNA encoding for a 16.7kDa, highly hydrophobic protein called MAL was described in T-lymphocyte (Alonso and Weissman, 1987). Later different laboratories independently identified MAL being also expressed in oligodendrocytes and Schwann cells *in vivo* and called thereafter myelin and lymphocyte protein (MAL, Schaeren-Wiemers et al., 1995b, Schaeren-Wiemers et al., 1995b), in rat primary oligodendrocytes (MVP17, Kim et al., 1995) and in polarized epithelial cells (VIP17, Zchetti et al., 1995). The myelin and lymphocyte protein MAL is a nonglycosylated integral membrane protein with four transmembrane domains that are separated by short hydrophilic segments (Alonso and Weissman, 1987, Schaeren-Wiemers et al., 1995b) (Figure 8).

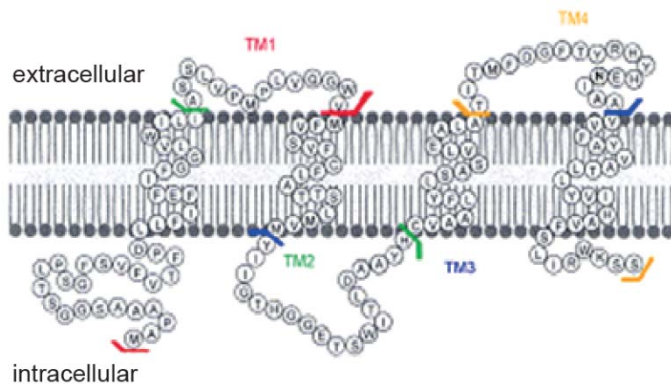


Figure 8: Protein structure of MAL. MAL is a highly hydrophobic tetraspan protein with only short hydrophilic segments. Modified after Schaeren-Wiemers et al., 1995.

Based on the structural similarity to the myelin proteolipid protein (PLP) and its solubility in organic solvents, MAL was suggested to be a proteolipid (Frank et al., 1998). Proteolipids are highly hydrophobic proteins, which are only soluble in organic solvents or in solutions containing strong detergents (Ting-Beall et al., 1979, Schlesinger, 1981, Lees et al., 1982). MAL was also identified to be incorporated into glycolipid-enriched membrane fractions, the so-called lipid rafts, pointing to its functional role in protein trafficking and sorting (Kim et al., 1995, Zchetti et al., 1995, Puertollano et al., 1999, Schaeren-Wiemers et al., 2004).

4.5.2. Expression pattern of MAL in the nervous system

In the nervous system, MAL is expressed by oligodendrocytes in the CNS and by Schwann cells in the PNS (Schaeren-Wiemers et al., 1995a, Schaeren-Wiemers et al., 1995b). In the CNS, MAL expression takes place during the later steps of myelination. Therefore, it could play a role in the final steps of myelin formation, such as stabilization and maintenance of the compact myelin sheath. MAL expression in Schwann cells starts already at embryonic

day 17 (E17), implicating a role in development (Frank et al., 1999). It is expressed by both myelinating and nonmyelinating Schwann cells, and is localized in compact myelin, but also in noncompact regions such as paranodal loops and Schmidt-Lanterman incisures (Erne et al., 2002).

4.5.3. Putative functional role of MAL

Besides the nervous system, MAL is localized in apical membranes of polarized epithelial cells of the kidney, gastrointestinal tract and thyroid gland (Zacchetti et al., 1995, Magyar et al., 1997, Frank et al., 1998, Martin-Belmonte et al., 1998, Cheong et al., 1999, Puertollano et al., 1999, Martin-Belmonte et al., 2000). MAL is present in vesicle structures within the apical part of polarized Madin-Darby canine kidney (MDCK) cells, suggesting that MAL might be a candidate component in vesicular sorting (Zacchetti et al., 1995). In agreement, another study reported that overexpression of MAL increases the apical transport and the apical surface in MDCK cells (Cheong et al., 1999). Deficiency of MAL causes accumulation of apical surface markers in post-Golgi compartments, whereas basolateral markers are not affected by reduced levels of MAL (Cheong et al., 1999). Further, MAL expression was detected on the apical surface of cells in the kidney and stomach epithelium (Frank et al., 1998). The importance of MAL in sorting of particular vesicles is underlined by a recent report indicating that MAL depletion decreases the rate by which uroplakins are inserted into the apical surface in MDCK cells (Zhou et al., 2012).

4.5.4. Phenotype of MAL overexpression in the peripheral nervous system

MAL overexpression leads to pathological apical membrane formation in kidney and stomach, demonstrating that its correct dosage is essential for proper function (Frank et al., 2000). In the PNS, mice overexpressing MAL manifest a delayed maturation of Remak bundles, and progressive segregation of unmyelinated axons (Frank et al., 2000, Buser et al., 2009b) (Figure 9A, B). In addition, polyaxonal myelination can occasionally be observed in MAL-overexpressing nerves (Figure 9C). One of the most important finding was the delayed onset of myelination in mice overexpressing MAL, which was reflected by hypomyelinated fibers during early development (Buser et al., 2009b) (Figure 9D, E). Along with changes on the morphological level, altered gene transcription and protein expression was detected in MAL-overexpressing mice. In sciatic nerves of newborn mice, reduced protein levels of the low affinity neurotrophin receptor p75^{NTR} were identified (Buser et al., 2009b) (Figure 9F). In line, also reduced mRNA expression levels of p75^{NTR} as well as of Sox10, ErbB2 and ErbB3 could be detected in sciatic nerves of newborn MAL-overexpressing mice (Buser et al., 2009b) (Figure 9G). These results suggested that altered p75^{NTR} expression in MAL-

overexpressing mice might be the cause of delayed onset of myelination, since distinct expression of p75^{NTR} has been shown to be essential for proper initiation of myelination (Cosgaya et al., 2002).

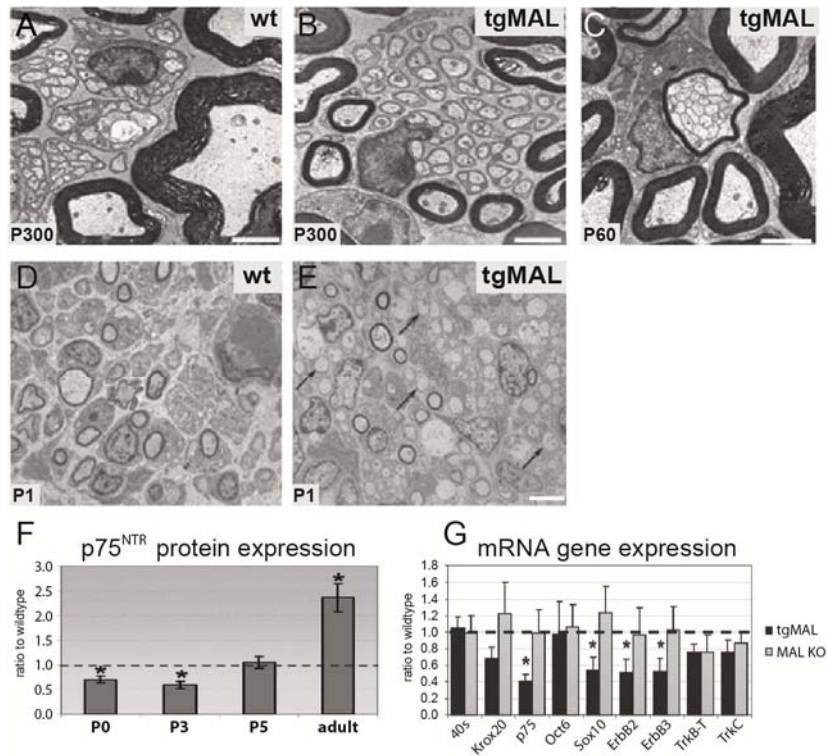


Figure 9: Phenotype of MAL overexpression in the PNS. (A, B) In adult mice, MAL overexpression leads to progressive segregation of unmyelinated axons. (C) Occasionally, polyaxonal myelination is observed. (D, E) Compared to wildtype mice, a retarded onset of myelination can be detected in newborn MAL-overexpressing mice, indicated by hypomyelinated fibers (arrows). (F) p75^{NTR} protein expression was reduced during early development in MAL-overexpressing sciatic nerves. (G) MAL overexpression in newborn mice leads to differentially expressed genes. Bar: A, B, C: 2 μ m, D, E: 5 μ m. Modified after Buser et al., 2009b.

4.5.5. Septin 6 is an interaction partner of MAL

To identify a potential intracellular binding partner of MAL, a postnatal mouse brain library was analyzed by a yeast two-hybrid screen, using the intracellular N-terminal domain of MAL as a bait (Buser et al., 2009a). This analysis identified Septin 6 (Sept6) as a potential interaction partner of MAL, which was confirmed by a GST-pull down assay (Buser et al., 2009a). Septins represent the fourth filamentous system of the cytoskeleton, and can interact with components of cellular membranes, as well as with actin filaments and microtubules (Saarikangas and Barral, 2011). This finding led to the hypothesis that the interaction of MAL and Septin 6 might be involved in the compartmentalization of the Schwann cell and in the sorting and trafficking of vesicles (Buser et al., 2009a).

5. Aim of the Work

Myelination is a remarkably complex and fascinating process in vertebrates, which is tightly orchestrated by Schwann cells during development. In addition to temporal regulation of the involved proteins, their proper localization in the different Schwann cell compartments is essential for accurate myelin formation. Despite decades of extensive research on myelin biology, the precise process of myelination is still not entirely understood. The transmembrane myelin and lymphocyte protein MAL is a component of lipid rafts, and it mediates the compartmentalization in polarized cells. In the PNS, MAL overexpression leads to a delayed onset of myelination, reflected in hypomyelinated fibers during early postnatal development. In addition to morphological changes, reduced expression levels of the myelin protein zero (P0, MPZ) as well as of the low affinity neurotrophin receptor p75^{NTR} were identified in MAL-overexpressing sciatic nerves. It was suggested that altered p75^{NTR} expression in MAL-overexpressing mice might be the cause of delayed onset of myelination, since distinct expression of p75^{NTR} is essential for proper initiation of myelination.

This thesis aimed to elucidate a functional link between MAL overexpression and the retarded onset of myelination. First, we planned to determine if the reduced expression of p75^{NTR} can be validated in MAL-overexpressing Schwann cells *in vitro*. For this purpose, primary mouse Schwann cell cultures were established, and their mRNA expression pattern was analyzed. Another important point to clarify was whether MAL-overexpressing Schwann cells are less responsive to axonal signals compared to wildtype cells. We embarked on downstream signaling pathways mediated by intracellular cAMP levels, neuregulin1, NGF and FGF1, and investigated whether they are functional in MAL-overexpressing Schwann cells. In order to gain better insight into the molecular mechanism leading to reduced expression of P0 and p75^{NTR}, a comprehensive data analysis of a microarray study was planned for MAL-overexpressing Schwann cells.

In another project, we planned to determine whether MAL overexpression directly leads to reduced expression of endogenous p75^{NTR}. To this end, wildtype Schwann cells were infected with a retroviral construct to overexpress MAL, and the p75^{NTR} expression was subsequently analyzed in these cells. We planned to investigate this direct link between MAL overexpression and reduced p75^{NTR} expression in the immortalized Schwann cell line S16 and in primary rat Schwann cells.

6. Material and Methods

6.1. Cell culture

6.1.1. Primary Schwann cell cultures

6.1.1.1. Primary mouse Schwann cell cultures

All reagents were supplied by Sigma-Aldrich, if not otherwise stated. Sciatic nerves of P1 mice were dissected aseptically, collected pairwise in 900µl cold DMEM (D6546), and centrifuged at 1'000rpm to gather them at the bottom of the tube. Nerves were first dissociated with 100µl 0.4% collagenase for 30 min at 37°C, and subsequently with 100µl 0.25% trypsin for additional 15 min. Then, the enzymatic reaction was stopped with 800µl DMEM supplemented with 10% FBS (herein called "SC medium"), and dissociated cells were centrifuged 5 min at 1'000rpm, resuspended in 320µl SC medium, and seeded on one well of a 24-well plates (Primaria™, BD Bioscience). The day after, 10µM antimitotic cytosine β-D-arabino-furanoside (AraC) was added for 24 h and repeated for additional 24 h to stop proliferation of fibroblasts. Thereafter, Schwann cells were passaged, and reseeded at the density of 25'000 cells per well in 320µl SC medium for stimulation assays. The purity of mouse Schwann cell cultures was determined by immunofluorescent stainings for p75^{NTR} and S100 and revealed in general more than 85% enrichment.

6.1.1.2. Stimulation assays of mouse Schwann cell cultures

Schwann cells were stimulated with 2, 20, 50 or 100µM forskolin (Sigma-Aldrich), 10 or 50ng/ml FGF1 (R&D Systems), 2.5 or 10nM heregulin-1β (Sigma-Aldrich; herein called neuregulin) or 20ng/ml NGF-β (Sigma-Aldrich) in SC medium for 24 h (mRNA analysis) or 72 h (protein analysis).

6.1.1.3. Primary rat Schwann cell cultures

All reagents were supplied by Sigma-Aldrich, if not otherwise stated. Rat Schwann cells were isolated as described with minor modifications (Brockes et al., 1979), and cultured according to a protocol kindly provided by Dies Meijer (Mandemakers et al., 2000). Sciatic nerves of P2 Sprague-Dawley rats were dissected, and collected in cold L-15 medium (Leibovitz) in a 35mm petri dish. Connective tissue was removed and the perineurial membrane was removed. The cells were dissociated with 2ml 0.1% collagenase in L-15 for 30 min at 37°C, and dissociated by pipetting up and down for five times every 10 min. Subsequently, 250µl 0.25% trypsin was added and the cells were incubated for additional 10 min at 37°C. The

protease activity was stopped by addition of L-15 supplemented with 10% FBS. Dissociated cells were centrifuged for 5 min at 1'000rpm at room temperature, and resuspended in DMEM (D6546) supplemented with 10% FBS, 10ng/ml NGF- β , L-glutamine, Pen/Strep (herein called "C_B medium"), thereafter seeded onto 10 cm plates (Primaria™, BD Bioscience), and incubated at 37°C, 5% CO₂.

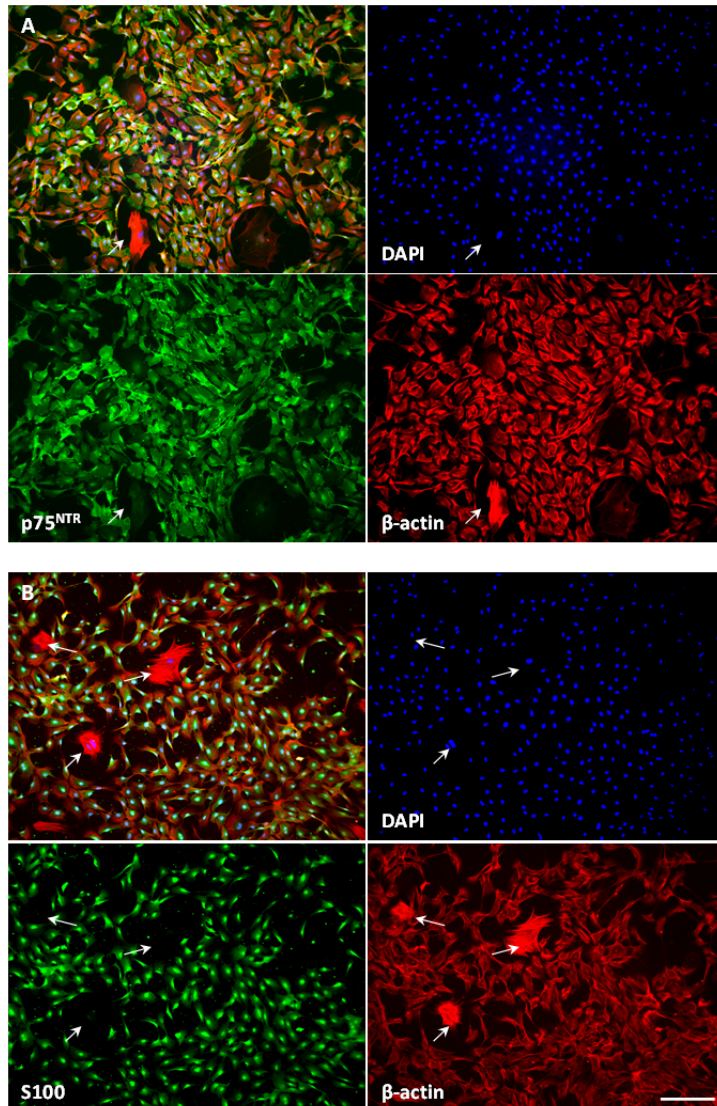


Figure 10: Establishment of proliferating rat Schwann cell cultures. Purity of rat Schwann cell cultures was determined by p75^{NTR} and S100 immunofluorescent microscopy. Schwann cells were positively stained for p75^{NTR} (A) and S100 (B), whereas remaining fibroblasts (arrows) were negative. They could be easily identified by their strong expression of β -actin. Bar: 200 μ m

The next day, cells were washed, and consecutively treated with 10 μ M AraC in C_B medium for three days to stop fibroblast proliferation. Thereafter, Schwann cell proliferation was induced by DMEM supplemented with 3% FBS, 5% NDF- β -conditioned medium (see below), 2 μ M forskolin and Pen/Strep (herein called "Schwann cell proliferating medium" (SCPM)). SCPM was replaced three times a week, and cells were passaged when semi-confluence was reached. In contrast to the original protocol advising the cold-jet method (Jirsova et al., 1997) for passaging, Schwann cells were incubated with 0.5ml 0.25% trypsin/EDTA for only

one minute at room temperature, and monitored by microscopy. Schwann cells got detached by strongly tapping at the side of the plate, while fibroblasts still remain attached to the plate, resulting in highly enriched Schwann cell cultures. The enzymatic reaction was stopped by addition of SCPM, cells were centrifuged for 5 min at 1'000 rpm, the pellet was resuspended in either SCPM for further expansion or in 45% DMEM/F12, 45% FBS and 10% DMSO for freezing.

To investigate the mRNA expression of distinct genes upon forskolin stimulation, 400'000 Schwann cells were seeded onto 6 well plates (Primaria™, BD Bioscience), cultured in SC medium for 24 h, followed by treatment with different concentrations of forskolin for another 24 h. For investigation of protein expression, 10'000 cells were seeded in a 150µl drop onto poly-L-lysine / laminin coated glass coverslips in DMEM supplemented with 1% FBS, incubated 48 h to deprive cells from mitogens, and then stimulated with 20µM forskolin for 72 h. Purity of proliferating rat Schwann cell cultures determined by immunofluorescent microscopy of p75^{NTR} and S100 revealed more than 95% pure Schwann cells (Figure 10).

Preparation of NDF-β conditioned medium:

A CHO cell line overexpressing NDF-β was generated by Elijor Peles (Weizmann Institute, Rehovot, Israel), and kindly provided by Dies Meijer. Cells were routinely grown in DMEM/F12 supplemented with 5% FBS, and split every three to four days. To obtain conditioned medium, a confluent plate was split 1:10, and the medium was replaced the next day with DMEM/F12 supplemented with 1% FBS, which was left on the cells for 72 h. The supernatant was collected, filtered, and aliquots were stored at -20°C. The freezing medium for the CHO cells contained 85% DMEM/F12, 10% FBS and 5% DMSO.

6.1.2. Standard cell cultures

All reagents were supplied by Sigma-Aldrich. The immortalized Schwann cell line S16 was cultured routinely in DMEM (D6546) supplemented with 10% FBS and 15µg/ml gentamycin on standard tissue culture plates and split every second or third day 1:5 to 1:8. The viral packaging cell line Phoenix_{Eco} and the fibroblast cell line NIH 3T3 were cultured in DMEM (D5796) supplemented with 10% FBS and 1x Penicillin/Streptomycin on standard tissue culture plates and split every second or third day 1:8 or 1:10.

6.2. Immunohistochemistry

6.2.1. Immunohistochemistry on cell cultures

Cells were washed with cold PBS, fixed with 4% PFA in PBS for 15 min and washed three times 15 min in PBS. Unspecific binding sites were impeded by incubation with blocking buffer containing 1% normal donkey serum (Chemicon Int.), 2% cold fish skin gelatin (Sigma-Aldrich), 0.15% Triton X-100 (Sigma-Aldrich) in PBS for 1 h at RT. Primary antibodies were incubated in blocking buffer at 4°C overnight (o.n.). The next day, cells were washed three times with PBS for 15 min and incubated with fluorochrome-coupled secondary antibodies and DAPI for 1 h at RT. Then, they were washed three times with PBS for 15 min, once with H₂O and embedded with Fluorsave (Calbiochem).

For O4 (sulfatide) and O1 (galactosylceramide) epitopes, undiluted primary antibodies were applied to unfixed cells for 30 min at RT. Thereafter, cells were washed with PBS and processed as described above for fixation and further staining.

6.2.2. Immunohistochemistry on fresh frozen mouse tissue

Cryostat sections of fresh frozen P7 mouse torso (10µm) were mounted on gelatin chrome alum - coated slides and fixed for 15min in 4% PFA in PBS. The following experimental steps were performed as described above.

6.2.3. Antibodies

The following primary antibodies were used for immunofluorescent stainings:

anti-β-actin (mouse, 1:200, Sigma-Aldrich), anti-GFAP (rabbit, 1:500, Dako), anti-Krox20 (rabbit, 1:300, Covance), anti-MBP (rat, 1:800, Chemicon), anti-neurofilament (mouse, 1:800, clone N52, Sigma-Aldrich), Hybridoma cells O1 (mouse, pure, provided by M. Schwab, Zürich, Switzerland), Hybridoma cells O4 (mouse, pure, provided by M. Schwab, Zürich, Switzerland), anti-Olig1 (rabbit, 1:2'000, Abcam), anti-P0 (mouse, 1:300, kindly provided by J. Archelos, Graz, Austria), anti-p75^{NTR} (rabbit, 1:500, Promega), anti-S100 (rabbit, 1:500, Dako), anti-tubulin (mouse, 1:800, Sigma-Aldrich).

The following secondary antibodies were used for immunofluorescent stainings:

donkey-anti-rabbit AlexaFluor488 (1:500, Jackson ImmunoResearch Laboratories), donkey-anti-rabbit DyLight549 (1:500, Jackson ImmunoResearch Laboratories), donkey-anti-mouse

AlexaFluor488 (1:500, Jackson ImmunoResearch Laboratories), donkey-anti-mouse DyLight549 (1:500, Jackson ImmunoResearch Laboratories), donkey-anti-rat AlexaFluor647 (1:500, Jackson ImmunoResearch Laboratories), DAPI (1.25 µg/ml; Molecular Probes) was used as cellular counter stain.

6.3.Expression analysis

6.3.1. RNA isolation of Schwann cells

Total RNA of Schwann cells was isolated using RNeasy Micro Kit (Qiagen) according to the manufacturer's protocol. Briefly, cells were washed with cold PBS and scraped off with 350µl RLT (containing guanidine salt; RNeasy Micro Kit) supplemented with β-mercaptoethanol. Cell suspension was frozen on dry ice, thawed and vigorously vortexed. One volume of 70% ethanol was added and total RNA was bound onto RNeasy Micro Spin Columns (Qiagen). The columns were washed twice with the high salt buffer RW1, once with buffer RPE and twice with 80% ethanol to remove remaining salt. Ethanol traces were removed by a centrifugation of 5 min in a new collection tube. The RNA was eluted with 14µl H₂O and stored at -80°C.

6.3.2. RNA isolation of sciatic nerves

Total RNA from sciatic nerves was isolated using the RNeasy Micro Kit (Qiagen) according to manufacturer's protocol. Sciatic nerves from two mice at P0 were pooled to one experimental sample, whereas sciatic nerves of a single animal older than P0 were used for RNA extraction. Sciatic nerves were homogenized with a polytron in 1ml Qiazol lysis reagent (Qiagen). After an incubation of 5 min at RT, 200µl chloroform was added and tubes were shaken vigorously for 15 s and incubated for 3 min. Then, the samples were centrifuged at 12'000xg for 15 min at 4°C, the aqueous phase was mixed with equal volume of 70% ethanol and loaded on RNeasy Micro Spin Columns (Qiagen). Samples were further processed as described above.

6.3.3. Reverse transcription reaction

Depending on purity of the samples, RNA was either precipitated by ethanol or used directly. First strand cDNA synthesis was performed with 80-500ng total RNA using Transcriptor Reverse Transcriptase (Roche). Respective amount of RNA was diluted to 12.5µl in H₂O and incubated with 50ng random hexamer primers (Roche) at 65°C for 5 min to break secondary RNA structures. Then, samples were placed on ice and 4µl 5x

transcription RT buffer, 2µl dNTP mix (10mM, Sigma-Aldrich) and 0.5µl Transcriptor reverse transcriptase enzyme (Roche) were added. Samples were incubated at 55°C for 30 min, followed by inactivation of the enzyme at 85°C for 5 min.

6.3.4. Quantitative RT-PCR analysis

6.3.4.1. Quantitative RT-PCR analysis

Quantitative RT-PCR was performed on the 7500 Fast Real-time PCR System (Applied Biosystems). Briefly, 4.6µl 2x Fast SYBR Master Mix (Applied Biosystems) were mixed with 3.6µl 560nM primer mix and applied onto a 96-well plate, and 1µl of the respective sample was added to the wells. The plate was sealed and centrifuged briefly to 1'000xg. The PCR program implemented 40 cycles with an annealing temperature of 60°C. The acquired mRNA copy numbers were normalized to the one of the 60S ribosomal protein subunit L13a.

6.3.4.2. Primer pairs for quantitative RT-PCR

Primer pairs for quantitative PCR were designed with Clone Manager software (Science and Educational Software) and NCBI PrimerBLAST. Suitable pairs were chosen to overlap exon/intron junctions to prevent amplification of genomic DNA (Table 1).

Primers used for qRT-PCR

Gene	Sequence	Gene	Sequence
m60s	5': GGA AGT ACC AGG CAG TGA CAG 3': GCA GGC ATG AGG CAA ACA G	mEgr3	5': CTC GGT AGC CCA TTA CAA TCA G 3': ATC GCC GCA GTT GGA ATA AG
mP0	5': CCT CTC AGG TCA CGC TCT ATG 3': GCC CGC TAA CCG CTA TTT C	mMAG	5': GTT TGC CCC CAT AAT CCT TCT G 3': TCC CTC TCC GTC TCA TTC ACA GTC
mp75 ^{NTR}	5': AGC GTG AGG AGG TCG AGA AG 3': CAT CAG CGG TCG GAA TGT GG		
mSox10	5': CAA GCT CTG GAG GTT GCT GA 3': CTG CCT TCC CGT TCT TCC G	r60s	5': GCC ATT GTG GCC AAG CAG GT 3': GTA GGC TTC AGC CGC ACA AC
mOct6	5': AGC CGC TGC TCA ACA AGT G 3': CTT CTC CAG TTG CAG GCT GTC	rP0	5': CCT CTC AGG TCA CGC TCT ATG 3': GCC CGC TAA CCG CTA TTT C
mKrox20	5': TCT ACC CGG TGG AAG ACC TC 3': CAG GGT ACT GTG GGT CAA TGG	rp75 ^{NTR}	5': CAC CGA CAA CCT CT TCC 3': AGT CTG CGT ATG GGT CTG
mcJun	5': TCT ACG ACG ATG CCC TCA ACG 3': GTG ATG TGC CCA TTG CTG GAC	rKrox20	5': TGA CCG CCA AGG CCG TAG ACA 3': ATG CCA TCT CCA GCC ACT CCG TT
mKrox24	5': CCG AGC GAA CAA CCC TAT G 3': AGC CGA GTA GAT GGG ACT G	rMAL	5': CAT CGC TGC AGT GGT GTT CGC 3': GAG CTC GAG CTA TGA AGA CTT CCA TCT GAT

Table 1: List of primer pairs. The itemized primers were utilized for qRT-PCR. m: mouse; r: rat

6.3.5. Whole genome expression profiling

Primary Schwann cell cultures derived from MAL-overexpressing mice and wildtype littermates were cultured and stimulated with 20 μ M forskolin for 24 h as described. A total of 36 cultures were investigated, complied by nine cultures per condition, derived from five independent experiments. For the *in vivo* analysis, sciatic nerves of MAL-overexpressing mice and wildtype littermates were dissected at the age of P0, P4, P7, P10 and P60. Microarray expression analysis was performed with 28 nerves from 14 mice pooled to seven experimental samples (n = 7) per genotype at P0 and P10, 20 nerves from 10 mice pooled to five experimental samples (n = 5) per genotype at P4 and P7, and six nerves from three mice (n = 3) per genotype at P60. Total RNA was isolated using RNeasy Micro Kit (Qiagen) according to the manufacturer's protocol. The following experimental procedures methods were kindly performed by Thomas Zeis. The RNA integrity number (RIN) of all samples was above 8, verified with the Agilent Bioanalyzer system. RNA was amplified and biotinylated using the Illumina TotalPrep RNA Amplification Kit (Applied Biosystems) according to the manufacturer's instructions. In vitro transcription was performed for 14 h o.n. and cRNA was hybridized to MouseWG-6 v2.0 Expression BeadChips from Illumina. Arrays were scanned using the iScan Reader (Illumina) and global median normalization of gene expression was performed with the GenomeStudio software (version 2011.1, Illumina). All data passed the quality control analysis was assessed by the Illumina on-board software (GenomeStudio, version 2011.1) and principal component analysis (Partek genomics Suite, version 6.6, Partek Inc.). Significantly differentially expressed genes were further analyzed with the Ingenuity Pathway Analysis (IPA) software (Ingenuity Systems) and the Database for Annotation, Visualization and Integrated Discovery (DAVID) (Huang da et al., 2009). Microarray data analysis was performed using Partek Genomic Suite software. Differentially expressed transcript of genes were identified by performing a three-way ANOVA (Genotype, Treatment, Array) and multiple testing corrections were done using the false discovery rate (FDR) method with a threshold p-value of 0.05 (Benjamini and Hochberg, 1995).

6.4. Generation of mCherry tagged MAL and PMP22 constructs

Retroviral constructs were generated for efficient delivery of genes into the genome of dividing cells. The pMX vector is based on the Moloney murine leukemia virus (MMLV) and provides the viral packaging signal, transcription and processing elements (Onishi et al., 1996).

6.4.1. Eliminating STOP sequence of the pMX-mCherry_{STOP} vector

For cloning of the pMX-mCherryMAL vector, the existing stop codon had to be eliminated from the pMX-mCherry backbone. The sequence of mCherry (without stop codon) was amplified by PCR from 10ng pMX-mCherry_{STOP} plasmid, using primers extended with the recognition sequences of the restriction endonucleases HindIII and NotI (Table 2). The purified PCR product was digested with HindIII and NotI at 37°C o.n. Subsequently, the linearized fragment was purified according to manufacturer's protocol (Qiaquick PCR purification kit, Qiagen) and ligated into digested pMX-mCherry_{STOP} using T4 DNA ligase (Roche) at 16°C for 4 h. Then, the construct was transfected into DH5 α chemically competent E.Coli according to routinely used protocols and plated on LB agar plates supplemented with ampicillin. The next day, successful insertion of the fragment was evaluated by PCR on colonies. Single positive clones were inoculated in LB medium supplemented with ampicillin, incubated at 37°C o.n., and the plasmid was isolated the following day using a Mini Prep Kit (Sigma) according to manufacturer's protocol. The DNA sequence was verified by sequencing (Microsynth), and pMX-mCherry_{clone 12} was chosen for further subcloning (Figure 11B).

6.4.2. Cloning MAL into the pMX-mCherry vector

Primers to amplify the MAL sequence from the β -actin-GFPMAL₂₋₁₈ plasmid were extended with the recognition sequences of the restriction endonucleases NotI and XhoI for cloning into the pMXmCherry backbone (Table 2). Following cloning steps were analogue to the one described above. Briefly, MAL was ligated into pMX-mCherry_{clone 12} and transformed into DH5 α cells. The resulting vector pMX-mCherryMAL_{clone10} was used for production of retroviral supernatant (Figure 11C)

6.4.3. Cloning PMP22 into the pMX-mCherry vector

The DNA sequence of PMP22 was amplified from cDNA derived from sciatic nerves of P14 C57/Bl6 mice with primers extended with the recognition sequences of the restriction endonucleases NotI and XhoI (Table 2). Following cloning steps were analogue to the one described above. Briefly, PMP22 was ligated into pMX-mCherry_{clone12} and transformed into DH5 α cells. The resulting vector pMX-mCherryPMP22_{clone2} was used for production of retroviral supernatant (Figure 11D).

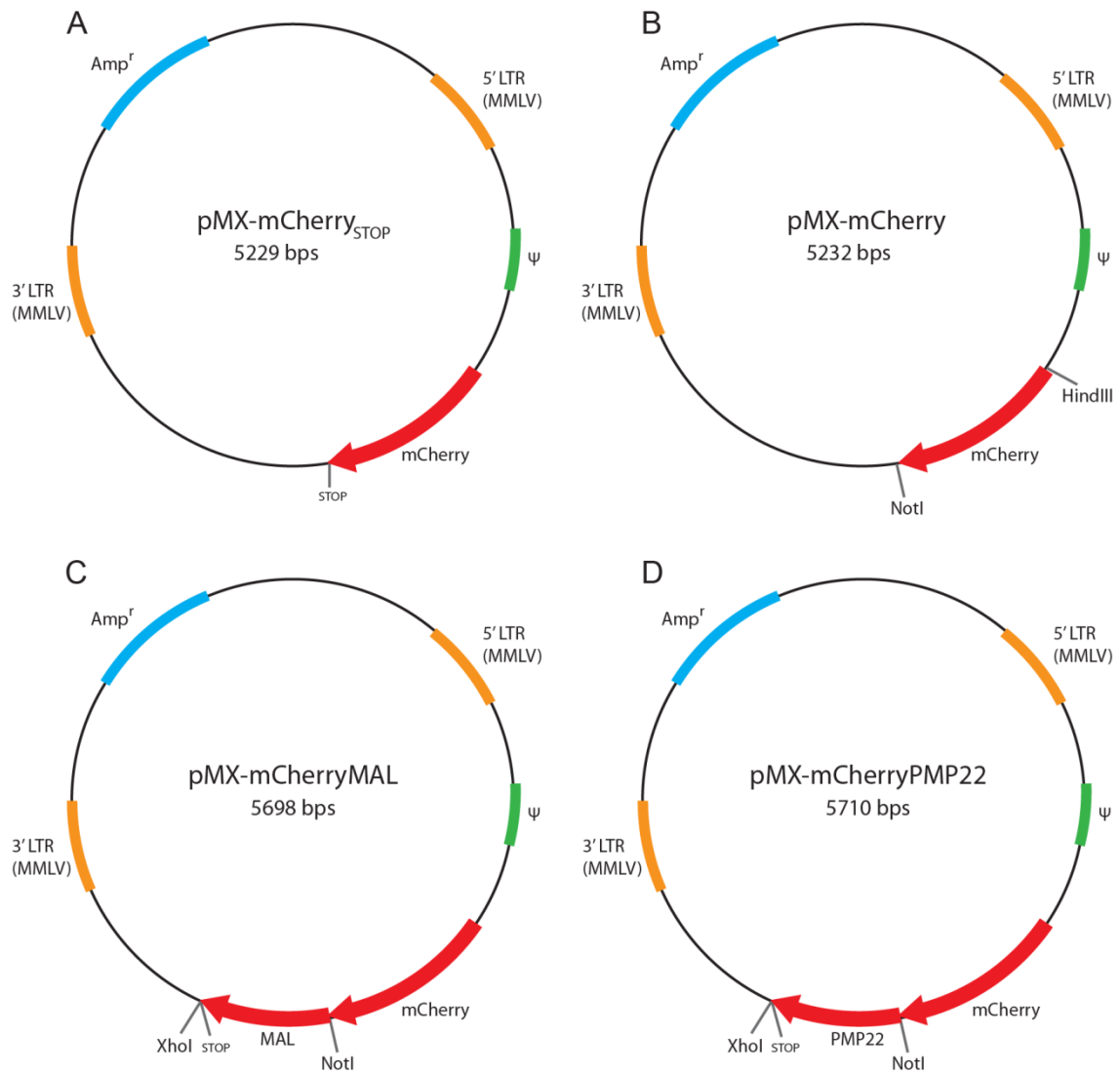


Figure 11: Cloned constructs for retroviral infections using the MMLV-based backbone pMX. The initial construct pMX-mCherry_{STOP} (A) was used as an infection control. After elimination of the stop codon (B), constructs to overexpress either MAL (C) or PMP22 (D) were generated.

6.4.4. Primer pairs for cloning the retroviral constructs

The following primer pairs were used to clone the expression constructs for retroviral infections:

Primer name	Restriction enzyme	Sequence
5' HindIII-mCherryMX:	5'- GAG AAGCTT	ATG GTG AGC AAG GGC GAG -3'
3'mCherryMX-NotI:	5'- GAG GCGGCCGC	CTT GTA CAG CTC GTC CAT G -3'
5' NotI-mCherryMAL:	5'- GAG GCGGCCGC G	ATG GCC CCA GCA GCA GC -3'
3'mCherryMAL-XhoI:	5'- GAG CTCGAG CTA	TGA AGA CTT CCA TCT GAT -3'
5' NotI-PMP22:	5'- GAG GCGGCCGC G	ATG CTT CTA CTC TTG TTG G -3'
3'PMP22-XhoI:	5'- GAG CTCGAG TCA	TTC GCG TTT CCG CAG G -3'

HindIII NotI XhoI STOP

Table 2: List of primer pairs used for cloning the retroviral constructs.

6.4.5. Production of retroviral stocks in Phoenix_{Eco} packaging cell line

Retroviral stocks were produced in the helper virus-free Phoenix_{Eco} packaging cell line (according to G. Nolan, Stanford, USA) with a calcium phosphate coprecipitation transfection. 4.5×10^6 cells were seeded onto a 10cm plate the afternoon prior transfection. Next morning, 9ml fresh medium was applied to the cells, followed by an incubation of 3 h at 37°C. For transfection, all reagents were prewarmed to RT. 25µg DNA was diluted to 438µl with H₂O, and 62µl 2M CaCl₂ was added. While vortexing, the DNA/CaCl₂ mix was added dropwise to 500µl 2x HBS pH 7.00. For accurate Ca-phosphate precipitation formation, the mixture was incubated for 15 min at RT. Meanwhile, 6µl 50mM chloroquine (Sigma-Aldrich) was applied to the cells on a 10cm culture plate to neutralize the lysosomal pH. The transfection mix was gently added dropwise onto the cells and the plates were incubated for 6 h at 37°C. Then, the cells were washed, and 10ml fresh medium was applied. After 48 h, supernatant was collected, centrifuged for 5 min at 1'700rpm at 4°C to collect cellular debris and was either directly used for viral infection or aliquots were snap frozen in N₂ and stored at -80°C.

6.4.6. Retroviral infection

A day prior infection, a distinct number of Schwann cells was seeded on either 6 well plates (Primaria™, BD Bioscience) or on PDL/laminin coated glass coverslips (12mm diameter). For retroviral infection, 8µg polybrene, a detergent to neutralize the charge repulsion on the cell surface, was added to 1ml undiluted viral stock and incubated on the cells for 6 h at 37°C. Then, cells were gently washed, and SCPM was added. The next morning, retroviral infection was repeated to increase infection efficiency. After 72 h, either protein or mRNA expression of the cells was analyzed. Applying this method, an infection efficiency of around 50% was achieved for rat Schwann cell cultures.

Cells	Experiment	Density	Plate / coating
Rat Schwann cells	RNA isolation	100'000cell/10ml	6well plate / Primaria™
Rat Schwann cells	Stainings	1'300cells/80µl	Glass coverslip / PDL+laminin

6.5. In Situ Hybridization

6.5.1. Cloning of the riboprobes

Primer pairs were designed with Clone Manager software (Science and Educational Software) and NCBI PrimerBLAST. The specificity of both, the primers, and the resulting cDNA sequences was investigated with NCBI BLAST to avoid unspecific binding of the probe.

Primers used to generate riboprobes

Ankrd1	5mAnkrd1-ISH-1235	: GCA CCA GTA TTC AGG CTT TC	3mAnkrd1-ISH-1705	: ACA TTT ACA GCG CGT GTC
Aqp1	5mAqp1-811-ISH	: TCA AAC CAC TGG ATT TTC TGG GT	3mAqp1-2408-ISH	: TAG GGA ACG GAG ACG AGT GT
Asgr1	5mNotI-mAsgr1-410-ISH	: TCT AGC GCG GCC GCA GCA CCC AGG GAA GTA GTG T	3Xhol-mAsgr1-1162-ISH	: TCT AGC CTC GAG ACC ACC AGG CAT CAT AC
Atf3	5mAtf3-ISH-1024	: TTA TCA TCC CGG CCA GTC	3mAtf3-ISH-1679	: GCT GTG GCT GTG GTT ATC
Col2A1	5mCol2A1-ISH-4700	: CCC GAA CCC TGA AAC AAC AC	3mCol2A1-ISH-4970	: GCG TCT GAC TCA CAC CAG ATA G
Dag1	5mDag1-ISH-1442	: TGC CTA CGC CTA CAT CTC C	3mDag1-ISH-2553	: GCC CGT CAC AGC AAT ACT C
Diras1	5HindIII-mDiras-ISH	: GAT TCA AAG CTT CCC ACC CCC ATT CTA TCT GC	3Xhol-mDiras-ISH	: TCT AGC CTC GAG CCG GCC TAC TTG GTC ATC TG
Dtna_1	5mNotI-mDtna_1-1333-ISH	: TCT AGC GCG GCC GCC ACA TCG TGC CTC CGA GAC C	3Xhol-mDtna_1-1681-ISH	: TCT AGC CTC GAG GTG CAC ACA GCT TTA TTG AGC A
Dtna_2	5mDtna_3-13-ISH	: GAC ACA GTG GAC GCC AGA	3mDtna_3-414-ISH	: TTG AGC CCT CAT CTC TGC AA
Entpd2	5HindIII-mEntpd2-ISH	: GAT TCA AAG CTT GTG ACT GCC AAC TAC CTG CT	3Xhol-mEntpd2-ISH	: TCT AGC CTC GAG GGG CTG CCC ATG TAG ACT TT
Gria1	5Xbal-mGria1-ISH	: GTT ACA TCT AGA AGA ATG GCA GAG TGG TCA GC	3mGria1-ISH	: TCT AGC CTC GAG CCA GGC CGT AGA CAA AAG GT
Hfe	5mHfe-ISH-177	: TGC CAC CGC GTT CAC ATT C	3mHfe-ISH-877	: GGC ATC CAG TGG TTG GTT GTC
Igfbp1	5mNotI-mIgfbp1-1066-ISH	: TCT AGC GCG GCC GCG ACA AAA GCA GCG ACC AAG G	33Xhol-mIgfbp1-1290-ISH	: TCT AGC CTC GAG ATT ATA TCT GGG TTT CCC TGC ATC C
Krt23_1	5mKrt23-1204-ISH	: TGA GTC AAG GCT GAA AGG ATC T	3mKrt22-1507-ISH	: ACT TCT TCT TTC ACT CAA AAA TTC C
Krt23_2	5mKrt23-3-ISH	: CGT CAG AGA GCT GAG ATA GC	3mKrt22-237-ISH	: CTT CTT CCA GAC CCC CAT GAT
Ldb2	5mLdb2-1492-ISH	: GAT TAC GCT GTC CAT AGG	3mLdb2-2537-ISH	: GAG CCA CTG TGT CTT TAC
Lmcd1	5mLmcd1-ISH-1130	: CTA CCA GCG TGT GGA AGA CC	3mLmcd1-ISH-1498	: CCT GGC AGG ATA CCA GTG TG
MAL	5mMAL-804-ISH	: AGA CTT CCT GGA TCA CAC TGG ATG	3mMAL-2452-ISH	: GGC TGT GTT AAG TGG GCA A
Moxd1_1	5mMoxd1_1-1750-ISH	: AAC GCA GAG TGG TCG ATT CA	3mMoxd1_1-2530-ISH	: CGG CTG GAC AGT GCT AGA AA
Moxd1_2	5mMoxd1_1-1082-ISH	: GGA GAT ATG ACG CAG GGG TG	3mMoxd1_1-1468-ISH	: TGG TGC TTA GTC CTC CCC AA
Olig1	5mOlig1-ISH-1339	: GCT CCC CAA CAG TGT CTA CC	3mOlig1-ISH-2082	: TCG GCT ACT GTC AAC AAC CC
Osbp13	5mOsbp13-ISH-7390	: TTC CTC CAC ACG GCT TTG	3mOsbp13-ISH-5165	: ACG GGC AGT GAC TTA CAG
P0	5mP0-742-ISH	: AAG GCT CAG TGC CAT GGA GA	3mP0-1733-ISH	: GTA GTG GTC AGA GGG CAT CG
p75	5mp75	: CGT GTC ATA AGC CTG AAG	3mp75	: GAG GTC TGG ATC TCA TAG TC
Pkfb4	5mPkfb4-1449-ISH	: CCG AGA CAG ACC TCA GAA TGT AG	3mPkfb4-2175-ISH	: ACA GGA TCC CCC GAA AGA GA
RhoU	5Xbal-mRhoU-278-ISH	: GTT ACA TCT AGA CAA CTT CTC GGC CGT GGT	3BamHI-mRhoU-2004-ISH	: TCT AGC GGA TCC AGG CCT TGC ACA TAC CTG TC
S100a4	5mS100a4_1-31-ISH	: TGG TCT GGT CTC AAC GGT TAC	3mS100a4_1-456-ISH	: ACA TGT GCG AAG AAG CCA GA
Sv2b	5mNotI-mSv2b-51-ISH	: TCT AGC GCG GCC GCC CCT CCA ACC TAT CCG GAA C	3Xhol-mSv2b-2487-ISH	: TCT AGC CTC GAG GGA GCC GCC AAT CAT CTT GA
Tnik	5Xbal-mTnik-2829-ISH	: GTT ACA TCT AGA AGA TGA GGA TCT GAC GGC AT	3HindIII-mTnik-4278-ISH	: GAT TCA AAG CTT GGG CAT TTC TCC CCA TTG GA
Vat11	5HindIII-mVat11-ISH	: GAT TCA AAG CTT GGG GAC AGC GAG AAC AAA GA	3Xhol-mVat11-ISH	: TCT AGC CTC GAG TGA AGG CGA ACC TTC CTG AC
Wnt16	5mWnt16_1-18-ISH	: ACC TTG GAA AGT GAG GGA AGC	3mWnt16_1-387-ISH	: ATG CCC AAC CAC ATC CAG TT

Table 3: Primers used to generate riboprobes.

Using standard molecular techniques, the fragment was cloned into the pCRII-TOPO vector (Invitrogen), transformed into chemically competent DH5 α E.Coli, and the direction of the insert was verified by sequencing (Microsynth). From a 150ml bacteria culture, the plasmid was isolated, and remaining RNase was removed using a phenol-chloroform extraction (1:1). Subsequently, an ethanol precipitation was performed and the cDNA was resuspended in a concentration of 1 μ g/ μ l. 10 μ g of the plasmid was linearized with itemized restriction enzymes at 37°C o.n. (Table 4).
































Gene	Size (bp)	Hydrolyzed	α -Sense	Sense	
Ankrd1	471		T7 / HindIII	Sp6 / XhoI	Sp6 HindIII  XhoI T7
Aqp1	1597	20'	T7 / HindIII	Sp6 / XhoI	Sp6 HindIII  XhoI T7
Asgr1	752		Sp6 / NotI	T7 / BamHI	T7 NotI  BamHI Sp6
Atf3	656		T7 / HindIII	Sp6 / XhoI	Sp6 HindIII  XhoI T7
Col2A1	271		T7 / HindIII	Sp6 / XhoI	Sp6 HindIII  XhoI T7
Dag1	1112	20'	Sp6 / XhoI	T7 / SpeI	T7 XhoI  SpeI Sp6
Diras1	1475	20'	T3 / HindIII	T7 / XhoI	T7 HindIII  XhoI T3
Dtna_1	348		T7 / HindIII	Sp6 / XhoI	Sp6 HindIII  XhoI T7
Dtna_2	401		Sp6 / XhoI	T7 / HindIII	T7 XhoI  HindIII Sp6
Entpd2	1096	20'	T3 / HindIII	T7 / XhoI	T7 HindIII  XhoI T3
Gria1	2208	30'	T7 / SpeI	Sp6 / XhoI	Sp6 SpeI  XhoI T7
Hfe	701		Sp6 / XhoI	T7 / HindIII	T7 XhoI  HindIII Sp6
Igsf10	1224	10'	Sp6 / NotI	T7 / BamHI	T7 NotI  BamHI Sp6
Krt23_1	303		Sp6 / XhoI	T7 / BamHI	T7 XhoI  BamHI Sp6
Krt23_2	234		Sp6 / XhoI	T7 / HindIII	T7 XhoI  HindIII Sp6
Ldb2	1045	10'	Sp6 / XhoI	T7 / BamHI	T7 XhoI  BamHI Sp6
Lmcd1	369		T7 / SpeI	Sp6 / XhoI	Sp6 HindIII  XhoI T7
MAL	1649	20'	T7 / HindIII	Sp6 / XhoI	Sp6 HindIII  XhoI T7
Moxd1_1	401		T7 / HindIII	Sp6 / XbaI	Sp6 HindIII  XbaI T7
Moxd1_2	386		T7 / HindIII	Sp6 / XhoI	Sp6 HindIII  XhoI T7
Olig1	744		Sp6 / XhoI	T7 / HindIII	T7 XhoI  HindIII Sp6
Osbp13	1176	20'	T7 / SpeI	Sp6 / XbaI	Sp6 SpeI  XbaI T7
P0	991	10'	T7 / SpeI	Sp6 / XhoI	Sp6 HindIII  XhoI T7
p75	1107	60'	Sp6 / XhoI	T7 / BamHI	T7 XhoI  BamHI Sp6
Pfkfb4	727		Sp6 / XbaI	T7 / HindIII	T7 XbaI  HindIII Sp6
RhoU	1726	20'	T7 / SpeI	Sp6 / NotI	Sp6 SpeI  NotI T7
S100a4	425		Sp6 / XhoI	T7 / HindIII	T7 XhoI  HindIII Sp6
Sv2b	2436	30'	Sp6 / NotI	T7 / BamHI	T7 NotI  BamHI Sp6
Tnik	725		Sp6 / XbaI	T7 / HindIII	T7 XbaI  HindIII Sp6
Vat1l	1896	20'	Sp6 / NotI	T7 / BamHI	T7 NotI  BamHI Sp6
Wnt16	369		Sp6 / XhoI	T7 / HindIII	T7 XhoI  HindIII Sp6

Table 4: List of cloned riboprobes for in situ hybridization. The itemized constructs were generated and linearized with the respective restriction enzymes.

6.5.2. DIG RNA labeling by in vitro transcription

In vitro transcription was performed on 2µg of purified cDNA with the RNA polymerases T3, T7 or SP6 (Roche) for 2 h at 37°C, using the 10x DIG RNA labeling mix according to the manufacturer's protocol (Roche). After transcription, DNA was removed by a DNase treatment for 15 min at 37°C. The amount of DIG labeled RNA was estimated on an agarose gel with a known standard of total RNA sample as comparison. Thereafter, cRNA was transferred onto a positively charged nylon membrane (Nytran N+ supercharged, 0.45µm; Schleicher&Schüll) by capillary transfer o.n. After crosslinking the RNA to the membrane with the Stratalinker₁₈₀₀ for 30 s, successful transfer was verified under UV light. Then, the membrane was rinsed in buffer B1 and was blocked in B2 for 30 min, followed by incubation of anti-DIG-AP antibody (1:5'000 in B1, Roche) for 1 h. The membrane was first washed in B1, then in B3 and immunological signal detection of the incorporated DIG was visualized by a color reaction in buffer B4. After around 5 min, when desired intensity was reached, the reaction was stopped in buffer B5.

For riboprobes longer than 1kb, an alkaline hydrolysis was performed with 30µl cRNA sample. 75µl of Mix A (pH 11; 5µl 1M DTT, 40µl 1M NaHCO₃, 60µl 1M Na₂CO₃, 395µl H₂O) were added and the reaction was incubated at 60°C for itemized time (Table 4). Alkaline hydrolysis was stopped by chilling the samples on ice and neutralized with 75µl Mix B (5µl 1M DTT, 5µl acetic acid, 100µl 1M NaOAc, 390µl H₂O). cRNA was precipitated in 2.5 volume 100% ethanol, 1/10 volume 4M LiCl and 1µl glycogen (Roche) and resuspended in 30µl H₂O ("stock probe"). For in situ hybridization, a "working probe" of approximately 10ng/µl was prepared in H₂O.

6.5.3. In situ hybridization

In situ hybridizations were performed as described previously (Schaeren-Wiemers and Gerfin-Moser, 1993). 16µm sections of fresh frozen tissue were mounted on SuperFrost Plus slides (Thermo Scientific), dried for 30 min at RT and fixed in freshly prepared 4% paraformaldehyde in PBS for 10 min. Then, slides were acetylated in 250ml H₂O with 3ml triethanolamine and 700µl acetic anhydride for 10 min and washed with PBS for another 3 x 15 min. The slides were subsequently incubated with 400µl pre-hybridizationbuffer in a humid chamber o.n. at RT. The next day, the DIG-labeled riboprobes were diluted in the pre-hybridization buffer and 100µl were applied per slide. A hybridization coverslip (Sigma-Aldrich) was placed onto the slide and sealed with rubber cement fixogum (Marabu). The metal boxes were sealed with tape and incubated at 72°C o.n. The next day, slides were transferred into prewarmed 5x SSC at 65°C and the coverslips were peeled off with forceps. After washing the slides in 0.2x SSC for 1h at 65°C, they were transferred to 0.2x at RT and

washed with buffer B1 for 5 min. Thereafter, B2 blocking buffer was applied to the tissue sections for 1 h at RT. Then, slides were incubated with the anti-DIG-AP antibody (1:5000 in B2, Roche) for 1 h, followed by 3 x 15 min washing steps in B1 and 5 min equilibration in B3. The color reaction was performed with B4 until desired intensity was reached. and was consecutively stopped in B5. For nuclear counterstaining, DAPI was incubated 1:25'000 in PBS for 5 min.

Riboprobe	Concentration (in prehybridization solution)
MAL	60 to 200 ng/ml
p75 ^{NTR}	60 to 200 ng/ml
P0	8 to 60 ng/ml

6.5.4. Buffer composition for in situ hybridization

B1:	0.1M Maleic acid (pH 7.5), 0.15M NaCl in H ₂ O; pH adjusted to 7.5 with NaOH
B2:	1% Blocking Reagent (Roche) in B1
B3:	100mM Tris-HCl, 100mM NaCl, 5mM MgCl ₂ in H ₂ O; pH adjusted to 9.5 with NaOH, filtered
B4:	45µl NBT (1g NBT in 1.3ml 70% Dimethylformamide, Sigma-Aldrich), 35µl BCIP (1g BCIP in 20ml 100% Dimethylformamide, Sigma-Aldrich), 2.4mg levamisole (Sigma-Aldrich) in 10ml B3
B5:	10mM Tris-HCl, 50mM EDTA in H ₂ O; pH adjusted to 8.0
Prehybridization buffer:	5x SSC, 50% Formamide, 5x Denhardt's solution, 0.2mg/ml Yeast RNA (Sigma-Aldrich), 0.1mg/ml Herring sperm DNA (Roche)
20x SSC:	3M NaCl, 0.3M Tris-sodium citrate dehydrate in H ₂ O
50x Denhardt's solution:	1% bovine serum albumin, 1% polyvinylpyrrolidone, 1% Ficoll 400

7. Results

7.1. MAL-dependent gene regulation in Schwann cells

7.1.1. Differential expression analysis on developing sciatic nerves

From our developmental study on PNS myelination, we identified that MAL overexpression led to delayed onset of myelination, reflected in hypomyelinated fibers during early development (Buser et al., 2009b). Besides changes on the morphological level, mRNA expression levels of the low affinity neurotrophin receptor $p75^{\text{NTR}}$ were significantly reduced in newborn MAL-overexpressing mice (Buser et al., 2009b). To further investigate the mRNA expression pattern during development, an expression analysis was performed on sciatic nerves by qRT-PCR. First, the mRNA expression levels of MAL were investigated. As expected, significant increases could be detected at all time points in MAL-overexpressing mice (Figure 12A). In line with protein expression, $p75^{\text{NTR}}$ mRNA expression was reduced in mice overexpressing mice between P0 and P10 (Figure 12B). At P60, significantly increased expression was detected in mice overexpressing MAL, presumably reflecting disturbed Remak bundle formation of nonmyelinating Schwann cells. For the myelin protein zero (P0), mRNA expression levels were reduced at P7 and P10 (Figure 12C).

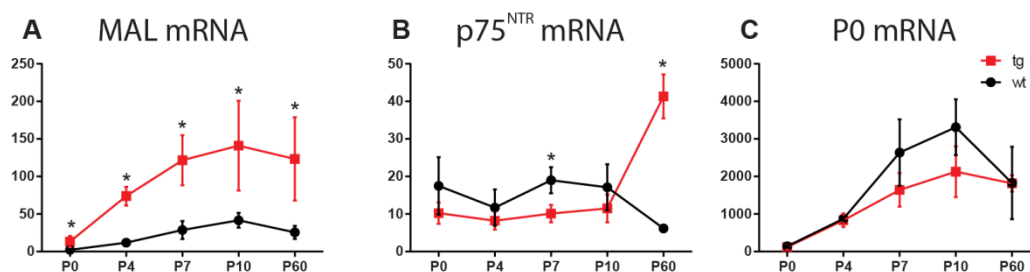


Figure 12: Expression analysis of developing sciatic nerves. mRNA expression levels of MAL (A), $p75^{\text{NTR}}$ (B) and P0 (C) was investigated on sciatic nerves of MAL-overexpressing mice and wildtype littermates by qRT-PCR. Data are normalized to the expression of 60s. Values represent the mean of five (P0, P10), four (P4, P7) and three (P60) independent samples. Error bars indicate the SD. *: p-value < 0.05

Next, we investigated whether the delayed myelination in MAL-overexpressing mice can be validated by in situ hybridization on transversal sections of a whole torso of P1 MAL-overexpressing mice and wildtype littermates (Figure 13). A strong expression of MAL was detected in the dorsal and ventral spinal roots and in peripheral nerves (Figure 13A, B; arrows, arrowheads and pN, respectively). In addition, strong expression was depicted in nonmyelinated Schwann cells of the sympathetic trunk (Figure 13A; ST), and in satellite cells in the dorsal root ganglion (DRG) (Figure 13D; asterisk). In the CNS, oligodendrocytes were only sparsely detected to express MAL (Figure 13D; star). Besides the nervous system, MAL was expressed in the innermost epithelial layer of the esophagus (Figure 13A, C; ES). In

wildtype tissue, only low expression of MAL was depicted at P1 (Figure 14A). Expression of $p75^{\text{NTR}}$ was detected mainly in neurons of the spinal cord and the dorsal root ganglion, whereas low expression levels were detected in the spinal roots and peripheral nerves (Figure 13E; SC, DRG and pN, respectively). Comparison between wildtype and MAL-overexpressing tissue revealed no difference in expression of $p75^{\text{NTR}}$ (Figure 14B). Expression of P0 was exclusively detected in spinal roots and peripheral nerves (Figure 13F). No altered expression of P0 could be identified in peripheral nerves overexpressing MAL compared to wildtype littermates (Figure 14C).

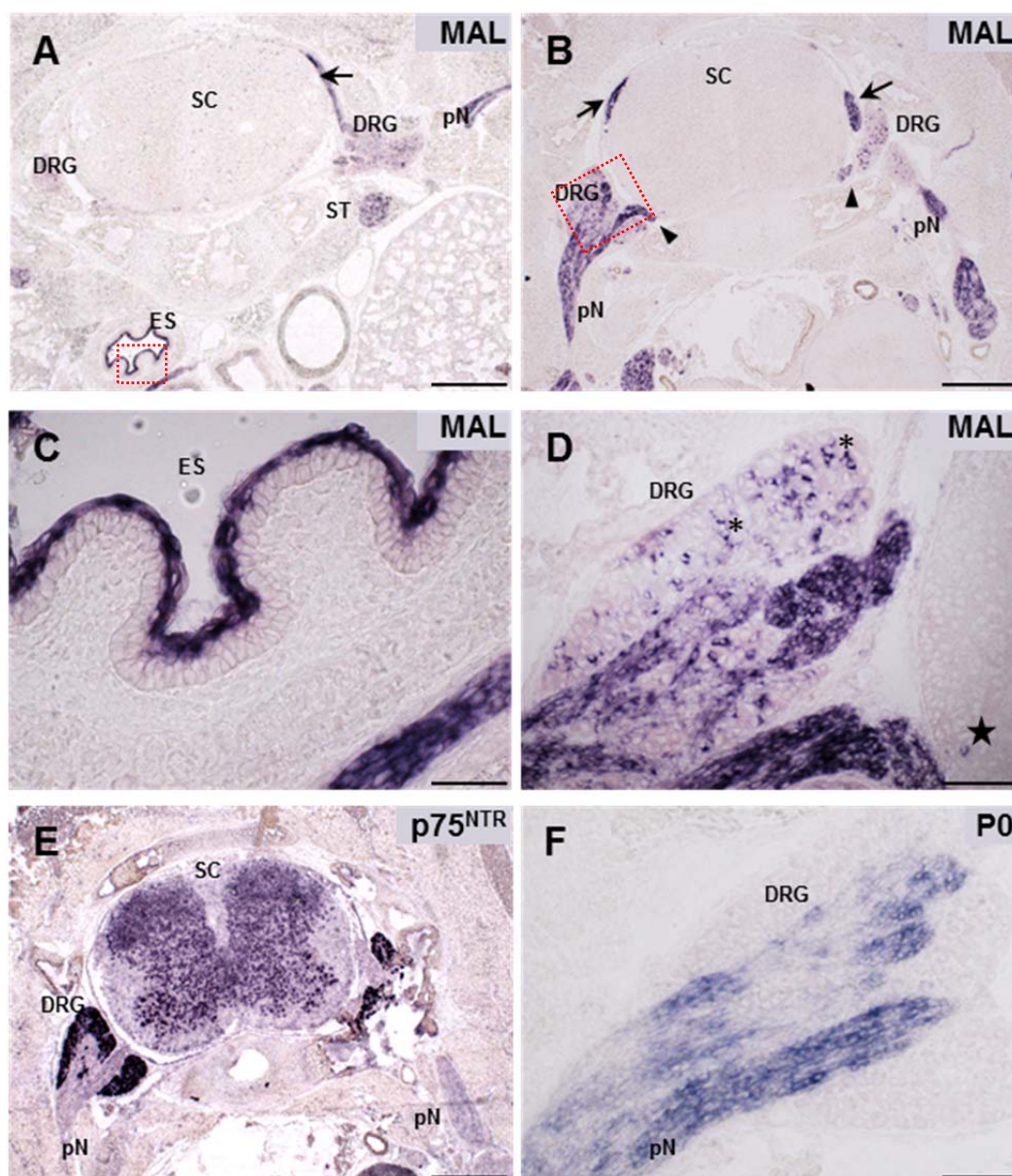


Figure 13: Expression pattern of MAL, $p75^{\text{NTR}}$ and P0 in P1 mice. (A-B) MAL expression could be depicted in the dorsal and ventral roots (arrows and arrowheads), in peripheral nerves (pN) and in the sympathetic trunk (ST). Also epithelial cells of the esophagus (ES) expressed MAL (C), as well as satellite cells (D, asterisk). In the CNS, only few oligodendrocytes expressed MAL at P1 (D, star). The expression of $p75^{\text{NTR}}$ was localized in dorsal root ganglia (DRG) and in neurons of the spinal cord (SC), whereas expression in peripheral nerves (pN) was at the detection limit (E). P0 was exclusively expressed in peripheral nerves (pN) (F). Bar: A, B, E: 500 μm , D, F: 100 μm , C: 50 μm

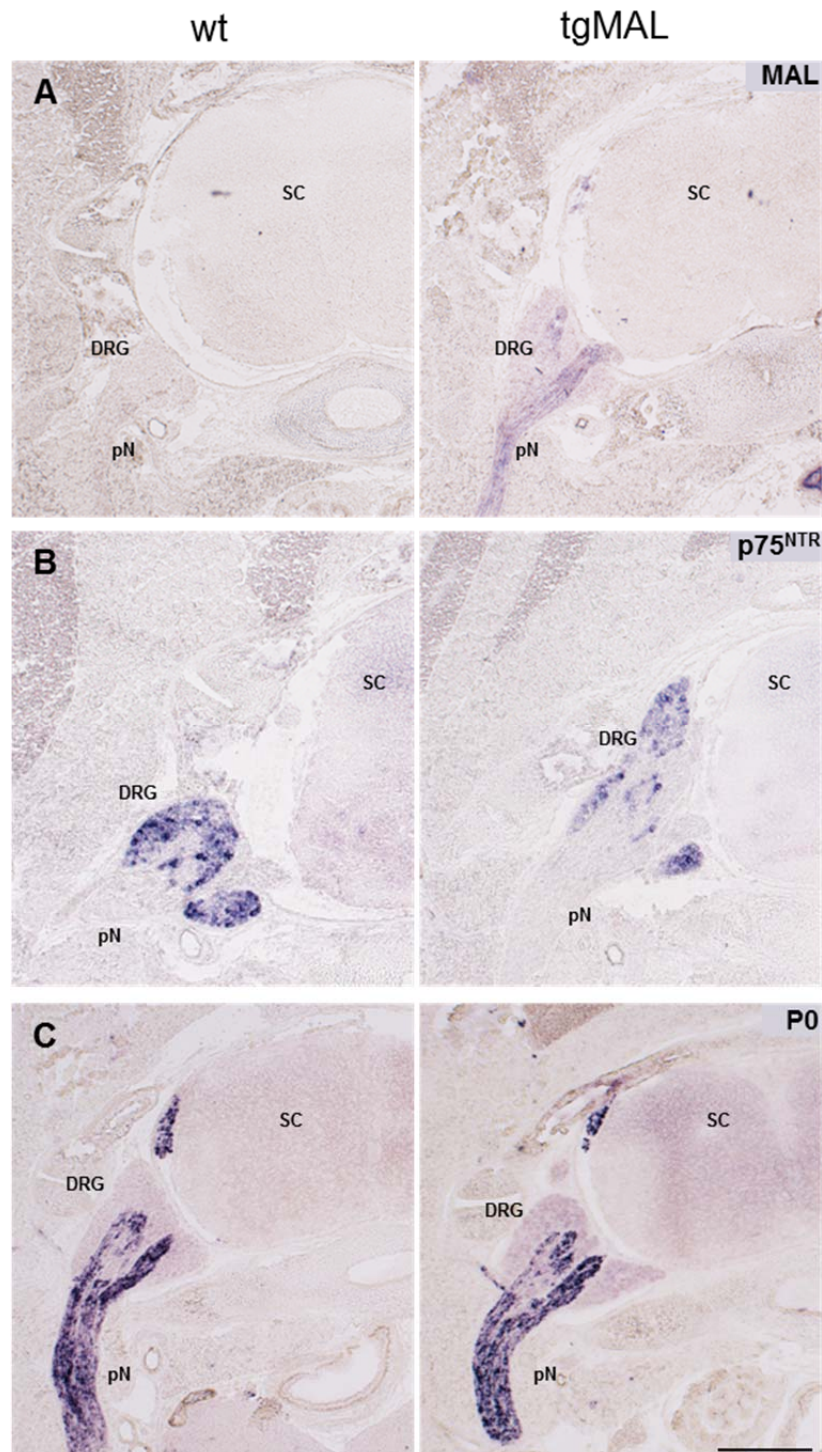


Figure 14: In situ hybridization of MAL, p75^{NTR} and P0 on the torso of MAL-overexpressing and wildtype mice. In MAL-overexpressing mice, a strong expression of MAL was detected in peripheral nerves (A, pN). For p75^{NTR}, no differential expression was detected between the genotypes. P0 was strongly expressed in peripheral nerves (pN), and no difference between wildtype and MAL-overexpressing was detected (C). wt: wildtype, tgMAL: MAL-overexpressing mice. SC: spinal cord, DRG: dorsal root ganglion, pN: peripheral nerve. Bar: 500µm

To summarize, a comparable expression of p75^{NTR} and P0 was detected between MAL-overexpressing mice and wildtype littermates by in situ hybridization.

7.1.2. Establishment of primary mouse Schwann cell cultures

Primary mouse Schwann cell cultures were investigated to study the molecular mechanisms of reduced P0 and p75^{NTR} expression by MAL overexpression. In general, *in vitro* investigations of Schwann cell differentiation and myelination were routinely performed with primary Schwann cells derived from rats. Therefore, protocols were adapted for mice, as mouse and rat Schwann cells react differently upon stimulating reagents (Yamada et al., 1995) (see Material and Methods for detailed protocol). Schwann cells were isolated from sciatic nerves of P1 C57/Bl6 mice. In contrast to rat nerves, the perineurium was not removed from murine nerves. The tissue was enzymatically dissociated with collagenase and trypsin, and the cells were cultured in high glucose DMEM supplemented with 10% FBS. Schwann cells were seeded onto PrimariaTM plates (with surface-modified polystyrene), and hence, no coating of the wells was necessary. Purity of primary mouse Schwann cell cultures was determined by immunofluorescent staining (Figure 15A-C). Schwann cells were identified by the marker S100 and p75^{NTR}, whereas residual fibroblasts could be identified by their size and strong β -actin- and tubulin expression (Figure 15A, C, arrows). Using this culturing method, an enrichment of >85% was achieved.

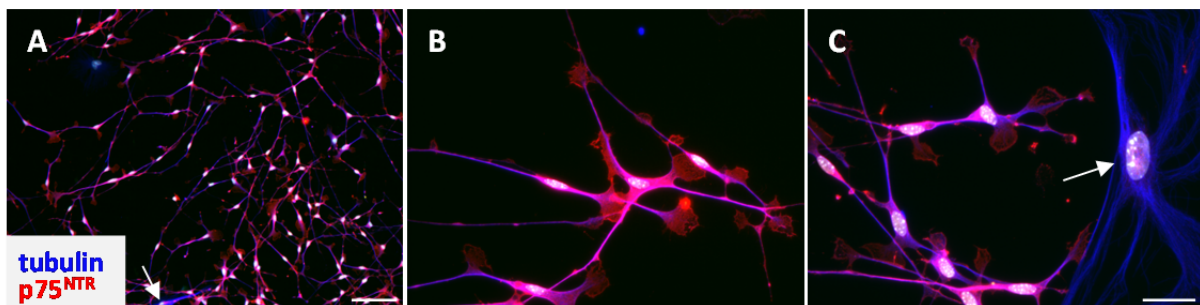


Figure 15: Establishment of primary mouse Schwann cell cultures. Primary mouse Schwann cell cultures were stained for p75^{NTR} and tubulin. All Schwann cells expressed p75^{NTR}, whereas fibroblasts (arrows) were negative for p75^{NTR}. DAPI was used as nuclear counter stain. Bar: A: 100 μ m, B, C: 20 μ m

7.1.3. Investigation of Schwann cell differentiation *in vitro*

We investigated whether Schwann cells overexpressing MAL can differentiate *in vitro* or whether they are less responsive to stimuli for Schwann cell differentiation, consequently leading to delayed onset of myelination. To investigate the molecular mechanisms of differentiation, Schwann cells were treated with forskolin, a generally used reagent to elevate intracellular cAMP. The consecutively activated cAMP response element-binding protein (CREB) signaling was previously shown to induce the expression of myelin-related genes in rat Schwann cells (Lemke and Chao, 1988, Monuki et al., 1989, Parkinson et al., 2003, Monje et al., 2009). Differentiation was measured by induction of myelin protein zero

(P0) expression. As stimulation assays were previously performed on rat Schwann cells, protocols had to be adopted for primary mouse Schwann cell cultures.

7.1.3.1. Stimulation with forskolin led to Schwann cell differentiation

To determine the role of forskolin on primary mouse Schwann cell cultures, Schwann cells derived from C57/Bl6 mice were stimulated with 2 μ M forskolin for one, four or five days (Figure 16A). Total RNA was isolated on the respective day, and the expression of the differentiation marker P0 was analyzed. Already after 24 h treatment, a strong induction of P0 transcription could be identified in stimulated Schwann cells, reflecting successful differentiation *in vitro*. Four and five days of stimulation did not result in an additional elevation of P0 mRNA expression. Next, the effect of progesterone was investigated. In rat Schwann cells, it was shown previously to induce Krox20 mRNA expression levels, a transcription factor expressed in differentiated Schwann cells (Guennoun et al., 2001). Upon stimulation with progesterone, an induced transcriptional activity for Krox20 could be detected in primary mouse Schwann cell cultures (Figure 16B). Treatment with forskolin led to a small induction of Krox20 expression (Figure 16B). In contrast to Krox20, stimulation with progesterone had no effect on the expression of P0 (Figure 16C). A strong induction of P0 mRNA expression could be detected upon forskolin treatment, validating our observation (Figure 16A). Stimulation with the cAMP elevating reagent forskolin was further investigated, as it resulted in a robust induction of the differentiation marker P0, indicating successful activation of the CREB signaling.

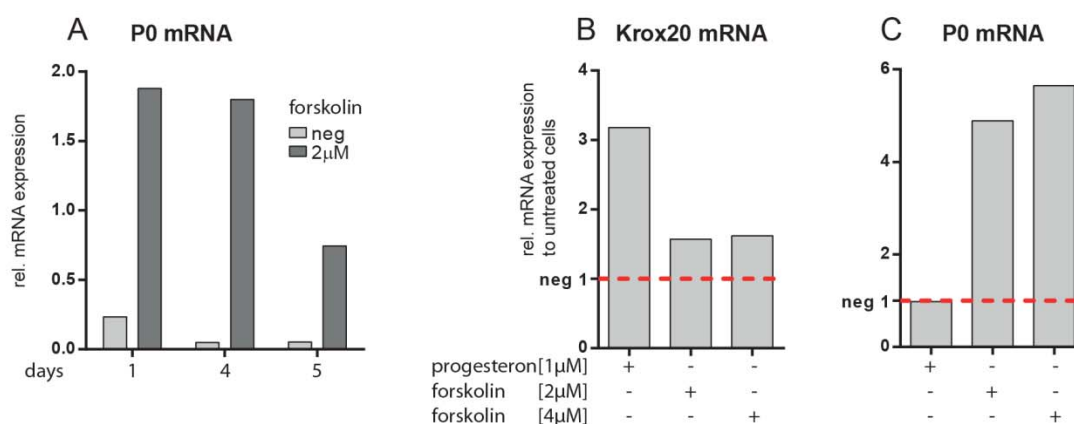


Figure 16: Schwann cell differentiation *in vitro*. (A) In an initial experiment, primary mouse Schwann cell cultures were stimulated with 2 μ M forskolin for 1, 4 or 5 days, and mRNA expression of P0 was investigated to determine Schwann cell differentiation. Already after 24 h, a strong induction of P0 expression was detected upon forskolin treatment. (B) Krox20 mRNA levels were increased with progesterone after 24 h, but not with forskolin. (C) In contrast, stimulation with progesterone did not influence P0 expression. Data were normalized to the expression of 60s, and mRNA expression levels in untreated samples were set to 1 (B, C).

In a next approach, transcription levels of P0, Krox20 and Oct6 were investigated in primary mouse Schwann cell cultures stimulated with forskolin for 24 h (Figure 17). To define the optimal concentration of forskolin, a dose response curve with 0, 2, 20 and 50 μ M forskolin was generated. The treatment resulted in a strong, dose-dependent induction of P0 transcription (Figure 17A). Upon stimulation, the mRNA expression of the transcription factor Krox20 was little induced (Figure 17B). Treatment with 2 and 20 μ M forskolin had also little effect on the expression of the transcription factor Oct6, whereas a strong induction could be detected with 50 μ M (Figure 17C). Investigation of p75^{NTR} expression revealed reduced transcription upon forskolin treatment (Figure 17D), resembling to some extent its decreasing expression during myelination (Buser et al., 2009b). For prospective mRNA expression analysis, 20 μ M forskolin was applied to the cultures for 24 h, which consequently led to increased P0 mRNA expression.

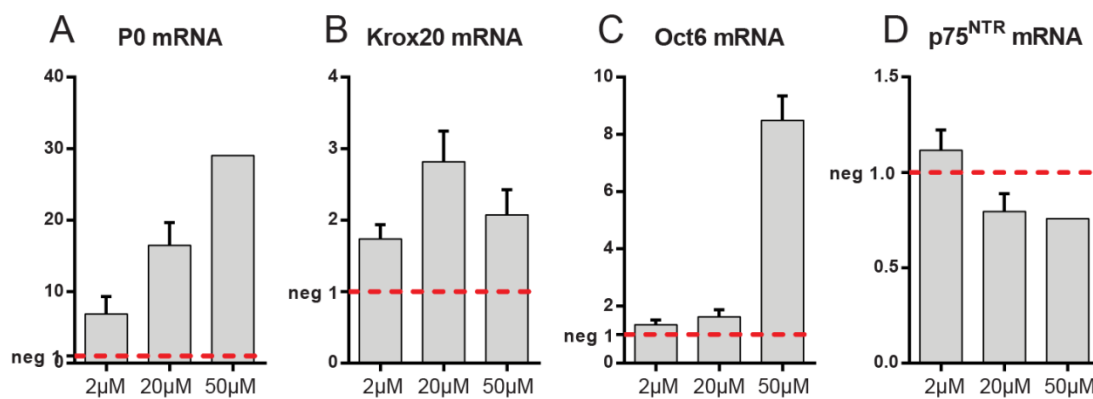


Figure 17: Stimulation with forskolin led to Schwann cell differentiation *in vitro*. Primary Schwann cells derived from C57/Bl6 mice were treated with different concentrations of forskolin for 24 h. Upon stimulation, a strong induction of P0 expression was depicted (A), whereas the induction of Krox20 mRNA was only small (B). Analysis of Oct6 revealed increased expression with only 50 μ M forskolin (C). Forskolin treatment led to decreased mRNA expression levels of p75^{NTR} (D). Values are normalized to the expression of 60s, and the expression levels of untreated cultures were set to 1. Data represent the mean of four independent experiments for 0, 2 and 20 μ M and 1 or 2 independent experiments for 50 μ M forskolin. Error bars indicate the SEM.

In addition to analysis of the mRNA expression, the protein expression of P0 and Krox20 was investigated by immunofluorescence microscopy (Figure 18A, B). For induction of protein expression, cells were stimulated with 2 or 20 μ M forskolin for 72 h; a culture stimulated with 2 μ M is shown for illustration (Figure 18B). A weak, cytoplasmic staining of P0 was detected under both conditions, and treatment with forskolin did not result in any detectable induction of P0 expression (Figure 18A, B, green). Further, nuclear Krox20 expression was depicted in few cells under both experimental conditions (Figure 18A, B, red, arrowhead), whereas most Krox20 was localized in the cytoplasm (Figure 18A, B arrows). In contrast to mRNA expression, no induction of P0 and Krox20 could be detected on the protein level. Though, Schwann cell morphology was changed to a more spindle-like

phenotype after treatment with forskolin, illustrated with stainings for p75^{NTR} (Figure 18C, D). No obvious difference in p75^{NTR} immunofluorescent intensity could be detected due to the forskolin treatment.

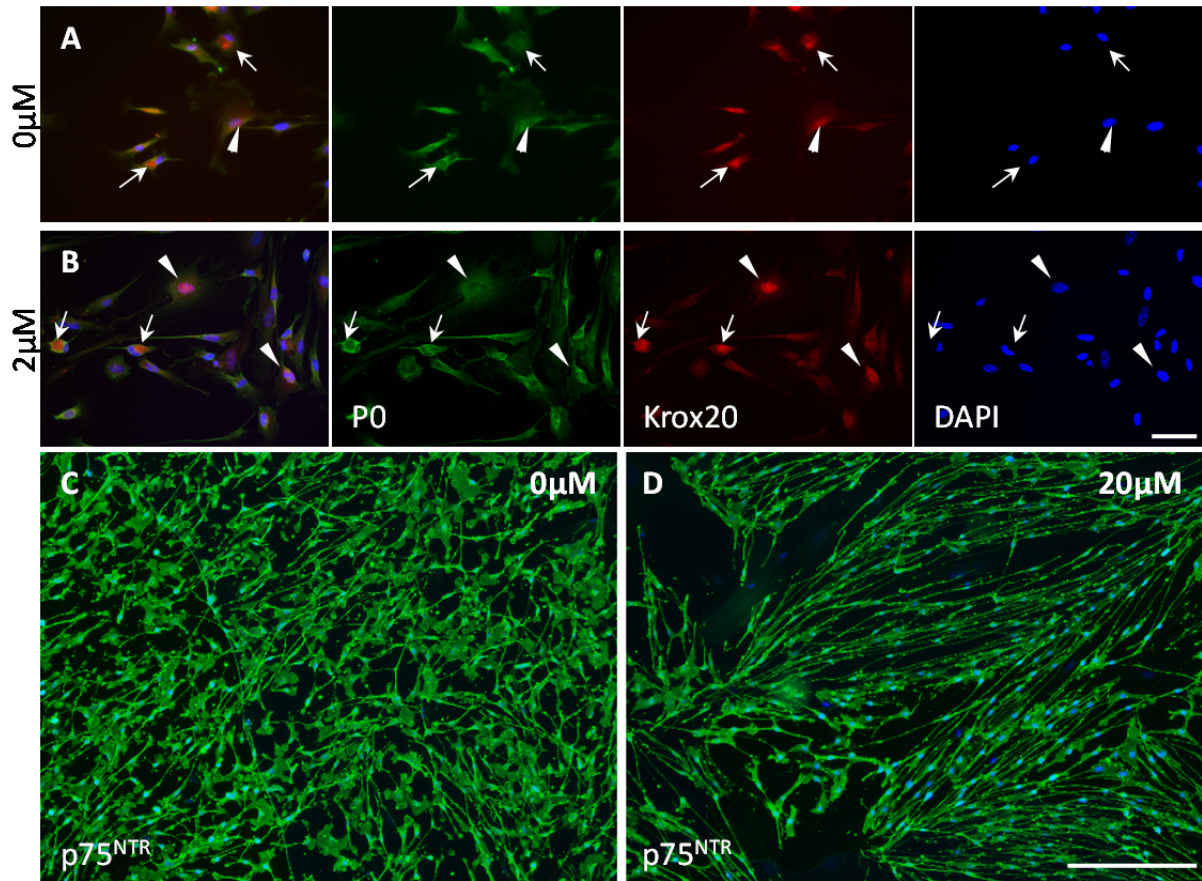


Figure 18: Stimulation of primary mouse Schwann cell cultures. Schwann cells were treated with forskolin for 72 h, and protein expression was analyzed by immunofluorescent stainings. (A, B) Upon stimulation, no induction of P0 expression could be depicted. Nuclear Krox20 expression was detected in only few cells (arrowheads), whereas most Krox20 was localized in the cytoplasm (arrows). There was no obvious difference in respect to P0 and Krox20 expression between stimulated and unstimulated cultures. (C, D) Stimulation with forskolin resulted in a morphological change of the Schwann cells, depicted by p75^{NTR} stainings (C, D). Bar: A, B: 50 μm, C, D: 200 μm

7.1.3.2. MAL-overexpressing Schwann cells manifest reduced P0 and p75^{NTR} expression

A major question was whether the retarded onset of myelination in MAL-overexpressing mice is due to impaired responsiveness of Schwann cells to axonal signals. Therefore, MAL-overexpressing Schwann cells were stimulated with 20 μM forskolin for 24 h to determine if they can activate the cAMP signaling pathway *in vitro* (Figure 19). A comparable induction of P0 transcription upon treatment was detected between wildtype and MAL-overexpressing cells, reflecting that they are able to activate the cAMP pathway (Figure 19A). Our data indicate that differentiation via CREB signaling pathway is functional in MAL-overexpressing Schwann cells. However, Schwann cells derived from MAL-overexpressing mice showed a

robust 50% reduction of P0 mRNA expression compared to wildtype littermates under both untreated and treated conditions.

Expression of p75^{NTR} in wildtype Schwann cells was reduced approximately 35% by forskolin stimulation (Figure 19B, wt⁺), corresponding to the *in vivo* situation in which p75^{NTR} expression was downregulated during myelination (Buser et al., 2009b). Along with the reduced expression of P0, Schwann cells overexpressing MAL manifested a 25% reduction in p75^{NTR} mRNA expression compared to wildtype cells (Figure 19B). This finding is coinciding with the observation of reduced p75^{NTR} expression in newborn mice overexpressing MAL (Buser et al., 2009b). As for wildtype cells, stimulation of MAL-overexpressing Schwann cells led to a 30% decrease of p75^{NTR} mRNA expression level, and still, a reduction of 20% compared to stimulated wildtype cells could be detected.

Our results demonstrate that the activation of the CREB signaling pathway is not affected by MAL overexpression, and did not improve reduced P0 and p75^{NTR} mRNA expression in MAL-overexpressing Schwann cells. Our analysis further revealed that P0 and p75^{NTR} were already reduced in unstimulated Schwann cells overexpressing MAL, suggesting that alteration in gene regulation due to MAL overexpression is taking place at an early stage of Schwann cell development.

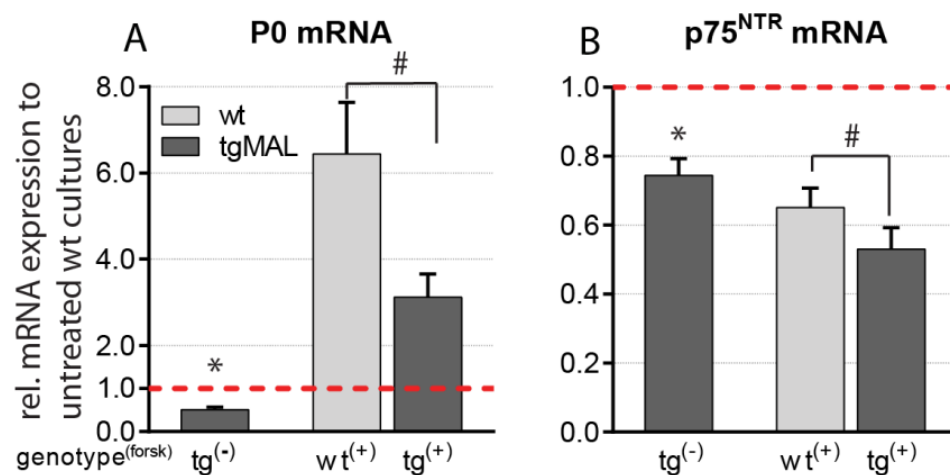


Figure 19: Differential expression analysis in primary Schwann cell cultures of MAL-overexpressing and wildtype mice. Schwann cells derived from P1 mice were cultured in the absence or the presence of 20 μ M forskolin for 24 h and analyzed by qRT-PCR. (A) The expression of P0 was significantly decreased in unstimulated and stimulated MAL-overexpressing Schwann cells. A substantial induction of P0 expression was investigated for both wildtype and MAL-overexpressing cells upon treatment. (B) Under both conditions, p75^{NTR} mRNA level was decreased in MAL-overexpressing mice. Upon treatment, p75^{NTR} expression was reduced in both genotypes. Data are normalized to the expression of 60s, and values for untreated wildtype were set to 1. Data derive from at least twenty independent experiments for unstimulated condition and at least nine independent experiments for stimulated condition. The error bars show the SEM. *: $p < 0.0001$; #: $p < 0.01$

7.1.3.3. Most transcription factors known to modulate P0 expression are unaffected by MAL overexpression

The expression levels of Sox10, Oct6, Krox20, cJun, Krox24, Egr3 and MAG were investigated in primary unstimulated mouse Schwann cell cultures to determine whether the reduced expression of P0 and p75^{NTR} in MAL-overexpressing Schwann cells is possibly caused by altered expression of transcription factors known to modulate Schwann cell development and differentiation (Figure 20). Since the effect of MAL overexpression was implicated to occur already before Schwann cell differentiation (Figure 19), the expression of transcripts of these genes was analyzed in untreated Schwann cells. First, the transcription factors Sox10, Oct6 and Krox20 were investigated, which were reported to modulate the expression of P0 (Topilko et al., 1994, Bermingham et al., 1996, Jaegle et al., 1996, Peirano et al., 2000). In MAL-overexpressing Schwann cells, Sox10 expression was slightly reduced ($p < 0.08$), validating previous *in vivo* observations (Buser et al., 2009b) (Figure 20). The expression of the transiently activated transcription factor Oct6 was slightly increased in MAL-overexpressing Schwann cells ($p < 0.06$). Furthermore, the mRNA expression levels of Krox20 were significantly increased in MAL-overexpressing Schwann cells compared to wildtype cells. Subsequently, the expression of cJun as a negative regulator for myelination was investigated (Parkinson et al., 2008), but no altered transcription was detected. The transcription factors Krox24 and Egr3 were investigated due to their ability to modulate p75^{NTR} expression (Gao et al., 2007), but the expression levels of both transcripts were not significantly changed. In contrast to the myelin-related gene P0, MAL overexpression did not influence the expression of the myelin-associated glycoprotein (MAG), which is also early expressed during Schwann cell development.

From our data, we can summarize that the expression of most transcription factors implicated in the modulation of P0 expression were not differentially regulated in MAL-overexpressing Schwann cells. Despite the fact that Krox20 expression was even increased, P0 mRNA levels were decreased in Schwann cells overexpressing MAL.

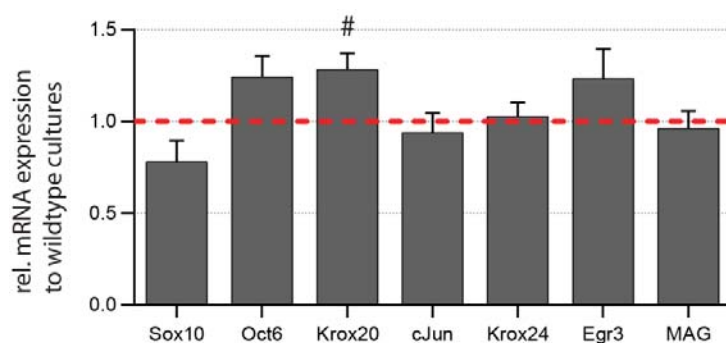


Figure 20: Transcripts of genes implicated in Schwann cell development and differentiation were investigated in untreated Schwann cells. The expression of most transcription factors was not affected by MAL overexpression. Values are normalized to the expression of 60s, and data of wildtype cultures were set to 1. The columns show the mean value of at least nine independent experiments, and the error bars indicate the SEM. #: $p < 0.01$

7.1.4. Investigation of other stimulation reagents

During development and differentiation, Schwann cells depend on accurate levels of different growth factors (Salzer et al., 1980, Anton et al., 1994, Cosgaya et al., 2002, Yamauchi et al., 2003, Chan et al., 2004, Taveggia et al., 2005). Therefore, neuregulin1, FGF1 and NGF were applied to the culture medium to determine whether their downstream signaling pathways are functional in MAL-overexpressing Schwann cells.

7.1.4.1. Neuregulin1 decreased forskolin-induced P0 expression

Accurate regulation of neuregulin1 signaling via ErbB receptors is vital for proper Schwann cell development and differentiation (Salzer et al., 1980, Taveggia et al., 2005). For this purpose, the effect of soluble neuregulin1 on primary mouse Schwann cell cultures was investigated. First, C57/Bl6 Schwann cells were treated with two different concentrations of neuregulin1, in the presence or absence of forskolin (Figure 21). Exogenous neuregulin1 resulted in slightly decreased transcription of P0 compared to untreated Schwann cells (Figure 21A). In agreement with previous observations, forskolin led to a robust induction of P0 mRNA expression levels. Application of combined treatment with neuregulin1 and forskolin abolished the forskolin-induced P0 transcription. In addition to P0, the mRNA expression levels of p75^{NTR} were investigated upon neuregulin1 stimulation (Figure 21B). A reduced expression of p75^{NTR} was detected with 2.5nM and 10nM neuregulin1 treatment. Stimulation with both forskolin and neuregulin1 did not significantly alter the transcription level of p75^{NTR} compared to stimulation with forskolin alone.

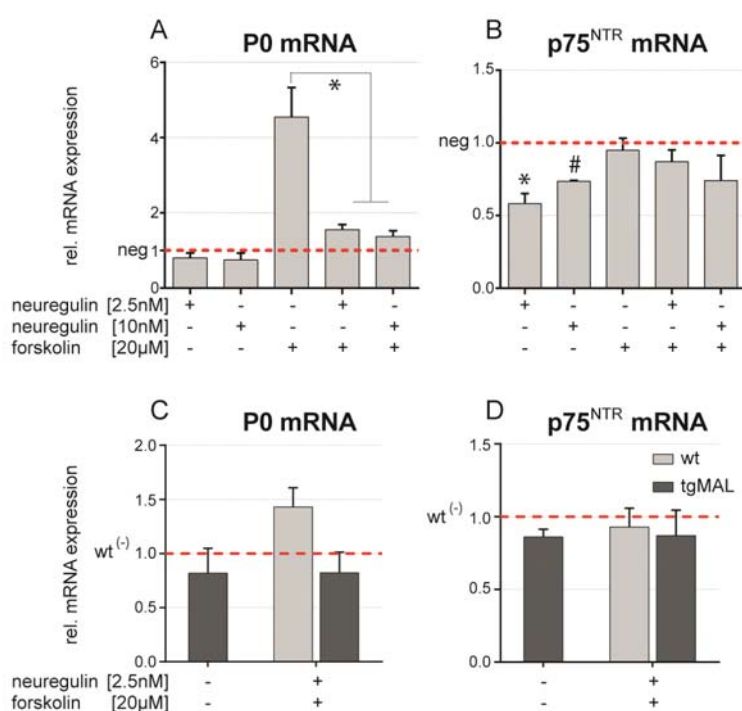


Figure 21: Effect of exogenous neuregulin1 on primary mouse Schwann cell cultures. (A) Stimulation with neuregulin1 abolished the forskolin-dependent induction of P0. (B) The expression of p75^{NTR} was decreased with neuregulin1. (C, D) Combined stimulation with neuregulin1 and forskolin did not change mRNA expression of P0 and p75^{NTR} in MAL-overexpressing Schwann cells compared to untreated wildtype cultures (wt⁽⁻⁾). In MAL-overexpressing Schwann cells, P0 expression was reduced under both conditions compared to wildtype cells. Values are normalized to the expression of 60s. Data represent the mean of at least three (A, B) or four (C, D) independent experiments, and error bars indicate the SEM. *: p-value < 0.001; #: p-value < 0.0001

Next, we investigated whether this treatment can improve the reduced P0 and p75^{NTR} expression in MAL-overexpressing Schwann cells. Combined stimulation with forskolin and neuregulin1 resulted in a small P0 mRNA induction in the wildtype, in accordance with Figure 21A (Figure 21C). In MAL-overexpressing cells, no effect upon the combined treatment with forskolin and neuregulin1 could be identified compared to untreated MAL-overexpressing Schwann cells. P0 mRNA expression was reduced under both conditions in Schwann cells overexpressing MAL compared to wildtype cells. Analysis of the p75^{NTR} expression revealed slightly reduced mRNA expression levels in untreated MAL-overexpressing Schwann cells compared to wildtype cells (Figure 21D). Upon stimulation, no difference between wildtype and transgenic cells could be observed.

7.1.4.2. Treatment with FGF1 did not improve P0 expression in MAL-overexpressing cells

A whole genome expression profiling was performed for peripheral nerve tissues at different developmental time points from wildtype and MAL-overexpressing mice. This study revealed a significant reduction of the fibroblast growth factor 1 (FGF1) in developing sciatic nerves of MAL-overexpressing mice (Figure 22).

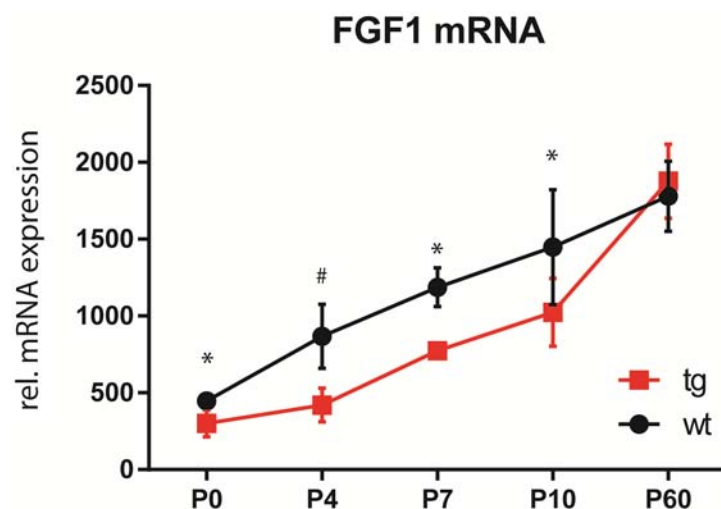


Figure 22: Reduced expression of FGF1 in developing MAL-overexpressing sciatic nerves. In MAL-overexpressing mice, reduced expression of the fibroblast growth factor 1 (FGF1) was detected at P0 to P10. Values are normalized to the global median. Data represent the mean value of seven (for P0, P10), five (for P4, P7) or three (for P60) experimental samples, and the error bars indicate the SD. Statistical analysis are based on a three-way ANOVA. #: p-value < 0.0001, *: p-value ≤ 0.05

These data may indicate that during development FGF1-mediated signaling pathways might have been impaired due to MAL overexpression. For this reason, we investigated whether exogenous FGF1 might improve transcriptional expression levels for P0 and p75^{NTR} in MAL-overexpressing Schwann cells (Figure 23). Untreated MAL-overexpressing Schwann cells showed reduced expression of P0 compared to wildtype cells (Figure 23A), in line with earlier findings. Addition of 10ng/ml FGF1 did not influence P0 transcription in wildtype Schwann cells as well as in MAL-overexpressing cells. Application of 50ng/ml FGF1 led to decreased mRNA expression levels of P0 in wildtype Schwann cells. In contrast, the

expression of P0 was not further reduced in MAL-overexpressing Schwann cells. Investigation of p75^{NTR} expression revealed reduced mRNA expression levels in untreated MAL-overexpressing Schwann cells (Figure 23B), in accordance with earlier observations. Similar as for P0 expression, addition of 10ng/ml FGF1 did not affect p75^{NTR} transcription. In wildtype cells, high dosage of FGF1 reduced p75^{NTR} expression to a comparable level as in untreated MAL-overexpressing Schwann cells, whereas mRNA expression levels of p75^{NTR} were not significantly influenced by 50ng/ml FGF1 in MAL-overexpressing cells. From these data we conclude that the downstream signaling of FGF1 seems not to be affected by MAL overexpression, because addition of FGF1 could not increase P0 expression to comparable wildtype levels.

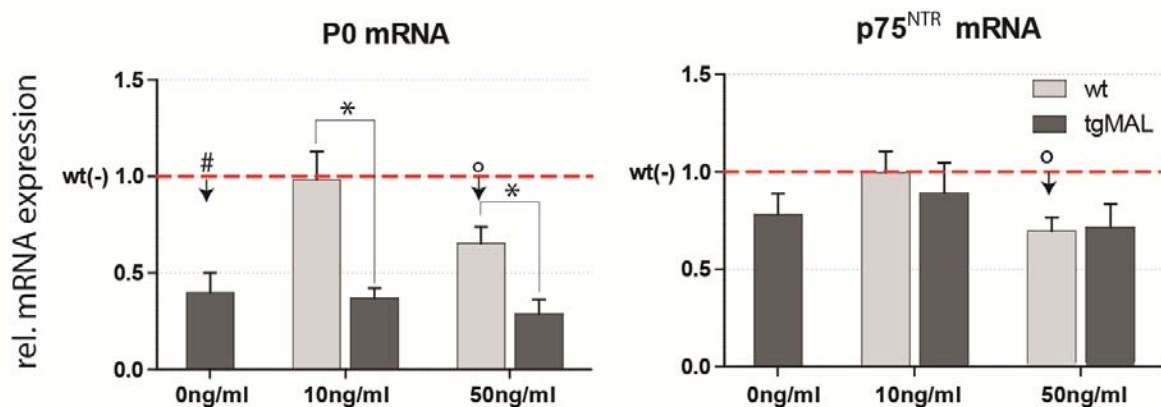


Figure 23: mRNA expression analysis upon stimulation with FGF1. (A) In wildtype Schwann cells, P0 mRNA levels were unaltered with 10ng/ml FGF1 and decreased with 50ng/ml. Stimulation with FGF1 did not lead to any alteration of P0 expression in Schwann cells overexpressing MAL. Under all stimulation conditions, P0 expression was reduced in MAL-overexpressing cells compared to wildtype cells. (B) In line with P0 expression, p75^{NTR} mRNA levels were reduced with 50ng/ml FGF1 in wildtype Schwann cells. In MAL-overexpressing Schwann cells, no changed expression of p75^{NTR} was detected under all conditions. Values are normalized to the expression of 60s, and the expression levels of untreated wildtype cultures (wt⁽⁻⁾) were set to 1. Data represent the mean of four independent experiments, and the error bars indicate the SEM. *: p-value < 0.05, °: p-value < 0.01, #: p-value < 0.005; arrows indicate significant differences to wt⁽⁻⁾.

7.1.4.3. NGF treatment increased P0 expression levels

In a next assay, we investigated the effect of the neurotrophin NGF on the expression of its low-affinity receptor p75^{NTR} and of P0 as a myelin-related gene. Application of 20ng/ml NGF resulted in an around 3-fold induction of P0 transcription (Figure 24A), in accordance with a report showing increased P0 protein expression in Schwann cell / DRG cocultures due to exogenous NGF (Chan et al., 2004). The addition of 20µM forskolin led to an induction of P0 expression of nearly six-fold, in accordance with our earlier observations. The combined treatment of forskolin and NGF resulted in a small additional elevation of P0 expression. Analysis of p75^{NTR} mRNA expression showed that stimulation with NGF led to increased mRNA levels, whereas treatment with forskolin reduced p75^{NTR} mRNA levels (Figure 24B).

Combination of exogenous NGF and forskolin also significantly increased p75^{NTR} expression compared to forskolin alone, highlighting the effect of NGF on p75^{NTR} induction.

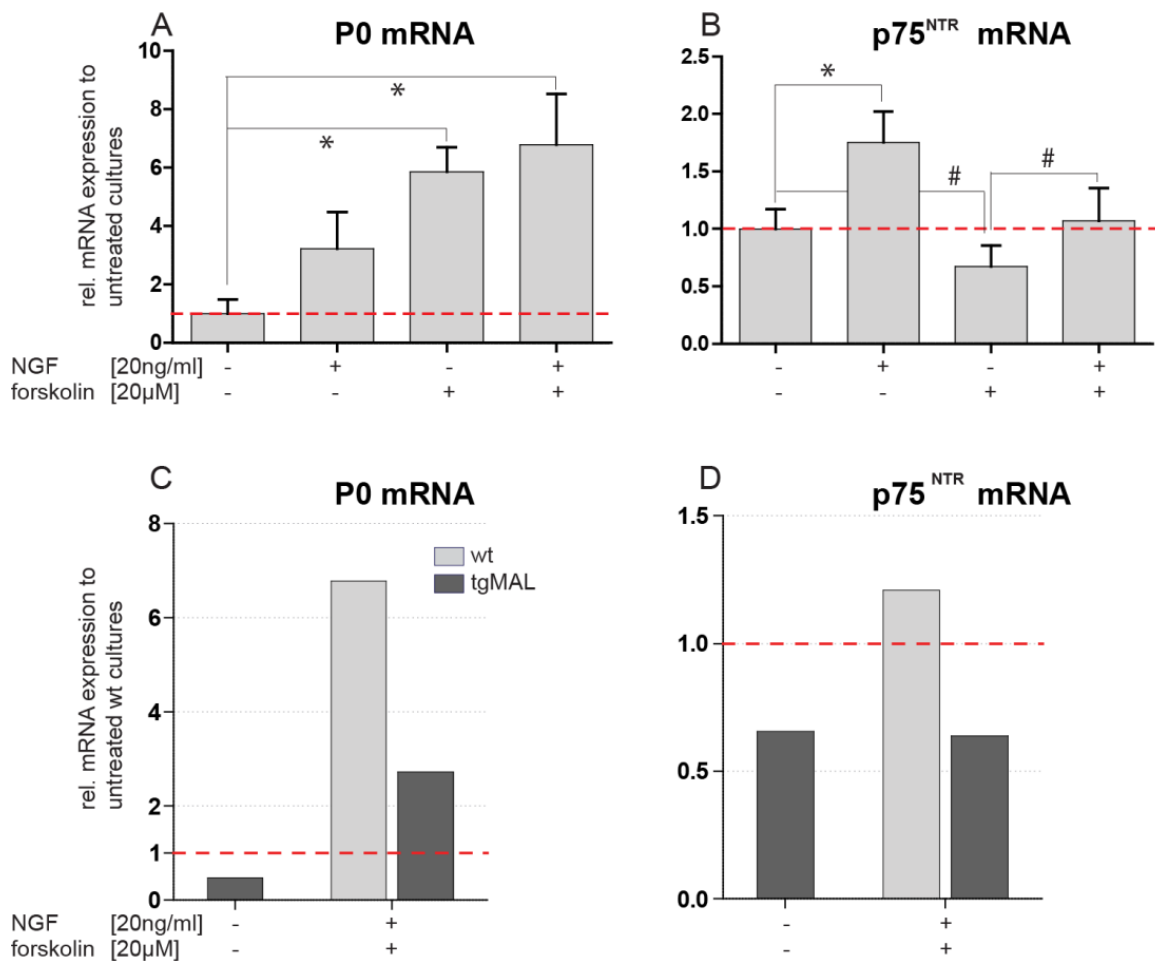


Figure 24: Investigation of exogenous NGF on primary mouse Schwann cell cultures. (A, B) Stimulation with NGF increased the expression of both P0 and p75^{NTR} in wildtype cells, in the presence or absence of forskolin. (C, D) Investigation of Schwann cells overexpressing MAL revealed comparable expression pattern of P0 and p75^{NTR} between wildtype and MAL-overexpressing cells. Transcriptional levels remained decreased in cells overexpressing MAL, indicating that stimulation with NGF was not affected by MAL overexpression. Values are normalized to the expression of 60s, and expression levels of unstimulated wildtype cultures were set to 1. (A, B): Data represent the mean of seven (negative, NGF/forskolin), four (forskolin) or three (NGF) independent experiments. The error bars indicate the SD. (C, D): Data points derived from a pilot experiment. *: p-value < 0.0005, #: p-value < 0.05.

In a pilot study, gene transcription levels of P0 and p75^{NTR} were compared between wildtype and MAL-overexpressing Schwann cells (Figure 24C, D). Combined stimulation with forskolin and NGF resulted in an around 6-fold induction of P0 expression for both wildtype and MAL-overexpressing Schwann cells, indicating that the activation of the signaling pathway mediated by NGF is not affected by MAL-overexpression (Figure 24C). However, a reduced expression of P0 was detected in untreated as well as in NGF-treated cells overexpressing MAL compared to wildtype cells. Further, the expression of p75^{NTR} was investigated in Schwann cells overexpressing MAL after combined treatment with NGF and

forskolin (Figure 24D). Stimulation with NGF and forskolin did not alter the transcription of p75^{NTR} in MAL-overexpressing Schwann cells, confirming data derived from wildtype cells (Figure 24B). Under both experimental conditions, p75^{NTR} mRNA levels were reduced in Schwann cells overexpressing MAL (Figure 24C).

7.1.5. Differential gene expression analysis in MAL-overexpressing Schwann cells

We could show that MAL overexpression leads to a robust reduction of P0 and p75^{NTR} expression, whereas most of the investigated transcripts of genes implicated in the regulation of the Schwann cell lineage were expressed at normal levels (Figure 20).

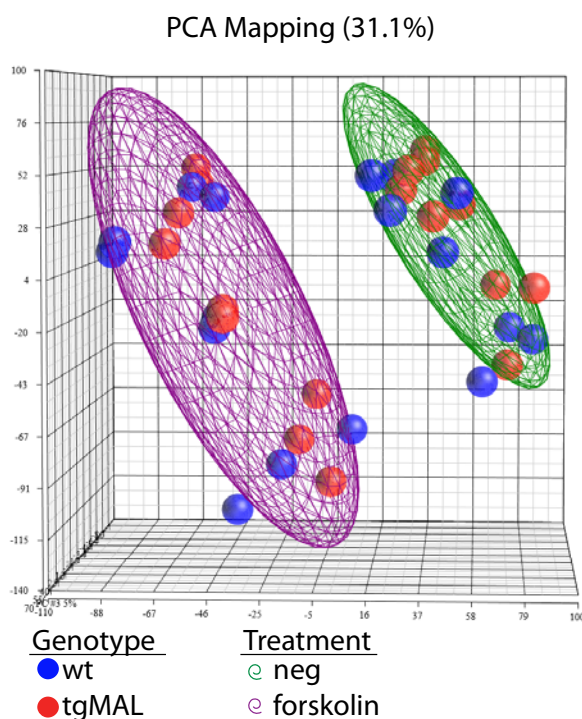


Figure 25: Microarray data illustrated by a principal component analysis (PCA). The expression of Schwann cells derived from either MAL-overexpressing mice (red) or wildtype littermates (blue) was determined by a whole genome expression profiling. Each dot represents an individual experimental sample. Two distinct clusters due to forskolin treatment can be identified (ellipsoids). PCA revealed no distinct clustering based on the genotype, indicating that only a small number of transcripts were differentially expressed in MAL-overexpressing Schwann cells.

To determine whether the transcriptional regulation of additional genes influencing the onset of myelination was altered in MAL-overexpressing Schwann cells, a whole genome expression assay covering more than 45'000 transcripts was performed for primary mouse Schwann cell cultures. In total, 36 samples were analyzed, compiled by nine independent samples of untreated and treated (20 μ M forskolin) Schwann cells derived from MAL-overexpressing mice and wildtype littermates. One coding DNA sequence may be represented by several distinct oligonucleotides (probes). For all examinations, probe-specific analysis was performed, allowing to identify MAL-dependent differentially expressed transcripts with high confidence. To investigate the effect of MAL overexpression on the global gene expression, data were visualized by an initial principal component

analysis (PCA) generated in Partek Genomics Suite (Figure 25, ellipsoids). Based on the genotype, no distinct clustering of MAL-overexpressing and wildtype samples was detected, suggesting that only a small number of transcripts were differently regulated in Schwann cells overexpressing MAL.

7.1.5.1. Majority of known genes in Schwann cells is unaffected by MAL overexpression

Selected transcripts of genes that are implicated in Schwann cell development, differentiation or myelination were analyzed using a three-way ANOVA to further investigate the effect of MAL overexpression (Table 5). First, transcription factors known in Schwann cells were investigated (Table 5A). This analysis revealed a small but significant reduction of Sox10 mRNA expression in MAL-overexpressing Schwann cells, in agreement with data generated by qRT-PCR (Figure 20). In general, however, transcription factors known to either positively or negatively modulate Schwann cell differentiation and myelination (e.g. Oct6, Krox20, Nab1, Nab2, NFatc3/4, Krox24, Egr3, Id2, cJun) were not significantly altered in MAL-overexpressing Schwann cells.

In addition to transcription factors, the expression of receptors implicated in neuregulin or neurotrophin signaling was investigated (Table 5B). In MAL-overexpressing Schwann cells, no altered expression for ErbB2, ErbB3, TrkB and TrkC could be detected compared to wildtype cells. However, two probes of the low affinity neurotrophins receptor p75^{NTR} were significantly reduced upon MAL overexpression, validating data revealed by qRT-PCR.

Analysis of myelin-related gene sequences showed the expected increase of MAL in MAL-overexpressing Schwann cells (Table 5C). Further, reduced mRNA expression of P0 could be confirmed. In addition, a significant reduction of the proteolipid protein plasmalogen (PIIp), a component of lipid rafts (Bosse et al., 2003) could be identified. Further, both probes of 2',3'-cyclic nucleotide 3' phosphodiesterase (CNPase, CNP) were significantly reduced in MAL-overexpressing Schwann cells. The expression of other myelin-related transcripts seemed not to be affected in MAL-overexpressing Schwann cells.

From these data analysis, we conclude that most investigated transcripts of genes implicated in Schwann cell development and differentiation showed comparable mRNA expression levels between MAL-overexpressing and wildtype Schwann cells. We identified that transcripts of a small number of genes were differentially expressed in MAL-overexpressing Schwann cells, but the consistent reduction of P0 and p75^{NTR} expression cannot be explained by these changes.

7. Results

Common name	Entrez ID	Ratio		Common name	Entrez ID	Ratio	
		tgMAL:wt	p-value			tgMAL:wt	p-value
A Transcription factor				Extra Cellular Matrix (ECM) /Polarization (continued)			
Early Growth Response 1 (Krox24)	Egr1	0.933	n.s.	Collagen typeV, α2	Col5a2	0.917	n.s.
Early Growth Response 2 (Krox20)	Egr2	0.894	n.s.	Collagen typeV, α2	Col5a2	1.116	n.s.
Early Growth Response 3	Egr3	1.045	n.s.	Collagen typeV, α3	Col5a3	1.005	n.s.
Inhibitor of DNA binding 2	Id2	0.888	n.s.	Collagen typeVI, α1	Col6a1	1.093	n.s.
Inhibitor of DNA binding 2	Id2	0.981	n.s.	Collagen typeVI, α1	Col6a1	1.015	n.s.
Inhibitor of DNA binding 4	Id4	1.135	n.s.	Collagen typeVI, α1	Col6a1	1.100	n.s.
Jun Oncogene (cJun)	Jun	0.928	n.s.	Collagen typeVI, α2	Col6a2	1.102	n.s.
Nab1, EGR-1-binding protein 1	Nab1	0.961	n.s.	Collagen typeVI, α2	Col6a2	1.037	n.s.
Nab1, EGR-1-binding protein 1	Nab1	1.026	n.s.	Collagen typeVI, α3	Col6a3	1.014	n.s.
Nab1, EGR-1-binding protein 1	Nab1	1.006	n.s.	Collagen typeVI, α3	Col6a3	1.082	n.s.
Nab1, EGR-1-binding protein 1	Nab1	1.004	n.s.	Dystroglycan	Dag1	0.838	0.0001
Nab2, EGR-1-binding protein 2	Nab2	1.067	n.s.	Dystroglycan	Dag1	0.891	0.0113
Nuclear factor of activated T cells, cytoplasmic 3 (Nfat4)	Nfat3	0.971	n.s.	Disks Large Homolog 1	Dlg1	not detected	
Nuclear factor of activated T cells, cytoplasmic 3 (Nfat4)	Nfat3	1.072	n.s.	Dedicator of Cytokinesis Protein 7	Dock7	1.000	n.s.
Nuclear factor of activated T cells, cytoplasmic 4 (Nfat3)	Nfat4	1.002	n.s.	Dedicator of Cytokinesis Protein 7	Dock7	0.963	n.s.
Paired Box Gene 3	Pax3	not on the array		Dystrophin-related Protein 2	Drp2	not detected	
POU Domain, class 3, Transcription factor 1 (Oct6, SCIP)	Pou3f1	0.873	n.s.	Dystrobrevin α	Dtna	0.799	<0.0001
SRY-box Containing Gene 10	Sox10	0.885	0.0103	Dystrobrevin α	Dtna	0.885	0.0186
SRY-box Containing Gene 2	Sox2	0.848	0.0039	Dystrobrevin α	Dtna	0.851	0.0003
SRY-box Containing Gene 2	Sox2	1.000	n.s.	Dystrobrevin α	Dtna	0.843	0.0100
Yin Yang 1	Yy1	not on the array		Dystrobrevin β	Dtnb	1.014	n.s.
B Receptor				Gliomedin			
A Disintegrin And Metallopeptidase Domain 22	Adam22	1.065	n.s.	Histone Deacetylase	HDAC1	not on the array	
v-Erb-b2 Erythroblastic Leukemia Viral Oncogene Homolog 2	ErbB2	0.937	n.s.	Histone Deacetylase	HDAC2	1.031	n.s.
v-Erb-b2 Erythroblastic Leukemia Viral Oncogene Homolog 3	ErbB3	not detected		Histone Deacetylase	HDAC2	0.981	n.s.
G protein-coupled receptor 126	Gpr126	0.982	n.s.	Perlecan (Heparan Sulfate Proteoglycan 2)	Hspg2	1.043	n.s.
Nerve Growth Factor Receptor (p75^{NTR})	Ngfr	0.896	0.0016	Perlecan (Heparan Sulfate Proteoglycan 2)	Hspg2	1.010	n.s.
Nerve Growth Factor Receptor (p75^{NTR})	Ngfr	0.886	0.0053	Perlecan (Heparan Sulfate Proteoglycan 2)	Hspg2	0.978	n.s.
Nerve Growth Factor Receptor (p75 ^{NTR})	Ngfr	0.930	n.s.	Integrin α1	Itga1	1.073	n.s.
Neurotrophic Tyrosine Kinase, Receptor, Type 2 (TrkB)	Ntrk2	1.069	n.s.	Integrin α1	Itga1	1.107	n.s.
Neurotrophic Tyrosine Kinase, Receptor, Type 3 (TrkC)	Ntrk3	1.008	n.s.	Integrin α6	Itga6	0.977	n.s.
Neurotrophic Tyrosine Kinase, Receptor, Type 3 (TrkC)	Ntrk3	1.064	n.s.	Integrin α7	Itga7	0.861	n.s.
C Myelin membranes				Integrin β1			
2',3'-cyclic nucleotide 3' phosphodiesterase (CNPase)	CNP	0.882	0.0037	Integrin β1	Itgb1	1.009	n.s.
2',3'-cyclic nucleotide 3' phosphodiesterase (CNPase)	CNP	0.869	0.0140	Integrin β1	Itgb1	1.077	n.s.
Gap Junction Protein α1 (Connexin 43)	Gja1	0.986	n.s.	Integrin β4	Itgb4	0.899	n.s.
Gap Junction Protein α4 (Connexin 37)	Gja4	not detected		Integrin β4	Itgb4	0.894	n.s.
Gap Junction Protein β1 (Connexin 32)	Gjb1	not detected		Laminin α1	Lama1	1.029	n.s.
Gap Junction Protein β2 (Connexin 26)	Gjb2	1.024	n.s.	Laminin α2	Lama2	0.994	n.s.
Gap Junction Protein γ3 (Connexin 29)	Gjc3	not on the array		Laminin α4	Lama4	not detected	
Lipin 1	Lpin1	1.031	n.s.	Laminin α5	Lama5	1.068	n.s.
Lipin 1	Lpin1	1.001	n.s.	Laminin β1	Lamb1-1	0.937	n.s.
Myelin-Associated Glycoprotein	Mag	0.930	n.s.	Laminin β2	Lamb2	1.020	n.s.
Myelin and Lymphocyte Protein	Mal	21.533	<0.0001	Laminin γ1	Lamc1	1.060	n.s.
Myelin and Lymphocyte Protein	Mal	12.687	<0.0001	Laminin γ1	Lamc1	1.038	n.s.
Myelin and Lymphocyte Protein	Mal	1.168	0.0001	Laminin γ2	Lamc2	0.983	n.s.
Myelin Basic Protein	Mbp	0.960	n.s.	Membrane Protein, Palmitoylated 5 (Pals1)	Mpp5	0.935	n.s.
Myelin Basic Protein	Mbp	0.913	n.s.	Neural Cell Adhesion Molecule (CD56)	Ncam1	1.059	n.s.
Myelin Basic Protein	Mbp	0.992	n.s.	Neural Cell Adhesion Molecule (CD56)	Ncam1	1.081	n.s.
Myelin Basic Protein	Mbp	0.974	n.s.	Neural Cell Adhesion Molecule (CD56)	Ncam1	1.102	n.s.
Myelin Protein Zero (P0)	Mpz	0.961	n.s.	Nidogen 1 (Entactin)	Nid1	0.907	n.s.
Myelin Protein Zero (P0)	Mpz	0.669	0.0003	Nidogen 1 (Entactin)	Nid1	1.003	n.s.
Neurofascin	Nfasc	not detected		Nidogen 2	Nid2	0.934	n.s.
Plasmolipin	Plip	0.801	0.0023	Partitioning Defective 3 Homolog (Par3)	Pard3	1.002	n.s.
Peripheral Myelin Protein 2	Pmp2	1.120	n.s.	Partitioning Defective 3 Homolog (Par3)	Pard3	0.970	n.s.
Peripheral Myelin Protein 22	Pmp22	1.147	n.s.	Partitioning Defective 3 Homolog (Par3)	Pard3	1.071	n.s.
Peripheral Myelin Protein 22	Pmp22	1.169	n.s.	Phosphatase and Tensin Homolog	Pten	0.991	n.s.
Periaxin	Prx	not detected		Phosphatase and Tensin Homolog	Pten	0.996	n.s.
D Cytoplasm				Ras-Related C3 Botulinum Substrate 1			
Growth Associated Protein 43	Gap43	1.033	n.s.	Ras Homolog Family Member A	Rhoa	not detected	
Glial Fibrillary Acidic Protein	Gfap	0.870	n.s.	Ras Homolog Family Member B	Rheb	0.975	n.s.
Glial Fibrillary Acidic Protein	Gfap	0.912	n.s.	Sarcoglycan α	Sgca	not detected	
S100 β	S100b	0.983	n.s.	Sarcoglycan δ	Sgcd	0.989	n.s.
E Extra Cellular Matrix (ECM) /Polarization				Sarcoglycan ε			
Aggrin	Aggrn	0.991	n.s.	Sarcoglycan γ	Sgcy	not detected	
Cell Division cycle 42	Cdc42	0.994	n.s.	Structural Maintenance of Chromosomes 3 (Bamacan)	Smc3	1.010	n.s.
Cadherin2 (Ncad)	Cdh2	0.996	n.s.	Syntrophin acidic 1	Snta1	0.982	n.s.
Collagen typeII, α1	Col2a1	1.454	0.0014	Syntrophin acidic 1	Snta1	1.011	n.s.
Collagen typeII, α1	Col2a1	1.419	0.0027	Syntrophin basic 1	Sntb1	0.990	n.s.
Collagen typeII, α1	Col2a1	1.330	0.0003	Syntrophin basic 2	Sntb2	0.907	n.s.
Collagen typeIV, α1	Col4a1	1.116	n.s.	Syntrophin basic 2	Sntb2	0.923	n.s.
Collagen typeIV, α5	Col4a5	1.154	0.0070	Syntrophin basic 2	Sntb2	1.029	n.s.
Collagen typeV, α1	Col5a1	0.999	n.s.	Syntrophin γ1	Sntg1	not detected	
Collagen typeV, α2	Col5a2	1.075	n.s.	Syntrophin γ2	Sntg2	not detected	
F Varia				Utrophin			
				Utrophin			
				Leucine-Rich Repeat LGI family, Member 4			
				Leucine-Rich Repeat LGI family, Member 4			

Table 5: Known genes in Schwann cells in MAL-overexpressing and wildtype Schwann cell cultures. A three-way ANOVA of microarray data revealed that the expression of most of the investigated transcripts of genes implicated in the Schwann cell development, differentiation and maintenance were unaltered in MAL-overexpressing cells. Based on a probe-specific analysis, several probes per gene were analyzed separately. The expression was normalized to the global median. Data indicate the ratio of expression of MAL-overexpressing to wildtype Schwann cells. $p \leq 0.01$ were accounted as significant. n.s.: not significant.

7.1.5.2. Several differentially expressed genes in MAL-overexpressing cells are associated with the extracellular matrix

We had a closer look at transcripts of genes localized in the extracellular matrix (ECM) of Schwann cells (Table 5E), since formation of the basal lamina is crucial for accurate myelination (Webster, 1971, Webster et al., 1973, Bunge et al., 1986, Feltri et al., 2002, Pietri et al., 2004, Yu et al., 2005, Grove et al., 2007). Statistical analysis revealed significantly reduced mRNA expression levels of α -dystrobrevin (Dtna) and dystroglycan (Dag1), two members of the dystrophin-glycoprotein complex. Transcripts of other members of this complex, such as β -dystrobrevin (Dtnb), sacroglycan (Sgcd), synthrophins (Snta1-Sntg2) and utrophin (Utrn) were unaltered. Additional analysis of the ECM revealed increased mRNA expression for collagen type II $\alpha 1$ (Col2a1) and collagen type IV $\alpha 5$ (Col4a5) in MAL-overexpressing Schwann cells. Further, normal expression levels were detected for different isoforms of integrin and laminin, as well as for entactin (nidogen, Nid1/2) and the proteoglycans agrin (Agrn), perlecan (Hspg2) and bamacan (Smc3). Investigation of transcripts of genes implicated in Schwann cell polarity revealed normal mRNA expression for disk large homolog (Dlg1), Par3 (Pard3) und Dock7 in MAL-overexpressing Schwann cells.

From this data analysis, we conclude that some components of the extracellular matrix such as α -dystrobrevin (Dtna), dystroglycan (Dag1) and collagen type II $\alpha 1$ (Col2a1) were differentially expressed in MAL-overexpressing Schwann cells.

7.1.5.3. MAL-dependent differential gene expression in Schwann cells

To investigate further the effect of MAL overexpression on gene transcription, microarray data were analyzed using a false discovery rate (FDR)-adjusted p-value of < 0.05 . This study revealed that the mRNA expression levels of 15 genes were reduced by at least 20% in MAL-overexpressing Schwann cells, whereas those of seven genes were increased (Table 6).

Common name	Entrez ID	Putative biological function	Role in Schwann cells	Ratio tgMAL:wt	p-value
Decreased due to MAL overexpression					
Glutamic Acid Decarboxylase 2 (Gad65)	Gad2	Decarboxylates glutamate to vesicular GABA	Detected in sciatic nerve extracts ¹	0.587	0.00000
Asialoglycoprotein Receptor 1	Asgr1	Mediates endocytosis of plasma glycoproteins in hepatocytes; turnover of glycoproteins ²	not reported	0.605	0.00000
Ectonucleoside Triphosphate Diphosphohydrolase 2 (NTPDase2)	Entpd2	Hydrolyzes extracellular ATP to ADP	Expressed in immature and nonmyelinating Schwann cells ³	0.622	0.00002
Keratin 23	Krt23	Intermediate filament for structural integrity in epithelial cells ⁴	not reported	0.643	0.00006
Synaptic Vesicle Glycoprotein 2 b	Sv2b	Integral membrane protein, essential for normal neurotransmission, proteoglycan at ECM ^{5,6}	Expressed on axonal side at node of Ranvier ⁷	0.669	0.00004
TRAF2 and NCK Interacting Kinase	Tnik	Regulates cytoskeleton by interaction with F-actin, activates JNK pathway ⁸	not reported	0.676	0.00000
DIRAS family, GTP-binding RAS-like 1	Diras1	Member of the small GTPase Ras family with only low GTPase activity, implicated in protein transport and localization ⁹	not reported	0.829	0.00000
Chloride Channel Calcium Activated 4	Cic4	N-terminal domain suggested to act as a zinc metalloprotease	not reported	0.693	0.00000
Vesicle Amine Transport Protein 1 Homolog-like	Vat1l	Zinc-containing alcohol dehydrogenase family	not reported	0.729	0.00004
Immunoglobulin Superfamily, Member 10	Igsf10	Member 10 of the immunoglobulin superfamily, is modulated by ECM in colorectal cancer cells ¹⁰	not reported	0.752	0.00001
6-phosphofructo-2-kinase/fructose-2,6-bisphosphatase 4	Pfkfb4	Regulates concentration of fructose 2,6-bisphosphate	Glycolysis present in Schwann cells	0.757	0.00000
Family With Sequence Similarity 213, Member B	Fam213b	-	not reported	0.767	0.00000
Glutamate Receptor, Ionotropic, AMPA1 (Gria, GluR-A, Glur1)	Gria1	Neurotransmission	Detected in a microarray study on human Schwann cell culture ¹¹	0.773	0.00004
Ras Homolog Family Member U (Wrch1)	Rhou	Member of Cdc42-related subfamily, induces actin reorganization and filopodia formation, required for F-actin polarization in the endoderm, implicated in activation of AKT and JNK ¹²⁻¹⁶	not reported	0.776	0.00006
α -Dystrobrevin	Dtna	Member of dystrophin-glycoprotein complex (links extracellular matrix to cytoskeleton)	Expressed in perineurium and Schwann cells ¹⁷	0.783	0.00001
				0.818	0.00002
				0.793	0.00000
				0.799	0.00001
Increased due to MAL overexpression					
Myelin And Lymphocyte Protein	Mal	Localized in lipid raft, trafficking & signaling; nervous system, epithelial cells	Overexpression leads to delayed onset of myelination, reduced p75 ^{NTR} expression and altered Remak bundle formation ¹⁸	21.533	0.00000
Monoxygenase, DBH-like 1	Moxd1	Predicted to hydroxylate a hydrophobic substrate in the endoplasmic reticulum	not reported	12.687	0.00000
Wingless-Related MMTV Integration Site 16	Wnt16	Secreted signaling protein, Wnt16B activates JNK pathway, regulates PI3-Kinase AKT pathway ^{19,20}	Wnt/beta-Catenin Signaling is important for expression of myelin genes ²¹	1.168	0.00006
S100 Calcium Binding Protein A4 (Mts1)	S100a4	Ca ²⁺ -binding protein in tumor metastasis, regulates cytoskeleton by binding to tropomyosin and non-muscle myosin II ²²⁻²³	Increased during peripheral nerve development ²⁴ , increased expression upon PMP22 overexpression ²⁵	1.564	0.00000
Oxysterol Binding Protein-like 3	Osbpl3	Intracellular lipid receptors. OSBP as sterol sensor; sterol-dependent scaffold for ERK pathway regulation	Oxysterol present in Schwann cells; it inhibits myelin gene expression in a Schwann cell line ²⁶	1.382	0.00001
Aquaporin 1	Aqp1	Water channel	Localized in peripheral nerves ²⁷	1.380	0.00007
LIM domain binding 2	Ldb2	Regulation of cell migration, biosensor that mediates communication between cytosolic and nuclear compartments ²⁸	not reported	1.279	0.00002
				1.270	0.00000
				1.266	0.00005
				1.235	0.00003

Table 6: Highly significantly changed mRNA expression due to MAL overexpression. The expression of MAL-overexpressing or wildtype Schwann cells was investigated by a whole genome expression analysis. Data were analyzed using a three-way ANOVA with an FDR-adjusted p-value of < 0.05, and genes with at least 20% expressional changes were taken into account. Fifteen transcripts of genes were decreased, whereas seven were increased in MAL-overexpressing Schwann cells. References: ¹Magnaghi et al., 2009; ²Rigopoulou et al., 2012; ³Braun et al., 2004; ⁴Zhang et al., 2001; ⁵Sinouris et al., 2008; ⁶Scranton et al., 1993; ⁷Zimmermann et al, 1996; ⁸Fu et al., 1999; ⁹Kontani et al., 2002; ¹⁰Zvibel et al., 2013; ¹¹Lee et al., 2004; ¹²Chuang et al., 2007; ¹³Feltri et al., 2008; ¹⁴Loebel et al, 2011; ¹⁵Ory et al., 2007; ¹⁶Tao et a., 2001; ¹⁷Albrechet et al., 2008; ¹⁸Buser et al., 2009; ¹⁹Binet et al., 2009; ²⁰Teh et al., 2006; ²¹Tawk et al., 2006; ²²Li et al., 2003; ²³Watanabe et al., 1993; ²⁴De Leon et al., 1991; ²⁵ten Asbroek et al., 2005; ²⁶Makoukji et al., 2011; ²⁷Gao et al., 2006; ²⁸Storbeck et al., 2009

Literature search revealed that the majority of the differentially expressed transcripts of genes were associated with the cytoskeleton organization. In addition to α -dystrobrevin (Dtna), we detected substantial transcriptional reduction of the intermediate filament keratin 23 (Krt23), the TRAF2 and NCK interacting kinase (Tnik) and the ras homolog family member U (RhoU, Wrch1) in MAL-overexpressing Schwann cells. A significantly increased expression in MAL-overexpressing Schwann cells was detected for the transcriptional cofactor LIM domain binding 2 (Ldb2) and the tropomyosin- and nonmuscle myosin II-binding protein S100a4 (Mts1).

In addition, we identified differentially expressed transcripts of genes that are implicated in intracellular signaling. In addition to RhoU and Tnik, significantly reduced mRNA expression could be detected for the GTP-binding protein Di-Ras1 (Diras1) in MAL-overexpressing

Schwann cells. In contrast, significantly increased expression levels of the secreted signaling protein Wnt16 and of the intracellular lipid receptor oxysterol binding protein-like 3 (Osbp13) were identified in Schwann cells overexpressing MAL.

A strong reduction could also be depicted for the glutamic acid decarboxylase 2 (Gad2, Gad65), as well as for the ionotropic glutamate receptor AMPA1 (Gria1, GluR-A, Glur1) and the asialoglycoprotein receptor 1 (Asgr1). A comparable reduction was identified for the ectonucleoside triphosphate diphosphohydrolase 2 (Entpd2, NTPDase2), whose expression was previously reported in immature and nonmyelinating Schwann cells (Braun et al., 2004). MAL overexpression resulted also in reduced mRNA expression levels of the chloride channel calcium activated 4 (Clca4), the vesicle amine transport protein 1 homolog-like (Vat1l), the proteoglycan synaptic vesicle glycoprotein 2B (Sv2b), the glycolysis-influencing gene 6-phosphofructo-2-kinase/fructose-2,6-biphosphatase 4 (Pfkfb4) and the member 10 of the immunoglobulin superfamily (Igsf10). Upon MAL overexpression, increased mRNA expression was detected for the water channel aquaporin 1 (Aqp1) and the monooxygenase DBH-like 1 (Moxd1).

To our knowledge, the expression of several of these genes has so far not been reported in the peripheral nervous system. Therefore, in situ hybridization stainings were performed to validate the altered mRNA expression in the costal arch of P10 wildtype mice. Unfortunately, no reliable signals could be detected due to their low expression levels (data not shown).

7.1.5.4. Hierarchical cluster analysis of differentially expressed genes

Genes with highly significantly altered mRNA expression in MAL-overexpressing Schwann cells were analyzed by a hierarchical cluster analysis and data were graphically represented using a heat map (Figure 26). Each column represents one experimental sample, whereas the rows show transcripts dysregulated in Schwann cells overexpressing MAL. An unambiguous separation between untreated and treated Schwann cells was detected, indicated by the green and purple bar. Further, most of the samples of the respective genotype cluster within the same stimulation condition. Hierarchical clustering of this data set resulted in three main clusters. The first two were compiled by genes whose mRNA expression levels were reduced in Schwann cells overexpressing MAL, and were subdivided into a set of transcripts with either induced or decreased expression due forskolin. The third cluster of the row dendrogram represented transcripts, which were increased in MAL-overexpressing compared to wildtype Schwann cells.

We can conclude the detected groups were formed in respect to their expressional regulation due to forskolin, but within the groups, no functional clustering of genes could be identified using hierarchical clustering analysis.

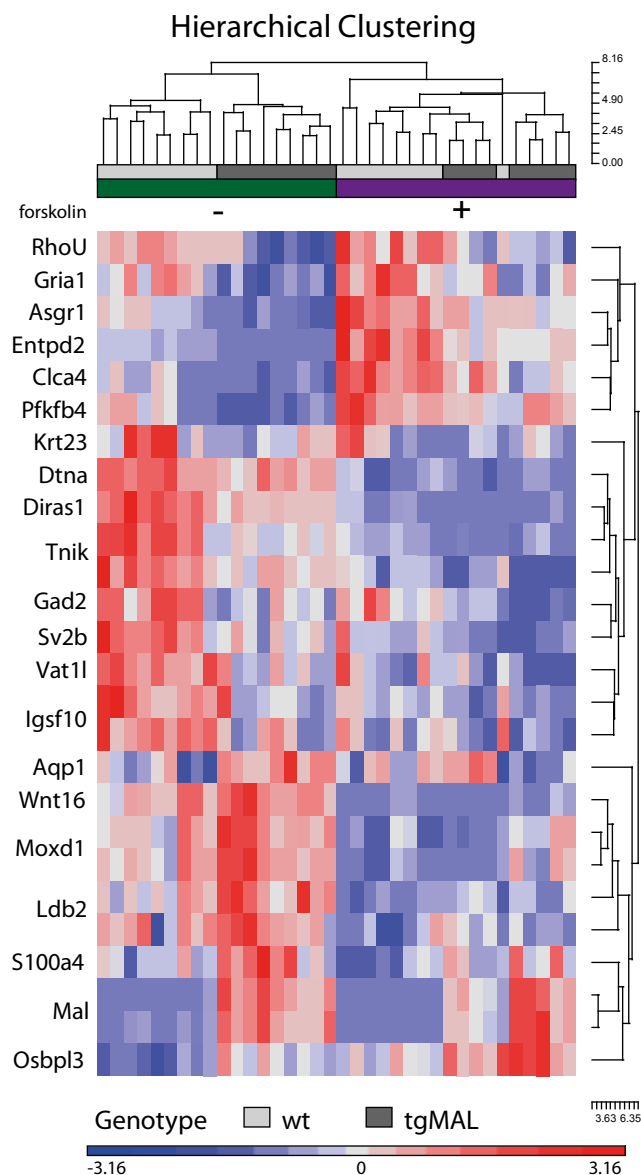


Figure 26: Hierarchic cluster of highly significantly altered gene expression upon MAL overexpression. The expression levels of the genes dysregulated with an FDR-adjusted p-value of < 0.05 were analyzed using a heat map. Each column depicts a single independent experimental sample, whereas the rows represent the altered genes. The similarity of gene expression between different samples was illustrated by the vertical distance on each branch of the dendrogram, whereas similarities between different genes were represented by the horizontal distances of the row dendrogram. A distinct separation between unstimulated and forskolin stimulated Schwann cells was determined and samples of the same genotype clustered well within a stimulation condition. The row dendrogram distinguished two main clusters of genes, representing either increased or decreased genes due to MAL overexpression, whereas the later can be subdivided into genes induced or reduced by forskolin. Grouping of genes was influenced mainly on their expression changes upon forskolin treatment.

7.1.5.5. Investigation of differentially expressed genes due to MAL overexpression in vivo

The expression pattern of the newly identified differentially expressed transcripts in Schwann cells overexpressing MAL were further investigated in sciatic nerves of MAL-overexpressing mice and wildtype littermates (Figure 27).

For that purpose, a whole genome expression array was performed on P0, P4, P7, P10 and P60 animals. In accordance with the *in vitro* observation, significantly reduced mRNA expression levels were detected for Entpd2, RhoU and Vat1l in developing MAL-

overexpressing sciatic nerves (Figure 27A-C). As expected, a strong induction of MAL mRNA levels could be depicted in MAL-overexpressing mice at every investigated time point (Figure 27D). In agreement with the *in vitro* observations, S100a4 mRNA expression was also increased in MAL-overexpressing nerves (Figure 27E). In comparison to primary mouse Schwann cell cultures, differential expression of *Igsf10*, *Pfkfb4*, *Krt23*, *Dtna*, *Sv2b*, *Moxd1*, *Aqp1*, *Osbpl3* and *Tnik* could not be identified, possibly due to their expression at background levels (data not shown), and the expression levels of *Gria1*, *Asgr1*, *Clca4*, *Diras1* and *Wnt16* were below background levels of the microarray. These data validate altered expression of several transcripts in peripheral nerves of MAL-overexpressing mice, underlining the influence of MAL on their transcriptional regulation both *in vivo* and *in vitro*.

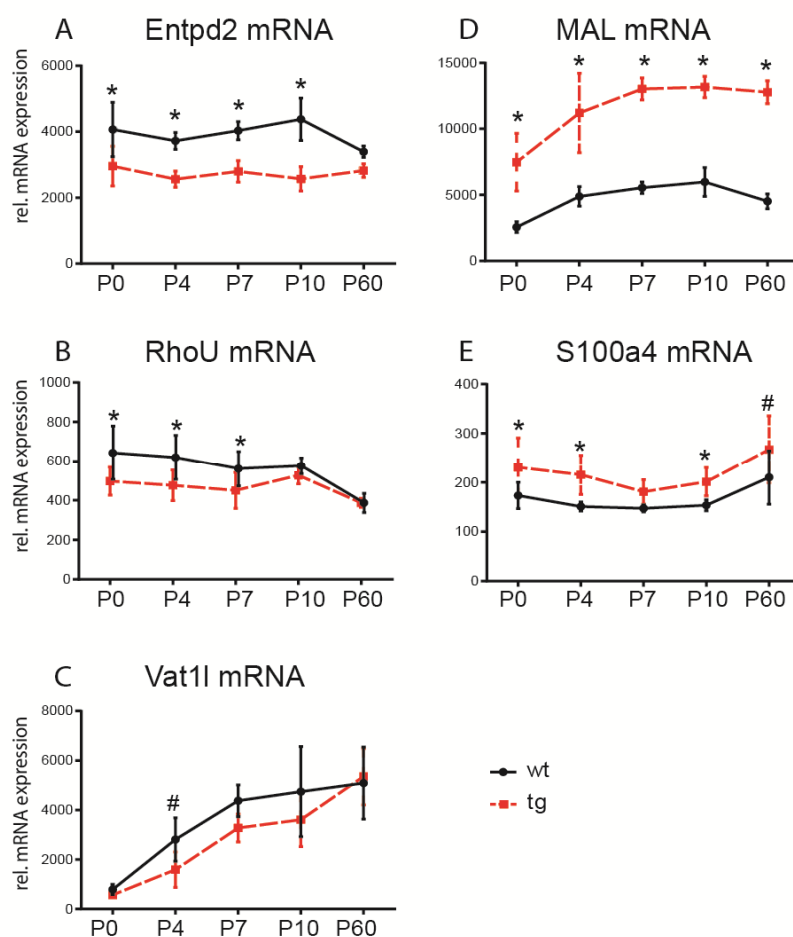


Figure 27: Investigation of mRNA expression in MAL-overexpressing mice and wildtype littermates. In a microarray approach, significantly altered transcripts in MAL-overexpressing Schwann cells were analyzed in P0, P4, P7, P10 and P60 sciatic nerves of MAL-overexpressing mice (red dots) and wildtype littermates (black dots). In line with the *in vitro* observation, RhoU, Entpd2 and Vat1l were decreased in MAL transgenic mice (A-C), whereas the expression of MAL and S100a4 was increased (D, E). Values are normalized to the global median. The dots show the mean value of seven (for P0, P10), five (for P4, P7) or three (for P60) experimental samples, and the error bars indicate the SD. *: p-value < 0.001, #: p-value < 0.05

7.1.5.6. Palmitoylation is an overrepresented annotation of genes reduced in MAL-overexpressing Schwann cells

A possible common functional role of the fifteen genes, whose transcripts were highly significantly decreased in MAL-overexpressing Schwann cells, was investigated by the Ingenuity pathway analysis (IPA, Ingenuity Systems) and the Database for Annotation, Visualization and Integrated Discovery v6.7 (DAVID). No common signaling pathway, protein-protein interactions or common transcriptional regulator for those genes was identified. However, functional annotation charts revealed that almost a third of the investigated genes (*Asgr1*, *Gria1*, *Gad2*, *RhoU*) were associated with the term palmitate ($p < 0.0005$). Palmitoylation is a reversible post-translational modification by covalently adding the saturated fatty acid palmitate to cysteine residues via thioester linkages (reviewed in Linder and Deschenes, 2007). This leads to increased protein hydrophobicity, and consequently facilitates interaction with lipid bilayer and targeting to lipid rafts. Furthermore, palmitoylation of proteins was shown to be important in regulating downstream signaling (reviewed in el-Husseini Ael and Brecht, 2002, Bijlmakers and Marsh, 2003, Hancock and Parton, 2005). Palmitoylation has been reported to be necessary for efficient targeting of myelin proteins to the plasma membrane (Schneider et al., 2005), and these data support the current concept for the functional role of MAL in sorting and trafficking of particular components to the plasma membrane (Schaeren-Wiemers et al., 2004).

Publication: Some of the data presented were submitted for publication.

Schmid D., T. Zeis, M. Sobrio and N. Schaeren-Wiemers. (2013). MAL overexpression leads to disturbed gene expression of components influencing the cytoskeleton organization and Schwann cell differentiation. *Manuscript submitted*

7.2. Investigation of a direct link between MAL overexpression and downregulation of p75^{NTR}

We could show reduced expression of p75^{NTR} in MAL-overexpressing Schwann cells. To determine whether overexpression of MAL directly leads to reduced p75^{NTR} expression, Schwann cells were infected with a retroviral construct to overexpress MAL, and the transcription of p75^{NTR} was subsequently analyzed.

7.2.1. Immortalized S16 Schwann cell line

The immortalized Schwann cell line S16 was established in 1989 by Richard H. Quarles (Goda et al., 1991), and derived from a primary rat Schwann cell culture that was immortalized by repetitive passaging. Using the S16 Schwann cell line, we investigated whether there is a putative direct link between MAL overexpression and the downregulation of p75^{NTR}. First, we determined whether this immortalized Schwann cell line can be compared to primary Schwann cells.

7.2.1.1. Morphological change and induction of Krox20 protein expression upon forskolin treatment

To investigate whether the differentiation of S16 Schwann cells *in vitro* is comparable to primary Schwann cells, they were stimulated with 0, 20 or 100 μM forskolin for 72 h, and their protein expression was subsequently analyzed by immunofluorescent microscopy (Figure 28). The most obvious difference was the morphological change due to forskolin; untreated S16 cells were flattened (Figure 28A, C, E), whereas stimulated cells manifested more processes (Figure 28B, D, F). In addition, a stronger DAPI staining was detected in all stimulated Schwann cells compared to unstimulated cells, suggesting higher transcriptional activity of the cell. The transcription factor Krox20, which is expressed in differentiated, pro-myelinating Schwann cells, was investigated as a differentiation marker (Figure 28A, B, red). Increased staining intensity of Krox20 was detected in the nucleus upon treatment with forskolin (Figure 28B, arrows). In addition, the hybridoma antibody O1 recognizing galactosylceramide (GalC) was used as a myelin lipid marker (Bansal and Pfeiffer, 1989). Already in untreated S16 cells, a robust expression of O1 was detected (Figure 28A, C, E; green). Stimulation with forskolin led to a moderate induction of O1 staining intensity, maybe evoked by changed morphology of the cell (Figure 28B, D, asterisk). The neurotrophin receptor p75^{NTR} was expressed in all untreated S16 cells (Figure 28C, red). Upon stimulation, the signal intensity of p75^{NTR} was increased compared to unstimulated controls (Figure 28D, red, asterisk). The intermediate filament GFAP, which is expressed in immature and nonmyelinating Schwann cells, was strongly expressed in unstimulated cells

(Figure 28E, red). In a subset of O1-positive cells, a reduction of the intermediate filament GFAP was observed (Figure 28E, arrows), in line with previous reports showing decreased GFAP expression in differentiated Schwann cells (Monje et al., 2009). However, some S16 cells remained strongly GFAP-positive upon forskolin stimulation, independent of O1 expression (Figure 28F).

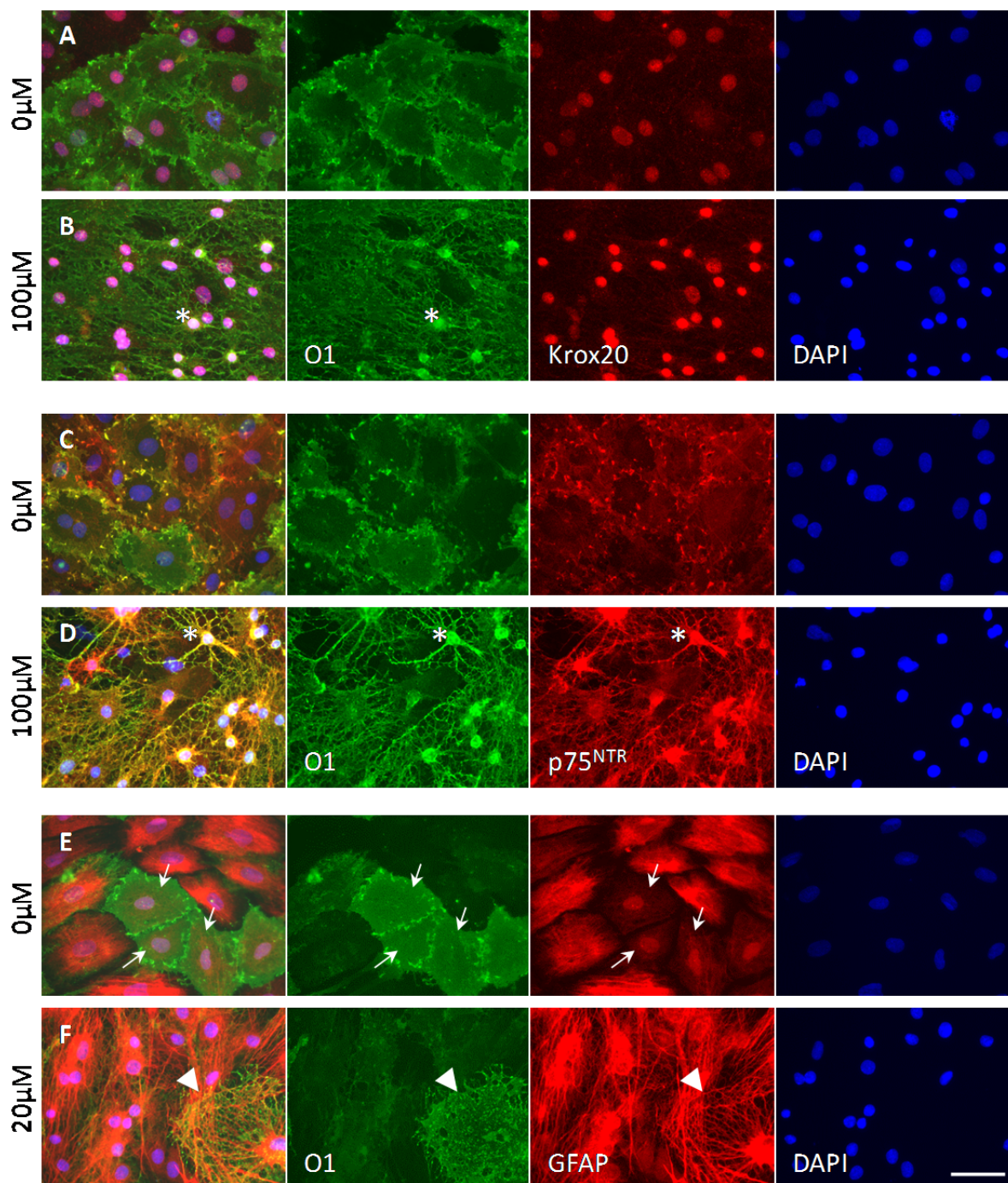


Figure 28: Treatment of the S16 cell line with forskolin. S16 Schwann cells were stimulated with different concentrations of forskolin for 72 h. A strong nuclear expression of Krox20 was detected upon stimulation (B). O1 was detected under both untreated and treated conditions (A-F). Occasionally, cells strongly coexpressing p75^{NTR} and O1 were detected in treated cultures (D, asterisk). In some cells, expression of the differentiation marker O1 was accompanied by decreased GFAP staining (E, arrows), whereas in others, GFAP remained strongly expressed (F, arrowhead). Note the morphological changes due to forskolin. Bar: 50µm

7.2.1.2. Forskolin treatment did not lead to a robust induction of P0 and Krox20 mRNA

The effect of forskolin treatment was further investigated on the mRNA expression levels in S16 Schwann cells. To determine whether a comparable induction of P0 transcription can be detected as in primary Schwann cell cultures, S16 Schwann cells were stimulated with 0, 2, 20, 50 or 100 μ M forskolin for 24 h. Forskolin treatment led to an increase of P0 mRNA expression level of around two-fold for 2 and 20 μ M forskolin (Figure 29A). Stimulation with 50 and 100 μ M forskolin had no effect on the P0 expression. No induction was detected for the transcription factor Krox20 at 2 and 20 μ M forskolin, and even a reduction was determined at higher concentrations (Figure 29B). Analysis of the neurotrophin receptor p75^{NTR} revealed an induced expression at all concentrations of forskolin (Figure 29C). This increased p75^{NTR} mRNA expression level is in agreement with the detected protein expression, as treated S16 cells were intensively positively stained for p75^{NTR} (Figure 28D).

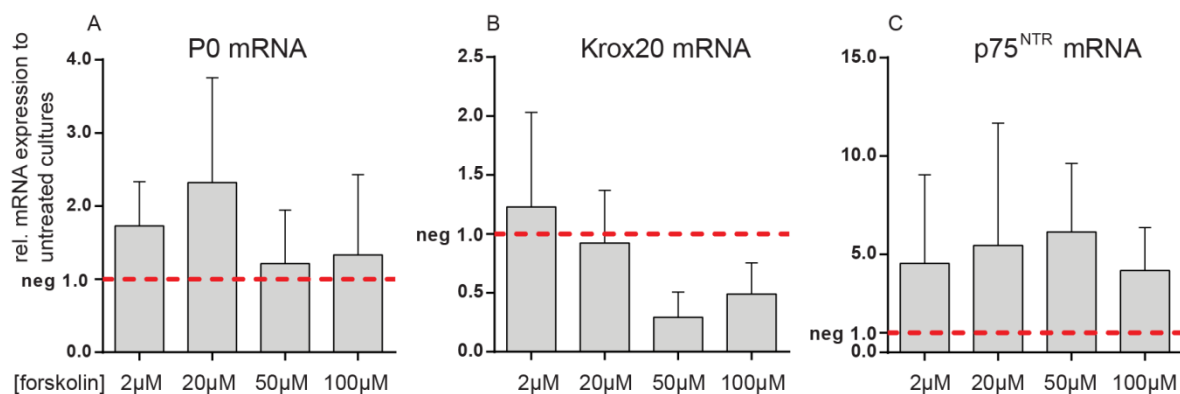


Figure 29: Expression analysis of S16 cell line upon treatment with forskolin. S16 Schwann cells were treated with different concentrations of forskolin for 24 h. (A) A small induction of P0 mRNA expression was detected with 2 and 20 μ M forskolin. (B) Krox20 expression level was not altered at 2 and 20 μ M and reduced at 50 and 100 μ M forskolin treatment. (C) For p75^{NTR} expression, all concentrations led to increased levels. Values are normalized to the expression of 60s, and expression levels of untreated cultures were set to 1. Data represent the mean of three independent experiments, and error bars indicate the SD.

The high standard deviation of qRT-PCR results might be explained by the heterogeneity of the cultures: Within one well, several distinct cell types could be identified. Regularly, patches of differentiated, O1- or O4-expressing S16 cells were detected in untreated cultures (Figure 28E, Figure 30A arrows). Furthermore, stimulation with forskolin did not lead to differentiation of all cells, reflected by occasionally observed O4-negative cells (Figure 30B, Figure 31C, D, arrowheads). These factors might distort the mRNA expression analysis, resulting in large standard deviations.

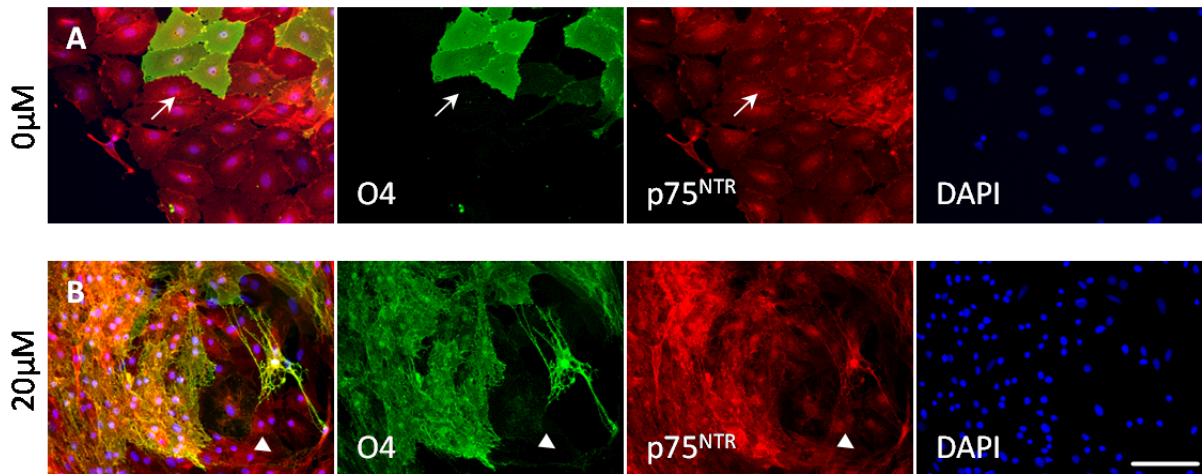


Figure 30: Heterogeneity of S16 cell cultures. (A) Within the same well, distinct differentiation stages could be detected, indicated by patches of differentiated, O4-positive cells under unstimulated condition (arrow). (B) Further, not all cells expressed O4 upon treatment with forskolin (arrowhead). Bar: 100µm

7.2.1.3. S16 cells manifested a nonphysiological morphology

Comparison of the morphology of S16 immortalized Schwann cells and primary Schwann cells revealed several differences. In S16 cell line, some cells showed unusual processes and strongly coexpressed p75^{NTR} and O1 or O4 (Figure 31A, B, asterisks), which was not observed in primary Schwann cells. These few p75^{NTR} and O1 positive S16 cells observed might be a consequence of disturbed lineage due to immortalization. In addition, several abnormally large cells could be depicted upon forskolin treatment (Figure 31C, D, arrows). Most of those large cells contained two up to five nuclei, which was not observed in primary Schwann cell cultures.

From this study, we conclude that the S16 cell line cannot be utilized as an alternative for primary Schwann cell cultures to investigate the functional role of MAL. Many cells showed an altered morphology, including multinuclear, abnormally large cells. Furthermore, forskolin-dependent PO mRNA induction was only minimal and variable, maybe due to heterogeneous cultures.

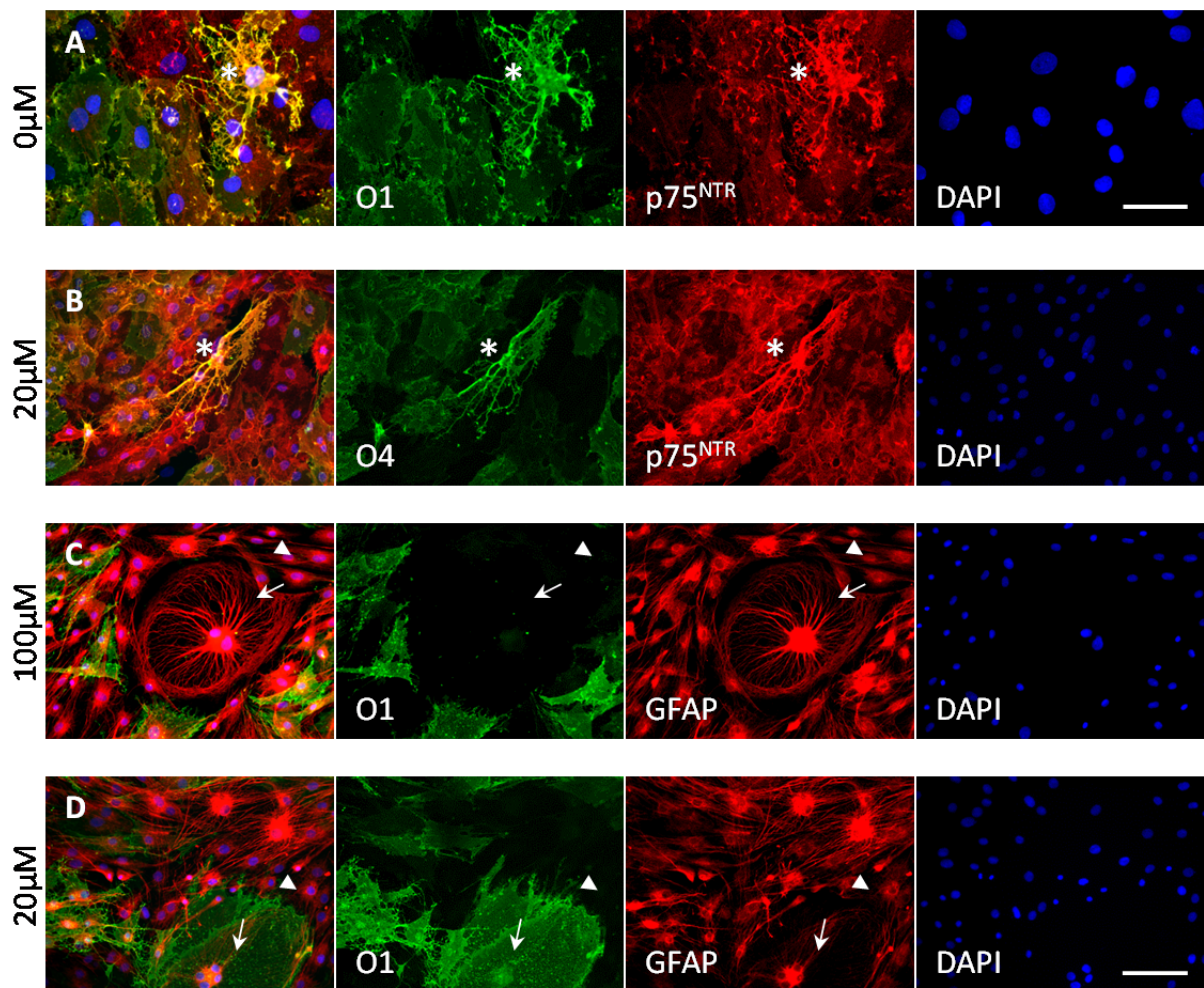


Figure 31: Nonphysiological morphology of S16 Schwann cells. (A, B) Occasionally, cells strongly coexpressed p75^{NTR} and O1 or O4 (asterisks). (C, D) Abnormally large, multinuclear cells were detected (C, D, arrows). Note that not all cells under differentiating conditions express O1 (arrow heads). Bars: A: 50µm, B-D: 100µm

7.2.2. Proliferating Rat Schwann cell cultures

We could show that the immortalized Schwann cell line S16 is not comparable to primary Schwann cell cultures. Therefore, rat Schwann cell cultures were investigated. In contrast to mouse Schwann cells, rat Schwann cells do proliferate *in vitro*, highlighting a valuable advantage since less animals have to be sacrificed. In addition, research on myelin biology was performed on rat Schwann cell cultures for the last decades, and many protocols are well established. In order to elucidate the role of MAL in rat Schwann cells, they first have to be infected with a retroviral construct to overexpress MAL.

7.2.2.1. Forskolin induced P0 and Krox20 expression and reduced p75^{NTR} mRNA levels

Rat Schwann cells proliferated in 2 μ M forskolin and conditioned medium (derived from NDF- β -overexpressing CHO cells) until high density was reached. Upon treatment with forskolin for 24 h, a nearly 6-fold induction of P0 expression could be detected with already 2 μ M forskolin (Figure 32A). Applying higher concentrations did not further increase P0 mRNA expression levels. The expression levels of Krox20 were increased continuously in a dose-dependent manner, reaching the highest induction with 50 μ M forskolin (Figure 32B). The mRNA levels for p75^{NTR} were steadily decreasing with higher concentrations (Figure 32C), in accordance to previous observations on primary mouse Schwann cell cultures.

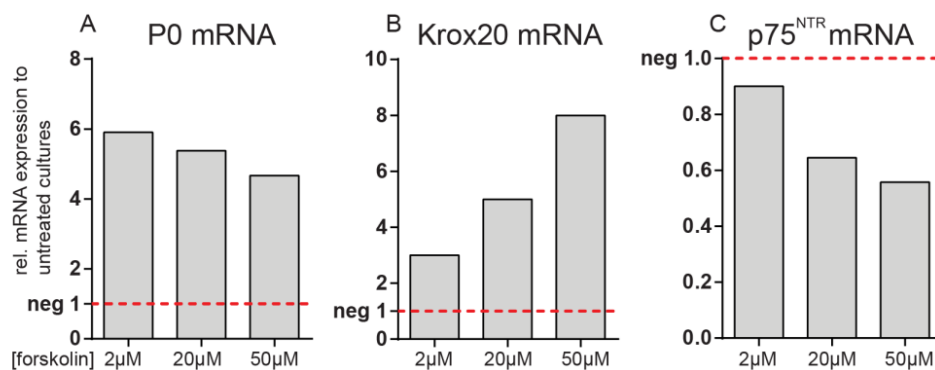


Figure 32: Treatment with forskolin induced transcription of differentiation marker in cultured rat Schwann cells. Stimulation with different concentrations of forskolin resulted in a strong induction of P0 (A) and Krox20 (B) expression and reduced mRNA levels of p75^{NTR} (C). Values are normalized to the expression of 60s, and the expression levels of unstimulated cultures were set to 1.

In addition to the analysis of the mRNA expression levels, protein expression of differentiation markers were investigated in rat Schwann cell cultures upon forskolin treatment. In untreated rat Schwann cells, strong p75^{NTR} protein expression could be detected, but no O1 staining was observed (Figure 33A). Stimulation with 20 μ M forskolin resulted in induced O1 expression in a subset of Schwann cells (Figure 33B, green). Upon

treatment, also decreased expression intensity of p75^{NTR} could be observed upon treatment (Figure 33B, red), in coincidence with mRNA expression analysis (Figure 32C). However, the induction of O1 did not consequently lead to reduced p75^{NTR} expression, indicated by some double positively labeled cells (Figure 33B, arrows). Cells left in the proliferating media SCPM (5% NDF- β -conditioned medium and 2 μ M forskolin) during the whole period, had similar staining intensities of p75^{NTR} and O1 as Schwann cells stimulated with 20 μ M forskolin (Figure 33C). An obvious effect of the stimulation is the morphological transformation. Untreated cells manifested the typical spindle-like pattern with elongated processes which is often observed in Schwann cells, whereas treated Schwann cells changed to a flattened phenotype, in agreement with previous observations in rat Schwann cells (Monje et al., 2010).

We can summarize that the effect of forskolin treatment is comparable between primary mouse and rat Schwann cell cultures. However, the highest induction of P0 expression was detected with 2 μ M forskolin, whereas P0 transcription was increased dose-dependently in mouse Schwann cells. In addition, morphological changes upon stimulation were distinct in rat Schwann cells compared to murine cells. Comparing to S16 immortalized Schwann cells, we can conclude that the differences between mouse and rat Schwann cell cultures were only small.

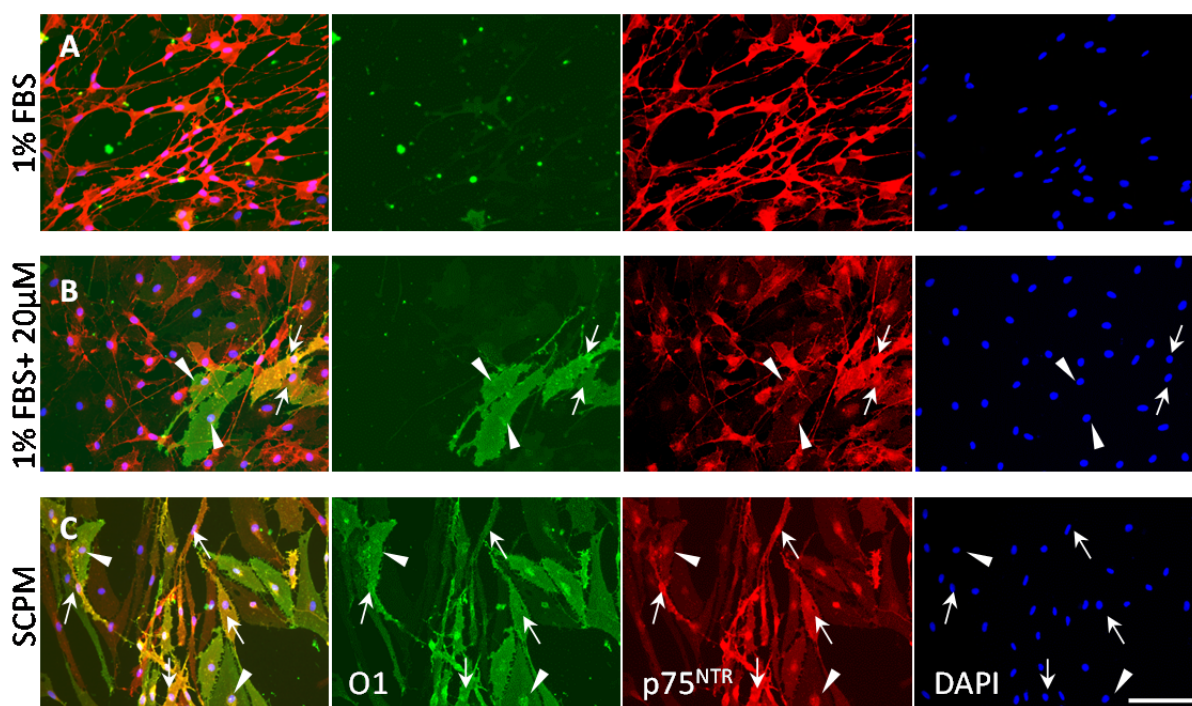


Figure 33: Differentiation of rat Schwann cell cultures. Rat Schwann cells were mitogen-deprived in 1% FBS for 48 h and then treated for 72 h in the absence (A) or presence of forskolin (B). Upon stimulation, induction of O1 expression was detected (arrowheads), whereas p75^{NTR} intensity was decreased. Some Schwann cells expressed both O1 and p75^{NTR} (arrows). Schwann cells kept in SCPM were strongly positive for O1 stainings (C). Bar: 100 μ m

7.2.2.2. Retroviral infection of rat Schwann cell cultures to overexpress MAL

To investigate whether MAL overexpression directly influences the expression of P0 and p75^{NTR}, rat Schwann cells were infected with a retroviral construct to overexpress MAL. Retroviral supernatant was applied to rat Schwann cells for twice 6 h, and protein and mRNA expression was analyzed after 72 h. Experiments were performed with uninfected and MAL-overexpressing cells, as well as with control cultures infected with only mCherry or mCherryPMP22 as another tetraspan protein.

7.2.2.2.1. mCherryMAL is localized in the plasma membrane of infected Schwann cells

First, the cellular localization of the overexpressed MAL and PMP22 was determined in infected rat Schwann cells (Figure 34).

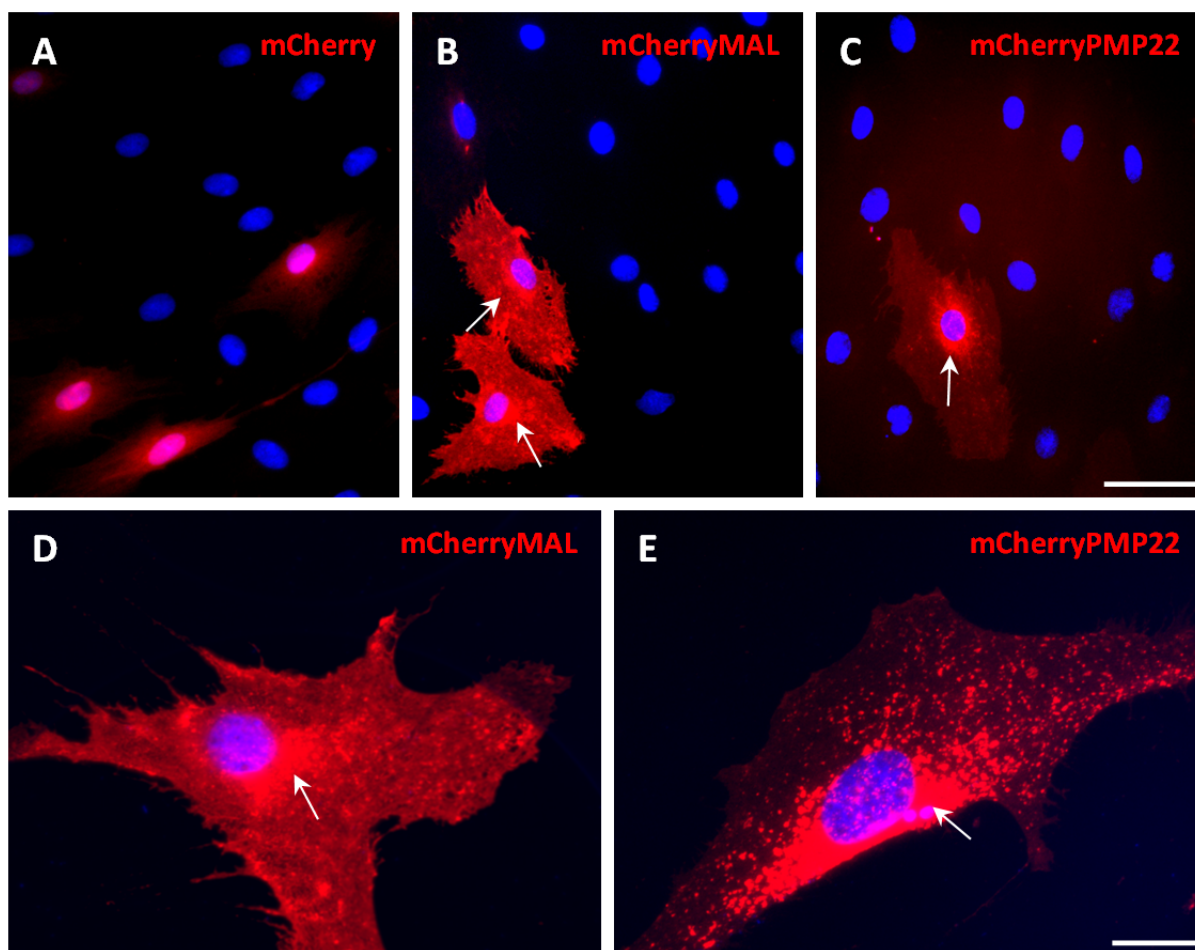


Figure 34: Retroviral infections of rat Schwann cells. Proliferating rat Schwann cells were retrovirally infected with constructs to overexpress the fusion protein mCherryMAL (B, D) or mCherryPMP22 (C, E). For infection control, cells were infected with mCherry alone (A). For the control mCherry, a cytoplasmic localization was detected (A). Overexpression of MAL resulted in a plasma membrane surface staining and some perinuclear accumulations, most likely representing the trans-Golgi network (B, D, arrow). In contrast, overexpressed PMP22 was only weakly detected in the plasma membrane, but predominantly in intracellular accumulations. Bar: A-C: 50 μ m, D, E: 20 μ m

For the fusion protein mCherryMAL, a plasma membrane surface staining was detected (Figure 34B, D). Further, accumulations near the nucleus were detected, which most likely represent the trans-Golgi network (TGN), where MAL is often localized *in vivo* (Figure 34B, D, arrows). Overexpression of PMP22 led to intracellular accumulation of the protein and only a weak autofluorescence on the plasma membrane could be depicted (Figure 34C, E). Infection with only the control vector pMXmCherry led to diffuse, cytoplasmic autofluorescence of mCherry (Figure 34A). These data confirmed the correct localization of the overexpressed proteins, indicating that the retroviral constructs were appropriately cloned. The optimal condition for retroviral infection of Schwann cells was obtained by varying the seeding density, time of infection and the amount of applied polybrene, and the infection efficiency could be raised to nearly 50% (data not shown).

7.2.2.2.2. MAL overexpression led to reduced p75^{NTR} protein expression in some infected Schwann cells

To investigate whether MAL overexpression was sufficient to reduce the expression of p75^{NTR}, infected rat Schwann cells were stained for p75^{NTR}. The autofluorescence of mCherry served as a marker for infected cells. Some cells overexpressing MAL could be detected that manifested lower p75^{NTR} staining intensity compared to uninfected Schwann cells (Figure 35A-C, arrows). On the other hand, several infected cells expressed p75^{NTR} protein at a comparable level as uninfected cells (Figure 35A-C, arrowheads). The intensity of p75^{NTR} staining was strongly varying even in uninfected cells and negative controls, reflected in some nearly undetectable p75^{NTR} stainings (Figure 35C, asterisk; Figure 10A). This observation of variable p75^{NTR} expression in uninfected cells did not allow a reliable quantification of p75^{NTR} staining intensities between infected and uninfected Schwann cells.

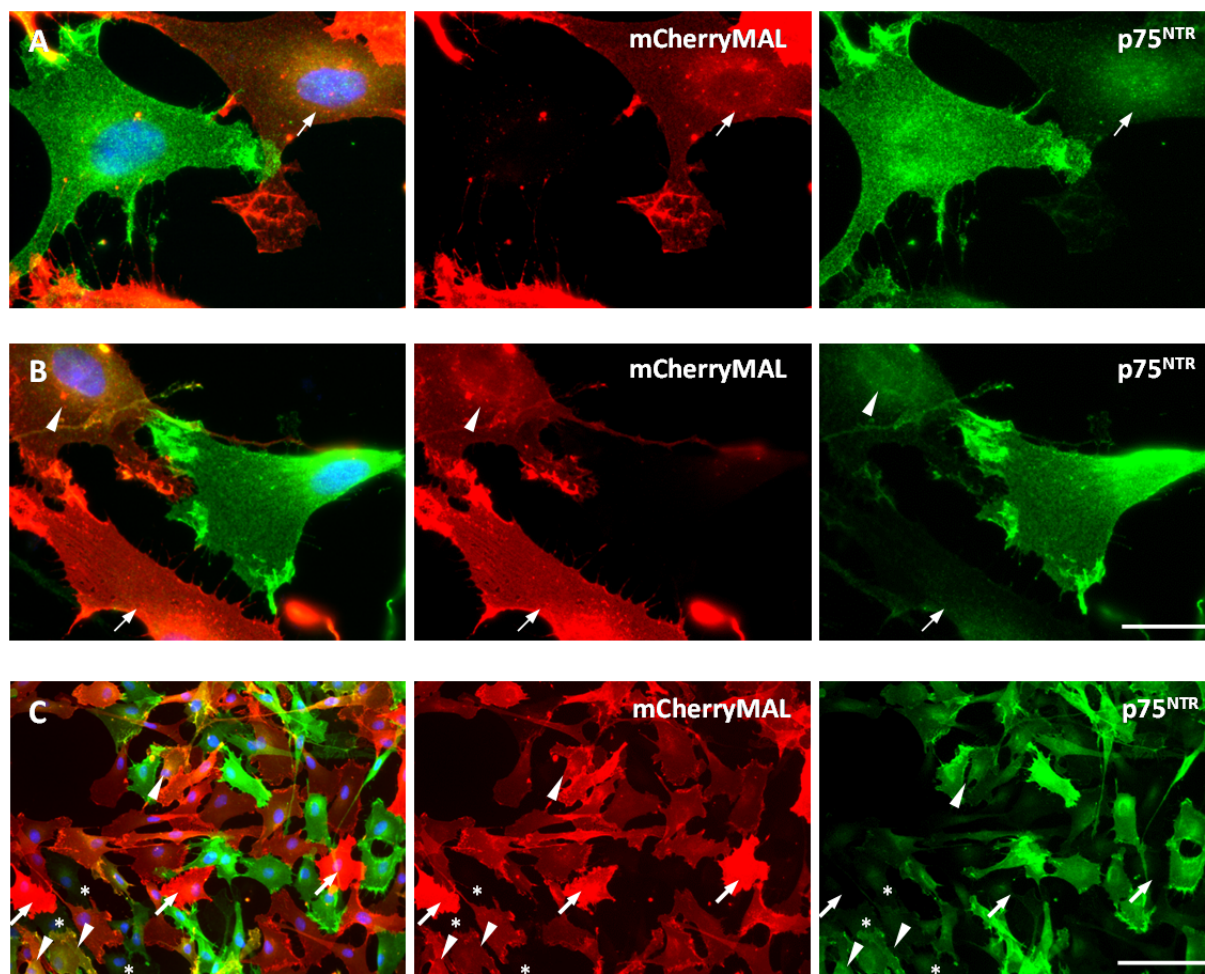


Figure 35: Some MAL-overexpressing rat Schwann cells manifested decreased p75^{NTR} expression. Proliferating rat Schwann cells were retrovirally infected to overexpress MAL, and their p75^{NTR} protein expression was analyzed by immunofluorescent microscopy. Some infected cells showed less p75^{NTR} expression compared to adjacent noninfected cells (arrows). In other infected cells, MAL overexpression had either no or only little effect on p75^{NTR} expression (arrowheads). Even in noninfected cells, the staining intensity of p75^{NTR} varied, indicated by Schwann cells with nearly undetectable p75^{NTR} expression levels (C, asterisks). Bar: A, B: 20 μ m, C: 100 μ m

7.2.2.2.3. Infection with pMXmCherryMAL resulted in a strong induction of MAL mRNA

The mRNA expression of p75^{NTR} was investigated upon MAL overexpression, as no reliable quantification of p75^{NTR} protein levels could be performed. To validate the retroviral construct to overexpress MAL, the mRNA expression levels of MAL were analyzed upon infection in rat Schwann cells (Figure 36A). A striking induction of MAL mRNA was measured by qRT-PCR, while MAL transcription was detected at background levels in uninfected, mCherry-infected and mCherryPMP22-infected cultures. Thereafter, the expression of p75^{NTR} was investigated to determine whether MAL overexpression is sufficient to reduce the transcription of p75^{NTR} (Figure 36B). No significant expressional alteration for p75^{NTR}

could be detected between the negative control, mCherry-, mCherryMAL- and mCherryPMP22-infected Schwann cells. Since the infection efficiency was only around 50%, the effect of MAL overexpression on the transcription activity of p75^{NTR} might have been masked.

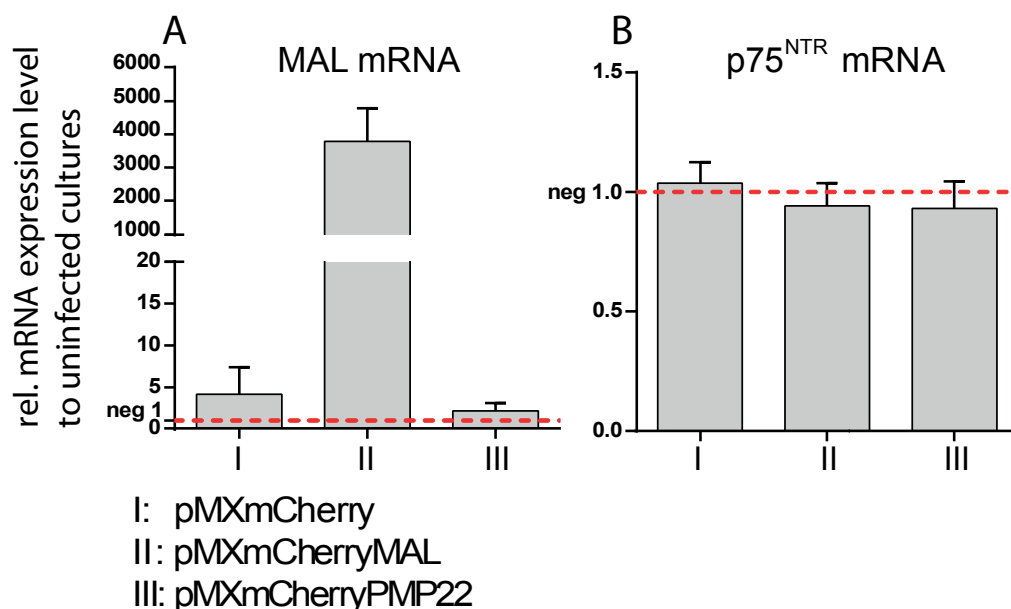


Figure 36 : Strong induction of MAL mRNA upon infection. Rat Schwann cells were either uninfected (neg, red line) or infected with either mCherry (I), mCherryMAL (II) or mCherryPMP22 (III). (A) Infection with pMXmCherryMAL resulted in a strong induction of MAL mRNA, whereas its expression was detected at background levels in uninfected or control-infected cells. (B) The expression of p75^{NTR} was not altered upon infection with neither constructs. Values are normalized to the expression of 60s, and expression levels of uninfected cultures were set to 1. Data represent the mean of at least four independent experiments, and error bars indicate the SEM.

7.2.2.2.4. Sorting of infected rat Schwann cell cultures to obtain a pure MAL-overexpressing cell population

To circumvent the issue of low infection efficiency, infected rat Schwann cell cultures were sorted using FACS methodology. Infected cultures were trypsinized and cells were resuspended in FACS buffer (1% BSA, 500mM EDTA in PBS) to 200cells/200 μ l. The infection marker mCherry was used to identify infected Schwann cells (\approx positive sort) (Figure 37A). In line, noninfected cells were sorted into another tube (\approx negative sort). Using this method, 100% pure populations of infected and noninfected cells were obtained.

Since no appropriate laser was available to excite mCherry at around 590nm, a 488nm laser was used, resulting in a maximal excitation of around 8%. Excitation of mCherry using the

488nm laser was feasible and mCherry signal could be detected (Figure 37B, purple bar). Infected cultures were sorted, resulting in a pure mCherry-positive and a mCherry-negative cell population, confirmed by reanalyzing the sorted samples (Figure 37C).

Using cells of the positive sorts of mCherry-infected and mCherryMAL-infected cultures, the direct effect of MAL overexpression on the expression of p75^{NTR} and P0 was investigated (Figure 37D-F). Despite a pure MAL-overexpressing population was analyzed, no alteration in the expression of p75^{NTR} and P0 could be depicted in MAL-overexpressing Schwann cells (Figure 37D, E). A strong induction of MAL expression was measured in rat Schwann cells infected with pMXmCherryMAL, validating that the infection to overexpress MAL worked (Figure 37F).

Further investigations revealed that infection alone already altered the gene transcription in Schwann cells, indicated by increased mRNA expression of P0 and p75^{NTR} in mCherry-overexpressing Schwann cells compared to uninfected cells (Figure 37G, H). Hence, gene insertion into the genome already affected transcriptional activity of the cells. It is possible that small deregulation caused by MAL overexpression could not be depicted, since infection with the control vector pMXmCherry already affected transcriptional regulation of our target genes. Therefore, retroviral infections of rat Schwann cell cultures were not further investigated.

Based on these findings, we could not determine whether there is a direct link between MAL overexpression and reduced expression of P0 and p75^{NTR}.

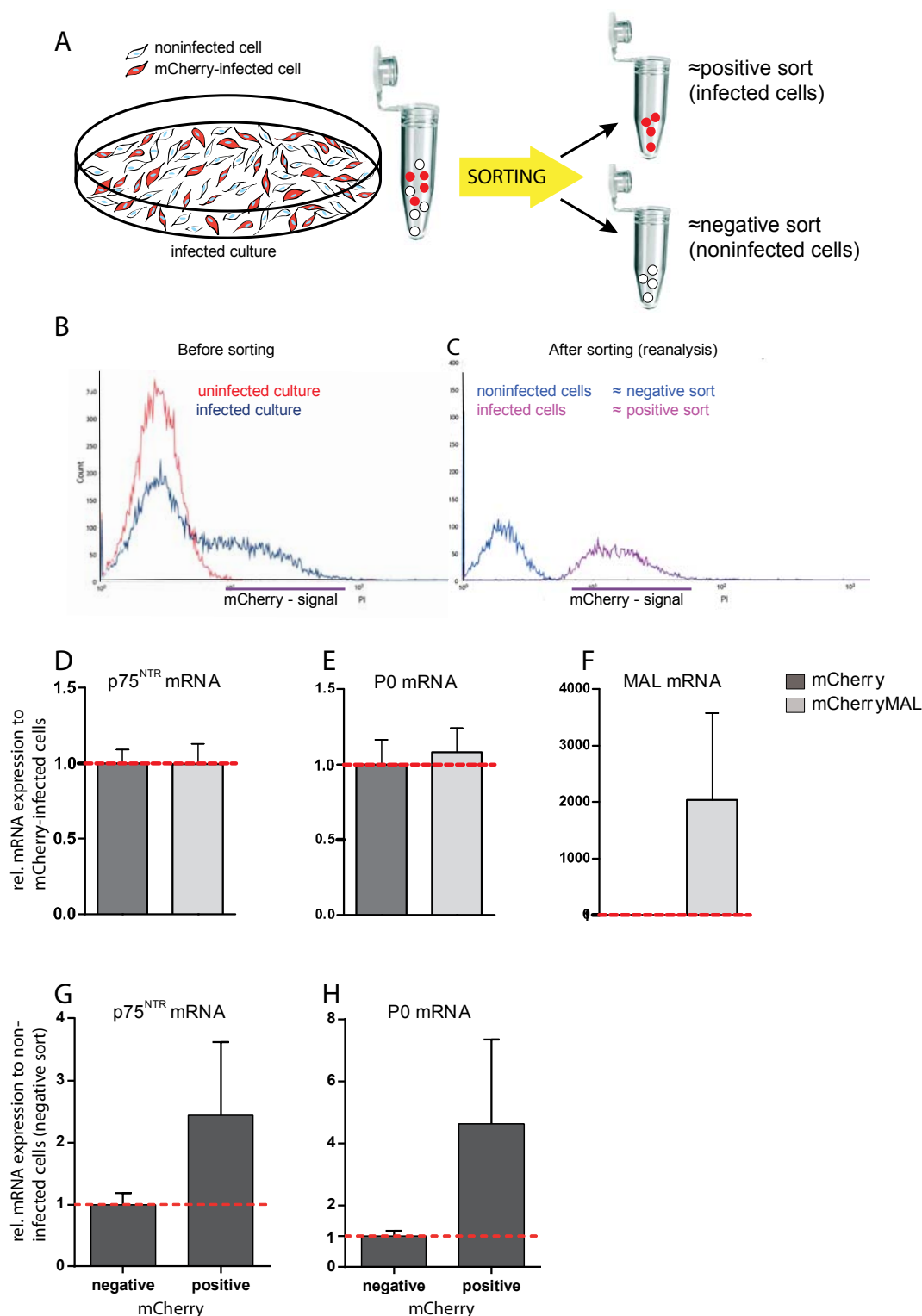


Figure 37: Sorting of infected rat Schwann cell cultures. (A) Using mCherry as an infection marker, infected and noninfected cells were sorted by FACS, resulting in two pure populations. (B) Monoparametric histogram shows the relative cell number on the y-axis and the two cell populations on the x-axis (mCherry positive: purple bar). (C) Reanalysis after sorting confirmed two pure populations of either noninfected or infected cells. (D, E) No altered transcription was detected for P0 and p75^{NTR} upon MAL overexpression. (F) A strong induction of MAL expression was determined upon MAL overexpression. (G, H) Comparison of negative and positive sort of mCherry-infected cultures revealed significantly increased mRNA expression of P0 and p75^{NTR} due to infection with the control vector pMXmCherry. Values are normalized to the expression of 60s, and expression levels of either mCherry-overexpressing samples (D-F) or noninfected samples (G, H) were set to 1. Data represent the mean of five independent experiments, and error bars indicate the SEM.

7.3. Transcriptional regulation induced by cAMP elevation in mouse Schwann cells

7.3.1. Forskolin-induced transcriptional regulation of genes involved in Schwann cell development

One key signaling pathway for Schwann cell differentiation and peripheral myelination is mediated by cAMP levels. This signal transduction pathway can be mimicked *in vitro* by either dibutyryl cAMP or forskolin, an adenylyl cyclase activator. In rat Schwann cell cultures, elevated intracellular cAMP levels by forskolin was shown previously to induce the expression of myelin-related gene (Monuki et al., 1989, Parkinson et al., 2003, Monje et al., 2009). Since rat and mouse Schwann cells were shown to react distinct upon stimulation reagents *in vitro* (Yamada et al., 1995), we investigated the effect of forskolin treatment on gene transcription in primary mouse Schwann cell cultures. Primary Schwann cells isolated from sciatic nerves of P1 mice were cultured in the presence or absence of forskolin for 24 h. We ascertained the optimal forskolin concentration of 20 μ M, resulting in robustly induced gene transcription of myelin protein zero (Mpz/P0), a commonly used marker for Schwann cell differentiation (Figure 16). A whole genome expression assay covering more than 45'000 transcripts was performed to identify transcriptional changes induced by elevated cAMP levels in mouse Schwann cells *in vitro*. 18 samples, comprised by nine independent samples of untreated and forskolin-treated Schwann cells were analyzed. One coding DNA sequence may be represented by several distinct oligonucleotides (called probes). For all examinations, probe-specific analysis was performed, allowing to identify differentially expressed transcripts with high confidence. About 22'000 transcripts were consistently expressed in cultured Schwann cells. To begin with, we analyzed forskolin-dependent transcriptional expression of genes that are implicated in Schwann cell development, differentiation and myelination (Table 7). For illustration, selected genes were schematically represented according to their temporal expression in the Schwann cell lineage (Figure 45).

Common name	Entrez ID	Ratio		Common name	Entrez ID	Ratio	
		20 to 0µM	p-value			20 to 0µM	p-value
A Transcription factor				D Lipid biosynthesis			
Early Growth Response 1 (Krox24)	Egr1	1.68	0.0063	ATP-binding cassette transporter D1	Abcd1	1.02	n.s.
Early Growth Response 2 (Krox20)	Egr2	1.27	n.s.	ATP citrate lyase	Acly	1.10	n.s.
Early Growth Response 3	Egr3	7.26	<0.0001	aldehyde dehydrogenase family 3, subfamily A2	Aldh3a2	1.08	n.s.
Inhibitor of DNA binding 2	Id2	2.12	<0.0001	aldehyde dehydrogenase family 3, subfamily A2	Aldh3a2	1.09	n.s.
Inhibitor of DNA binding 2	Id2	1.37	<0.0001	arylsulfatase A (ASA)	Arsa	1.10	n.s.
Inhibitor of DNA binding 4	Id4	1.98	0.0118	Cyp27a1	Cyp27a1	not detected	
Jun Oncogen (cJun)	Jun	0.62	<0.0001	7-dehydrocholesterol reductase	Dhcr7	1.04	n.s.
Nab1, EGR-1-binding protein 1	Nab1	0.99	n.s.	fatty acid 2-hydroxylase	Fa2h	not detected	
Nab1, EGR-1-binding protein 1	Nab1	1.05	n.s.	fatty acid binding protein 7 (Bibp, Bfabp)	Fabp7	not detected	
Nab1, EGR-1-binding protein 1	Nab1	0.98	n.s.	fatty acid synthase	Fasn	not detected	
Nab1, EGR-1-binding protein 1	Nab1	1.11	n.s.	galactose-3-O-sulfotransferase 1 (Cst, Gcst)	Gal3st1	1.30	n.s.
Nab2, EGR-1-binding protein 2	Nab2	1.36	<0.0001	galactosylceramidase	Galc	1.04	n.s.
Paired Box Gene 3	Pax3	not detected		glyceronephosphate O-acyltransferase (Dhapat)	Gnpat	0.99	n.s.
POU Domain, class 3, TF 1 (Oct6, SCIP)	Pou3f1	4.38	0.0181	3-hydroxy-3-methylglutaryl-Coenzyme A reductase	Hmgcr	0.95	n.s.
SRY-box Containing Gene 10	Sox10	1.05	n.s.	phytanoyl-CoA hydroxylase	Phyh	not detected	
SRY-box Containing Gene 2	Sox2	0.88	n.s.	sphingosine-1-phosphate receptor 1 (S1p)	S1pr1	not detected	
SRY-box Containing Gene 2	Sox2	0.93	n.s.	SREBP cleavage activating protein	Scap	1.15	n.s.
AP2α	Tcfap2a	0.75	0.0133	stearoyl-Coenzyme A desaturase 1 (Scd)	Scd1	1.61	<0.0001
AP2α	Tcfap2a	0.82	0.0139	sphingomyelin phosphodiesterase 1	Smpd1	0.95	n.s.
Yin Yang 1	Yy1	not detected		sphingomyelin phosphodiesterase 1	Smpd1	1.20	n.s.
B Receptor				sphingomyelin phosphodiesterase 1	Smpd1	1.20	n.s.
v-Erb-b2 Erythroblastic Leukemia Viral Oncogene 2	Erbb2	1.34	0.0073	sterol regulatory element binding transcription factor 1	Sreb1	1.12	n.s.
v-Erb-b2 Erythroblastic Leukemia Viral Oncogene 3	Erbb3	not detected		sterol regulatory element binding factor 2 (SREBP-2)	Sreb2	1.03	n.s.
G protein-coupled receptor 126	Gpr126	1.15	n.s.	sterol regulatory element binding factor 2 (SREBP-2)	Sreb2	1.01	n.s.
Nerve Growth Factor Receptor (p75^{NTR})	Ngfr	0.89	0.0123	UDP-glucose ceramide glucosyltransferase (Gcs)	Ugcg	1.18	0.0078
Nerve Growth Factor Receptor (p75 ^{NTR})	Ngfr	0.92	n.s.	UDP-glucose ceramide glucosyltransferase (Gcs)	Ugcg	1.22	0.0172
Nerve Growth Factor Receptor (p75 ^{NTR})	Ngfr	0.92	n.s.	UDP galactosyltransferase 8A (Cgt, mCerGT)	Ugt8a	1.16	0.0126
Neurotrophic Tyrosine Kinase, Receptor 2 (TrkB)	Ntrk2	1.26	0.0045	E Varia			
Neurotrophic Tyrosine Kinase, Receptor 3 (TrkC)	Ntrk3	1.29	0.0018	Cadherin19	Cdh19	0.59	0.0003
Neurotrophic Tyrosine Kinase, Receptor 3 (TrkC)	Ntrk3	1.26	0.0068	Cadherin19	Cdh19	0.62	0.0021
C Myelin				Cadherin2 (Ncad)	Cdh2	0.80	0.0010
2',3'-cyclic nucleotide 3' phosphodiesterase	CNP	1.02	n.s.	Disks Large Homolog 1	Dlg1	not detected	
2',3'-cyclic nucleotide 3' phosphodiesterase	CNP	1.18	n.s.	Dedicator of Cytokinesis Protein 7	Dock7	0.99	n.s.
Gap Junction Protein α1 (Connexin 43)	Gja1	1.80	0.0023	Dedicator of Cytokinesis Protein 7	Dock7	1.12	n.s.
Gap Junction Protein α4 (Connexin 37)	Gja4	not detected		Dystrophin-related Protein 2	Drp2	1.08	n.s.
Gap Junction Protein β1 (Connexin 32)	Gjb1	not detected		Endothelin	Edn1	0.44	n.s.
Gap Junction Protein β2 (Connexin 26)	Gjb2	1.33	n.s.	Growth Associated Protein 43	Gap43	0.50	<0.0001
Gap Junction Protein γ3 (Connexin 29)	Gjc3	not on the array		Glial Fibrillary Acidic Protein	Gfap	1.10	n.s.
Lipin 1	Lpin1	1.37	0.0008	Glial Fibrillary Acidic Protein	Gfap	1.52	0.0041
Lipin 1	Lpin1	1.32	0.0004	Histone Deacetylase	HDAC1	not on the array	
Myelin-Associated Glycoprotein	Mag	0.98	n.s.	Histone Deacetylase	HDAC2	0.93	n.s.
Myelin and Lymphocyte Protein	Mal	1.06	n.s.	Leucine-Rich Repeat LGI family, Member 4	Lgi4	1.26	0.0105
Myelin and Lymphocyte Protein	Mal	1.37	n.s.	Leucine-Rich Repeat LGI family, Member 4	Lgi4	1.87	0.0002
Myelin Basic Protein (variant 1-7)	Mbp	0.10	<0.0001	Membrane Protein, Palmitoylated 5 (Pals1)	Mpp5	0.95	n.s.
Myelin Basic Protein (variant 1, 2, 4)	Mbp	0.80	<0.0001	Partitioning Defective 3 Homolog (Par3)	Pard3	1.02	n.s.
Myelin Basic Protein (variant 8)	Mbp	0.92	n.s.	Partitioning Defective 3 Homolog (Par3)	Pard3	1.03	n.s.
Myelin Basic Protein (variant 1-8)	Mbp	0.40	<0.0001	Partitioning Defective 3 Homolog (Par3)	Pard3	1.04	n.s.
Myelin Protein Zero (P0)	Mpz	3.41	0.0001	Phosphatase and Tensin Homolog	Pten	0.99	n.s.
Myelin Protein Zero (P0)	Mpz	1.12	n.s.	Phosphatase and Tensin Homolog	Pten	1.12	n.s.
Neurofascin	Nfasc	not detected		RAS-Related C3 Botulinum Substrate 1	Rac1	0.91	n.s.
Plasmolipin	Plip	0.64	0.0018	Ras Homolog Family Member A	Rhoa	not detected	
Peripheral Myelin Protein 2	Pmp2	0.98	n.s.	Ras Homolog Family Member B	Rhob	1.05	n.s.
Peripheral Myelin Protein 22	Pmp22	1.51	n.s.	S100 β	S100b	not detected	
Peripheral Myelin Protein 22	Pmp22	1.52	0.0037				
Periaxin	Prx	not detected					

Table 7: Differential gene expression analysis on transcripts known in Schwann cells. The expression levels of gene transcripts, which are important for Schwann cell development, differentiation and myelination were analyzed. The strongest induced mRNA expression levels were detected for Pou3f1, Egr3 and Mpz. *: note that Mbp variants 7 and 8 are coding for Golli-Mbp, and are not expressed in myelin. Data are based on a two-way ANOVA and unadjusted p-values < 0.01 were accounted as significant.

Analysis of transcription factors revealed that activation of the adenylyl cyclase by forskolin strongly induced the mRNA expression levels of Oct6 (Pou3f1, Table 7A), a major target of cAMP signaling in Schwann cells (Monuki et al., 1989). Increased transcription was also detected for Krox24 (Egr1), Egr3, the Egr1-binding protein 2 (Nab2) and for the inhibitor of DNA binding 2 and 4 (Id2, Id4). A slightly, but not significant, increased expression could be detected for Krox20 (Egr2), in line with data derived from qRT-PCR (Figure 17B). In addition, forskolin treatment reduced the mRNA expression levels of the transcription factors AP2 α (Tcfap2a) and cJun (Jun), which is in line with their expression in neural crest cells, Schwann cell precursors and immature Schwann cells, respectively, and downregulation during development (reviewed in Jessen and Mirsky, 2005). For Sox10, which is expressed during the whole Schwann cell lineage, no forskolin-dependent regulation was observed. Investigation of receptors, which were implicated in Schwann cell signaling, revealed that the expression levels of the tyrosine kinase receptors ErbB2, TrkB (Ntrk2) and TrkC (Ntrk3) were significantly increased by forskolin treatment (Table 7B).

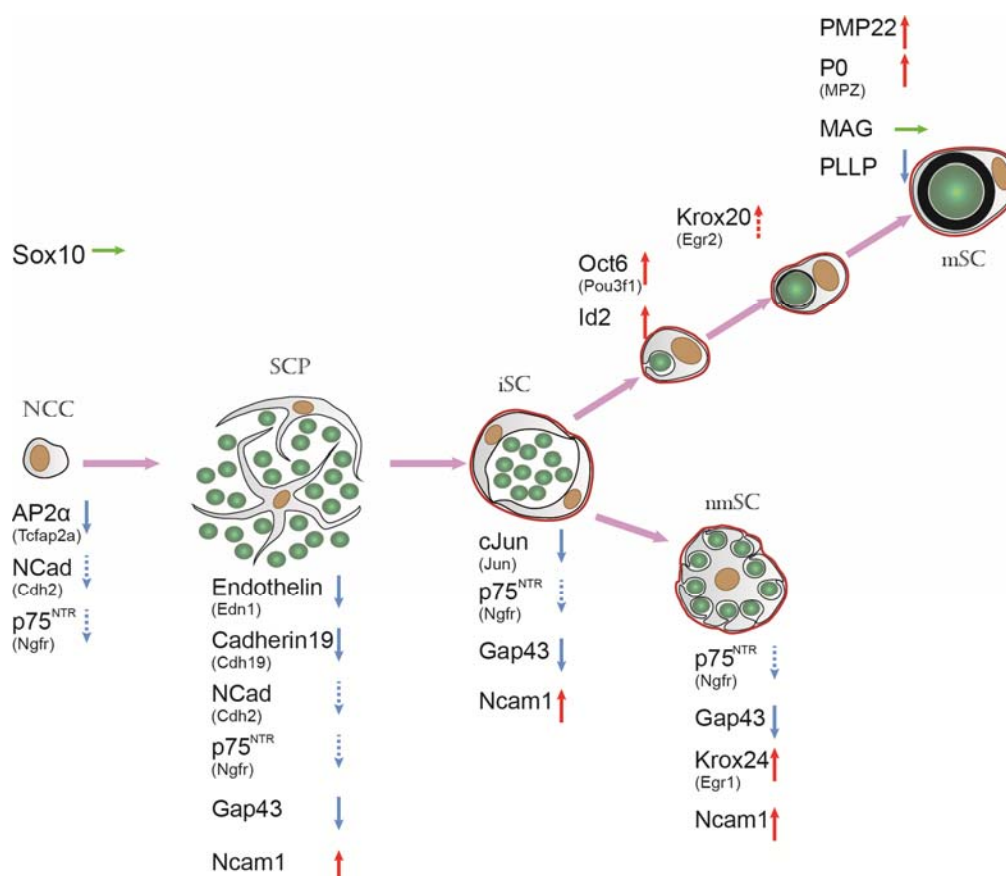


Figure 38: Schematic illustration of genes implicated in the Schwann cell lineage. Selected genes of Table6, which are specific for a distinct Schwann cell stage, were schematically grouped. Genes implicated in neural crest cells, Schwann cell precursors or immature Schwann cells showed reduced mRNA expression levels upon forskolin treatment (blue arrows), whereas increased expression could be detected for some myelin-related genes (red arrows). Dashed arrows indicate only slightly differentially expressed transcripts. Red line: Basal lamina. NCC: Neural crest cell, SCP: Schwann cell precursor, iSC: immature Schwann cell, mSC: myelinating Schwann cell, nmSC: nonmyelinating Schwann cell. Figure adapted to Jessen et al., 2005.

Forskolin treatment resulted also in increased transcription of the myelin-related genes *Mpz*, peripheral myelin protein 22 (*Pmp22*) and *lipin1* (*Lpn1*) (Table 7C). No transcriptional induction could be detected for 2',3'-cyclic nucleotide 3' phosphodiesterase (*Cnp*), the myelin-associated glycoprotein (*Mag*) and the myelin and lymphocyte protein (*Mal*). However, reduced expression levels of plasmalipin (*Plip*) and myelin basic protein (*Mp*) were detected in treated Schwann cells, which was not expected (Gillen et al., 1996, Lemke and Chao, 1988, Monje et al., 2009). Sequence analysis of the *Mbp* probes revealed that they code also for Golli *Mbp* variants that have a distinct expression pattern and function during glia development compared to classical MBP isoforms (Campagnoni et al., 1993, Pribyl et al., 1996). The expression levels of periaxin (*Prx*) and neurofascin (*Nfasc*) were not detected.

During myelination, the synthesis of lipids is important for accurate myelin formation. We analyzed transcripts involved in lipid biosynthesis in Schwann cells in order to investigate whether they are differentially expressed upon forskolin-treatment *in vitro* (Table 7D). Significantly increased transcription levels were detected for the stearoyl-Coenzyme A desaturase 1 (*Scd1*) and the UDP-glucose ceramide glucosyltransferase (*Ugcg*, also known as *Gcs*). Further, also UDP galactosyltransferase 8A (*Ugt8a*, also known as *Cgt* and *mCerGT*), the rate-limiting enzyme of the cerebroside biosynthesis, showed increased transcription due to elevation of intracellular cAMP levels by forskolin.

Our data analysis revealed that forskolin treatment induces differential expression of a particular set of genes in cultured Schwann cells that are implicated in Schwann cell differentiation *in vivo*. In particular, forskolin treatment led to reduced expression of genes that are expressed in neural crest cells and Schwann cell precursors, such as *AP2 α* , endothelin (*Edn1*), cadherin 19 (*Cdh19*) and *Gap43*, known to be downregulated during Schwann cell differentiation (reviewed in Jessen and Mirsky, 2005). Otherwise, a number of transcripts known to play a role in Schwann cell differentiation *in vivo*, such as *Oct6*, *MPZ*, *ErbB2*, *TrkB* and *TrkC* were increased upon forskolin treatment in cultured Schwann cells. Still, the expression levels of other transcripts known to be induced during Schwann cell differentiation were not altered, suggesting that their activation might occur independently.

7.3.2. General forskolin-induced transcriptional regulation in Schwann cells

To further investigate the effect of forskolin on transcriptional regulation in cultured mouse Schwann cell, microarray data were analyzed using a false discovery rate (FDR)-adjusted p-value of < 0.05 . This study revealed that 330 transcripts were upregulated by at least 1.5-fold, whereas 305 transcripts were downregulated due to forskolin treatment (Appendix I). The myelin protein *Mpz* was identified among the 25 strongest induced genes, confirming forskolin-induced Schwann cell differentiation *in vitro* (Table 8A). The strongest transcriptional induction was detected for the sclerostin domain containing 1 (*Sostdc1*), the pleckstrin homology domain containing family A (*Plekha4*) and the extracellular matrix protein spondin 2 (*Spon2*). Further, a highly significant increase in transcription was identified for the transcription factor *Egr3*, the fibroblast growth factor 7 (*Fgf7*), the transforming growth factor beta receptor III (*Tgfbr3*), the endothelin receptor type B (*Ednrb*), as well as for the proteoglycan decorin (*Dcn*).

Strongest downregulation due to forskolin treatment was detected for the mRNA expression of protocadherin 20 (*Pcdh20*, also known as *Pcdh13*), phosphodiesterase 1B (*Pde1b*) and leucin-rich repeats and transmembrane domains 1 (*Lrtm1*), each represented by two transcripts (Table 8B). The oligodendrocytes transcription factor 1 (*Olig1*) was the only transcription factor identified among the 25 strongest reduced transcripts. Strong transcriptional reduction was also identified for the chondroitin sulfate proteoglycan 4 (*Cspg4*, also known as neuron-glia antigen 2 (NG2)), the proteoglycan aggrecan (*Acan*), and the secreted matrix Gla protein (*Mgp*). The platelet-derived growth factor subunit B (*Pdgfb*) was also shown to be strongly reduced in forskolin-treated Schwann cells.

In summary, cAMP elevation led to differential expression of more than 600 transcripts in primary mouse Schwann cell cultures. Among the 25 strongest induced genes, *Mpz* was the only typically so far known myelin-related gene, disclosing the possibility that new genes important for Schwann cell differentiation were identified by this microanalysis.

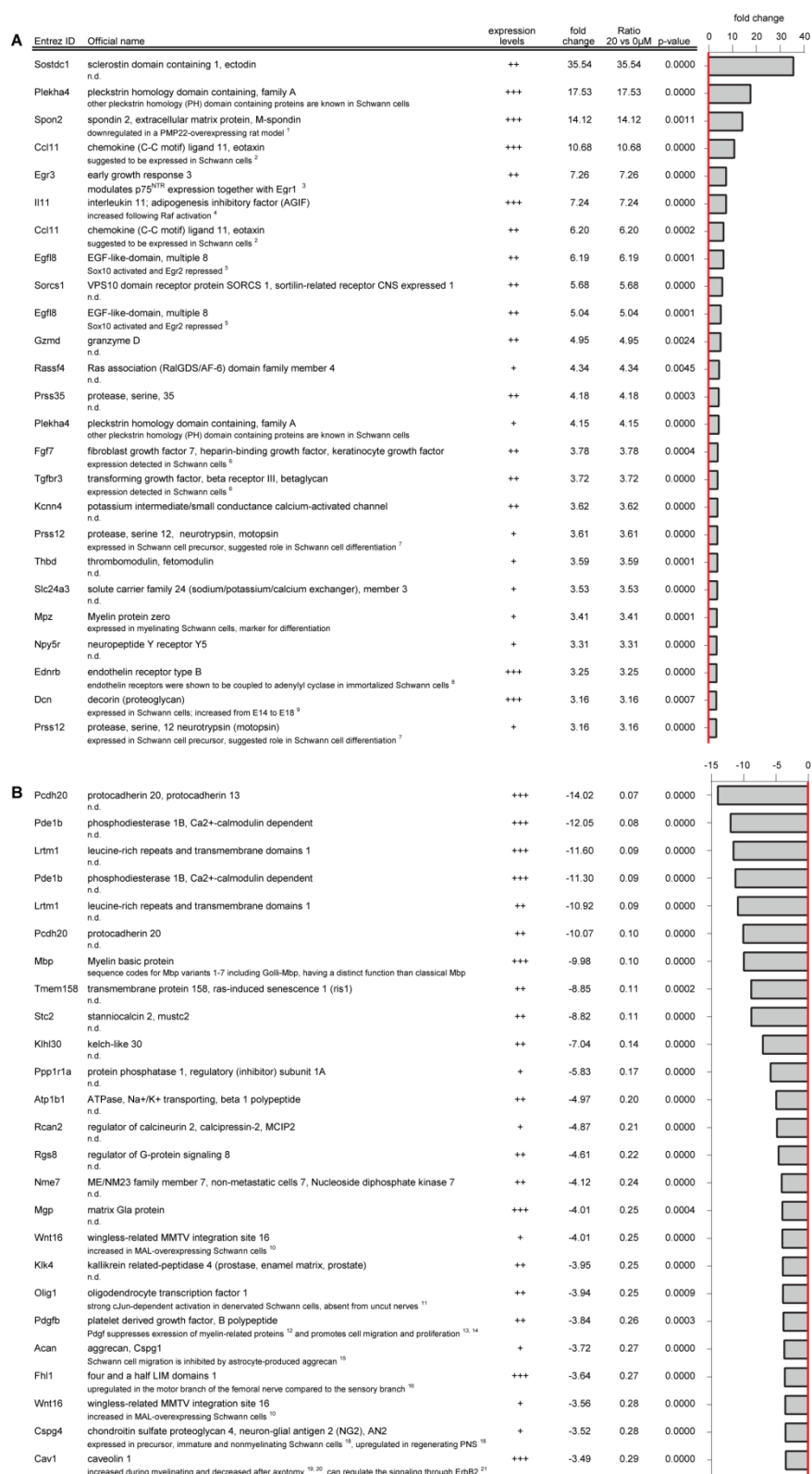


Table 8: The most highly differentially regulated transcripts by forskolin. Microarray data of Schwann cells cultured in the presence or absence of forskolin were analyzed using a two-way ANOVA with an FDR-adjusted p-value < 0.05. The 25 transcripts with the strongest increased (A) or reduced (B) mRNA expression levels in treated Schwann cells were itemized. The fold change was graphically illustrated. n.d.: not determined. Expression levels in Schwann cells are indicated y +, ++, or +++. ¹Vigo et al., 2005 ²Yang et al., 1998 ³Gao et al., 2007 ⁴Napoli et al., 2012 ⁵Srinivasan et al., 2012 ⁶Thomas and de Vries, 2007 ⁷Wolfer et al., 2001 ⁸Wilkins et al., 1997 ⁹Hanemann et al., 1993 ¹⁰Schmid et al., 2013, submitted for publication ¹¹Arthur-Farraj et al., 2012 ¹²Ogata et al., 2004 ¹³De Donatis et al., 2008 ¹⁴Jiang et al., 2013 ¹⁵Monje et al., 2009 ¹⁶Afshari et al., 2010 ¹⁷Jesuraj et al., 2012 ¹⁸Schneider et al., 2001 ¹⁹Rezajooi et al., 2004 ²⁰Mikol et al., 1999 ²¹Mikol et al., 2002 ²²Tan et al., 2002

7.3.3. Olig1 expression in the peripheral nervous system

Olig1 was among the 25 strongest downregulated transcripts caused by forskolin treatment. While Olig1 is known to play an important functional role in differentiation of oligodendrocytes precursor cells (Li et al., 2007), its role in Schwann cell development is not well known. Immunofluorescent microscopy localized Olig1 expression in the cytoplasm of cultured mouse Schwann cells, identified by p75^{NTR} (Figure 39).

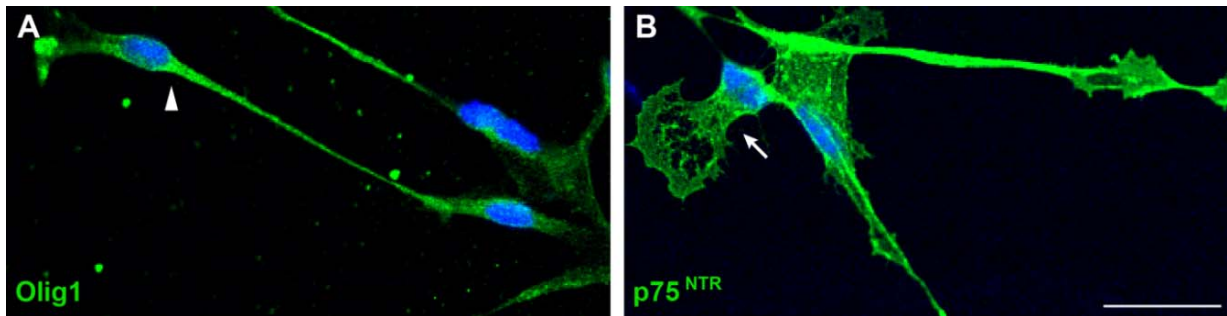


Figure 39: p75^{NTR} and Olig1 expression in primary mouse Schwann cell cultures. (A) Olig1 expression was mainly detected in the cytoplasm of cultured Schwann cells (arrowhead). (B) p75^{NTR} was strongly expressed within the plasma membrane of cultured Schwann cells (arrow). Bar: 20 μ m

Immunofluorescent colocalization analysis of P7 sciatic nerves revealed Olig1 immunofluorescent signal primarily in MBP-negative areas consisting of small diameter axons identified by neurofilament (Figure 40A, insert and Figure 40B, arrows). These areas are reminiscent of Remak bundles evident by the expression of p75^{NTR}, a marker for nonmyelinating Schwann cells (Figure 41A, insert, arrow). On longitudinal nerve sections, p75^{NTR}-positive Schwann cells were associated with multiple unmyelinated, small caliber fibers (Figure 41B, arrows), whereas Schwann cells myelinating large caliber MBP-positive fibers did not express p75^{NTR} (Figure 41B, arrowheads). Our data demonstrate a comparable expression pattern of Olig1 with p75^{NTR} in Schwann cells *in vitro* and *in vivo*, suggesting a role in immature and in nonmyelinating Schwann cells.

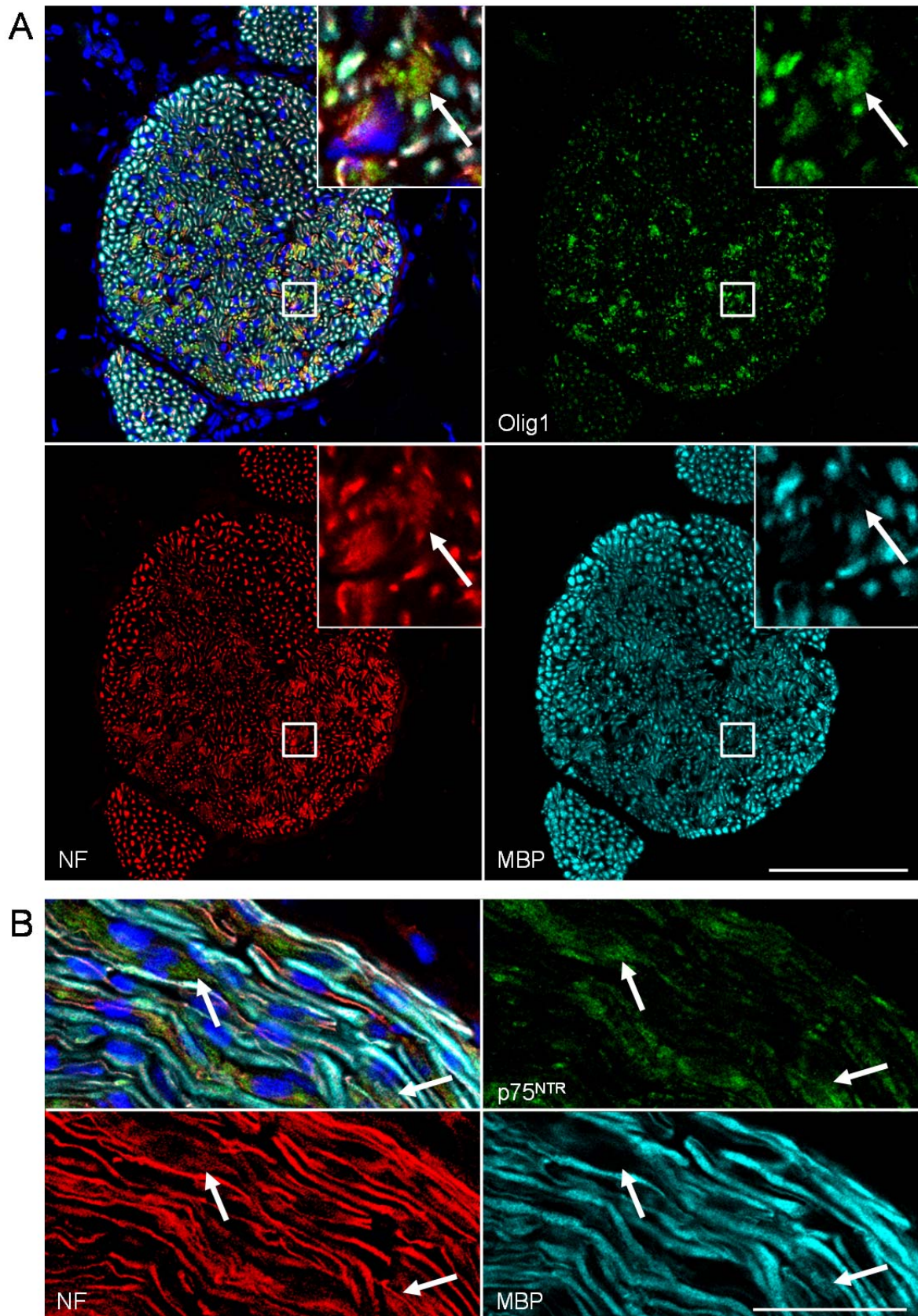


Figure 40: Localization of Olig1 in nonmyelinating Schwann cells. Immunofluorescent stainings of transversal (A) and longitudinal (B) tissue sections of sciatic nerves from P7 mice revealed Olig1 immunofluorescence in Remak bundles, which were identified by a bundle of unmyelinated (MBP-negative) small diameter axons (arrows). NF: neurofilament. Bar: A: 100 μ m, B: 20 μ m

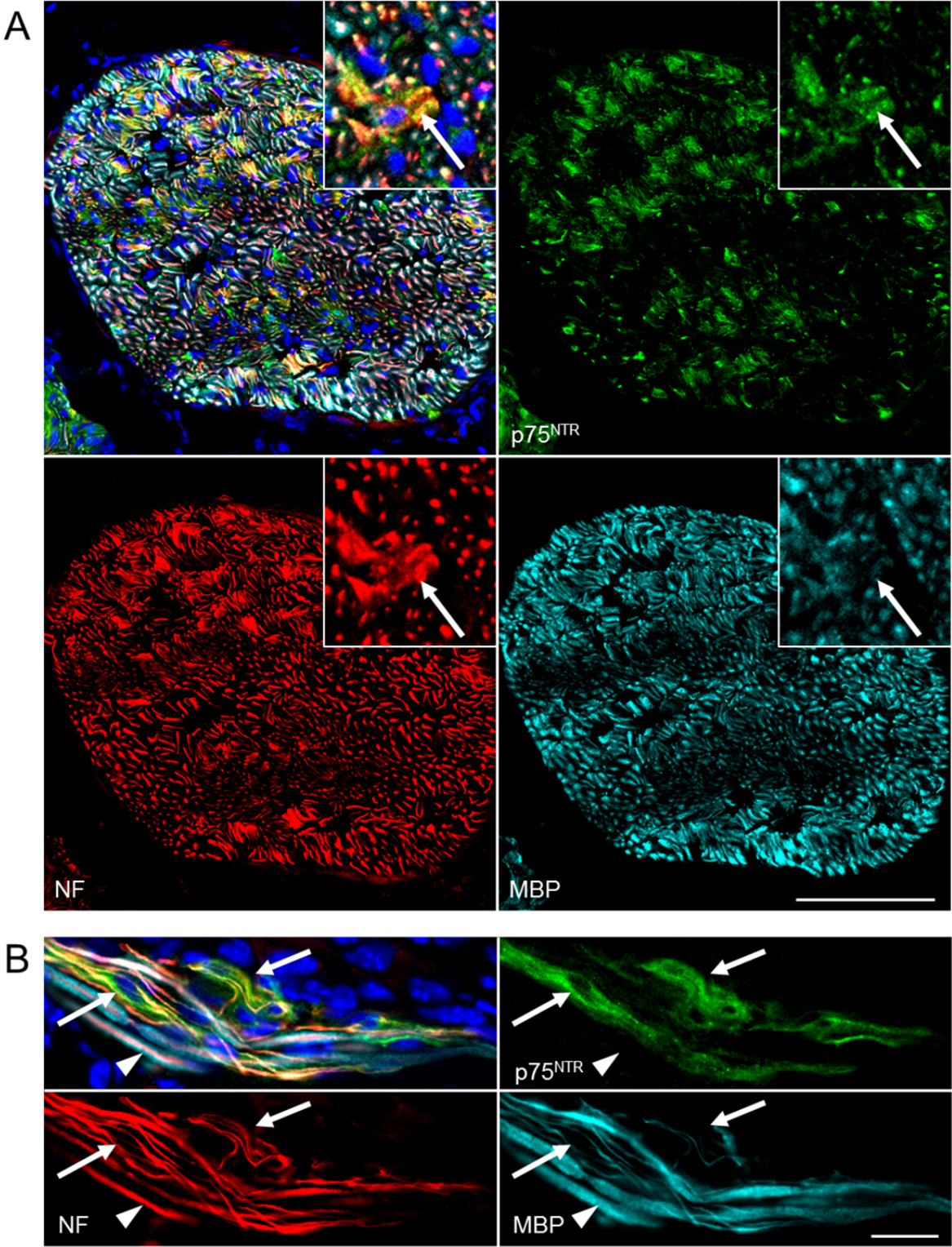


Figure 41: Localization of p75^{NTR} in nonmyelinating Schwann cells. Immunofluorescent stainings of transversal (A) and longitudinal (B) tissue sections of sciatic nerves from P7 mice revealed p75^{NTR} immunofluorescence in nonmyelinating Schwann cells (arrows) localized around a bundle of small diameter axons. Myelinating Schwann cells were p75^{NTR}-negative (arrowheads). NF: neurofilament. Bar: A: 100µm, B: 20µm

7.3.4. Analysis of possible target regulators

Putative forskolin-dependent upstream regulators were identified by the interactive pathway analysis (IPA) of Ingenuity Systems, based on the highly significantly deregulated transcripts (Appendix I). The highest significantly proposed upstream regulator was identified as “forskolin”, validating the stimulation assay (

Table 9). Further, three kinases playing a role in regulation of the NF- κ B pathway were suggested as upstream regulators, namely the inhibitor of NF- κ B kinase subunit α (CHUK), the I- κ B kinase subunit γ (IKBKG) and the I- κ B kinase subunit β (IKKB). These findings validate the stimulation assay, since the transcription factor NF- κ B was demonstrated as a target gene of the PKA (Yoon et al., 2008). In addition, the signal transducer and activator of transcription 3 (Stat3) was proposed to be involved in the regulation of some of the identified differentially expressed genes. Also the transcription factor Sox10 was suggested as an upstream regulator of forskolin-dependent differentially expressed gene transcripts, such as Mpz and Pmp22.

Upstream regulator	Common name	Predicted activation state	Activation z-score	p-value of overlap
forskolin		Activated	2.508	3.90E-15
CHUK	Inhibitor of nuclear factor kappa-B kinase subunit alpha	Activated	2.387	4.83E-15
IKBKG	Inhibitor of kappaB kinase subunit gamma	Activated	2.982	1.61E-13
IKKB	Inhibitor of kappaB kinase subunit beta	Activated	2.985	1.21E-10
STAT3	Signal transducer and activator of transcription 3	Activated	2.462	8.81E-07
CEBPB	C/EBP-beta, NF-IL6	Activated	2.201	5.81E-06
SOX10	SRY-box containing gene 10	Activated	2.200	1.57E-05
HOXC8	Homeobox C8	Activated	2.000	6.41E-03
Tnf (family)	Tumor necrosis factor	Activated	2.132	9.84E-03
HOXC6	Homeobox C6	Activated	2.000	1.51E-02
ZNF217	Zinc finger protein 217	Activated	2.236	3.36E-02
PTPRJ	Protein tyrosine phosphatase, receptor type, J	Activated	2.000	4.33E-02
NOTCH1	Notch1	Inhibited	-2.318	8.05E-06
SRF	Serum response factor	Inhibited	-2.668	1.12E-05
TGFB3	Transforming growth factor, beta 3	Inhibited	-2.559	3.31E-05
KLF4	Kruppel-like factor 4	Inhibited	-2.599	5.93E-04
Nfat (family)	Nuclear factor of activated T cells	Inhibited	-2.121	6.60E-04
LYN	Yamaguchi sarcoma viral (v-yes-1) oncogene homolog	Inhibited	-2.186	4.21E-03
RAC1	RAS-related C3 botulinum substrate 1	Inhibited	-2.173	5.11E-03
MAP2K1/2	Mek1/2	Inhibited	-2.177	9.43E-03
MKL1	MKL (megakaryoblastic leukemia)/myocardin-like 1	Inhibited	-2.160	1.26E-02
SFTPA1	Surfactant associated protein A1	Inhibited	-2.200	3.19E-02
IKZF1	IKAROS family zinc finger 1	Inhibited	-2.433	3.92E-02

Table 9: Investigation of putative upstream regulators. Differentially expressed transcripts in differentiated Schwann cells were analyzed in respect to their potential upstream regulators. As expected, forskolin was proposed as the most significant target regulator.

We further investigated which target regulators might have been inhibited due to the elevation of intracellular cAMP. Notch1 was identified as the most significant inhibited upstream regulator. This observation is well in line with the negative effect of Notch signaling on peripheral myelination (Woodhoo et al., 2009). In addition, inhibitory modulation was proposed for the serum response factor (SRF), which was implicated in the

binding to the serum response element (SRE). Further, also the small GTP binding protein Rac1 was proposed as an inhibitory upstream regulator, as well as the MAP2-kinases MEK1 and 2.

An important question is whether there are putative transcription factor binding sites in promoter regions of coregulated genes, allowing to identify transcription factors that might cause some of the observed alterations. Using TransFind, a web-based software tool, the affinity of a transcription factor to the putative promoters of the genes (-300 to +100) was predicted *in silico* (Kielbasa et al., 2010). First, genes with induced mRNA expression levels due to forskolin were analyzed (Table 10A). Data analysis revealed that three transcription factor matrixes were overrepresented in the set of induced transcripts. The most significant prediction was for the matrix of KROX transcription factors, identified in 14 out of 252 genes ($p < 0.000025$). The KROX family contains Krox24 (Egr1), Krox20 (Egr2), Egr3 and NGFI-C (Egr4) and the distally related Wilms' tumor 1 (WT1) (Chavrier et al., 1988, Lemaire et al., 1988, Call et al., 1990, Gessler et al., 1990, Patwardhan et al., 1991, Crosby et al., 1992). In addition to KROX, binding sites for the transcription factors spermatogenic leucine zipper 1 (Spz1) and Wilms' tumor 1 (Wt1) were significantly overrepresented in forskolin-induced genes. We could further identify that several genes with reduced mRNA expression levels due to forskolin contain a binding site for the transcription factor HeLa E-box binding protein (HEB, also known as REB or transcription factor 12, Tcf12) or the myocyte enhancer factor-2 (MEF-2) (Table 10B).

A Positive set: Increased due to forskolin treatment

Rank	TF matrix i	p-value	FDR	Hits in positive set	Hits in negative set
1	KROX_Q6	<0.0001	0.01	14 (5.55%) ^a	486 (1.43%) ^b
2	SPZ_01	0.0004	0.03	12 (4.76%)	488 (1.43%)
3	WT1_Q6	0.0004	0.03	12 (4.76%)	488 (1.43%)

Supporting transcripts of positive set:

- 1 Twist2, Kif26a, Pik3r1, Ctcb, Emb, Cacna1h, Bcl2l11, Slc24a, Crabp2, Olfml3, Camk2n1, Reln, Fgfr1, Crif1
- 2 Bmp4, Emb, Clcf1, Scd1, Camk2n1, Cxcl1, Tgfb3, Tcf3, Ybx, Il11, Crif1
- 3 Twist2, Appl2, Aatk, Col14a1, Emb, Pde10a, Slc24a3, Tgfb3, Il11, Crif1

B Positive set: Decreased due to forskolin treatment

Rank	TF matrix i	p-value	FDR	Hits in positive set	Hits in negative set
1	HEB_Q6	0.0001	0.01	13 (4.94%)	487 (1.43%)
2	MEF2_Q6_01	0.0001	0.01	13 (4.94%)	487 (1.43%)

Supporting transcripts of positive set:

- 1 Des, Lypd1, Slamf9, Plxna2, Igf1, A530088H08Rik (Pirt), Mef2c, Leprel1, Cdkn1a, Klk8, Galnt4, Spbs4, Tmem158
- 2 Gpbar1, Igf1, Tcap, Hdac5, D030072B18Rik (Hdac9), Ckb, Hist1h2af, Hspb3, Myom1, Jun, Csrp3, Inpp1, 2610524A10Rik (Dzip1)

Table 10: Promoter analysis to investigate significantly enriched transcription factor binding sites. Three putative transcription factor binding sites could be identified for gene transcripts increased due to forskolin treatment (A), whereas two putative binding sites could be detected for decreased gene transcripts (B). TF: Transcription factor. ^a number and percentage of genes that contain specific transcription factor binding site among submitted transcripts; ^b number and percentage of genes that contain specific transcription factor binding site among all genes.

7.3.5. GO-annotation analysis in differentiated Schwann cells

The usage of gene ontology (GO) annotations allows analyzing differentially expressed genes by means of a controlled vocabulary. Gene transcripts that were deregulated due to forskolin treatment were analyzed in respect to the categories of cellular components, molecular functions and biological processes (illustrated in Figure 42; data from Table 11).

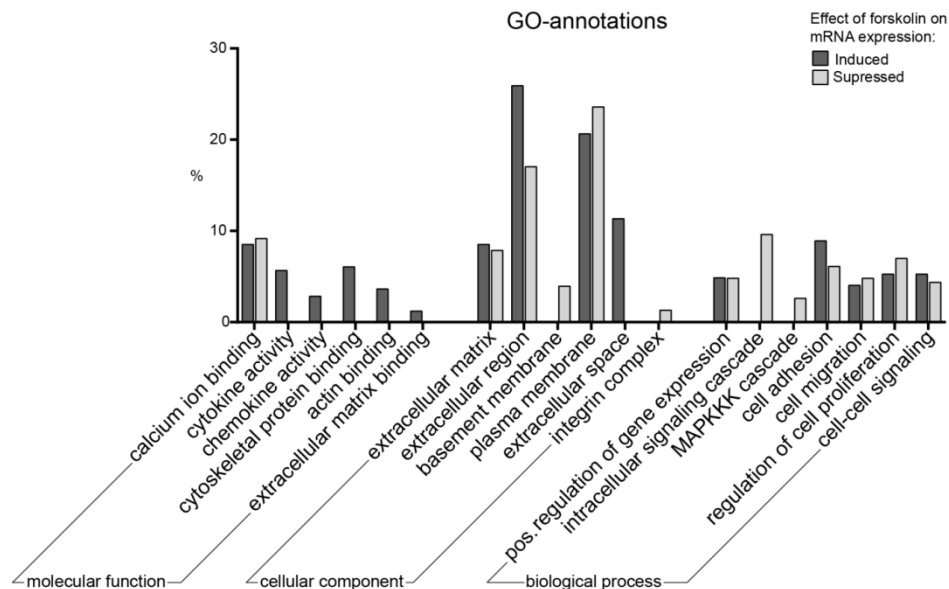


Figure 42: GO-annotation analysis of differentially expressed genes due to forskolin. Analysis of molecular functions revealed that several transcripts increased with forskolin are associated with cytoskeletal protein and actin binding. Both sets of transcript either increased or decreased due to forskolin manifested association to the cellular component of extracellular matrix and to plasma membrane. The term of basement membrane and integrin complex was exclusively enriched in forskolin-reduced transcripts. GO-annotation analysis of transcripts decreased with forskolin showed an enrichment of genes implicated in intracellular signaling cascade and in the MAPKK cascade.

Analysis of molecular functions revealed that forskolin-induced transcripts were associated with cytoskeletal protein binding, actin binding and extracellular matrix binding. Further, induced transcripts were associated with cytokine and chemokine activity. The annotation of calcium ion binding is represented in both sets of transcripts, with either induced or reduced mRNA expression levels due to forskolin. Investigation of GO-annotations on cellular components revealed a high association of both sets of transcripts with the extracellular region and with the plasma membrane. In addition, several differentially expressed transcripts were associated with the extracellular matrix. In contrast to induced transcripts, genes with reduced mRNA expression levels due to forskolin showed enrichment for the annotations basement membrane and integrin complex. We could identify that both increased and decreased transcripts were associated with cell adhesion, migration and proliferation, as well as cell-cell signaling. Further, the terms of intracellular signaling cascade and MAPKKK cascade were detected only in the set of transcripts with reduced expression.

A Induced gene transcripts**Molecular Function**

Category	Identification	Term	Count	%	p-value
GOTERM_MF_FAT	GO:0005509~	calcium ion binding	21	8.50	6.26E-03
<small>GAINT2, SVEP1, NCAID, NID1, MMP15, DLK1, SLIT2, NID1, SUT3, SLIT3, THBD, GNPTAB, SLC24A3, CACNA1H, RELN, EGFL8, VCAN, SPON2, ENTDP2, PROS1, DST, AOC3</small>					
GOTERM_MF_FAT	GO:0005125~	cytokine activity	14	5.67	4.13E-07
<small>BMP4, CXCL1, IL6, GDF1, CXCL1, IL33, KITL, CXCL12, CCL7, IL11, CCL11, CXCL14, PPBP, CLCF1</small>					
GOTERM_MF_FAT	GO:0008009~	chemokine activity	7	2.83	9.46E-06
<small>CCL11, CXCL1, CXCL14, PPBP, CXCL1, CXCL12, CCL7</small>					
GOTERM_MF_FAT	GO:0008092~	cytoskeletal protein binding	15	6.07	8.96E-04
<small>CLMN, BCL2L1, FARP2, CORO2B, FMN2, TRIM2, SYN1, TMOO2, MFAP2, EPR4, IL14B, CLASP1, LOC100044177, ADD3, DST, SYNPO</small>					
GOTERM_MF_FAT	GO:0003779~	actin binding	9	3.64	3.25E-02
<small>CORO2B, FMN2, SYN1, CLMN, TMOO2, LOC100044177, DST, ADD3, SYNPO</small>					
GOTERM_MF_FAT	GO:0050840~	extracellular matrix binding	3	1.21	4.27E-02
<small>NID1, DCN, SHH</small>					

Cellular Component

Category	Identification	Term	Count	%	p-value
GOTERM_CC_FAT	GO:0031012~	extracellular matrix	21	8.50	7.29E-09
<small>BMP4, MATN2, FMOD, CTRHC1, LUM, ADAMTS15, NID1, MMP15, DCN, PRELP, LAMA1, COL14A1, CRISPLD2, PTN, TGFB3, RELN, MFAP2, VCAN, SPON2, ENTDP2, PRSS12</small>					
GOTERM_CC_FAT	GO:0005576~	extracellular region	64	25.91	1.97E-15
<small>CTRHC1, AEBP1, GDF1, FGF7, CRHBP, CXCL12, SHH, IL11, OLFML3, CLCF1, SOSTDC1, LGI4, SEMA3B, SPON2, PRSS35, MATN2, MMP15, SLIT2, SLIT3, PRELP, THBD, PPBP, PLA2G7, STC1, RELN, VCAN, MFAP2, EGFL8, CTSS, PROS1, HSD17B11, CXCL1, GALNT2, DHH, FMOD, LUM, ADAMTS15, CLCF1, CXCL1, DCN, IL33, CCL7, CRISPLD2, C1QTNF1, PTN, ENTDP2, PRSS12, PRL2C2, BMP4, IL6, SVEP1, NID1, KITL, SOD3, CCL11, LAMA1, COL14A1, CXCL14, SFRP1, FXR1, USH, TGFB3, PLAU, IGFBP5</small>					
GOTERM_CC_FAT	GO:0005886~	plasma membrane	51	20.65	2.76E-02
<small>SLC16A11, FGFRL1, GJA1, DLX1, SHH, EDNRB, UGT1A6B, SLC24A3, UGT1A6A, GNG2, ROBO2, LOC100044177, CEACAM2, RAP2A, MMP15, PTPRU, PTPRN, NCAM1, UGT1A10, THBD, SGM3, CTSS, KCNH2, DST, ADD3, PMEP1A, ADC3, DHH, ITGB4, KCNA6, CXCL1, CDH5, ALCAM, IGSF11, SYN1, ITGB8, SYNPO, TMEM45A, LOC100047606, IL6, SMAD3, NPY1R, KITL, NPY5R, CAMK2N1, FZD6, GPR153, SLC17A8, KCNN4, ABCA4, TGFB3, CACNA1H, TNK2</small>					
GOTERM_CC_FAT	GO:0005615~	extracellular space	28	11.34	5.93E-10
<small>CXCL1, DHH, GDF1, CRHBP, IL33, CXCL1, CXCL12, SHH, CCL7, IL11, CLCF1, SOSTDC1, C1QTNF1, PRL2C2, BMP4, IL6, KITL, SLIT2, SOD3, SLIT3, CCL11, THBD, CXCL14, PLA2G7, FXR1, RELN, STC1, IGFBP5</small>					

Biological Process

Category	Identification	Term	Count	%	p-value
GOTERM_BP_FAT	GO:0010628~	positive regulation of gene expression	12	4.86	7.48E-02
<small>BMP4, HDAC4, IL6, CEBPB, KLF13, GUS1, BCL3, SMAD3, RORR, SHH, IL11, PRL2C2</small>					
GOTERM_BP_FAT	GO:0007155~	cell adhesion	22	8.91	2.82E-05
<small>AEBP1, SVEP1, ITGB4, NID1, CXCL1, PTPRU, KITL, LOC100045228, CDH5, BCL2L1, ALCAM, NCAM1, LAMA1, IGSF11, COL14A1, ITGB8, RELN, ROBO2, VCAN, SPON2, DST, AOC3</small>					
GOTERM_BP_FAT	GO:0016477~	cell migration	10	4.05	5.42E-03
<small>EDNRB, GJA1, RELN, CXCL1, NR2F2, CXCL12, KITL, PLAU, SHH, DCX1</small>					
GOTERM_BP_FAT	GO:0042127~	regulation of cell proliferation	13	5.26	6.71E-02
<small>BMP4, IL6, FGF7, FGFRL1, SMAD3, KITL, SHH, CDH5, IL11, HDAC4, TGFB3, PLAU, PRL2C2</small>					
GOTERM_BP_FAT	GO:0007267~	cell-cell signaling	13	5.26	6.81E-04
<small>BMP4, DHH, IL6, EGR3, FGF7, GJA1, FZD2, LOC100045228, SHH, NPY5R, SYN1, TMOO2, PPP3CA</small>					

B Suppressed gene transcripts**Molecular Function**

Category	Identification	Term	Count	%	p-value
GOTERM_MF_FAT	GO:0005509~	calcium ion binding	21	9.17	4.67E-03
<small>PCDH20, ITGA1, ANXA1, MGP, PAD2, MMP17, LPCAT2, PCDH17, CALB2, MYL9, GALNT4, ITGAS, GSN, LOC638935, CDH19, VSNL1, TGM2, THBS1, CDH10, SNTA1, EHD4, DTNA</small>					

Cellular Component

Category	Identification	Term	Count	%	p-value
GOTERM_CC_FAT	GO:0031012~	extracellular matrix	18	7.86	3.98E-07
<small>WNT16, WNT10B, PTPR21, TNC, ADAMTS15, COL15A1, CDCD80, COL28A1, MMP17, COL5A2, COL4A5, THSD4, ACAN, TGM2, ADAMTS1, AGRN, ADAMTS12, COL8A1</small>					
GOTERM_CC_FAT	GO:0005576~	extracellular region	39	17.03	2.33E-04
<small>WNT16, PDGFB, PDGFA, PGF, TNC, ADAMTS15, CD109, COL28A1, GDNF, FAM132B, C1QTNF3, GSN, TGM2, ACAN, LOXL4, ADAMTS12, AGRN, HTRA3, COL8A1, THBS1, KLK8, WNT10B, STC2, PTPR21, COL15A1, CDCD80, IGF1, MMP17, MGP, ENDD1, COL5A2, COL4A5, 119000215RIK, SRPX2, THSD4, NPPB, ADAMTS1, PRSS23, IGFBP3</small>					
GOTERM_CC_FAT	GO:0005604~	basement membrane	9	3.93	3.82E-06
<small>TNC, ACAN, COL15A1, CCD80, COL28A1, ADAMTS1, AGRN, COL8A1, COL4A5</small>					
GOTERM_CC_FAT	GO:0005886~	plasma membrane	54	23.58	2.29E-03
<small>LOC100049310, LYR1, ATRB1, GABRB3, CSPG4, LGN6, KCN12, CALB2, MCF2L, MRP, DIRAS1, DYSF, DES, SV2B, RHOC, GPR176, INPPL1, CRYAB, RFXP3, MDGA2, MMP17, RFTN1, TNS3, CD80, GPR41, VAMP5, HSPB1, GAP43, ACVR1, CAV1, UMS2, PCDH20, CD109, ITGB5, PTK2, PRR1, TGM2, PPAP2A, DTNA, CNKSR2, IRGM1, FLT1, ANXA1, ITGA1, ATP1A2, PCDH17, ABCB4, P2RX5, ITGAS, RGS3, CDH19, CD200, CDH10, SNTA1</small>					
GOTERM_CC_FAT	GO:0008305~	integrin complex	3	1.31	4.90E-02
<small>ITGAS, ITGA1, ITGB5</small>					

Biological Process

Category	Identification	Term	Count	%	p-value
GOTERM_BP_FAT	GO:0010628~	positive regulation of gene expression	11	4.80	8.37E-02
<small>MEF2C, WNT10B, ETS1, MEOX1, IRF6, JUN, FOXO1, IGF1, CREB5, AGRN, HMG1A</small>					
GOTERM_BP_FAT	GO:0007242~	intracellular signaling cascade	22	9.61	4.75E-03
<small>CNKSR2, S430435G22RIK, CAV1, TNK1, RFXP3, STMN4, CSPG4, SPSB4, PEA15A, RASL12, RCAN2, MCF2L, TNS3, DIRAS1, NUPR1, DOK5, GAB1, TGM2, GUCY1A3, MAPK9, RHOC, GADD45B</small>					
GOTERM_BP_FAT	GO:0000165~	MAPKKK cascade	6	2.62	1.39E-02
<small>CAV1, DOK5, GAB1, CSPG4, MAPK9, GADD45B</small>					
GOTERM_BP_FAT	GO:0007155~	cell adhesion	14	6.11	2.30E-02
<small>INPPL1, PCDH20, TNC, ITGA1, COL15A1, COL28A1, ITGB5, PCDH17, ITGAS, CDH19, ACAN, THBS1, COL8A1, CDH10</small>					
GOTERM_BP_FAT	GO:0016477~	cell migration	11	4.80	8.43E-04
<small>TNS3, PTK2, FLT1, PDGFB, PLXNA2, CSPG4, ITGA1, PRKG1, APBB2, GDNF, ACVR1</small>					
GOTERM_BP_FAT	GO:0042127~	regulation of cell proliferation	16	6.99	2.94E-03
<small>CAV1, PDGFB, PDGFA, INPPL1, ANXA1, IGF1, FOXO1, PMAIP1, TNS3, CDKN1A, NUPR1, CD80, IRF6, JUN, TGM2, IGFBP3</small>					
GOTERM_BP_FAT	GO:0007267~	cell-cell signaling	10	4.37	1.04E-02
<small>KLK8, PTK2, WNT10B, GABRB3, PDGFA, TNC, SV2B, AGRN, ATP1A2, GDNF</small>					

Table 11: GO-annotation analysis of differentially expressed genes due to forskolin treatment. Data of the Figure 42. In forskolin-induced genes, several genes were associated with GO-annotations for cell differentiation and cell adhesion, migration and motility (A). Several forskolin-repressed genes were associated with intracellular signaling, such as the MAPKKK cascade (B).

Taken together, annotation analysis identified a high number of forskolin-dependent differentially expressed transcripts that were associated with the term extracellular matrix, highlighting its important role during Schwann cell differentiation. Further, forskolin had a negative effect on genes associated with intracellular MAP-kinase signaling pathway, which was implicated in Schwann cell dedifferentiation before (Harrisingh et al., 2004).

7.3.6. Pathway analysis implicated in Schwann cell differentiation

To identify putative signaling cascades in forskolin-dependent differentially expressed transcripts, the Kyoto Encyclopedia of Genes and Genomes (KEGG) pathway analysis was performed using DAVID software (Table 12). First, the set of genes with forskolin-induced mRNA expression was investigated (Table 12A). We could detect that 5% of the transcripts were associated with the cytokine-cytokine receptor pathway, such as interleukin 6 (Il6), chemokine (C-X-C motif) ligand 1 (Cxcl1) and chemokine (C-C motif) ligand 2 (Ccl2). Also this analysis revealed that several differentially regulated gene transcripts might be implicated in the extracellular matrix (ECM) - receptor interaction, such as laminin α 1 (Lama1), integrin β 4 (Itgb4) and collagen type II α 1 (Col2a1). In addition, an enrichment of the NOD-like receptor signaling pathway, the TGF- β signaling pathway as well as the focal adhesion pathway could be identified in the set of transcripts positively regulated by forskolin.

A Set of genes with increased mRNA expression levels due to forskolin

Identification	Pathway	%	p-value
mmu04060	Cytokine-cytokine receptor interaction	5.10	0.00020
mmu04512	ECM-receptor interaction	2.38	0.00446
mmu04621	NOD-like receptor signaling pathway	2.04	0.00528
mmu04360	Axon guidance	2.72	0.01129
mmu04350	TGF-beta signaling pathway	2.04	0.02338
mmu04510	Focal adhesion	3.06	0.03265

B Set of genes with decreased mRNA expression levels due to forskolin

Identification	Pathway	%	p-value
mmu04510	Focal adhesion	7.02	<0.00001
mmu04512	ECM-receptor interaction	3.31	0.00028
mmu04115	p53 signaling pathway	2.89	0.00060
mmu04810	Regulation of actin cytoskeleton	3.72	0.01811
mmu04012	ErbB signaling pathway	2.07	0.04833
mmu04010	MAPK signaling pathway	3.72	0.05746

Table 12: KEGG pathway analysis of differentially expressed transcripts in primary mouse Schwann cell cultures. Gene with induced (A) as well as genes with reduced mRNA expression levels (B) due to forskolin treatment were analyzed using the software DAVID. Both sets manifested enrichment for the ECM-receptor interaction and for focal adhesion. % of total submitted genes (294 for A, 242 for B).

Pathway analysis of transcripts which are reduced due to forskolin revealed a strong enrichment for the focal adhesion pathway (Table 12B). In line with induced transcripts, ECM-receptor interaction was also proposed as a putative pathway for the set of genes with decreased mRNA expression due to forskolin. Furthermore, the p53 signaling pathway, the ErbB signaling pathway as well as the MAPK signaling pathway were identified to be overrepresented in this set of transcripts.

Based on pathway analysis, we conclude that a number of differentially regulated transcripts were associated with the ECM-receptor interaction as well as with the focal adhesion pathway, implicating that a major effect of forskolin might be the modulation of the ECM and the cytoskeleton.

7.3.7. Forskolin-induced regulation of components of the extracellular matrix

To determine the effect of elevated cAMP levels by forskolin on transcriptional regulation of components of the ECM and the basal lamina, a list of selected genes known to be expressed in Schwann cells was compiled (Table 13) and schematically illustrated (Figure 43). Most of the investigated components of the basal lamina showed differentially expressed mRNA expression levels upon forskolin treatment. A strong and highly significant reduction could be detected for α -dystrobrevin (Dtna), a member of the dystrophin-glycoprotein complex (DGC). The expression levels of other members of this complex such as dystroglycan (Dag1) and different isoforms of syntrophin (Snt) were not significantly regulated by forskolin. The DGC is linked to the basal lamina by interaction with agrin or laminin. For agrin (Agrn), a reduced expression was identified, whereas the expression levels for laminin α 1, α 2 (Lama1, Lama2) and laminin γ 1 (Lamc1) were increased. Slightly reduced expression was detected for laminin γ 2 (Lamc2), and no transcriptional regulation due to forskolin treatment was identified for laminin α 5, β 1 and β 2 (Lama5, Lamb1, Lamb2).

Investigation of the laminin receptor integrin manifested that forskolin treatment reduced the transcription of integrins such as the integrin α 1, α 2, α 5, β 1 and β 5 (Itga1, Itga2, Itga5, Itgb1 and Itgb5). In contrast, forskolin treatment induced the transcription of integrin β 4 and β 8 (Itgb4 and Itgb8), in agreement with a previous study reporting elevated integrin β 4 expression during development and upon forskolin treatment in rat Schwann cells (Feltri et al., 1994).

Common name	Entrez ID	Ratio		Common name	Entrez ID	Ratio	
		20 to 0 μ M	p-value			20 to 0 μ M	p-value
Agtrin	Agri	0.60	0.0001	Integrin α 7	Itga7	0.83	n.s.
Cell Division cycle 42	Cdc42	0.86	n.s.	Integrin α 9	Itga9	not detected	
Collagen typeII, α2	Col2a1	1.80	0.0130	Integrin β1	Itgb1	0.71	0.0028
Collagen typeII, α 2	Col2a1	1.52	n.s.	Integrin β 1	Itgb1	0.80	n.s.
Collagen typeII, α2	Col2a1	1.36	0.0125	Integrin β 2	Itgb2	0.92	n.s.
Collagen typeIV, α 1	Col4a1	1.15	n.s.	Integrin β 3	Itgb3	not detected	
Collagen typeIV, α2	Col4a2	1.27	0.0091	Integrin β4	Itgb4	1.63	<0.0001
Collagen typeIV, α5	Col4a5	0.63	<0.0001	Integrin β4	Itgb4	1.68	0.0002
Collagen typeIV, α5	Col4a5	0.71	0.0011	Integrin β5	Itgb5	0.54	0.0001
Collagen typeV, α 1	Col5a1	1.01	n.s.	Integrin β 6	Itgb6	1.03	n.s.
Collagen typeV, α2	Col5a2	0.66	0.0036	Integrin β8	Itgb8	1.48	0.0001
Collagen typeV, α 2	Col5a2	0.91	n.s.	Integrin β8	Itgb8	1.59	<0.0001
Collagen typeV, α2	Col5a2	0.74	0.0099	Laminin α1	Lama1	1.75	0.0022
Collagen typeV, α 3	Col5a3	0.84	n.s.	Laminin α2	Lama2	1.35	0.0046
Collagen typeVI, α 1	Col6a1	1.00	n.s.	Laminin α 4	Lama4	not detected	
Collagen typeVI, α 1	Col6a1	0.86	n.s.	Laminin α 5	Lama5	0.80	n.s.
Collagen typeVI, α 1	Col6a1	1.05	n.s.	Laminin β 1	Lamb1-1	1.08	n.s.
Collagen typeVI, α 2	Col6a2	0.99	n.s.	Laminin β 2	Lamb2	1.00	n.s.
Collagen typeVI, α 2	Col6a2	1.00	n.s.	Laminin γ 1	Lamc1	1.01	n.s.
Collagen typeVI, α 3	Col6a3	0.88	n.s.	Laminin γ1	Lamc1	1.21	0.0024
Collagen typeVI, α3	Col6a3	0.71	<0.0001	Laminin γ2	Lamc2	0.82	0.0167
Dystroglycan	Dag1	1.15	n.s.	Neural Cell Adhesion Molecule (CD56)	Ncam1	1.39	0.0010
Dystroglycan	Dag1	1.19	n.s.	Neural Cell Adhesion Molecule (CD56)	Ncam1	2.20	<0.0001
Dystrobrevin α	Dtna	0.40	<0.0001	Neural Cell Adhesion Molecule (CD56)	Ncam1	1.52	0.0026
Dystrobrevin α	Dtna	0.60	0.0001	Nidogen 1 (Entactin)	Nid1	1.77	<0.0001
Dystrobrevin α	Dtna	0.71	0.0007	Nidogen 1 (Entactin)	Nid1	1.88	<0.0001
Dystrobrevin α	Dtna	0.76	0.0030	Nigoden 2	Nid2	1.48	0.0008
Dystrobrevin β	Dtnb	1.00	n.s.	Sarcoglycan α	Sgca	not detected	
Perlecan (Heparan Sulfate Proteoglycan 2)	Hspg2	0.89	n.s.	Sarcoglycan ϵ	Sgce	not detected	
Perlecan (Heparan Sulfate Proteoglycan 2)	Hspg2	1.43	0.0040	Sarcoglycan γ	Sgcy	not detected	
Perlecan (Heparan Sulfate Proteoglycan 2)	Hspg2	1.32	0.0141	Bamacan	Smc3	0.86	n.s.
Integrin α1	Itga1	0.76	0.0006	Syntrophin acidic 1	Snta1	0.93	n.s.
Integrin α1	Itga1	0.49	<0.0001	Syntrophin acidic 1	Snta1	0.49	<0.0001
Integrin α 10	Itga10	0.95	n.s.	Syntrophin basic 1	Sntb1	0.85	n.s.
Integrin α 11	Itga11	1.19	n.s.	Syntrophin basic 2	Sntb2	0.99	n.s.
Integrin α 11	Itga11	1.21	n.s.	Syntrophin basic 2	Sntb2	1.18	n.s.
Integrin α2	Itga2	0.76	0.0054	Syntrophin basic 2	Sntb2	0.90	n.s.
Integrin α 3	Itga3	1.03	n.s.	Syntrophin γ 1	Sntg1	not detected	
Integrin α5	Itga5	0.64	0.0003	Syntrophin γ 2	Sntg2	not detected	
Integrin α5	Itga5	0.65	0.0075	Utrophin	Utrn	not detected	
Integrin α 6	Itga6	0.80	n.s.				

Table 13: Effect of forskolin treatment on mRNA expression of known components of the ECM in Schwann cells. Data analysis of microarray was performed by a two-way ANOVA and unadjusted p-value < 0.01 were accounted as significant. Forskolin had a regulatory effect on the majority of investigated ECM-associated genes. n.s.: not significant

Collagen fibers are another major component of the ECM. Elevation of cAMP levels by forskolin led to a significant induction of all three probes of collagen type II α 1 (Col2a1), in line with a previous report (D'Antonio et al., 2006). Collagen type IV showed highly significantly decreased mRNA expression levels for the chain α 5 (Col4a5), whereas those of α 2 (Col4a2) were increased upon Schwann cell differentiation *in vitro*. Forskolin treatment also led to slightly reduced transcription of collagen V α 2 (Col5a2) and of collagen VI α 3 (Col6a3). Additional analysis of basal lamina components revealed significantly increased mRNA expression levels of nidogen1 (entactin, Nid1), nidogen2 (entactin 2, Nid2) and of the proteoglycan perlecan (Hspg2).

From these data, we conclude that cAMP elevation by forskolin has a strong impact on transcriptional regulation of a variety of ECM-associated genes in cultured Schwann cells, probably reflecting the morphological changes occurring upon Schwann cell differentiation.

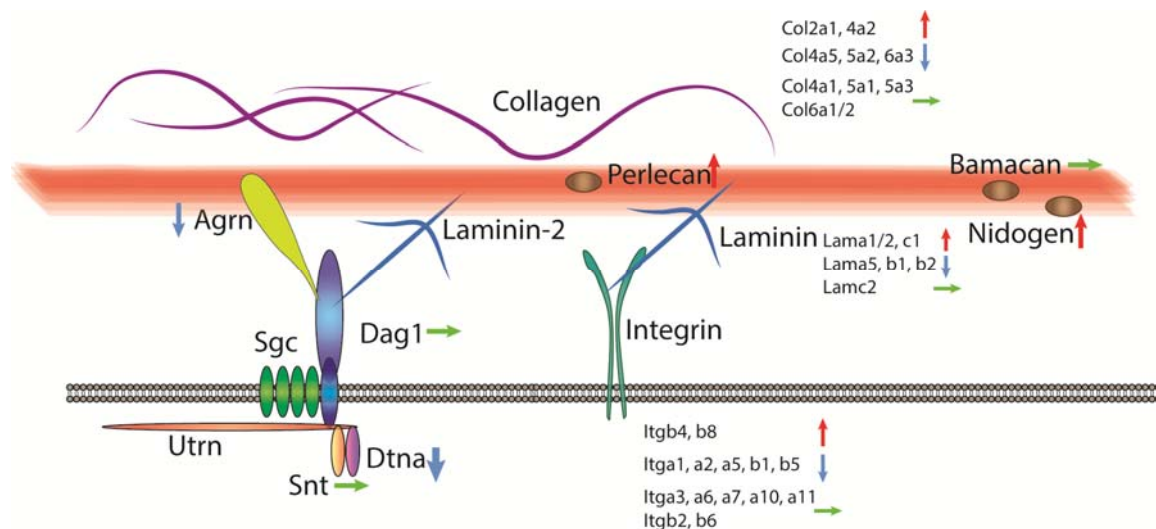


Figure 43: Schematic illustration of components of the extracellular matrix and the basal lamina in Schwann cells. The effect of forskolin on gene expression of selected genes associated with the extracellular matrix and the basal lamina (red line) was shown by blue (reduced), red (increased) or green (unaltered) arrows. Data derive from Table 13.

7.3.8. Correlation analysis between *in vivo* and *in vitro* samples

Elevation of intracellular cAMP by forskolin is often used as an *in vitro* model for Schwann cell differentiation. Therefore, the expression data from naive and forskolin-treated Schwann cells and from sciatic nerve tissues taken from P0, P4, P7, P10 and P60 were examined by a principal component analysis (PCA) to identify similarities or differences between the experimental samples (Figure 44A). Well-defined clusters could be identified for both untreated and treated Schwann cell cultures (Figure 44A, red and blue dots, respectively). Additional distinct clusters could be detected for samples of the different developmental time points of peripheral nerves (Figure 44A, green dots). The PCA for the developmental *in vivo* samples showed a well-defined clusters and the time points closely neighbor each other (Figure 44A and C). P60 nerve samples formed an individual cluster, reflecting that their expression is distinct. The PCA also illustrated that the expression pattern identified in cultured Schwann cells did not overlap with those of the peripheral nerve tissues, which is also reflected by the dendrogram analysis of hierarchical clustering (Figure 44B).

The effect on elevated cAMP levels on the Schwann cell lineage was further investigated by analyzing only transcripts which were differentially expressed with an FDR-adjusted p-value below 0.05 due to forskolin treatment (Figure 44C, D). By PCA, distinct clusters could be depicted for samples of treated or untreated Schwann cell cultures (Figure 44C). Hierarchical cluster analysis revealed further that forskolin-treated Schwann cell samples associate within the same branch as the samples derived from the nerve tissues (Figure

44D, arrow), indicating some corresponding expression pattern. Still, the majority of differentially expressed transcripts elicited by forskolin treatment do not resemble the *in vivo* situation.

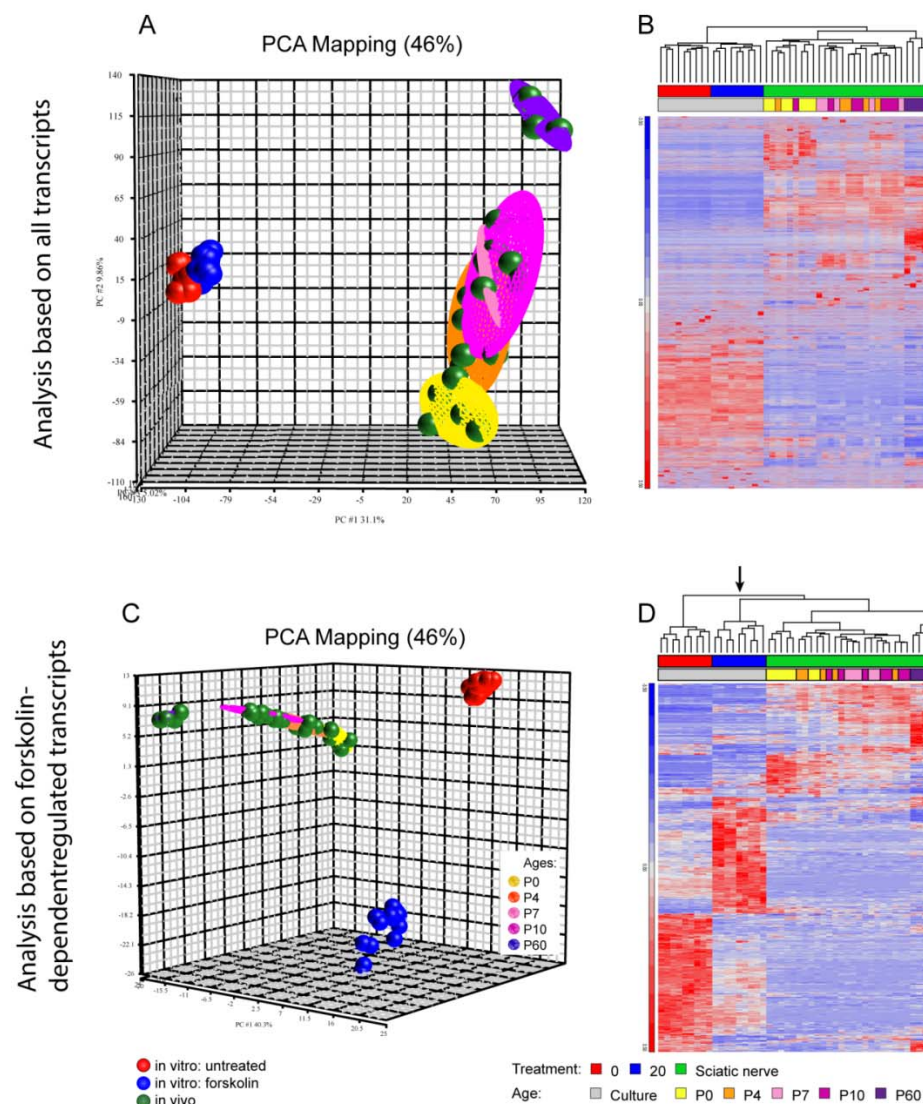


Figure 44: Comparison analysis of gene expression between primary mouse Schwann cell cultures and developing sciatic nerve samples. (A, B) Analysis of the whole genome revealed distinct gene transcription between *in vivo* and *in vitro*, illustrated by PCA (A). A well-defined cluster can be depicted of developing nerve samples, whereas P60 form an individual cluster. Distinct expression between primary Schwann cell cultures and *in vivo* samples could be confirmed by a heat map analysis, indicated by the dendrogram (B). (C, D) Analysis based on only forskolin-dependent differentially expressed transcripts resulted in distinct clusters between treated and untreated Schwann cells, as well as between *in vivo* and *in vitro* (C). Heat map analysis revealed that forskolin-treated Schwann cells associate within the same branch as the samples derived from the nerve tissues (D, arrow).

Publication: The data presented will be submitted for publication.

Schmid D., T. Zeis and N. Schaeren-Wiemers. (2013). Transcriptional regulation induced by cAMP elevation in mouse Schwann cells. *Manuscript in preparation, submission planned for June 2013*

8. Discussion

8.1. MAL-dependent gene regulation in Schwann cells

MAL-dependent gene regulation in primary mouse Schwann cell cultures

A previous study on PNS development revealed that MAL overexpression leads to a delayed onset of myelination, hypomyelinated fibers and reduced P0 and p75^{NTR} expression in newborn mice (Buser et al., 2009b). In agreement with these *in vivo* observations, we could detect significantly reduced mRNA expression levels for P0 and p75^{NTR} in MAL-overexpressing Schwann cells. Since the reduced expression was already determined before Schwann cell differentiation, the effect of MAL might be implicated during early developmental stages. Herein this study, we further demonstrated that primary mouse Schwann cells overexpressing MAL can activate the CREB signaling pathway upon treatment with forskolin, reflected by a comparable induction of P0 expression between MAL-overexpressing and wildtype Schwann cells. Further, stimulation with neuregulin1, FGF1 and NGF could not improve the reduced P0 expression level in MAL-overexpressing Schwann cells. These data indicate that the downstream signaling pathways mediated by these growth factors were not affected by MAL overexpression. Another important intracellular signaling pathway during Schwann cell differentiation and myelination is the PI3-kinase/Akt pathway. Reduced activity of this pathway was shown to result in impaired myelination (Maurel and Salzer, 2000, Ogata et al., 2004, Goebbels et al., 2010). Therefore, we investigated whether the PI3-kinase/Akt signaling pathway is functional in MAL-overexpressing mice. Analysis of phosphorylation of Akt, a key effector of PI3-kinase, revealed no difference due to MAL overexpression, neither *in vivo* nor *in vitro* (Master thesis of Monia Sobrio, 2013). Addition of neuregulin1 to Schwann cells resulted in an induced phosphorylation of Akt, suggesting that the PI3-kinase pathway is functional. Differential expression analysis of genes implicated to be regulated upon activation of the Raf-kinase (Napoli et al., 2012) revealed no transcriptional alterations in Schwann cells overexpressing MAL, demonstrating that also the ERK pathway is not affected by MAL overexpression (data not shown). We conclude that despite the fact that cAMP signaling and PI3-kinase cascade can be activated in MAL-overexpressing Schwann cells, significantly reduced expression levels of P0 and p75^{NTR} were detected. This reduction was determined already in untreated Schwann cells before differentiation, pointing to the effect of MAL during early developmental stages.

Most transcription factors implicated in Schwann cell differentiation were not affected by MAL overexpression

To determine whether altered expression of distinct transcription factors might have led to the reduced expression of P0 observed in MAL-overexpressing Schwann cells, several transcription factors were investigated, known to play a vital role during Schwann cell development and differentiation. In MAL-overexpressing Schwann cells, slightly reduced mRNA expression of Sox10 could be observed, which was also reported *in vivo* (Buser et al., 2009b). On the contrary, qRT-PCR analysis revealed increased transcription levels for Krox20. Despite the fact that Krox20 mRNA is increased in MAL-overexpressing Schwann cells, the expression of P0 was robustly reduced. It was shown previously that viral overexpression of Krox20 consequently induced P0 expression in 3T3 fibroblasts, even if this cell line normally does not express P0 (Parkinson et al., 2004). However, also another report showed that normal Krox20 expression could not improve reduced P0 expression in PMP22-overexpressing mice with a strongly impaired myelination (Kinter et al., 2013). This is in line with a recent study on mTOR mutant mice, in which decreased P0 expression but normal Krox20 expression levels were determined (Sherman et al., 2012). In MAL-overexpressing Schwann cells, no increased expression levels were observed for transcripts known for negative modulation of myelination, such as cJun, Id2, Krox24 and Dock7 (recently reviewed in Heinen et al., 2013).

MAL overexpression led to differentially expressed transcripts of genes associated with cytoskeleton organization and extracellular matrix

Besides functional regulatory pathways for myelination, analysis of the microarray revealed that transcripts of a set of genes implicated in the regulation of the cytoskeleton were differentially expressed in primary MAL-overexpressing Schwann cell cultures (Figure 45).

A strong reduction was detected for the intermediate filament keratin 23 (Krt23), which is a member of the type I keratin family (Zhang et al., 2001). In contrast to actin and microtubules, keratin filaments lack polarity. For Krt18, an interaction partner of Krt23, keratin monomers were shown to appear at the cell periphery close to the plasma membrane, and to be transported along actin fibers, allowing intermediate filament network reorganization (Kolsch et al., 2009) (Figure 45B). In Schwann cells, only little is known about the expression of keratins. But our analysis revealed that Krt23 and Krt10 were substantially expressed in Schwann cells *in vitro*, whereas other keratin transcripts were not detected in primary Schwann cell cultures. Thus, reduced expression of Krt23 in

MAL-overexpressing Schwann cells might debilitate integration of keratin monomers into the keratin filament network that is mediated by actin fibers.

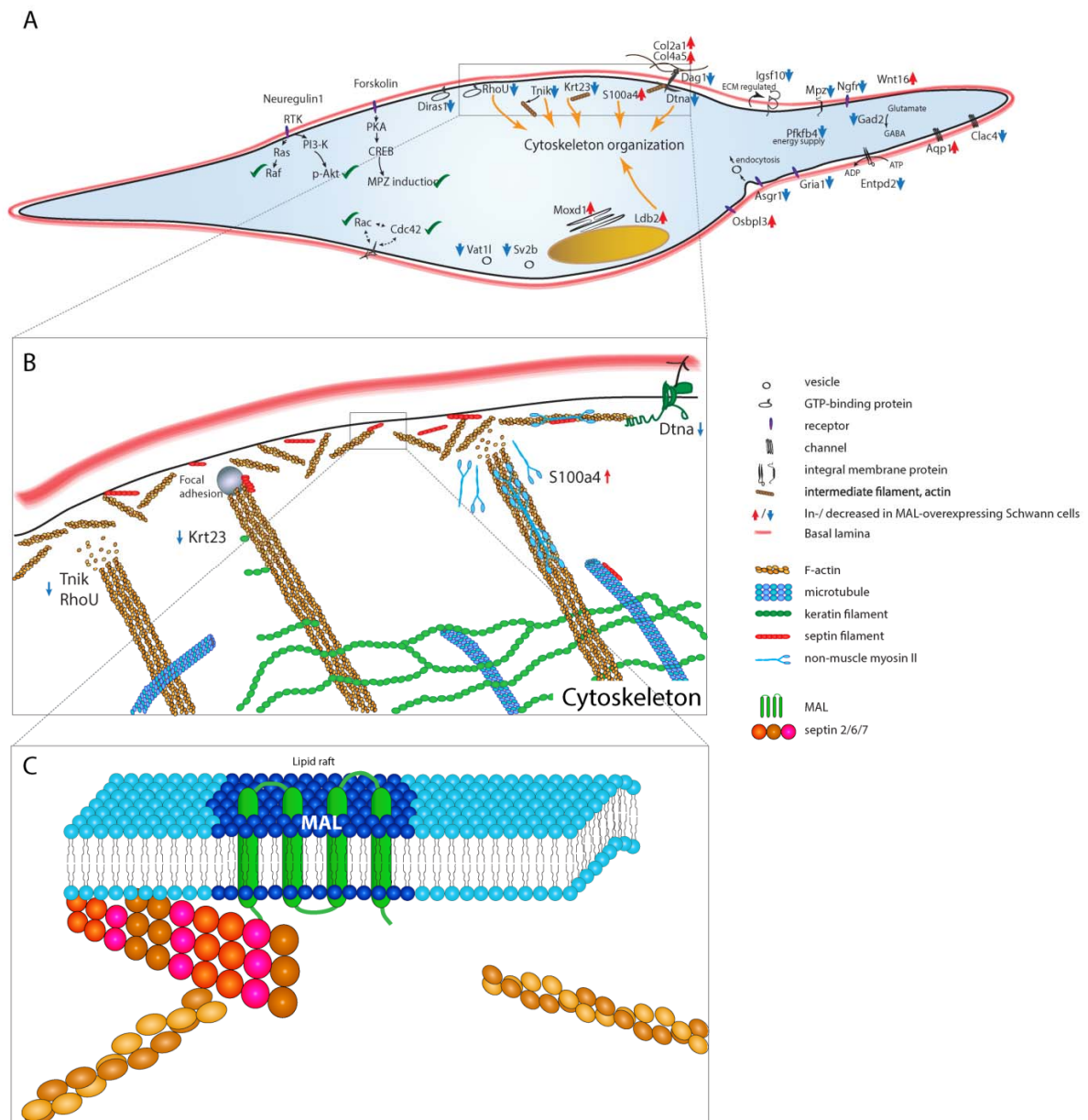


Figure 45: Schematic illustration of putative functional roles of the identified differentially expressed transcripts in MAL-overexpressing Schwann cells. (A) Forskolin-dependent induction of MPZ as well as phosphorylation of Akt were unaffected by MAL overexpression. Microarray analysis revealed that a number of differentially expressed transcripts in MAL-overexpressing Schwann cells were associated with the cytoskeleton organization. (B) Tnik and RhoU were reported to induce disruption of F-actin, whereas S100a4 promotes the disassembly of myosin II filaments. Keratin monomers were shown to be transported along actin fibers to integrate into the intermediate filament network. Septins may interact with components of cellular membranes, with actin filaments and with microtubules. α -dystrobrevin is a component of the dystrophin glycoprotein complex, which binds to actin filaments. (C) The lipid raft protein MAL interacts with the cytoskeleton protein septin 6, which forms a heterotrimer with septin 7 and the actin-associated protein septin 2.

Further, decreased expression was depicted for the Traf and Nck-interacting kinase (Tnik). Tnik belongs to the germinal center kinase (GCK) family and was postulated to have two independent functions (Fu et al., 1999). It specifically activates the JNK pathway, but it also induces disruption of F-actin and by that inhibits cell spreading (Figure 45B). Its functional role in Schwann cells is not yet known, but it might be a novel candidate involved in modulating early events of Schwann cell differentiation, in which JNK and actin are known to play an important role (Fernandez-Valle et al., 1997, Parkinson et al., 2004).

Along these lines, we identified reduced expression of RhoU/Wrch1 in MAL-overexpressing Schwann cells. RhoU is also implicated to activate the JNK signaling pathway, and was shown to be essential to maintain F-actin polarization, too (Tao et al., 2001, Ory et al., 2007) (Figure 45B). In a comparable manner to Tnik, RhoU overexpression was shown to result in dissolution of F-actin stress fibers (Tao et al., 2001). The observed reduced expression of Tnik and RhoU in MAL-overexpressing Schwann cells may influence their potential to induce disassembly of F-actin, and by that may modulate cytoskeleton dynamics important for Schwann cell membrane mobility.

Increased expression in Schwann cells overexpressing MAL was detected for S100a4, a member of the EF-hand family of calcium-binding protein. S100a4 inhibits the assembly of non-muscle myosin II monomers into filaments and promotes the disassembly of myosin II filaments (Li et al., 2003) (Figure 45B). Non-muscle myosin II is implicated in regulating cell migration, integrin-mediated cell adhesion and polarity by remodeling the actin cytoskeleton (reviewed in (Vicente-Manzanares et al., 2009)). In Schwann cells, myosin II was shown to be necessary for peripheral myelination, indicated by reduced number of myelin segments and reduction of myelin proteins induced by RNA interference (RNAi) of myosin II in myelinating cocultures (Wang et al., 2008). In addition, RNAi of myosin II resulted in reduced expression of laminin $\alpha 2$ chain and impaired basal lamina assembly (Wang et al., 2008). Increased S100a4 in MAL-overexpressing Schwann cells might increase the disassembly of myosin II filaments, and thereby, influencing actin filament stability. Along this line, we observed reduced expression of CNPase (CNP), a prenylated myelin protein, interacting with tubulin heterodimers and involved in microtubule and F-actin reorganization, which is necessary for process outgrowth in oligodendrocytes (Lee et al., 2005).

Although immunofluorescent analysis for tubulin and actin did not reveal obvious changes in the cytoskeletal morphology between MAL-overexpressing and wildtype Schwann cells (data not shown), we cannot rule out that minor subcellular changes occurred. Besides microtubules, actin filaments and intermediate filaments, a fourth filamentous system is

known in Schwann cells, namely the family of septins (Buser et al., 2009a). Septins form higher-order filaments by heteromeric assembly, and can interact with components of cellular membranes, as well as with actin filaments and microtubules (reviewed in (Saarikangas and Barral, 2011)). Septins are involved in membrane compartmentalization and vesicle transport in polarized cells including Schwann cells. A whole set of septins are expressed in Schwann cells throughout development and in the adult, and localized in particular cellular compartments (Buser et al. 2009a). In addition, MAL was shown to interact with septin 6, which in turn is associated with particular septins and actin, probably establishing specialized scaffolds in distinct myelin compartments (Buser et al., 2009a) (Figure 45C). Due to this direct link between MAL and a component of the cytoskeleton, it is tempting to speculate about the modulatory role of MAL in plasma membrane mobility.

During Schwann cell development and differentiation, accurate cytoskeleton organization is crucial, and altered cytoskeleton organization might influence the onset of myelination by disturbing radial sorting. Two important modulators for radial sorting are the Rho family GTPases Rac1 and Cdc42 (reviewed in Chan, 2007). However, analysis of downstream targets of the Rac1 and Cdc42 signaling pathways revealed no altered transcription in MAL-overexpressing Schwann cells, proposing that these signaling cascades were not affected by MAL overexpression (data not shown). In addition to cytoskeleton organization, a number of transcripts of genes associated with the extracellular matrix were differentially regulated in Schwann cells overexpressing MAL. Microarray analysis revealed that transcripts of α -dystrobrevin and dystroglycan, two members of the dystrophin-glycoprotein complex, were significantly decreased. In dystroglycan-deficient mice, a subset of axons is abnormally sorted and polyaxonal myelination can be observed (Saito et al., 2003), coincident with observations in MAL-overexpressing mice that occasionally myelinate a bundle of several axons together (Buser et al., 2009b). In addition, shorter internodal length can be detected in dystroglycan-deficient mice (Court et al., 2009), correlating with a previous findings, in which shorter internodal length for mice overexpressing MAL were reported (Buser et al., 2009b). Unlike the *in vitro* observation, no altered expression for α -dystrobrevin could be determined in sciatic nerves of MAL-overexpressing mice compared to wildtype littermates. *In vivo*, the reduced expression level of this gene transcript might have been masked due to normal expression levels in the perineurium, which is composed of five to six layers of basement membrane (Akert et al., 1976); in contrast, only one layer is present in Schwann cells. Further analysis of genes expressed in the ECM revealed an increased expression for collagen type II α 1 (Col2a1) in MAL-overexpressing mice. Collagen II is the major collagen in cartilage tissue, and its expression was shown in several tissues such as kidney, lung, brain, liver and skin (Sandberg et al., 1993). In the peripheral nervous system, Col2a1 was

previously reported in both myelinating and nonmyelinating Schwann cells (D'Antonio et al., 2006), but its functional role in differentiation or myelination is not yet known. In line, the expression of collagen IV $\alpha 5$ (Col4a5) was slightly increased in MAL-overexpressing Schwann cells, known to be synthesized in cultured Schwann cells (Carey et al., 1983). A recent study showed that the expression of the member 10 of the immunoglobulin superfamily (Igsf10), which was highly significantly reduced in MAL-overexpressing Schwann cells, is modulated by the ECM (Zvibel et al., 2013), emphasizing a functional effect of MAL on the ECM composition.

In addition to proper gene expression levels of ECM members, accurate sulfatide levels are required to anchor laminin-1 ($\alpha 1\beta 1\gamma 1$) and laminin-2 ($\alpha 2\beta 1\gamma 1$) to Schwann cells and consequently to assemble the basal lamina (Li et al., 2005, McKee et al., 2007). Interestingly, previous reports showed that MAL binds sulfatide (Frank et al., 1998, Saravanan et al., 2004). This finding leads to the speculation that MAL-dependent binding of sulfatide might impair functional integrity of laminins into the basal lamina, resulting in disturbed integrin- and dystroglycan-mediated signaling.

Proper assembly of the basal lamina is not only important for accurate radial sorting, but also for the signaling pathways PI3-kinase/Akt and Ras/MAPK, which are associated with signal transduction downstream of integrins and laminins (Colognato et al., 2002, Yang et al., 2005, Yu et al., 2005, Barros et al., 2009). Additionally, laminin expression is essential for proper neuregulin signaling (Yu et al., 2005). *In vivo* and *in vitro*, we demonstrated that phosphorylation of Akt is not affected by MAL overexpression. However, we cannot exclude any altered signaling via this pathway, which might result in slightly delayed myelination. Another implication of laminin is the activation of Fyn, which can activate members of the small Rho GTPases, such as Rac1 and Cdc42 and modulate process outgrowth by influencing actin cytoskeleton (Hoshina et al., 2007). From our data, we hypothesize that the disturbed regulation of essential components of the basal lamina and the ECM might result in altered downstream signaling influencing accurate myelination in MAL-overexpressing mice.

MAL overexpression altered expression of genes associated with palmitate

Bioinformatic analysis of highly significantly reduced genes in MAL-overexpressing Schwann cells revealed an enrichment of the term palmitate. Palmitoylation is a reversible post-translational modification by covalently adding the saturated fatty acid palmitate to cysteine residues via thioester linkages (reviewed in Linder and Deschenes, 2007). This leads to increased protein hydrophobicity and consequently facilitates interaction with lipid bilayers. Long chain saturated free fatty acids such as palmitate accumulate in membrane lipid rafts and influence the lipid environment, which might result in altered downstream signaling by affecting receptor functions (reviewed in Simons and Toomre, 2000). In Schwann cells, palmitoylation is required to translocate p75^{NTR} protein into cholesterol-rich domains of the plasma membrane, which is crucial for subsequent cleavage by the γ -secretase (Underwood et al., 2008). Further, palmitoylation of PMP22 and PLP is implicated in the efficient protein transport to the plasma membrane (Schneider et al., 2005, Zoltewicz et al., 2012). The protein MAL is an important component of lipid rafts and is localized in the trans-Golgi network, where lipid rafts are constituted. It is tempting to speculate that MAL overexpression alters the composition of lipid rafts, consequently disturbing the balance of accurate palmitate amount in particular signaling platforms. Thus, altered palmitoylation might lead to impaired downstream signaling influencing the efficiency of myelination in newborn MAL-overexpressing mice.

Investigation of a direct link between MAL overexpression and downregulation of p75^{NTR}

We could detect reduced p75^{NTR} expression in MAL-overexpressing Schwann cells, both *in vivo* and *in vitro*. Therefore, we investigated whether overexpression of MAL might directly result in reduced p75^{NTR} expression. For this purpose, wildtype Schwann cells were infected with a construct to overexpress MAL, and the expression of p75^{NTR} was subsequently analyzed. First, the immortalized Schwann cell line S16 was investigated to determine whether these cells are comparable to primary Schwann cells. Already in naive cells, a strong expression of the myelin lipid marker O1 could be detected, which is in contrary to untreated primary mouse Schwann cells (own observations) and adult rat Schwann cell cultures (Monje et al., 2009, Monje et al., 2010). Also the increased expression of both protein and mRNA of p75^{NTR} in forskolin-treated S16 cells is in disagreement to previous reports on primary Schwann cell cultures (Morgan et al., 1991, Monje et al., 2010). These findings highlighted that the immortalized S16 Schwann cell line cannot be compared to primary Schwann cells, excluding them as a culture system to determine a direct link

between MAL overexpression and reduced p75^{NTR} expression. In addition, primary rat Schwann cell cultures were established, and cells were infected with a retroviral construct to overexpress MAL. Data analysis revealed that retroviral infection per se already altered the transcription of the target genes P0 and p75^{NTR}. Hence, their expression pattern could not reliably be analyzed in cells infected with a construct to overexpress MAL. Therefore, it was not possible to determine a possible link between MAL overexpression and reduced p75^{NTR} expression.

Conclusion

Our presented study showed that MAL overexpression leads to significantly reduced expression of P0 and p75^{NTR} in primary mouse Schwann cell cultures. This differential expression was observed despite normal expression of most transcription factors, receptors, myelin-related genes and components of the extracellular matrix, important for Schwann cell development, differentiation and myelination. We also identified a set of genes differentially expressed in a MAL-dependent manner that are implicated in the regulation of cytoskeleton organization and plasma membrane mobility, proposing them as novel candidates for influencing myelination.

8.2. Transcriptional regulation induced by cAMP elevation in cultured mouse Schwann cells

Accurate peripheral myelination depends on a variety of signals and growth factors. One of the key signaling pathways is mediated by the second messenger cAMP, which activates the CREB signaling pathway, reflected by induced expression of myelin-related genes (Monuki et al., 1989, Morgan et al., 1991, Parkinson et al., 2003, Monje et al., 2009). The elevation of intracellular cAMP levels by either dibutyryl-cAMP or forskolin is the classically used stimulation assay to mimic Schwann cell differentiation *in vitro*. The effect of forskolin treatment on Schwann cells was analyzed by a comprehensive microarray study on primary mouse Schwann cell cultures. In addition to the myelin-related genes known to be regulated by forskolin *in vitro*, we identified many so far disregarded genes to be expressed by Schwann cells in culture. The generated database provides new insights for the community into the molecular mechanisms of Schwann cell differentiation.

In a first step, we focused on genes which were reported to be expressed at a distinct stage of the Schwann cell lineage (Figure 38). Investigation of genes expressed in neural crest cells, Schwann cell precursors and immature Schwann cells revealed that elevation of cAMP levels by forskolin reduced their transcription levels, such as those of the transcription factors AP2 α and cJun or the adhesion proteins NCad and cadherin 19 (Cdh19). In line with previous studies, we observed induced transcription of genes expressed in differentiated Schwann cells, such as the myelin-related genes Mpz and Pmp22 (Lemke and Chao, 1988, Monje et al., 2009). However, no increased expression could be detected for Mag, contrary to previous reports showing increased protein levels upon cAMP elevation in rat Schwann cell cultures (Monje et al., 2009, Monje et al., 2010). The mRNA expression levels for plasmalogen (Plp) were reduced upon treatment, although its expression during peripheral development was previously reported to correlate with myelination (Gillen et al., 1996). In addition to induced myelin-related genes, also increased mRNA expression levels of the transcription factors Oct6 and Krox20 could be detected in differentiated Schwann cells, in agreement with previous reports (Monuki et al., 1989, Parkinson et al., 2003). In line, we and others found strong induction of Id2 expression after elevation of intracellular cAMP in Schwann cell cultures (Stewart et al., 1997, Thatikunta et al., 1999, Mager et al., 2008). We could also identify significantly increased expression for Krox24, the major transcription factor in nonmyelinating Schwann cells. This observation suggests that treatment with forskolin might also influence the nonmyelinating Schwann cell lineage. Induced transcription of Krox24 can be explained by the fact that the Krox24 promoter contains a cAMP response element (CRE) (reviewed in Thiel et al., 2010). Further, increased

transcriptional activity of Krox24 by forskolin is in line with detected transactivation of Krox24 by CREB signaling in gonadotrophs (Mayer et al., 2008, Mayer and Thiel, 2009). Besides Krox24, also the related transcription factor Egr3 was significantly increased in treated Schwann cells. Together with Krox24, it modulates the expression of p75^{NTR} (Gao et al., 2007), which in turn is critical for the onset of peripheral myelination (Cosgaya et al., 2002). Hence, increased expression of both Krox24 and Egr3 suggests that regulation of p75^{NTR} might be also important for Schwann cell differentiation *in vitro*. Analysis of tyrosine kinase receptors revealed that transcripts coding for ErbB2, TrkB and TrkC were increased in treated Schwann cells, suggesting that forskolin treatment not only activates CREB signaling but also might influence other intracellular signaling pathways mediated by tyrosine kinase receptors in Schwann cells as previously suggested (Stewart et al., 1996, Kim et al., 1997, Cohen and Frame, 2001, Grimes and Jope, 2001, Ogata et al., 2004, Monje et al., 2006, Monje et al., 2010).

Regulation of ECM components is dependent on intracellular cAMP levels

Data analysis revealed that a set of strongly differentially expressed transcripts due to forskolin treatment are associated to components of the ECM. Increased mRNA expression levels could be identified for the secreted extracellular matrix protein spondin2 (Spon2) and for decorin (Dcn), a chondroitin sulphate proteoglycan known to be expressed in Schwann cells (Hanemann et al., 1993). These data are in agreement with previous reports showing an upregulation of decorin during embryonic Schwann cell development (Buchstaller et al., 2004, D'Antonio et al., 2006). In line, the proteoglycan thrombomodulin (Thbd), whose transcription was highly significantly increased in treated Schwann cells, was previously shown to be induced in endothelial and leukemia cell lines after elevation of intracellular cAMP levels (Ito et al., 1990, Maruyama et al., 1991, Archipoff et al., 1993). Another increased transcript associated with ECM was neurotrypsin (motopsin, Prss12), a serine protease known to cleave agrin (Reif et al., 2007). Upon treatment with forskolin, reduced transcription was detected for the secreted matrix Gla protein (Mgp) and the proteoglycan aggrecan (Acan). To investigate whether differentially expressed gene transcripts might have a common function, they were analyzed in respect to their GO-annotations. In line with gene expression analysis, the enriched term of “extracellular matrix” could be identified for both sets, either transcripts increased or decreased after forskolin treatment. In addition, pathway analysis revealed that the interaction of ECM with its receptors was enriched in differentially expressed gene transcripts. Further, we could detect that the transcripts of agrin (Agrn), collagen IV $\alpha 1$ (Col4a1) and collagen V $\alpha 1$ (Col5a1) were strongly

expressed in primary mouse Schwann cell cultures compared to other transcripts known in Schwann cells (data not shown). This observation is in line with a previous report showing that rat Schwann cells synthesize and secrete collagen IV *in vitro* (Carey et al., 1983).

During Schwann cell differentiation and radial sorting *in vivo*, considerable modifications of the plasma membrane occur. The sole axon-glia interaction transforms into a glia-glia interaction on one side, and an axon-glia interaction on the other side of the same membrane elongation. Hence, expressional changes of adhesion molecules and components of the extracellular matrix are vital for proper function and polarization *in vivo*. From our data, we conclude that one of the major effects of forskolin is the regulation of the ECM, indicating that changes of the ECM also occur in Schwann cell differentiation *in vitro*.

Olig1 as a new candidate gene in nonmyelinating Schwann cells

Among the 25 gene transcripts, which were strongly decreased due to forskolin treatment, we identified the transcription factor Olig1. In the CNS, Olig1 is essential for the differentiation of oligodendrocyte precursor cells into mature oligodendrocytes (Xin et al., 2005, Li et al., 2007). However, its role in the PNS is not well known yet. First, we confirmed its expression in primary mouse Schwann cells by immunofluorescent microscopy. Immunofluorescence analysis on sciatic nerve tissue sections revealed that Olig1 was localized in nonmyelinating Schwann cells. This finding in nonmyelinating Schwann cells is well in line with the observed decreased mRNA expression level upon forskolin treatment. Previously, Olig1 was reported in injured nerves (Arthur-Farraj et al., 2012), suggesting its expression also in denervated Schwann cells. We propose Olig1 as a possible new transcription factor of the nonmyelinating Schwann cell lineage, whose expression was negatively regulated by elevation of intracellular cAMP levels.

Highly significantly differential gene expression induced by elevated cAMP

Analysis of the strongest forskolin-dependent regulated transcripts identified the fibroblast growth factor 7 (Fgf7), which is also known as keratinocyte growth factor (Kgf). The mitogen Fgf7 was shown to regulate differentiation in epithelial cells (Marchese et al., 1990). Its expression in human Schwann cells was identified already previously (Thomas and De Vries, 2007). In primary mouse Schwann cells, we could examine that Fgf7 was strongly increased

after forskolin treatment. This finding is in accordance with recent reports showing that stimulation with forskolin led to increased *Fgf7* expression in dermal papilla cells and in primary fibroblasts (Iino et al., 2007, Scott et al., 2012). Another significantly induced gene was the endothelin receptor type b (*Ednrb*), which is coupled to the adenylyl cyclase (Wilkins et al., 1997). Also for *PDGF β* , reduced expression was detected in differentiated Schwann cells, in accordance with reports showing the functional role of PDGF in cell migration and proliferation (De Donatis et al., 2008, Monje et al., 2009, Jiang et al., 2013). Our result of decreased *PDGF β* in differentiated Schwann cells is also in agreement with the finding that exogenous PDGF led to suppression of the expression of myelin-related proteins in rat Schwann cells (Ogata et al., 2004). Further, a decreased expression of the nucleoside diphosphate kinase 7 (*Nme7*) was detected in stimulated Schwann cells. For embryonic stem cells, it was recently demonstrated that reduction of *Nme7* by RNAi induces cell differentiation (Wang et al., 2012), suggesting that its reduced expression in treated Schwann cells might also induce cell differentiation.

The strongest forskolin-induced reduction was detected for the transcription of the protocadherin 20 (*Pcdh20*). This cell adhesion molecule belongs to non-clustered protocadherins, and its expression was analyzed particularly in the CNS (Kim et al., 2007). To our knowledge, *Pcdh20* expression has not yet been investigated in the PNS. In primary mouse Schwann cells, we detected high expression levels of both transcripts in naive Schwann cells (data not shown). Upon forskolin treatment, transcription of *Pcdh20* was highly significantly reduced, maybe reflecting morphological changes of the cells in conjunction with differentially expressed adhesion molecules. Forskolin treatment resulted also in strongly reduced transcription of the calcium - and calmodulin-dependent phosphodiesterase 1B (*Pde1b*). As for *Pcdh20*, gene transcripts of *Pde1b* were strongly expressed in untreated Schwann cell cultures. This enzyme was reported to hydrolyze the second messengers cAMP and cGMP, consequently regulating their cellular levels (reviewed in Bender and Beavo, 2006, Omori and Kotera, 2007). Hence, elevated intracellular levels of cAMP by forskolin treatment might directly suppress the expression of *Pde1b*. The third transcript which was strongly reduced in forskolin-treated Schwann cells was the leucine-rich repeat and transmembrane domain-containing protein 1 (*Lrtm1*). In naive Schwann cells, a strong expression of both transcripts could be detected. The functional role of the *Lrtm1* protein is not known. Leucine-rich repeat proteins in general were shown to be involved in cell adhesion and polarization, cytoskeleton dynamics and neural development (reviewed in Kobe and Kajava, 2001), proposing *Lrtm1* as a new candidate gene in cell adhesion in Schwann cells, comparable to the cell adhesion molecule *Pcdh20*.

Forskolin treatment led also to reduced expression of the transmembrane protein 158 (Ris1), which was shown to be upregulated in response to activation of the Ras pathway (Barradas et al., 2002, Iglesias et al., 2006, Birch et al., 2008). Since the Ras/Raf/Mek/Erk signaling pathway blocks Schwann cell differentiation (Harrisingh et al., 2004, Ogata et al., 2004), a decreased activity of this pathway is expected upon differentiation with forskolin, subsequently leading to reduce expression of Tmem158. The hypothesis of reduced activity of the MAP-kinase cascade was validated by an analysis of putative pathways, revealing that reduced genes in treated Schwann cells are often associated to the MAP-kinase pathway in genes reduced in differentiated Schwann cells. In addition, the MAPK-kinases Mek1/2 could be identified as possible target regulators of genes with a reduced expression after forskolin treatment. Inhibitory modulation was also proposed for the target regulator serum response factor (SRF), which is implicated in the binding to the serum response element (SRE). A recent study suggested cell proliferation through phosphorylation of SRF by the MAPK signaling cascade in HeLa cells (Eto et al., 2010). In line, Rac1, that was identified as a putative negative target regulator of the differentially expressed transcripts, was recently demonstrated as a negative regulator of Schwann cell differentiation by upregulating cJun and downregulating Krox20 through the JNK pathway (Shin et al., 2013). Upstream analysis further revealed that three members of the NF- κ B pathway are putative target regulators. This is in accordance to the observation, that the activation of NF- κ B is vital for peripheral myelination (Nickols et al., 2003). NF- κ B was shown to be phosphorylated and activated by the PKA (Yoon et al., 2008).

Distinct gene expression between Schwann cells *in vitro* and developing peripheral nerves

In vivo, developing peripheral nerves, represented by the time points P0, P4, P7 and P10, formed well-defined clusters illustrated by a principle component analysis (PCA). Samples of mature nerves at P60 constituted an individual cluster, indicating distinct gene expression compared to younger time points. Clusters could also be identified for treated as well as untreated Schwann cells. Comparison of gene expression between samples derived from primary mouse Schwann cells and samples of developing sciatic nerves revealed significant differences. The differences in gene expression between *in vivo* and *in vitro* might be explained by the fact that there is a constant interaction and reciprocal signaling between axons and Schwann cells *in vivo*, which is absent in primary mouse Schwann cell cultures. Furthermore, the *in vivo* system is more sophisticated, since other cells such as endothelial cells and fibroblasts are present in the nerve extract, whereas only Schwann cells were analyzed in the culture. Cultured Schwann cells are more synchronized, in contrast to

Schwann cells in peripheral nerves, where an overlap of distinct Schwann cell stages can be observed during early development. These data indicate that caution has to be exercised when comparing primary Schwann cell cultures to *in vivo* analysis, despite the finding that forskolin-treated Schwann cells associate within the same branch of the dendrogram as the nerve samples.

Conclusion

From our study, we conclude that a major role of forskolin is the regulation of genes associated with the ECM, underlining its importance during Schwann cell differentiation. In addition, a negative modulatory effect on differentiation was detected for the MAP-kinase and Rac1 signaling pathway, confirming previous studies.

9. Outlook

In primary MAL-overexpressing mouse Schwann cell cultures, a distinct set of gene transcripts were differentially regulated compared to wildtype cells. Analysis of a microarray study on MAL-overexpressing Schwann cells revealed that several of those transcripts are associated with the cytoskeleton organization, as well as with the extracellular matrix and the basal lamina assembly (Figure 45).

It might be promising to further investigate the effect of MAL overexpression on the cytoskeleton organization and the plasma membrane mobility by a comprehensive immunofluorescent colocalization study. Due to the restricted size of Schwann cells, this analysis might be performed in either the NIH 3T3 fibroblast cell line or in Madine-Darby canine kidney (MDCK) cells, transfected with a construct to overexpress MAL. Confocal analysis of immunofluorescent stainings for cytoskeleton proteins, such as F-actin, microtubules, keratins or septins might reveal whether overexpression of MAL directly influence the cytoskeleton organization. These transfected cells might be further analyzed by an *in vitro* scratch assay (Liang et al., 2007), to determine if MAL dosage has a direct effect on cell migration and plasma membrane mobility.

It is not yet known how MAL overexpression leads to decreased expression of components of the basal lamina. It was previously reported that expression of galactosyl-sulfatide is necessary to anchor laminin-1 ($\alpha1\beta1\gamma1$) and laminin-2 ($\alpha2\beta1\gamma1$) to Schwann cell surfaces, and is therefore important for accurate basal lamina assembly (Li et al., 2005, McKee et al., 2007). Since MAL binds the glycosphingolipid sulfatide (Frank et al., 1998, Saravanan et al., 2004), its overexpression might influence functional integrity of laminin into the basal lamina by affecting sulfatide levels. A possible functional link of MAL overexpression and sulfatide-dependent assembly of the basal lamina might be studied in mouse embryonic lung fibroblast cells (MEFs). Despite fibroblasts produce components of the basal lamina, they do not assemble a basal lamina on their cell surface (Cornbrooks et al., 1983, Marinkovich et al., 1993). Previously, treatment with sulfatide was shown to lead to the formation of a basal lamina even in fibroblasts, detected by electron microscopy (Li et al., 2005). It might be elucidated whether fibroblasts transfected with a construct to overexpress MAL are able to assemble a continuous basal lamina in the presence of sulfatide or whether MAL overexpression is sufficient to inhibit the sulfatide-driven formation of the basal lamina.

To investigate whether basal lamina formation is altered due to MAL overexpression, MAL-overexpressing nerves might be analyzed by electron microscopy. An embryonic developmental study between E16 and E19 might indicate if not only the onset of

myelination, but also the formation of the basal lamina is retarded in MAL-overexpressing mice. In addition to electron microscopy, immunofluorescent stainings for collagen and integrin on embryonic nerves might reveal an impaired or discontinuous basal lamina in MAL-overexpressing mice compared to wildtype littermates.

Another relevant point is whether and how MAL overexpression alters lipid composition in the plasma membrane. To answer this question, myelin membrane extracts as well as membranes of detergent-insoluble glycosphingolipid/cholesterol-rich membrane domains (so-called lipid rafts) might be analyzed by lipidomics. Of particular interest are the levels of sulfatides, which influence basal lamina assembly (Li et al., 2005, McKee et al., 2007) and cholesterol, an important regulator for accurate myelination (Saher et al., 2005, Saher et al., 2009, Verheijen et al., 2009). In addition, oxidized cholesterol (oxysterol) was shown previously to inhibit myelin-related gene expression (Makoukji et al., 2011). Since MAL overexpression leads to increased expression of the intracellular lipid receptor oxysterol binding protein-like 3 (Osbp13), a comprehensive study on the lipid composition might be instrumental to open new perspectives about the functional role of MAL.

A promising, although sophisticated, attempt is to further investigate the effect of the differentially expressed transcripts in MAL-overexpressing Schwann cell cultures by viral infections. A rescue experiment might be performed by overexpressing genes which were decreased in MAL-overexpressing Schwann cells, such as α -dystrobrevin (Dtna), RhoU and keratin 23 (Krt23). Subsequent analysis of P0 and p75^{NTR} expression might reveal whether their reduced expression in MAL-overexpressing Schwann cells could be ameliorated. In line, gene transcripts, which were increased in MAL-overexpressing cells, such as S100a4 or the oxysterol binding protein-like 3 (Osbp13), might be reduced in the culture by RNA interference (RNAi). The retroviral backbone pMX cannot be used, because primary mouse Schwann cells do not proliferate in culture. In addition, I could demonstrate that already the infection alone with the pMX vector alters gene transcription in mouse Schwann cells. Hence, a lentiviral expression system (e.g. the HIV-1-based vector pLVX-Puro) might be applied for those difficult-to-infect and nonproliferative Schwann cells. This rescue experiment might contribute to improved knowledge about the cause and the consequence of MAL-dependent gene regulation.

10. References

- Afshari FT, Kwok JC, White L, Fawcett JW (2010) Schwann cell migration is integrin-dependent and inhibited by astrocyte-produced aggrecan. *Glia* 58:857-869.
- Akert K, Sandri C, Weibel ER, Peper K, Moor H (1976) The fine structure of the perineural endothelium. *Cell and tissue research* 165:281-295.
- Albrecht DE, Sherman DL, Brophy PJ, Froehner SC (2008) The ABCA1 cholesterol transporter associates with one of two distinct dystrophin-based scaffolds in Schwann cells. *Glia* 56:611-618.
- Alonso MA, Weissman SM (1987) cDNA cloning and sequence of MAL, a hydrophobic protein associated with human T-cell differentiation. *Proceedings of the National Academy of Sciences of the United States of America* 84:1997-2001.
- Anton ES, Weskamp G, Reichardt LF, Matthew WD (1994) Nerve growth factor and its low-affinity receptor promote Schwann cell migration. *Proceedings of the National Academy of Sciences of the United States of America* 91:2795-2799.
- Archipoff G, Beretz A, Bartha K, Brisson C, de la Salle C, Froget-Leon C, Klein-Soyer C, Cazenave JP (1993) Role of cyclic AMP in promoting the thromboresistance of human endothelial cells by enhancing thrombomodulin and decreasing tissue factor activities. *British journal of pharmacology* 109:18-28.
- Ariga M, Nedachi T, Akahori M, Sakamoto H, Ito Y, Hakuno F, Takahashi S (2000) Signalling pathways of insulin-like growth factor-I that are augmented by cAMP in FRTL-5 cells. *The Biochemical journal* 348 Pt 2:409-416.
- Arthur-Farraj P, Wanek K, Hantke J, Davis CM, Jayakar A, Parkinson DB, Mirsky R, Jessen KR (2011) Mouse schwann cells need both NRG1 and cyclic AMP to myelinate. *Glia* 59:720-733.
- Arthur-Farraj PJ, Latouche M, Wilton DK, Quintes S, Chabrol E, Banerjee A, Woodhoo A, Jenkins B, Rahman M, Turmaine M, Wicher GK, Mitter R, Greensmith L, Behrens A, Raivich G, Mirsky R, Jessen KR (2012) c-Jun reprograms Schwann cells of injured nerves to generate a repair cell essential for regeneration. *Neuron* 75:633-647.
- Bansal R, Pfeiffer SE (1989) Reversible inhibition of oligodendrocyte progenitor differentiation by a monoclonal antibody against surface galactolipids. *Proceedings of the National Academy of Sciences of the United States of America* 86:6181-6185.
- Barradas M, Gonos ES, Zebedee Z, Kolettas E, Petropoulou C, Delgado MD, Leon J, Hara E, Serrano M (2002) Identification of a candidate tumor-suppressor gene specifically activated during Ras-induced senescence. *Experimental cell research* 273:127-137.
- Barros CS, Nguyen T, Spencer KSR, Nishiyama A, Colognato H, Muller U (2009) beta 1 integrins are required for normal CNS myelination and promote AKT-dependent myelin outgrowth. *Development* 136:2717-2724.
- Bellacosa A, Testa JR, Staal SP, Tschlis PN (1991) A retroviral oncogene, akt, encoding a serine-threonine kinase containing an SH2-like region. *Science* 254:274-277.

- Bender AT, Beavo JA (2006) Cyclic nucleotide phosphodiesterases: molecular regulation to clinical use. *Pharmacological reviews* 58:488-520.
- Benjamini Y, Hochberg Y (1995) Controlling the false discovery rate: a practical and powerful approach to multiple testing. *J Roy Stat Soc Ser B* 57:289-300.
- Benninger Y, Thurnherr T, Pereira JA, Krause S, Wu X, Chrostek-Grashoff A, Herzog D, Nave KA, Franklin RJ, Meijer D, Brakebusch C, Suter U, Relvas JB (2007) Essential and distinct roles for cdc42 and rac1 in the regulation of Schwann cell biology during peripheral nervous system development. *The Journal of cell biology* 177:1051-1061.
- Bermingham JR, Jr., Scherer SS, O'Connell S, Arroyo E, Kalla KA, Powell FL, Rosenfeld MG (1996) Tst-1/Oct-6/SCIP regulates a unique step in peripheral myelination and is required for normal respiration. *Genes & development* 10:1751-1762.
- Bernier G, De Repentigny Y, Mathieu M, David S, Kothary R (1998) Dystonin is an essential component of the Schwann cell cytoskeleton at the time of myelination. *Development* 125:2135-2148.
- Bijlmakers MJ, Marsh M (2003) The on-off story of protein palmitoylation. *Trends in cell biology* 13:32-42.
- Binet R, Ythier D, Robles AI, Collado M, Larrieu D, Fonti C, Brambilla E, Brambilla C, Serrano M, Harris CC, Pedoux R (2009) WNT16B is a new marker of cellular senescence that regulates p53 activity and the phosphoinositide 3-kinase/AKT pathway. *Cancer research* 69:9183-9191.
- Birch AH, Quinn MC, Filali-Mouhim A, Provencher DM, Mes-Masson AM, Tonin PN (2008) Transcriptome analysis of serous ovarian cancers identifies differentially expressed chromosome 3 genes. *Molecular carcinogenesis* 47:56-65.
- Birchmeier C, Nave KA (2008) Neuregulin-1, a key axonal signal that drives Schwann cell growth and differentiation. *Glia* 56:1491-1497.
- Bosse F, Hasse B, Pippirs U, Greiner-Petter R, Muller HW (2003) Proteolipid plasmalogen: localization in polarized cells, regulated expression and lipid raft association in CNS and PNS myelin. *Journal of neurochemistry* 86:508-518.
- Braun N, Sevigny J, Robson SC, Hammer K, Hanani M, Zimmermann H (2004) Association of the ecto-ATPase NTPDase2 with glial cells of the peripheral nervous system. *Glia* 45:124-132.
- Brockes JP, Fields KL, Raff MC (1979) Studies on cultured rat Schwann cells. I. Establishment of purified populations from cultures of peripheral nerve. *Brain research* 165:105-118.
- Buchstaller J, Sommer L, Bodmer M, Hoffmann R, Suter U, Mantei N (2004) Efficient isolation and gene expression profiling of small numbers of neural crest stem cells and developing Schwann cells. *The Journal of neuroscience : the official journal of the Society for Neuroscience* 24:2357-2365.
- Bunge RP (1993) Expanding roles for the Schwann cell: ensheathment, myelination, trophism and regeneration. *Current opinion in neurobiology* 3:805-809.

- Bunge RP, Bunge MB, Cochran M (1978) Some factors influencing the proliferation and differentiation of myelin-forming cells. *Neurology* 28:59-67.
- Bunge RP, Bunge MB, Eldridge CF (1986) Linkage between axonal ensheathment and basal lamina production by Schwann cells. *Annual review of neuroscience* 9:305-328.
- Buonanno A, Fischbach GD (2001) Neuregulin and ErbB receptor signaling pathways in the nervous system. *Current opinion in neurobiology* 11:287-296.
- Buser AM, Erne B, Werner HB, Nave KA, Schaeren-Wiemers N (2009a) The septin cytoskeleton in myelinating glia. *Molecular and cellular neurosciences* 40:156-166.
- Buser AM, Schmid D, Kern F, Erne B, Lazzati T, Schaeren-Wiemers N (2009b) The myelin protein MAL affects peripheral nerve myelination: a new player influencing p75 neurotrophin receptor expression. *The European journal of neuroscience* 29:2276-2290.
- Call K, Glaser T, Ito CY, Buckler AJ, Pelletier J, Haber DA, Rose EA, Kral A, Yeger H, Lewis WH, Jones C, Housman DE (1990) Isolation and characterization of a zinc finger polypeptide gene at the human chromosome 11 Wilms' tumor locus. *Cell* 60:509-520.
- Campagnoni AT, Pribyl TM, Campagnoni CW, Kampf K, Amur-Umarjee S, Landry CF, Handley VW, Newman SL, Garbay B, Kitamura K (1993) Structure and developmental regulation of Golli-mbp, a 105-kilobase gene that encompasses the myelin basic protein gene and is expressed in cells in the oligodendrocyte lineage in the brain. *The Journal of biological chemistry* 268:4930-4938.
- Carey DJ, Eldridge CF, Cornbrooks CJ, Timpl R, Bunge RP (1983) Biosynthesis of type IV collagen by cultured rat Schwann cells. *The Journal of cell biology* 97:473-479.
- Chan JR (2007) Myelination: all about Rac 'n' roll. *The Journal of cell biology* 177:953-955.
- Chan JR, Cosgaya JM, Wu YJ, Shooter EM (2001) Neurotrophins are key mediators of the myelination program in the peripheral nervous system. *Proceedings of the National Academy of Sciences of the United States of America* 98:14661-14668.
- Chan JR, Watkins TA, Cosgaya JM, Zhang C, Chen L, Reichardt LF, Shooter EM, Barres BA (2004) NGF controls axonal receptivity to myelination by Schwann cells or oligodendrocytes. *Neuron* 43:183-191.
- Chavrier P, Zerial M, Lemaire P, Almendral J, Bravo R, Charnay P (1988) A gene encoding a protein with zinc fingers is activated during G0/G1 transition in cultured cells. *The EMBO journal* 7:29-35.
- Chen ZL, Strickland S (2003) Laminin gamma1 is critical for Schwann cell differentiation, axon myelination, and regeneration in the peripheral nerve. *The Journal of cell biology* 163:889-899.
- Cheong KH, Zacchetti D, Schneeberger EE, Simons K (1999) VIP17/MAL, a lipid raft-associated protein, is involved in apical transport in MDCK cells. *Proceedings of the National Academy of Sciences of the United States of America* 96:6241-6248.

- Chernousov MA, Yu WM, Chen ZL, Carey DJ, Strickland S (2008) Regulation of Schwann cell function by the extracellular matrix. *Glia* 56:1498-1507.
- Chuang YY, Valster A, Coniglio SJ, Backer JM, Symons M (2007) The atypical Rho family GTPase Wrch-1 regulates focal adhesion formation and cell migration. *Journal of cell science* 120:1927-1934.
- Cody RL, Wicha MS (1986) Clustering of cell surface laminin enhances its association with the cytoskeleton. *Experimental cell research* 165:107-116.
- Cohen P, Frame S (2001) The renaissance of GSK3. *Nature reviews Molecular cell biology* 2:769-776.
- Cognato H, Baron W, Avellana-Adalid V, Relvas JB, Baron-Van Evercooren A, Georges-Labouesse E, French-Constant C (2002) CNS integrins switch growth factor signalling to promote target-dependent survival. *Nat Cell Biol* 4:833-841.
- Cognato H, Winkelmann DA, Yurchenco PD (1999) Laminin polymerization induces a receptor-cytoskeleton network. *The Journal of cell biology* 145:619-631.
- Cornbrooks CJ, Carey DJ, McDonald JA, Timpl R, Bunge RP (1983) In vivo and in vitro observations on laminin production by Schwann cells. *Proceedings of the National Academy of Sciences of the United States of America* 80:3850-3854.
- Cosgaya JM, Chan JR, Shooter EM (2002) The neurotrophin receptor p75NTR as a positive modulator of myelination. *Science* 298:1245-1248.
- Court FA, Hewitt JE, Davies K, Patton BL, Uncini A, Wrabetz L, Feltri ML (2009) A laminin-2, dystroglycan, utrophin axis is required for compartmentalization and elongation of myelin segments. *The Journal of neuroscience : the official journal of the Society for Neuroscience* 29:3908-3919.
- Court FA, Wrabetz L, Feltri ML (2006) Basal lamina: Schwann cells wrap to the rhythm of space-time. *Current opinion in neurobiology* 16:501-507.
- Crosby SD, Veile RA, Donis-Keller H, Baraban JM, Bhat RV, Simburger KS, Milbrandt J (1992) Neural-specific expression, genomic structure, and chromosomal localization of the gene encoding the zinc-finger transcription factor NGFI-C. *Proceedings of the National Academy of Sciences of the United States of America* 89:6663.
- D'Antonio M, Michalovich D, Paterson M, Droggiti A, Woodhoo A, Mirsky R, Jessen KR (2006) Gene profiling and bioinformatic analysis of Schwann cell embryonic development and myelination. *Glia* 53:501-515.
- Davis RJ (2000) Signal transduction by the JNK group of MAP kinases. *Cell* 103:239-252.
- De Donatis A, Comito G, Buricchi F, Vinci MC, Parenti A, Caselli A, Camici G, Manao G, Ramponi G, Cirri P (2008) Proliferation versus migration in platelet-derived growth factor signaling: the key role of endocytosis. *The Journal of biological chemistry* 283:19948-19956.
- De Leon M, Van Eldik LJ, Shooter EM (1991) Differential regulation of S100 beta and mRNAs coding for S100-like proteins (42A and 42C) during development and after lesion of rat sciatic nerve. *Journal of neuroscience research* 29:155-162.

- Dong Z, Brennan A, Liu N, Yarden Y, Lefkowitz G, Mirsky R, Jessen KR (1995) Neu differentiation factor is a neuron-glia signal and regulates survival, proliferation, and maturation of rat Schwann cell precursors. *Neuron* 15:585-596.
- el-Husseini Ael D, Bredt DS (2002) Protein palmitoylation: a regulator of neuronal development and function. *Nature reviews Neuroscience* 3:791-802.
- Erne B, Sansano S, Frank M, Schaeren-Wiemers N (2002) Rafts in adult peripheral nerve myelin contain major structural myelin proteins and myelin and lymphocyte protein (MAL) and CD59 as specific markers. *Journal of neurochemistry* 82:550-562.
- Eto K, Hommyo A, Yonemitsu R, Abe S (2010) ErbB4 signals Neuregulin1-stimulated cell proliferation and c-fos gene expression through phosphorylation of serum response factor by mitogen-activated protein kinase cascade. *Molecular and cellular biochemistry* 339:119-125.
- Falls DL (2003) Neuregulins and the neuromuscular system: 10 years of answers and questions. *Journal of neurocytology* 32:619-647.
- Feltri ML, Graus Porta D, Previtali SC, Nodari A, Migliavacca B, Cassetti A, Littlewood-Evans A, Reichardt LF, Messing A, Quattrini A, Mueller U, Wrabetz L (2002) Conditional disruption of beta 1 integrin in Schwann cells impedes interactions with axons. *The Journal of cell biology* 156:199-209.
- Feltri ML, Scherer SS, Nemni R, Kamholz J, Vogelbacker H, Scott MO, Canal N, Quaranta V, Wrabetz L (1994) Beta 4 integrin expression in myelinating Schwann cells is polarized, developmentally regulated and axonally dependent. *Development* 120:1287-1301.
- Feltri ML, Suter U, Relvas JB (2008) The function of RhoGTPases in axon ensheathment and myelination. *Glia* 56:1508-1517.
- Fernandez-Valle C, Gorman D, Gomez AM, Bunge MB (1997) Actin plays a role in both changes in cell shape and gene-expression associated with Schwann cell myelination. *The Journal of neuroscience : the official journal of the Society for Neuroscience* 17:241-250.
- Flores AI, Narayanan SP, Morse EN, Shick HE, Yin X, Kidd G, Avila RL, Kirschner DA, Macklin WB (2008) Constitutively active Akt induces enhanced myelination in the CNS. *The Journal of neuroscience : the official journal of the Society for Neuroscience* 28:7174-7183.
- Frank M (2000) MAL, a proteolipid in glycosphingolipid enriched domains: functional implications in myelin and beyond. *Progress in neurobiology* 60:531-544.
- Frank M, Atanasoski S, Sancho S, Magyar JP, Rulicke T, Schwab ME, Suter U (2000) Progressive segregation of unmyelinated axons in peripheral nerves, myelin alterations in the CNS, and cyst formation in the kidneys of myelin and lymphocyte protein-overexpressing mice. *Journal of neurochemistry* 75:1927-1939.
- Frank M, Schaeren-Wiemers N, Schneider R, Schwab ME (1999) Developmental expression pattern of the myelin proteolipid MAL indicates different functions of MAL for

- immature Schwann cells and in a late step of CNS myelinogenesis. *Journal of neurochemistry* 73:587-597.
- Frank M, van der Haar ME, Schaeren-Wiemers N, Schwab ME (1998) rMAL is a glycosphingolipid-associated protein of myelin and apical membranes of epithelial cells in kidney and stomach. *The Journal of neuroscience : the official journal of the Society for Neuroscience* 18:4901-4913.
- Fu CA, Shen M, Huang BC, Lasaga J, Payan DG, Luo Y (1999) TNIK, a novel member of the germinal center kinase family that activates the c-Jun N-terminal kinase pathway and regulates the cytoskeleton. *The Journal of biological chemistry* 274:30729-30737.
- Gao H, He C, Fang X, Hou X, Feng X, Yang H, Zhao X, Ma T (2006) Localization of aquaporin-1 water channel in glial cells of the human peripheral nervous system. *Glia* 53:783-787.
- Gao X, Daugherty RL, Tourtellotte WG (2007) Regulation of low affinity neurotrophin receptor (p75(NTR)) by early growth response (Egr) transcriptional regulators. *Molecular and cellular neurosciences* 36:501-514.
- Garratt AN, Britsch S, Birchmeier C (2000a) Neuregulin, a factor with many functions in the life of a schwann cell. *BioEssays : news and reviews in molecular, cellular and developmental biology* 22:987-996.
- Garratt AN, Voiculescu O, Topilko P, Charnay P, Birchmeier C (2000b) A dual role of erbB2 in myelination and in expansion of the schwann cell precursor pool. *The Journal of cell biology* 148:1035-1046.
- Gessler M, Poustka A, Cavenee W, Neve RL, Orkin SH, Bruns GA (1990) Homozygous deletion in Wilms tumours of a zinc-finger gene identified by chromosome jumping. *Nature* 343:774-778.
- Gillen C, Gleichmann M, Greiner-Petter R, Zoidl G, Kupfer S, Bosse F, Auer J, Muller HW (1996) Full-length cloning, expression and cellular localization of rat plasmalogen mRNA, a proteolipid of PNS and CNS. *The European journal of neuroscience* 8:405-414.
- Goda S, Hammer J, Kobiler D, Quarles RH (1991) Expression of the myelin-associated glycoprotein in cultures of immortalized Schwann cells. *Journal of neurochemistry* 56:1354-1361.
- Goebbels S, Oltrogge JH, Kemper R, Heilmann I, Bormuth I, Wolfer S, Wichert SP, Mobius W, Liu X, Lappe-Siefke C, Rossner MJ, Groszer M, Suter U, Frahm J, Boretius S, Nave KA (2010) Elevated phosphatidylinositol 3,4,5-trisphosphate in glia triggers cell-autonomous membrane wrapping and myelination. *The Journal of neuroscience : the official journal of the Society for Neuroscience* 30:8953-8964.
- Grimes CA, Jope RS (2001) CREB DNA binding activity is inhibited by glycogen synthase kinase-3 beta and facilitated by lithium. *Journal of neurochemistry* 78:1219-1232.
- Grove M, Komiyama NH, Nave KA, Grant SG, Sherman DL, Brophy PJ (2007) FAK is required for axonal sorting by Schwann cells. *The Journal of cell biology* 176:277-282.

- Guennoun R, Benmessahel Y, Delespierre B, Gouezou M, Rajkowski KM, Baulieu EE, Schumacher M (2001) Progesterone stimulates Krox-20 gene expression in Schwann cells. *Brain research Molecular brain research* 90:75-82.
- Hancock JF, Parton RG (2005) Ras plasma membrane signalling platforms. *The Biochemical journal* 389:1-11.
- Hanemann CO, Kuhn G, Lie A, Gillen C, Bosse F, Spreyer P, Muller HW (1993) Expression of decorin mRNA in the nervous system of rat. *The journal of histochemistry and cytochemistry : official journal of the Histochemistry Society* 41:1383-1391.
- Hanoune J, Defer N (2001) Regulation and role of adenylyl cyclase isoforms. *Annual review of pharmacology and toxicology* 41:145-174.
- Harrisingh MC, Perez-Nadales E, Parkinson DB, Malcolm DS, Mudge AW, Lloyd AC (2004) The Ras/Raf/ERK signalling pathway drives Schwann cell dedifferentiation. *The EMBO journal* 23:3061-3071.
- Heinen A, Lehmann HC, Kury P (2013) Negative regulators of schwann cell differentiation- novel targets for peripheral nerve therapies? *Journal of clinical immunology* 33 Suppl 1:S18-26.
- Holmes WE, Sliwkowski MX, Akita RW, Henzel WJ, Lee J, Park JW, Yansura D, Abadi N, Raab H, Lewis GD, et al. (1992) Identification of heregulin, a specific activator of p185erbB2. *Science* 256:1205-1210.
- Horiuchi K, Zhou HM, Kelly K, Manova K, Blobel CP (2005) Evaluation of the contributions of ADAMs 9, 12, 15, 17, and 19 to heart development and ectodomain shedding of neuregulins beta1 and beta2. *Developmental biology* 283:459-471.
- Hoshina N, Tezuka T, Yokoyama K, Kozuka-Hata H, Oyama M, Yamamoto T (2007) Focal adhesion kinase regulates laminin-induced oligodendroglial process outgrowth. *Genes Cells* 12:1245-1254.
- Hu X, Hicks CW, He W, Wong P, Macklin WB, Trapp BD, Yan R (2006) Bace1 modulates myelination in the central and peripheral nervous system. *Nat Neurosci* 9:1520-1525.
- Huang da W, Sherman BT, Lempicki RA (2009) Systematic and integrative analysis of large gene lists using DAVID bioinformatics resources. *Nature protocols* 4:44-57.
- Iglesias D, Fernandez-Peralta AM, Nejda N, Daimiel L, Azcoita MM, Oliart S, Gonzalez-Aguilera JJ (2006) RIS1, a gene with trinucleotide repeats, is a target in the mutator pathway of colorectal carcinogenesis. *Cancer genetics and cytogenetics* 167:138-144.
- Iino M, Ehama R, Nakazawa Y, Iwabuchi T, Ogo M, Tajima M, Arase S (2007) Adenosine stimulates fibroblast growth factor-7 gene expression via adenosine A2b receptor signaling in dermal papilla cells. *The Journal of investigative dermatology* 127:1318-1325.
- Ito T, Ogura M, Morishita Y, Takamatsu J, Maruyama I, Yamamoto S, Ogawa K, Saito H (1990) Enhanced expression of thrombomodulin by intracellular cyclic AMP-

- increasing agents in two human megakaryoblastic leukemia cell lines. *Thrombosis research* 58:615-624.
- Jaegle M, Mandemakers W, Broos L, Zwart R, Karis A, Visser P, Grosveld F, Meijer D (1996) The POU factor Oct-6 and Schwann cell differentiation. *Science* 273:507-510.
- Jessen KR, Mirsky R (2005) The origin and development of glial cells in peripheral nerves. *Nature reviews Neuroscience* 6:671-682.
- Jesuraj NJ, Nguyen PK, Wood MD, Moore AM, Borschel GH, Mackinnon SE, Sakiyama-Elbert SE (2012) Differential gene expression in motor and sensory Schwann cells in the rat femoral nerve. *Journal of neuroscience research* 90:96-104.
- Jiang H, Qu W, Li Y, Zhong W, Zhang W (2013) Platelet-derived growth factors-BB and Fibroblast Growth Factors-base induced proliferation of Schwann cells in a 3D environment. *Neurochemical research* 38:346-355.
- Jin F, Dong B, Georgiou J, Jiang Q, Zhang J, Bharioke A, Qiu F, Lommel S, Feltri ML, Wrabetz L, Roder JC, Eyer J, Chen X, Peterson AC, Siminovitch KA (2011) N-WASp is required for Schwann cell cytoskeletal dynamics, normal myelin gene expression and peripheral nerve myelination. *Development* 138:1329-1337.
- Jirsova K, Soodar P, Mandys V, Bar PR (1997) Cold jet: a method to obtain pure Schwann cell cultures without the need for cytotoxic, apoptosis-inducing drug treatment. *Journal of neuroscience methods* 78:133-137.
- Johnson GL, Lapadat R (2002) Mitogen-activated protein kinase pathways mediated by ERK, JNK, and p38 protein kinases. *Science* 298:1911-1912.
- Jung-Testas I, Schumacher M, Bugnard H, Baulieu EE (1993) Stimulation of rat Schwann cell proliferation by estradiol: synergism between the estrogen and cAMP. *Brain research Developmental brain research* 72:282-290.
- Kielbasa SM, Klein H, Roeder HG, Vingron M, Bluthgen N (2010) TransFind--predicting transcriptional regulators for gene sets. *Nucleic acids research* 38:W275-280.
- Kim HA, DeClue JE, Ratner N (1997) cAMP-dependent protein kinase A is required for Schwann cell growth: interactions between the cAMP and neuregulin/tyrosine kinase pathways. *Journal of neuroscience research* 49:236-247.
- Kim SY, Chung HS, Sun W, Kim H (2007) Spatiotemporal expression pattern of non-clustered protocadherin family members in the developing rat brain. *Neuroscience* 147:996-1021.
- Kim T, Fiedler K, Madison DL, Krueger WH, Pfeiffer SE (1995) Cloning and characterization of MVP17: a developmentally regulated myelin protein in oligodendrocytes. *Journal of neuroscience research* 42:413-422.
- Kinter J, Lazzati T, Schmid D, Zeis T, Erne B, Lutzelschwab R, Steck AJ, Pareyson D, Peles E, Schaeren-Wiemers N (2013) An essential role of MAG in mediating axon-myelin attachment in Charcot-Marie-Tooth 1A disease. *Neurobiology of disease* 49:221-231.
- Kobe B, Kajava AV (2001) The leucine-rich repeat as a protein recognition motif. *Current opinion in structural biology* 11:725-732.

- Kolsch A, Windoffer R, Leube RE (2009) Actin-dependent dynamics of keratin filament precursors. *Cell motility and the cytoskeleton* 66:976-985.
- Kontani K, Tada M, Ogawa T, Okai T, Saito K, Araki Y, Katada T (2002) Di-Ras, a distinct subgroup of ras family GTPases with unique biochemical properties. *The Journal of biological chemistry* 277:41070-41078.
- Kyriakis JM, Avruch J (2001) Mammalian mitogen-activated protein kinase signal transduction pathways activated by stress and inflammation. *Physiological reviews* 81:807-869.
- Le N, Nagarajan R, Wang JY, Araki T, Schmidt RE, Milbrandt J (2005) Analysis of congenital hypomyelinating Egr2Lo/Lo nerves identifies Sox2 as an inhibitor of Schwann cell differentiation and myelination. *Proceedings of the National Academy of Sciences of the United States of America* 102:2596-2601.
- Lee J, Gravel M, Zhang R, Thibault P, Braun PE (2005) Process outgrowth in oligodendrocytes is mediated by CNP, a novel microtubule assembly myelin protein. *The Journal of cell biology* 170:661-673.
- Lee PR, Cohen JE, Tendi EA, Farrer R, GH DEV, Becker KG, Fields RD (2004) Transcriptional profiling in an MPNST-derived cell line and normal human Schwann cells. *Neuron glia biology* 1:135-147.
- Lees MB, Chao BH, Laursen RA, L'Italien JJ (1982) A hydrophobic tryptic peptide from bovine white matter proteolipid. *Biochimica et biophysica acta* 702:117-124.
- Lemaire P, Revelant O, Bravo R, Charnay P (1988) Two mouse genes encoding potential transcription factors with identical DNA-binding domains are activated by growth factors in cultured cells. *Proceedings of the National Academy of Sciences of the United States of America* 85:4691-4695.
- Lemke G, Chao M (1988) Axons regulate Schwann cell expression of the major myelin and NGF receptor genes. *Development* 102:499-504.
- Lemke G, Kuhn R, Monuki ES, Weinmaster G (1990) Transcriptional controls underlying Schwann cell differentiation and myelination. *Annals of the New York Academy of Sciences* 605:248-253.
- Li H, Lu Y, Smith HK, Richardson WD (2007) Olig1 and Sox10 interact synergistically to drive myelin basic protein transcription in oligodendrocytes. *The Journal of neuroscience : the official journal of the Society for Neuroscience* 27:14375-14382.
- Li S, Liquari P, McKee KK, Harrison D, Patel R, Lee S, Yurchenco PD (2005) Laminin-sulfatide binding initiates basement membrane assembly and enables receptor signaling in Schwann cells and fibroblasts. *The Journal of cell biology* 169:179-189.
- Li ZH, Spektor A, Varlamova O, Bresnick AR (2003) Mts1 regulates the assembly of nonmuscle myosin-IIA. *Biochemistry* 42:14258-14266.
- Liang CC, Park AY, Guan JL (2007) In vitro scratch assay: a convenient and inexpensive method for analysis of cell migration in vitro. *Nature protocols* 2:329-333.

- Liffers ST, Maghnouj A, Munding JB, Jackstadt R, Herbrand U, Schulenburg T, Marcus K, Klein-Scory S, Schmiegel W, Schwarte-Waldhoff I, Meyer HE, Stuhler K, Hahn SA (2011) Keratin 23, a novel DPC4/Smad4 target gene which binds 14-3-3epsilon. *BMC cancer* 11:137.
- Linder ME, Deschenes RJ (2007) Palmitoylation: policing protein stability and traffic. *Nature reviews Molecular cell biology* 8:74-84.
- Loebel DA, Studdert JB, Power M, Radziewicz T, Jones V, Coultas L, Jackson Y, Rao RS, Steiner K, Fossat N, Robb L, Tam PP (2011) Rho maintains the epithelial architecture and facilitates differentiation of the foregut endoderm. *Development* 138:4511-4522.
- Mager GM, Ward RM, Srinivasan R, Jang SW, Wrabetz L, Svaren J (2008) Active gene repression by the Egr2.NAB complex during peripheral nerve myelination. *The Journal of biological chemistry* 283:18187-18197.
- Magnaghi V, Parducz A, Frasca A, Ballabio M, Procacci P, Racagni G, Bonanno G, Fumagalli F (2010) GABA synthesis in Schwann cells is induced by the neuroactive steroid allopregnanolone. *Journal of neurochemistry* 112:980-990.
- Magyar JP, Ebensperger C, Schaeren-Wiemers N, Suter U (1997) Myelin and lymphocyte protein (MAL/MVP17/VIP17) and plasmalogen are members of an extended gene family. *Gene* 189:269-275.
- Makoukji J, Shackelford G, Meffre D, Grenier J, Liere P, Lobaccaro JM, Schumacher M, Massaad C (2011) Interplay between LXR and Wnt/beta-catenin signaling in the negative regulation of peripheral myelin genes by oxysterols. *The Journal of neuroscience : the official journal of the Society for Neuroscience* 31:9620-9629.
- Mandemakers W, Zwart R, Jaegle M, Walbeehm E, Visser P, Grosveld F, Meijer D (2000) A distal Schwann cell-specific enhancer mediates axonal regulation of the Oct-6 transcription factor during peripheral nerve development and regeneration. *The EMBO journal* 19:2992-3003.
- Marchese C, Rubin J, Ron D, Faggioni A, Torrisi MR, Messina A, Frati L, Aaronson SA (1990) Human keratinocyte growth factor activity on proliferation and differentiation of human keratinocytes: differentiation response distinguishes KGF from EGF family. *Journal of cellular physiology* 144:326-332.
- Marinkovich MP, Keene DR, Rimberg CS, Burgeson RE (1993) Cellular origin of the dermal-epidermal basement membrane. *Developmental dynamics : an official publication of the American Association of Anatomists* 197:255-267.
- Martin-Belmonte F, Kremer L, Albar JP, Marazuela M, Alonso MA (1998) Expression of the MAL gene in the thyroid: the MAL proteolipid, a component of glycolipid-enriched membranes, is apically distributed in thyroid follicles. *Endocrinology* 139:2077-2084.
- Martin-Belmonte F, Puertollano R, Millan J, Alonso MA (2000) The MAL proteolipid is necessary for the overall apical delivery of membrane proteins in the polarized epithelial Madin-Darby canine kidney and fischer rat thyroid cell lines. *Molecular biology of the cell* 11:2033-2045.

- Maruyama I, Soejima Y, Osame M, Ito T, Ogawa K, Yamamoto S, Dittman WA, Saito H (1991) Increased expression of thrombomodulin on the cultured human umbilical vein endothelial cells and mouse hemangioma cells by cyclic AMP. *Thrombosis research* 61:301-310.
- Maurel P, Einheber S, Galinska J, Thaker P, Lam I, Rubin MB, Scherer SS, Murakami Y, Gutmann DH, Salzer JL (2007) Nectin-like proteins mediate axon Schwann cell interactions along the internode and are essential for myelination. *The Journal of cell biology* 178:861-874.
- Maurel P, Salzer JL (2000) Axonal regulation of Schwann cell proliferation and survival and the initial events of myelination requires PI 3-kinase activity. *The Journal of neuroscience : the official journal of the Society for Neuroscience* 20:4635-4645.
- Mayer SI, Thiel G (2009) Calcium influx into MIN6 insulinoma cells induces expression of Egr-1 involving extracellular signal-regulated protein kinase and the transcription factors Elk-1 and CREB. *European journal of cell biology* 88:19-33.
- Mayer SI, Willars GB, Nishida E, Thiel G (2008) Elk-1, CREB, and MKP-1 regulate Egr-1 expression in gonadotropin-releasing hormone stimulated gonadotrophs. *Journal of cellular biochemistry* 105:1267-1278.
- McKee KK, Harrison D, Capizzi S, Yurchenco PD (2007) Role of laminin terminal globular domains in basement membrane assembly. *The Journal of biological chemistry* 282:21437-21447.
- Meier C, Parmantier E, Brennan A, Mirsky R, Jessen KR (1999) Developing Schwann cells acquire the ability to survive without axons by establishing an autocrine circuit involving insulin-like growth factor, neurotrophin-3, and platelet-derived growth factor-BB. *The Journal of neuroscience : the official journal of the Society for Neuroscience* 19:3847-3859.
- Meintanis S, Thomaidou D, Jessen KR, Mirsky R, Matsas R (2001) The neuron-glia signal beta-neuregulin promotes Schwann cell motility via the MAPK pathway. *Glia* 34:39-51.
- Melendez-Vasquez CV, Einheber S, Salzer JL (2004) Rho kinase regulates schwann cell myelination and formation of associated axonal domains. *The Journal of neuroscience : the official journal of the Society for Neuroscience* 24:3953-3963.
- Michailov GV, Sereda MW, Brinkmann BG, Fischer TM, Haug B, Birchmeier C, Role L, Lai C, Schwab MH, Nave KA (2004) Axonal neuregulin-1 regulates myelin sheath thickness. *Science* 304:700-703.
- Mikol DD, Hong HL, Cheng HL, Feldman EL (1999) Caveolin-1 expression in Schwann cells. *Glia* 27:39-52.
- Mikol DD, Scherer SS, Duckett SJ, Hong HL, Feldman EL (2002) Schwann cell caveolin-1 expression increases during myelination and decreases after axotomy. *Glia* 38:191-199.

- Monje PV, Bartlett Bunge M, Wood PM (2006) Cyclic AMP synergistically enhances neuregulin-dependent ERK and Akt activation and cell cycle progression in Schwann cells. *Glia* 53:649-659.
- Monje PV, Rendon S, Athauda G, Bates M, Wood PM, Bunge MB (2009) Non-antagonistic relationship between mitogenic factors and cAMP in adult Schwann cell re-differentiation. *Glia* 57:947-961.
- Monje PV, Soto J, Bacallao K, Wood PM (2010) Schwann cell dedifferentiation is independent of mitogenic signaling and uncoupled to proliferation: role of cAMP and JNK in the maintenance of the differentiated state. *The Journal of biological chemistry* 285:31024-31036.
- Monk KR, Naylor SG, Glenn TD, Mercurio S, Perlin JR, Dominguez C, Moens CB, Talbot WS (2009) A G protein-coupled receptor is essential for Schwann cells to initiate myelination. *Science* 325:1402-1405.
- Monk KR, Oshima K, Jors S, Heller S, Talbot WS (2011) Gpr126 is essential for peripheral nerve development and myelination in mammals. *Development* 138:2673-2680.
- Montero JC, Yuste L, Diaz-Rodriguez E, Esparis-Ogando A, Pandiella A (2000) Differential shedding of transmembrane neuregulin isoforms by the tumor necrosis factor-alpha-converting enzyme. *Molecular and cellular neurosciences* 16:631-648.
- Monuki ES, Weinmaster G, Kuhn R, Lemke G (1989) SCIP: a glial POU domain gene regulated by cyclic AMP. *Neuron* 3:783-793.
- Morgan L, Jessen KR, Mirsky R (1991) The effects of cAMP on differentiation of cultured Schwann cells: progression from an early phenotype (04+) to a myelin phenotype (P0+, GFAP-, N-CAM-, NGF-receptor-) depends on growth inhibition. *The Journal of cell biology* 112:457-467.
- Napoli I, Noon LA, Ribeiro S, Kerai AP, Parrinello S, Rosenberg LH, Collins MJ, Harrisingh MC, White IJ, Woodhoo A, Lloyd AC (2012) A central role for the ERK-signaling pathway in controlling Schwann cell plasticity and peripheral nerve regeneration in vivo. *Neuron* 73:729-742.
- Nave KA (2010) Myelination and the trophic support of long axons. *Nature reviews Neuroscience* 11:275-283.
- Nave KA, Salzer JL (2006) Axonal regulation of myelination by neuregulin 1. *Current opinion in neurobiology* 16:492-500.
- Nave KA, Trapp BD (2008) Axon-glial signaling and the glial support of axon function. *Annual review of neuroscience* 31:535-561.
- Nickols JC, Valentine W, Kanwal S, Carter BD (2003) Activation of the transcription factor NF-kappaB in Schwann cells is required for peripheral myelin formation. *Nat Neurosci* 6:161-167.
- Nishida E, Gotoh Y (1993) The MAP kinase cascade is essential for diverse signal transduction pathways. *Trends in biochemical sciences* 18:128-131.

- Nishimoto S, Nishida E (2006) MAPK signalling: ERK5 versus ERK1/2. *EMBO reports* 7:782-786.
- Nodari A, Zambroni D, Quattrini A, Court FA, D'Urso A, Recchia A, Tybulewicz VL, Wrabetz L, Feltri ML (2007) Beta1 integrin activates Rac1 in Schwann cells to generate radial lamellae during axonal sorting and myelination. *The Journal of cell biology* 177:1063-1075.
- Ogata T, Iijima S, Hoshikawa S, Miura T, Yamamoto S, Oda H, Nakamura K, Tanaka S (2004) Opposing extracellular signal-regulated kinase and Akt pathways control Schwann cell myelination. *The Journal of neuroscience : the official journal of the Society for Neuroscience* 24:6724-6732.
- Omori K, Kotera J (2007) Overview of PDEs and their regulation. *Circulation research* 100:309-327.
- Onishi M, Kinoshita S, Morikawa Y, Shibuya A, Phillips J, Lanier LL, Gorman DM, Nolan GP, Miyajima A, Kitamura T (1996) Applications of retrovirus-mediated expression cloning. *Experimental hematology* 24:324-329.
- Ory S, Brazier H, Blangy A (2007) Identification of a bipartite focal adhesion localization signal in RhoU/Wrch-1, a Rho family GTPase that regulates cell adhesion and migration. *Biology of the cell / under the auspices of the European Cell Biology Organization* 99:701-716.
- Parkinson DB, Bhaskaran A, Arthur-Farraj P, Noon LA, Woodhoo A, Lloyd AC, Feltri ML, Wrabetz L, Behrens A, Mirsky R, Jessen KR (2008) c-Jun is a negative regulator of myelination. *The Journal of cell biology* 181:625-637.
- Parkinson DB, Bhaskaran A, Droggiti A, Dickinson S, D'Antonio M, Mirsky R, Jessen KR (2004) Krox-20 inhibits Jun-NH2-terminal kinase/c-Jun to control Schwann cell proliferation and death. *The Journal of cell biology* 164:385-394.
- Parkinson DB, Dickinson S, Bhaskaran A, Kinsella MT, Brophy PJ, Sherman DL, Sharghi-Namini S, Duran Alonso MB, Mirsky R, Jessen KR (2003) Regulation of the myelin gene periaxin provides evidence for Krox-20-independent myelin-related signalling in Schwann cells. *Molecular and cellular neurosciences* 23:13-27.
- Patwardhan S, Gashler A, Siegel MG, Chang LC, Joseph LJ, Shows TB, Le Beau MM, Sukhatme VP (1991) EGR3, a novel member of the Egr family of genes encoding immediate-early transcription factors. *Oncogene* 6:917-928.
- Peirano RI, Goerich DE, Riethmacher D, Wegner M (2000) Protein zero gene expression is regulated by the glial transcription factor Sox10. *Molecular and cellular biology* 20:3198-3209.
- Pietri T, Eder O, Brea MA, Topilko P, Blanche M, Brakebusch C, Fassler R, Thiery JP, Dufour S (2004) Conditional beta1-integrin gene deletion in neural crest cells causes severe developmental alterations of the peripheral nervous system. *Development* 131:3871-3883.
- Poliak S, Peles E (2003) The local differentiation of myelinated axons at nodes of Ranvier. *Nature reviews Neuroscience* 4:968-980.

- Porstmann T, Griffiths B, Chung YL, Delpuech O, Griffiths JR, Downward J, Schulze A (2005) PKB/Akt induces transcription of enzymes involved in cholesterol and fatty acid biosynthesis via activation of SREBP. *Oncogene* 24:6465-6481.
- Previtali SC, Nodari A, Taveggia C, Pardini C, Dina G, Villa A, Wrabetz L, Quattrini A, Feltri ML (2003) Expression of laminin receptors in schwann cell differentiation: evidence for distinct roles. *The Journal of neuroscience : the official journal of the Society for Neuroscience* 23:5520-5530.
- Pribyl TM, Campagnoni CW, Kampf K, Kashima T, Handley VW, McMahon J, Campagnoni AT (1996) Expression of the myelin proteolipid protein gene in the human fetal thymus. *Journal of neuroimmunology* 67:125-130.
- Puertollano R, Martin-Belmonte F, Millan J, de Marco MC, Albar JP, Kremer L, Alonso MA (1999) The MAL proteolipid is necessary for normal apical transport and accurate sorting of the influenza virus hemagglutinin in Madin-Darby canine kidney cells. *The Journal of cell biology* 145:141-151.
- Raman M, Chen W, Cobb MH (2007) Differential regulation and properties of MAPKs. *Oncogene* 26:3100-3112.
- Reichardt LF (2006) Neurotrophin-regulated signalling pathways. *Philosophical transactions of the Royal Society of London Series B, Biological sciences* 361:1545-1564.
- Reif R, Sales S, Hettwer S, Dreier B, Gisler C, Wolfel J, Luscher D, Zurlinden A, Stephan A, Ahmed S, Baici A, Ledermann B, Kunz B, Sonderegger P (2007) Specific cleavage of agrin by neurotrypsin, a synaptic protease linked to mental retardation. *FASEB journal : official publication of the Federation of American Societies for Experimental Biology* 21:3468-3478.
- Rezajooi K, Pavlides M, Winterbottom J, Stallcup WB, Hamlyn PJ, Lieberman AR, Anderson PN (2004) NG2 proteoglycan expression in the peripheral nervous system: upregulation following injury and comparison with CNS lesions. *Molecular and cellular neurosciences* 25:572-584.
- Riethmacher D, Sonnenberg-Riethmacher E, Brinkmann V, Yamaai T, Lewin GR, Birchmeier C (1997) Severe neuropathies in mice with targeted mutations in the ErbB3 receptor. *Nature* 389:725-730.
- Rigopoulou EI, Roggenbuck D, Smyk DS, Liaskos C, Mytilinaiou MG, Feist E, Conrad K, Bogdanos DP (2012) Asialoglycoprotein receptor (ASGPR) as target autoantigen in liver autoimmunity: lost and found. *Autoimmunity reviews* 12:260-269.
- Robinson MJ, Cobb MH (1997) Mitogen-activated protein kinase pathways. *Current opinion in cell biology* 9:180-186.
- Saarikangas J, Barral Y (2011) The emerging functions of septins in metazoans. *EMBO reports* 12:1118-1126.
- Saher G, Brugger B, Lappe-Siefke C, Mobius W, Tozawa R, Wehr MC, Wieland F, Ishibashi S, Nave KA (2005) High cholesterol level is essential for myelin membrane growth. *Nat Neurosci* 8:468-475.

- Saher G, Quintes S, Mobius W, Wehr MC, Kramer-Albers EM, Brugger B, Nave KA (2009) Cholesterol Regulates the Endoplasmic Reticulum Exit of the Major Membrane Protein P0 Required for Peripheral Myelin Compaction. *J Neurosci* 29:6094-6104.
- Saito F, Moore SA, Barresi R, Henry MD, Messing A, Ross-Barta SE, Cohn RD, Williamson RA, Sluka KA, Sherman DL, Brophy PJ, Schmelzer JD, Low PA, Wrabetz L, Feltri ML, Campbell KP (2003) Unique role of dystroglycan in peripheral nerve myelination, nodal structure, and sodium channel stabilization. *Neuron* 38:747-758.
- Salzer JL, Williams AK, Glaser L, Bunge RP (1980) Studies of Schwann cell proliferation. II. Characterization of the stimulation and specificity of the response to a neurite membrane fraction. *The Journal of cell biology* 84:753-766.
- Sandberg MM, Hirvonen HE, Elima KJ, Vuorio EI (1993) Co-expression of collagens II and XI and alternative splicing of exon 2 of collagen II in several developing human tissues. *The Biochemical journal* 294 (Pt 2):595-602.
- Saravanan K, Schaeren-Wiemers N, Klein D, Sandhoff R, Schwarz A, Yaghootfam A, Gieselmann V, Franken S (2004) Specific downregulation and mistargeting of the lipid raft-associated protein MAL in a glycolipid storage disorder. *Neurobiology of disease* 16:396-406.
- Schaeren-Wiemers N, Bonnet A, Erb M, Erne B, Bartsch U, Kern F, Mantei N, Sherman D, Suter U (2004) The raft-associated protein MAL is required for maintenance of proper axon-glia interactions in the central nervous system. *The Journal of cell biology* 166:731-742.
- Schaeren-Wiemers N, Gerfin-Moser A (1993) A single protocol to detect transcripts of various types and expression levels in neural tissue and cultured cells: in situ hybridization using digoxigenin-labelled cRNA probes. *Histochemistry* 100:431-440.
- Schaeren-Wiemers N, Schaefer C, Valenzuela DM, Yancopoulos GD, Schwab ME (1995a) Identification of new oligodendrocyte- and myelin-specific genes by a differential screening approach. *Journal of neurochemistry* 65:10-22.
- Schaeren-Wiemers N, Valenzuela DM, Frank M, Schwab ME (1995b) Characterization of a rat gene, rMAL, encoding a protein with four hydrophobic domains in central and peripheral myelin. *The Journal of neuroscience : the official journal of the Society for Neuroscience* 15:5753-5764.
- Schlesinger MJ (1981) Proteolipids. *Annual review of biochemistry* 50:193-206.
- Schneider A, Lander H, Schulz G, Wolburg H, Nave KA, Schulz JB, Simons M (2005) Palmitoylation is a sorting determinant for transport to the myelin membrane. *Journal of cell science* 118:2415-2423.
- Schneider S, Bosse F, D'Urso D, Muller H, Sereda MW, Nave K, Niehaus A, Kempf T, Schnolzer M, Trotter J (2001) The AN2 protein is a novel marker for the Schwann cell lineage expressed by immature and nonmyelinating Schwann cells. *The Journal of neuroscience : the official journal of the Society for Neuroscience* 21:920-933.
- Scott TL, Christian PA, Kesler MV, Donohue KM, Shelton B, Wakamatsu K, Ito S, D'Orazio J (2012) Pigment-independent cAMP-mediated epidermal thickening protects against

- cutaneous UV injury by keratinocyte proliferation. *Experimental dermatology* 21:771-777.
- Scranton TW, Iwata M, Carlson SS (1993) The SV2 protein of synaptic vesicles is a keratan sulfate proteoglycan. *Journal of neurochemistry* 61:29-44.
- Sherman DL, Krols M, Wu LM, Grove M, Nave KA, Gangloff YG, Brophy PJ (2012) Arrest of myelination and reduced axon growth when Schwann cells lack mTOR. *The Journal of neuroscience : the official journal of the Society for Neuroscience* 32:1817-1825.
- Shin YK, Jang SY, Park JY, Park SY, Lee HJ, Suh DJ, Park HT (2013) The Neuregulin-Rac-MKK7 pathway regulates antagonistic c-jun/Krox20 expression in Schwann cell dedifferentiation. *Glia* 61:892-904.
- Shirakabe K, Wakatsuki S, Kurisaki T, Fujisawa-Sehara A (2001) Roles of Meltrin beta /ADAM19 in the processing of neuregulin. *The Journal of biological chemistry* 276:9352-9358.
- Simons K, Toomre D (2000) Lipid rafts and signal transduction. *Nature reviews Molecular cell biology* 1:31-39.
- Simons M, Trotter J (2007) Wrapping it up: the cell biology of myelination. *Current opinion in neurobiology* 17:533-540.
- Sinouris EA, Skandalis SS, Kilia V, Theocharis AD, Theocharis DA, Ravazoula P, Vynios DH, Papageorgakopoulou N (2009) Keratan sulfate-containing proteoglycans in sheep brain with particular reference to phosphacan and synaptic vesicle proteoglycan isoforms. *Biomedical chromatography : BMC* 23:455-463.
- Smyth N, Vatansever HS, Murray P, Meyer M, Frie C, Paulsson M, Edgar D (1999) Absence of basement membranes after targeting the LAMC1 gene results in embryonic lethality due to failure of endoderm differentiation. *The Journal of cell biology* 144:151-160.
- Sobue G, Shuman S, Pleasure D (1986) Schwann cell responses to cyclic AMP: proliferation, change in shape, and appearance of surface galactocerebroside. *Brain research* 362:23-32.
- Sparrow N, Manetti ME, Bott M, Fabianac T, Petrilli A, Bates ML, Bunge MB, Lambert S, Fernandez-Valle C (2012) The actin-severing protein cofilin is downstream of neuregulin signaling and is essential for Schwann cell myelination. *The Journal of neuroscience : the official journal of the Society for Neuroscience* 32:5284-5297.
- Spiegel I, Adamsky K, Eshed Y, Milo R, Sabanay H, Sarig-Nadir O, Horresh I, Scherer SS, Rasband MN, Peles E (2007) A central role for Necl4 (SynCAM4) in Schwann cell-axon interaction and myelination. *Nat Neurosci* 10:861-869.
- Srinivasan R, Sun G, Keles S, Jones EA, Jang SW, Krueger C, Moran JJ, Svaren J (2012) Genome-wide analysis of EGR2/SOX10 binding in myelinating peripheral nerve. *Nucleic acids research* 40:6449-6460.
- Stewart HJ, Bradke F, Taberner A, Morrell D, Jessen KR, Mirsky R (1996) Regulation of rat Schwann cell Po expression and DNA synthesis by insulin-like growth factors in vitro. *The European journal of neuroscience* 8:553-564.

- Stewart HJ, Zoidl G, Rossner M, Brennan A, Zoidl C, Nave KA, Mirsky R, Jessen KR (1997) Helix-loop-helix proteins in Schwann cells: a study of regulation and subcellular localization of Ids, REB, and E12/47 during embryonic and postnatal development. *Journal of neuroscience research* 50:684-701.
- Storbeck CJ, Wagner S, O'Reilly P, McKay M, Parks RJ, Westphal H, Sabourin LA (2009) The Ldb1 and Ldb2 transcriptional cofactors interact with the Ste20-like kinase SLK and regulate cell migration. *Molecular biology of the cell* 20:4174-4182.
- Tan W, Rouen S, Barkus KM, Dremina YS, Hui D, Christianson JA, Wright DE, Yoon SO, Dobrowsky RT (2003) Nerve growth factor blocks the glucose-induced down-regulation of caveolin-1 expression in Schwann cells via p75 neurotrophin receptor signaling. *The Journal of biological chemistry* 278:23151-23162.
- Tao W, Pennica D, Xu L, Kalejta RF, Levine AJ (2001) Wrch-1, a novel member of the Rho gene family that is regulated by Wnt-1. *Genes & development* 15:1796-1807.
- Taveggia C, Zanazzi G, Petrylak A, Yano H, Rosenbluth J, Einheber S, Xu X, Esper RM, Loeb JA, Shrager P, Chao MV, Falls DL, Role L, Salzer JL (2005) Neuregulin-1 type III determines the ensheathment fate of axons. *Neuron* 47:681-694.
- Tawk M, Makoukji J, Belle M, Fonte C, Trousson A, Hawkins T, Li H, Ghandour S, Schumacher M, Massaad C (2011) Wnt/beta-catenin signaling is an essential and direct driver of myelin gene expression and myelinogenesis. *The Journal of neuroscience : the official journal of the Society for Neuroscience* 31:3729-3742.
- Teh MT, Blaydon D, Ghali LR, Briggs V, Edmunds S, Pantazi E, Barnes MR, Leigh IM, Kelsell DP, Philpott MP (2007) Role for WNT16B in human epidermal keratinocyte proliferation and differentiation. *Journal of cell science* 120:330-339.
- ten Asbroek AL, Verhamme C, van Groenigen M, Wolterman R, de Kok-Nazaruk MM, Baas F (2005) Expression profiling of sciatic nerve in a Charcot-Marie-Tooth disease type 1a mouse model. *Journal of neuroscience research* 79:825-835.
- Tep C, Kim ML, Opincariu LI, Limpert AS, Chan JR, Appel B, Carter BD, Yoon SO (2012) Brain-derived neurotrophic factor (BDNF) induces polarized signaling of small GTPase (Rac1) protein at the onset of Schwann cell myelination through partitioning-defective 3 (Par3) protein. *The Journal of biological chemistry* 287:1600-1608.
- Thatikunta P, Qin W, Christy BA, Tennekoon GI, Rutkowski JL (1999) Reciprocal Id expression and myelin gene regulation in Schwann cells. *Molecular and cellular neurosciences* 14:519-528.
- Thiel G, Mayer SI, Muller I, Stefano L, Rössler OG (2010) Egr-1-A Ca(2+)-regulated transcription factor. *Cell calcium* 47:397-403.
- Thomas SL, De Vries GH (2007) Angiogenic expression profile of normal and neurofibromin-deficient human Schwann cells. *Neurochemical research* 32:1129-1141.
- Ting-Beall HP, Lees MB, Robertson JD (1979) Interactions of Folch-Lees proteolipid apoprotein with planar lipid bilayers. *The Journal of membrane biology* 51:33-46.

- Topilko P, Schneider-Maunoury S, Levi G, Baron-Van Evercooren A, Chennoufi AB, Seitanidou T, Babinet C, Charnay P (1994) Krox-20 controls myelination in the peripheral nervous system. *Nature* 371:796-799.
- Underwood CK, Reid K, May LM, Bartlett PF, Coulson EJ (2008) Palmitoylation of the C-terminal fragment of p75(NTR) regulates death signaling and is required for subsequent cleavage by gamma-secretase. *Molecular and cellular neurosciences* 37:346-358.
- Vartanian T, Goodearl A, Lefebvre S, Park SK, Fischbach G (2000) Neuregulin induces the rapid association of focal adhesion kinase with the erbB2-erbB3 receptor complex in schwann cells. *Biochemical and biophysical research communications* 271:414-417.
- Verheijen MHG, Camargo N, Verdier V, Nadra K, Charles ASD, Medard JJ, Luoma A, Crowther M, Inouye H, Shimano H, Chen S, Brouwers JF, Helms JB, Feltri ML, Wrabetz L, Kirschner D, Chrast R, Smit AB (2009) SCAP is required for timely and proper myelin membrane synthesis. *P Natl Acad Sci USA* 106:21383-21388.
- Vicente-Manzanares M, Ma X, Adelstein RS, Horwitz AR (2009) Non-muscle myosin II takes centre stage in cell adhesion and migration. *Nature reviews Molecular cell biology* 10:778-790.
- Vigo T, Nobbio L, Hummelen PV, Abbruzzese M, Mancardi G, Verpoorten N, Verhoeven K, Sereda MW, Nave KA, Timmerman V, Schenone A (2005) Experimental Charcot-Marie-Tooth type 1A: a cDNA microarrays analysis. *Molecular and cellular neurosciences* 28:703-714.
- Wang CH, Ma N, Lin YT, Wu CC, Hsiao M, Lu FL, Yu CC, Chen SY, Lu J (2012) A shRNA functional screen reveals Nme6 and Nme7 are crucial for embryonic stem cell renewal. *Stem cells* 30:2199-2211.
- Wang H, Tewari A, Einheber S, Salzer JL, Melendez-Vasquez CV (2008) Myosin II has distinct functions in PNS and CNS myelin sheath formation. *The Journal of cell biology* 182:1171-1184.
- Watanabe Y, Usada N, Minami H, Morita T, Tsugane S, Ishikawa R, Kohama K, Tomida Y, Hidaka H (1993) Calvasculin, as a factor affecting the microfilament assemblies in rat fibroblasts transfected by src gene. *FEBS letters* 324:51-55.
- Webster HD (1971) The geometry of peripheral myelin sheaths during their formation and growth in rat sciatic nerves. *The Journal of cell biology* 48:348-367.
- Webster HD, Martin R, O'Connell MF (1973) The relationships between interphase Schwann cells and axons before myelination: a quantitative electron microscopic study. *Developmental biology* 32:401-416.
- Wegner AM, Nebhan CA, Hu L, Majumdar D, Meier KM, Weaver AM, Webb DJ (2008) N-wasp and the arp2/3 complex are critical regulators of actin in the development of dendritic spines and synapses. *The Journal of biological chemistry* 283:15912-15920.
- Weiner JA, Chun J (1999) Schwann cell survival mediated by the signaling phospholipid lysophosphatidic acid. *Proceedings of the National Academy of Sciences of the United States of America* 96:5233-5238.

- Wen D, Peles E, Cupples R, Suggs SV, Bacus SS, Luo Y, Trail G, Hu S, Silbiger SM, Levy RB, et al. (1992) Neu differentiation factor: a transmembrane glycoprotein containing an EGF domain and an immunoglobulin homology unit. *Cell* 69:559-572.
- Wilkins PL, Suchovsky D, Berti-Mattera LN (1997) Immortalized schwann cells express endothelin receptors coupled to adenylyl cyclase and phospholipase C. *Neurochemical research* 22:409-418.
- Willem M, Garratt AN, Novak B, Citron M, Kaufmann S, Rittger A, DeStrooper B, Saftig P, Birchmeier C, Haass C (2006) Control of peripheral nerve myelination by the beta-secretase BACE1. *Science* 314:664-666.
- Wolfer DP, Lang R, Cinelli P, Madani R, Sonderegger P (2001) Multiple roles of neurotrypsin in tissue morphogenesis and nervous system development suggested by the mRNA expression pattern. *Molecular and cellular neurosciences* 18:407-433.
- Wood PM, Bunge RP (1975) Evidence that sensory axons are mitogenic for Schwann cells. *Nature* 256:662-664.
- Woodhoo A, Alonso MB, Droggiti A, Turmaine M, D'Antonio M, Parkinson DB, Wilton DK, Al-Shawi R, Simons P, Shen J, Guillemot F, Radtke F, Meijer D, Feltri ML, Wrabetz L, Mirsky R, Jessen KR (2009) Notch controls embryonic Schwann cell differentiation, postnatal myelination and adult plasticity. *Nat Neurosci* 12:839-847.
- Xin M, Yue T, Ma Z, Wu FF, Gow A, Lu QR (2005) Myelinogenesis and axonal recognition by oligodendrocytes in brain are uncoupled in Olig1-null mice. *The Journal of neuroscience : the official journal of the Society for Neuroscience* 25:1354-1365.
- Yamada H, Komiyama A, Suzuki K (1995) Schwann cell responses to forskolin and cyclic AMP analogues: comparative study of mouse and rat Schwann cells. *Brain research* 681:97-104.
- Yamauchi J, Chan JR, Shooter EM (2003) Neurotrophin 3 activation of TrkC induces Schwann cell migration through the c-Jun N-terminal kinase pathway. *Proceedings of the National Academy of Sciences of the United States of America* 100:14421-14426.
- Yang DR, Bierman J, Tarumi YS, Zhong YP, Rangwala R, Proctor TM, Miyagoe-Suzuki Y, Takeda S, Miner JH, Sherman LS, Gold BG, Patton BL (2005) Coordinate control of axon defasciculation and myelination by laminin-2 and -8. *J Cell Biol* 168:655-666.
- Yang Y, Loy J, Ryseck RP, Carrasco D, Bravo R (1998) Antigen-induced eosinophilic lung inflammation develops in mice deficient in chemokine eotaxin. *Blood* 92:3912-3923.
- Yarden Y, Sliwkowski MX (2001) Untangling the ErbB signalling network. *Nature reviews Molecular cell biology* 2:127-137.
- Yoon C, Korade Z, Carter BD (2008) Protein kinase A-induced phosphorylation of the p65 subunit of nuclear factor-kappaB promotes Schwann cell differentiation into a myelinating phenotype. *The Journal of neuroscience : the official journal of the Society for Neuroscience* 28:3738-3746.
- Yoon S, Seger R (2006) The extracellular signal-regulated kinase: multiple substrates regulate diverse cellular functions. *Growth factors* 24:21-44.

- Yu WM, Chen ZL, North AJ, Strickland S (2009) Laminin is required for Schwann cell morphogenesis. *Journal of cell science* 122:929-936.
- Yu WM, Feltri ML, Wrabetz L, Strickland S, Chen ZL (2005) Schwann cell-specific ablation of laminin gamma 1 causes apoptosis and prevents proliferation. *J Neurosci* 25:4463-4472.
- Zacchetti D, Peranen J, Murata M, Fiedler K, Simons K (1995) VIP17/MAL, a proteolipid in apical transport vesicles. *FEBS letters* 377:465-469.
- Zhang JS, Wang L, Huang H, Nelson M, Smith DI (2001) Keratin 23 (K23), a novel acidic keratin, is highly induced by histone deacetylase inhibitors during differentiation of pancreatic cancer cells. *Genes, chromosomes & cancer* 30:123-135.
- Zhou G, Liang FX, Romih R, Wang Z, Liao Y, Ghiso J, Luque-Garcia JL, Neubert TA, Kreibich G, Alonso MA, Schaeren-Wiemers N, Sun TT (2012) MAL facilitates the incorporation of exocytic uroplakin-delivering vesicles into the apical membrane of urothelial umbrella cells. *Molecular biology of the cell* 23:1354-1366.
- Zimmermann H (1996) Accumulation of synaptic vesicle proteins and cytoskeletal specializations at the peripheral node of Ranvier. *Microscopy research and technique* 34:462-473.
- Zoltewicz SJ, Lee S, Chittoor VG, Freeland SM, Rangaraju S, Zacharias DA, Notterpek L (2012) The palmitoylation state of PMP22 modulates epithelial cell morphology and migration. *ASN neuro* 4:409-421.
- Zvibel I, Wagner A, Pasmanik-Chor M, Varol C, Oron-Karni V, Santo EM, Halpern Z, Kariv R (2013) Transcriptional profiling identifies genes induced by hepatocyte-derived extracellular matrix in metastatic human colorectal cancer cell lines. *Clinical & experimental metastasis* 30:189-200.

11. Appendix I: Differentially expressed transcripts

A list of differentially expressed transcripts in differentiated Schwann cells (20 μ M forskolin) was compiled with an FDR-adjusted p-value < 0.05. The 25 genes with the highest positive or negative fold changes are highlighted in red.

Differentially expressed transcripts due to forskolin				Differentially expressed transcripts due to forskolin			
Column ID	p-value	Mean Ratio (20 vs. 0)	Fold Change (20 vs. 0)	Column ID	p-value	Mean Ratio Column #	Fold Change Column ID
1190002N15Rik	0.000058	0.64	-1.56	Aebp1	0.000212	1.51	1.51
1200002N14Rik	0.000123	1.81	1.81	Agri	0.000056	0.60	-1.66
1200009O22Rik	0.000792	1.51	1.51	Alcam	0.000004	2.07	2.07
1700007G11Rik	0.001151	0.62	-1.61	Aldh1a3	0.000514	0.53	-1.89
1700021K19Rik	0.000002	0.38	-2.64	Aldh1a3	0.000066	0.37	-2.71
1700024G10Rik	0.000123	0.57	-1.75	Ankrd39	0.000578	0.64	-1.57
1700025G04Rik	0.000250	0.66	-1.52	Anp32e	0.000013	0.63	-1.59
1700029G01Rik	0.000010	1.62	1.62	Anxa1	0.000020	0.55	-1.81
1810011O10Rik	0.000007	1.71	1.71	Aoc3	0.004084	1.65	1.65
2010004A03Rik	0.000020	0.55	-1.82	Apbb2	0.000860	0.58	-1.74
2210410E06Rik	0.000001	0.58	-1.72	App2	0.000006	1.83	1.83
2310022B05Rik	0.000000	0.48	-2.07	Atf3	0.000309	0.30	-3.32
2310022M17Rik	0.000140	0.60	-1.66	Atp1a2	0.000001	0.65	-1.53
2310043L02Rik	0.000356	0.56	-1.79	Atp1b1	0.000028	0.20	-4.97
2310043N10Rik	0.000304	1.67	1.67	Axud1	0.000509	0.63	-1.59
2410004L22Rik	0.000876	0.60	-1.67	Baal	0.000001	2.94	2.94
2610524A10Rik	0.000000	0.55	-1.82	Baal	0.000000	2.67	2.67
2700094K13Rik	0.000059	0.63	-1.59	BC020002	0.000003	0.58	-1.74
2810428I15Rik	0.000113	0.60	-1.68	BC020108	0.000497	1.92	1.92
2810439F02Rik	0.000018	1.79	1.79	BC050210	0.000374	0.66	-1.51
2810439F02Rik	0.000164	2.17	2.17	Bcl2l1	0.000002	2.04	2.04
3300005D01Rik	0.000069	0.42	-2.39	Bcl3	0.002488	1.65	1.65
4632401N01Rik	0.000001	2.01	2.01	Bcl7a	0.000049	1.58	1.58
4732458O05Rik	0.000590	0.65	-1.55	Bmf	0.000011	2.66	2.66
4732460K03Rik	0.000034	0.43	-2.34	Bmp4	0.002119	1.54	1.54
4833412C05Rik	0.000000	0.55	-1.83	Bok	0.000087	0.61	-1.64
4833431D13Rik	0.002122	1.59	1.59	Btbd11	0.000002	0.64	-1.57
4932416A11Rik	0.000002	1.94	1.94	C1qtnf1	0.000020	1.65	1.65
4933421H10Rik	0.001195	1.62	1.62	C1qtnf3	0.000535	0.58	-1.73
5430406J06Rik	0.000006	1.68	1.68	C1qtnf3	0.000110	0.62	-1.60
5430435G22Rik	0.000031	0.48	-2.07	Cacna1h	0.000931	1.69	1.69
5430435G22Rik	0.000001	0.53	-1.90	Calb2	0.000450	0.42	-2.39
5530400B01Rik	0.001020	1.53	1.53	Camk2n1	0.000029	2.10	2.10
5730409K12Rik	0.000002	0.66	-1.50	Camk2n1	0.000005	2.11	2.11
5730478M09Rik	0.000008	0.61	-1.63	Capn5	0.000282	1.69	1.69
6330403K07Rik	0.000004	2.67	2.67	Cav1	0.000000	0.29	-3.49
6330403M23Rik	0.000059	1.58	1.58	Ccdc80	0.000057	0.63	-1.58
9430064K01Rik	0.000273	1.60	1.60	Ccl11	0.000186	6.20	6.20
9530064J02	0.000098	0.66	-1.52	Ccl11	0.000004	10.68	10.68
9930031P18Rik	0.000422	1.99	1.99	Ccl7	0.003240	2.16	2.16
A130010C12Rik	0.000124	1.51	1.51	Ccl7	0.000333	1.92	1.92
A130082M07Rik	0.000031	0.62	-1.62	Ccrn4l	0.000008	0.58	-1.73
A430103B12Rik	0.000309	1.60	1.60	Cd109	0.000001	0.42	-2.37
A530088H08Rik	0.000022	0.53	-1.90	Cd109	0.000000	0.32	-3.14
A730085F06Rik	0.000008	1.59	1.59	Cd200	0.000000	0.51	-1.97
Aadacl1	0.000185	1.59	1.59	Cd200	0.000032	0.62	-1.61
Aatk	0.000216	1.65	1.65	Cd80	0.001090	0.60	-1.67
Abcb4	0.000045	0.46	-2.17	Cda	0.003023	1.51	1.51
Abcc4	0.000040	2.01	2.01	Cdca3	0.003955	0.65	-1.53
Abr	0.000084	1.83	1.83	Cdh10	0.000047	0.56	-1.80
Acaa2	0.003101	0.64	-1.55	Cdh19	0.002132	0.62	-1.62
Acan	0.000000	0.27	-3.72	Cdh19	0.000342	0.59	-1.69
Acan	0.000000	0.41	-2.43	Cdh5	0.003800	1.50	1.50
Acot1	0.000001	1.99	1.99	Cdk5rap2	0.000423	0.63	-1.58
Acta2	0.000053	0.64	-1.57	Cdkn1a	0.001536	0.59	-1.71
Acta2	0.000068	0.65	-1.55	Cdkn1c	0.003230	1.80	1.80
Acta2	0.000005	0.60	-1.65	Ceacam2	0.001093	1.58	1.58
Actg2	0.000016	0.61	-1.64	Cebpb	0.000479	2.04	2.04
Acvr1	0.000391	0.66	-1.51	Ch25h	0.000010	0.54	-1.87
Adamts1	0.000306	0.61	-1.63	Chst2	0.002840	0.65	-1.53
Adamts12	0.000001	0.52	-1.93	Ckb	0.000006	0.65	-1.55
Adamts15	0.000116	1.56	1.56	Clasp1	0.000006	1.53	1.53
Adamts15	0.000251	0.61	-1.65	Clca4	0.001403	1.50	1.50
Add3	0.000000	2.24	2.24	Clcf1	0.000005	1.69	1.69
Add3	0.000000	2.00	2.00	Clcf1	0.000107	1.54	1.54

11. Appendix I: Differentially expressed transcripts

Differentially expressed transcripts due to forskolin				Differentially expressed transcripts due to forskolin			
Column ID	p-value	Mean Ratio (20 vs. 0)	Fold Change (20 vs. 0)	Column ID	p-value	Mean Ratio (20 vs. 0)	Fold Change (20 vs. 0)
Clcf1	0.000077	1.58	1.58	Emb	0.002300	2.50	2.50
Clmn	0.000030	1.62	1.62	En1	0.000490	0.52	-1.93
Cnksr2	0.000001	0.51	-1.96	Enc1	0.000343	0.35	-2.88
Cnn2	0.003388	0.67	-1.50	Endod1	0.000006	0.48	-2.09
Col14a1	0.000005	2.73	2.73	Entpd2	0.004328	1.92	1.92
Col14a1	0.000000	2.63	2.63	Epb4.1l4b	0.000001	2.62	2.62
Col15a1	0.000009	0.48	-2.10	Epb4.1l4b	0.000001	2.66	2.66
Col28a1	0.000051	0.58	-1.72	Errfi1	0.000249	2.87	2.87
Col4a5	0.000017	0.63	-1.60	Ets1	0.000000	0.58	-1.72
Col5a2	0.003559	0.66	-1.51	Fabp3	0.000109	0.57	-1.75
Col8a1	0.001428	0.63	-1.59	Fam132b	0.000808	0.62	-1.61
Coro2b	0.000026	1.77	1.77	Fam134b	0.000030	2.04	2.04
Cpne8	0.001910	0.61	-1.64	Fam171b	0.002227	0.42	-2.40
Crabp2	0.000175	2.09	2.09	Farp2	0.000002	1.85	1.85
Creb5	0.000039	0.52	-1.92	Fgf7	0.000437	3.78	3.78
Crhbp	0.000006	1.83	1.83	Fgfr1	0.000243	1.97	1.97
Crispld2	0.000948	1.61	1.61	Fhl1	0.000000	0.32	-3.13
Crif1	0.000001	1.53	1.53	Fhl1	0.000000	0.32	-3.13
Cryab	0.000033	0.55	-1.83	Fjx1	0.000168	1.97	1.97
Csmd2	0.000700	1.63	1.63	Fjx1	0.000243	1.65	1.65
Cspg4	0.000000	0.28	-3.52	Fkh18	0.000072	0.54	-1.86
Csrp3	0.000332	0.64	-1.56	Flt1	0.000003	0.52	-1.94
Cthrc1	0.000000	2.39	2.39	Fmn2	0.000246	1.57	1.57
Ctsb	0.002984	1.53	1.53	Fmnl3	0.000000	0.59	-1.70
Cx3c1	0.003110	1.76	1.76	Fmnl3	0.000001	0.56	-1.80
Cxcl1	0.002912	2.01	2.01	Fmod	0.001786	2.03	2.03
Cxcl12	0.003575	1.91	1.91	Foxi2	0.000000	1.88	1.88
Cxcl12	0.001442	1.81	1.81	Foxo1	0.001664	0.55	-1.81
Cxcl14	0.000115	2.57	2.57	Frm4a	0.000512	1.63	1.63
Cxcl14	0.000860	1.72	1.72	Fxyd3	0.001011	2.34	2.34
Cyp2d22	0.000081	1.66	1.66	Fxyd5	0.000003	0.61	-1.65
D030063E12	0.000000	1.86	1.86	Fxyd5	0.000181	0.64	-1.56
D030072B18Rik	0.000001	0.66	-1.51	Fxyd5	0.000149	0.64	-1.57
D0H45114	0.000004	1.66	1.66	Fyb	0.000083	0.56	-1.78
D12Ert4553e	0.000619	1.68	1.68	Fzd2	0.000048	1.52	1.52
D16Ert472e	0.000045	1.55	1.55	Fzd6	0.000004	1.80	1.80
D1Ert471e	0.002910	0.60	-1.67	Fzd6	0.000000	2.17	2.17
D330020A13Rik	0.000001	1.85	1.85	Gab1	0.000001	0.42	-2.41
D330027H18Rik	0.000000	0.60	-1.66	Gabrb3	0.000818	0.53	-1.89
D630040I23Rik	0.000030	0.60	-1.67	Gabrb3	0.000046	0.59	-1.70
Dap	0.000018	0.66	-1.51	Gadd45b	0.000003	0.54	-1.87
Dbndd2	0.000000	0.48	-2.06	Galnt2	0.000000	1.61	1.61
Dclk1	0.000575	1.73	1.73	Galnt2	0.000003	1.74	1.74
Dcn	0.002973	2.90	2.90	Galnt2	0.000020	1.84	1.84
Dcn	0.000668	3.16	3.16	Galnt4	0.001064	0.53	-1.88
Ddit4	0.000000	2.27	2.27	Gap43	0.000036	0.50	-2.00
Ddit4l	0.003681	1.50	1.50	Gas2l3	0.000054	1.68	1.68
Depdc6	0.000878	1.59	1.59	Gas2l3	0.001408	1.59	1.59
Des	0.000003	0.50	-1.99	Gdf1	0.000021	1.73	1.73
Dhh	0.000000	1.80	1.80	Gdnf	0.002929	0.65	-1.54
Dhx32	0.000032	0.57	-1.75	Gdpd5	0.000309	1.66	1.66
Diras1	0.000001	0.41	-2.47	Gfap	0.004051	1.52	1.52
Dlk1	0.000515	1.69	1.69	Gja1	0.002280	1.80	1.80
Dlk1	0.000030	2.10	2.10	Glis1	0.000486	1.82	1.82
Dm15	0.000049	0.58	-1.73	Gng2	0.001858	1.63	1.63
Dok5	0.000002	0.59	-1.70	Gng2	0.000472	1.74	1.74
Dok5	0.000147	0.64	-1.55	Gnptab	0.000001	1.57	1.57
Dst	0.000612	1.55	1.55	Gp38	0.000927	1.65	1.65
Dstn	0.000018	0.67	-1.50	Gpbar1	0.000420	0.63	-1.58
Dtna	0.000000	0.40	-2.51	Gpr137b	0.000095	1.60	1.60
Dtna	0.000082	0.60	-1.67	Gpr153	0.000252	1.52	1.52
Dusp4	0.000370	0.66	-1.52	Gpr176	0.000000	0.41	-2.43
Dusp4	0.000914	0.61	-1.64	Gpr23	0.000011	1.58	1.58
Dusp8	0.000026	1.71	1.71	Gse1	0.000033	1.59	1.59
Dysf	0.000000	0.55	-1.82	Gsn	0.001129	0.62	-1.61
E230013M07Rik	0.000000	5.49	5.49	Gsta4	0.000677	1.67	1.67
E330035H20Rik	0.000004	1.71	1.71	Gstm1	0.000002	1.63	1.63
Ednrb	0.000001	3.25	3.25	Gucy1a3	0.002333	0.61	-1.65
Ednrb	0.000000	2.32	2.32	Gzmd	0.002338	1.61	1.61
Ednrb	0.000000	2.05	2.05	Gzmd	0.002419	4.95	4.95
EG574403	0.002279	1.53	1.53	Gzme	0.003553	3.09	3.09
Egfl8	0.000068	6.19	6.19	Gzme	0.003961	2.22	2.22
Egfl8	0.000104	5.04	5.04	Hdac4	0.002296	1.54	1.54
Egr3	0.000001	7.26	7.26	Hdac5	0.000754	0.65	-1.53
Ehd4	0.000029	0.62	-1.60	Hdac5	0.000002	0.60	-1.67

11. Appendix I: Differentially expressed transcripts

Differentially expressed transcripts due to forskolin				Differentially expressed transcripts due to forskolin			
Column ID	p-value	Mean Ratio (20 vs. 0)	Fold Change (20 vs. 0)	Column ID	p-value	Mean Ratio (20 vs. 0)	Fold Change (20 vs. 0)
Hebp1	0.000440	0.63	-1.59	Lgr6	0.000055	0.66	-1.50
Heyl	0.000240	0.57	-1.74	Lhfp	0.000068	1.68	1.68
Hist1h2af	0.000275	0.66	-1.52	Lhfp	0.000288	1.76	1.76
Hist1h2ah	0.004376	0.63	-1.60	Lhfp	0.000142	1.52	1.52
Hmga1	0.000010	0.53	-1.89	Lims2	0.000000	0.42	-2.38
Hs2st1	0.000000	0.66	-1.51	Lims2	0.000000	0.45	-2.23
Hs3st3a1	0.000307	0.55	-1.80	Lims2	0.000000	0.49	-2.05
Hsd11b1	0.000535	1.60	1.60	Lip1	0.000001	0.53	-1.87
Hsd17b11	0.000239	1.59	1.59	Lip1	0.000084	0.61	-1.64
Hspa1l	0.000110	0.61	-1.65	Liph	0.000176	1.82	1.82
Hspb1	0.000062	0.38	-2.66	Liph	0.000193	2.34	2.34
Hspb2	0.000037	0.53	-1.88	LOC100044177	0.000006	3.09	3.09
Hspb3	0.000005	0.50	-2.00	LOC100045228	0.000279	2.20	2.20
Htra3	0.000998	0.63	-1.59	LOC100047214	0.000075	1.63	1.63
Id1	0.002180	1.50	1.50	LOC100047268	0.000292	2.02	2.02
Id2	0.000000	2.12	2.12	LOC100047583	0.000444	0.35	-2.82
Idb2	0.000000	3.03	3.03	LOC100047606	0.000006	1.82	1.82
Ifit2	0.002078	0.66	-1.51	LOC100047619	0.000125	0.63	-1.58
Igf1	0.000049	0.63	-1.60	LOC100047659	0.000003	3.07	3.07
Igf1	0.000001	0.53	-1.89	LOC100047808	0.000013	0.41	-2.47
Igfbp3	0.000001	0.40	-2.47	LOC100048721	0.000468	1.52	1.52
Igfbp3	0.000227	0.50	-2.02	LOC218877	0.000013	1.72	1.72
Igfbp5	0.000000	1.85	1.85	LOC234081	0.000026	0.53	-1.88
Igfbp5	0.000001	2.09	2.09	LOC240672	0.000010	0.40	-2.50
Igfbp5	0.000000	2.14	2.14	LOC638935	0.000007	0.52	-1.92
Igsf11	0.000003	2.77	2.77	LOC666036	0.000000	0.54	-1.85
Igsf11	0.000007	2.77	2.77	Loxl4	0.000133	0.55	-1.82
Igsf4a	0.000000	0.46	-2.16	Lpcat2	0.001179	0.58	-1.74
Ikbkg	0.000001	1.63	1.63	Lrrc17	0.002276	1.71	1.71
Il11	0.000000	7.24	7.24	Lrrn3	0.000000	0.42	-2.39
Il33	0.003905	1.75	1.75	Lrrtm2	0.000941	1.92	1.92
Il6	0.002469	1.51	1.51	Lrtm1	0.000010	0.09	-11.60
Inpp5a	0.000009	0.55	-1.83	Lrtm1	0.000018	0.09	-10.92
Inpp5a	0.000004	0.53	-1.89	Lum	0.001457	1.98	1.98
Inpp5f	0.002289	1.59	1.59	Lypd1	0.000378	0.64	-1.57
Inppl1	0.000558	0.65	-1.54	Mapk9	0.000262	0.65	-1.53
Iqgap2	0.000585	2.17	2.17	Matn2	0.000001	1.62	1.62
Irf6	0.000001	0.38	-2.61	Mbp	0.000000	0.10	-9.98
Irgm1	0.004311	0.66	-1.51	Mbp	0.000016	0.40	-2.51
Itga1	0.000000	0.49	-2.05	Mcf2l	0.000045	0.55	-1.81
Itga5	0.000262	0.64	-1.56	Mdga2	0.000225	0.65	-1.53
Itgb4	0.000036	1.63	1.63	Mdh1	0.000175	0.59	-1.70
Itgb4	0.000177	1.68	1.68	Me2	0.000729	0.66	-1.51
Itgb5	0.000096	0.54	-1.86	Mef2c	0.000068	0.46	-2.19
Itgb8	0.000002	1.59	1.59	Mef2c	0.000000	0.33	-3.03
Itpk1	0.001470	0.63	-1.59	Mef2c	0.000000	0.36	-2.81
Ivl	0.000291	0.56	-1.79	Meox1	0.000124	0.67	-1.50
Jun	0.000020	0.62	-1.61	Mertk	0.002382	1.64	1.64
Kcna6	0.000028	1.60	1.60	Mfap2	0.000007	1.55	1.55
Kcna6	0.000011	1.62	1.62	Mfap2	0.000203	1.69	1.69
Kcnab1	0.000363	0.65	-1.54	Mgll	0.000063	0.57	-1.76
Kcnab1	0.003562	0.67	-1.50	Mgll	0.000002	0.46	-2.18
Kcnh2	0.000017	2.08	2.08	Mgll	0.000180	0.53	-1.88
Kcnh2	0.000028	1.77	1.77	Mgp	0.000448	0.25	-4.01
Kcnj12	0.000169	0.64	-1.55	Mgst1	0.000900	1.88	1.88
Kcnk13	0.000001	0.40	-2.49	Mgst1	0.000695	2.66	2.66
Kcnk5	0.000000	2.08	2.08	Mid1ip1	0.000558	0.66	-1.52
Kcnk5	0.000000	2.12	2.12	Mid2	0.000001	0.40	-2.49
Kcnn4	0.000000	3.62	3.62	Mmd2	0.001290	1.50	1.50
Kif21a	0.000013	1.59	1.59	Mmp15	0.000371	1.90	1.90
Kif26a	0.000000	1.51	1.51	Mmp17	0.000003	0.41	-2.45
Kitl	0.000289	1.76	1.76	Moxd1	0.000020	0.58	-1.73
Klf13	0.000042	1.75	1.75	Moxd1	0.000012	0.59	-1.70
Klhl26	0.000002	1.70	1.70	Mpz	0.000072	3.41	3.41
Klhl30	0.000000	0.14	-7.04	Myl9	0.000527	0.64	-1.57
Klk4	0.000008	0.25	-3.95	Myom1	0.000651	0.66	-1.53
Klk8	0.000001	0.33	-3.04	Ncald	0.003406	1.58	1.58
Krt23	0.001666	0.64	-1.57	Ncam1	0.000030	2.20	2.20
Lama1	0.002195	1.75	1.75	Ncam1	0.002629	1.52	1.52
Lbh	0.000000	0.35	-2.88	Ndrp1	0.000000	2.21	2.21
Lbh	0.000000	0.34	-2.98	Ndr1	0.000000	2.12	2.12
Leprel1	0.000001	0.52	-1.93	Nedd4l	0.000017	0.65	-1.53
Leprel1	0.000000	0.34	-2.94	Nek1	0.001319	1.63	1.63
Lgi4	0.000215	1.87	1.87	Nid1	0.000002	1.77	1.77
Lgmn	0.000000	0.52	-1.94	Nid1	0.000050	1.88	1.88

11. Appendix I: Differentially expressed transcripts

Differentially expressed transcripts due to forskolin				Differentially expressed transcripts due to forskolin			
Column ID	p-value	Mean Ratio (20 vs. 0)	Fold Change (20 vs. 0)	Column ID	p-value	Mean Ratio (20 vs. 0)	Fold Change (20 vs. 0)
Nme7	0.000042	0.55	-1.80	Prss23	0.000005	0.53	-1.89
Nme7	0.000002	0.24	-4.12	Prss35	0.000339	4.18	4.18
Nme7	0.000011	0.29	-3.42	Psmd8	0.000000	0.61	-1.64
Nnat	0.000008	2.15	2.15	Ptgjs	0.001424	0.66	-1.51
Nppb	0.000184	0.54	-1.84	Ptk2	0.000012	0.64	-1.56
Npr3	0.002365	2.86	2.86	Ptn	0.000005	2.82	2.82
Npr3	0.000730	1.59	1.59	Ptpla	0.000513	0.64	-1.55
Npr3	0.001797	1.84	1.84	Ptprm	0.000128	1.51	1.51
Npy1r	0.000012	2.37	2.37	Ptprt	0.000007	0.64	-1.56
Npy5r	0.000007	2.79	2.79	Ptpru	0.000005	1.62	1.62
Npy5r	0.000000	3.31	3.31	Ptpru	0.000054	1.88	1.88
Nr2f2	0.000111	1.66	1.66	Ptprz1	0.000096	0.30	-3.32
Nrbp2	0.000756	1.68	1.68	Ramp3	0.000009	2.31	2.31
Nupr1	0.000923	0.57	-1.76	Ramp3	0.000019	2.88	2.88
Olfml3	0.000735	1.86	1.86	Rap2a	0.000000	2.33	2.33
Olig1	0.000857	0.25	-3.94	Rasl12	0.000656	0.60	-1.66
Osbpl3	0.000140	1.50	1.50	Rassf4	0.002989	1.54	1.54
OTTMUSG00000002196	0.000113	0.43	-2.31	Rassf4	0.004456	4.34	4.34
P2rx5	0.000000	0.36	-2.80	Rbms3	0.000031	1.81	1.81
P2ry1	0.000036	0.60	-1.67	Rbmx	0.000060	0.65	-1.54
Pacsin2	0.000118	0.66	-1.52	Rbpms2	0.000045	0.66	-1.52
Padi2	0.000025	0.62	-1.62	Rcan2	0.000008	0.21	-4.87
Parp14	0.000000	2.04	2.04	Rcan2	0.000000	0.35	-2.85
Pbk	0.001506	0.58	-1.73	Rcsd1	0.001466	0.66	-1.52
Pcdh17	0.001548	0.54	-1.87	Rdh5	0.000477	1.66	1.66
Pcdh20	0.000000	0.07	-14.02	Reln	0.000030	2.73	2.73
Pcdh20	0.000000	0.10	-10.07	Rftn1	0.000688	0.60	-1.66
Pdcd4	0.000169	1.53	1.53	Rgs16	0.000001	0.33	-3.01
Pde10a	0.000072	1.52	1.52	Rgs3	0.000000	0.58	-1.72
Pde1a	0.002561	1.71	1.71	Rgs8	0.000010	0.22	-4.61
Pde1a	0.002365	2.00	2.00	Rhoc	0.000149	0.67	-1.50
Pde1b	0.000000	0.09	-11.30	Rin1	0.000002	0.63	-1.60
Pde1b	0.000000	0.08	-12.05	Rnf125	0.001748	1.68	1.68
Pde4b	0.000000	2.54	2.54	Robo2	0.000845	1.62	1.62
Pde4d	0.000069	1.71	1.71	Rorb	0.000038	1.62	1.62
Pde7b	0.000053	1.84	1.84	Rrm2	0.000226	0.64	-1.56
Pdgfa	0.000747	0.64	-1.57	Rxfp3	0.000103	0.60	-1.67
Pdgfb	0.000314	0.26	-3.84	Satb1	0.000000	0.32	-3.16
Pea15	0.000001	0.53	-1.89	Scd1	0.000039	1.61	1.61
Pea15a	0.000191	0.57	-1.74	sc1000981.1_40	0.003147	1.56	1.56
Pgf	0.000002	0.44	-2.27	Sema3b	0.000002	2.00	2.00
Phgdh	0.000025	0.53	-1.90	Sema3b	0.000436	1.69	1.69
Pik3r1	0.000294	1.69	1.69	Sema6b	0.002104	1.83	1.83
Pitpnc1	0.003041	1.62	1.62	Sema6b	0.000987	1.71	1.71
Pkig	0.000001	1.71	1.71	39692	0.000066	0.66	-1.51
Pla2g7	0.000083	1.93	1.93	Sfrp1	0.003690	1.96	1.96
Plau	0.000221	2.41	2.41	Sfrp1	0.000487	1.88	1.88
Pld3	0.000022	1.71	1.71	Sgk1	0.002665	1.89	1.89
Plekha4	0.000000	4.15	4.15	Sgsm3	0.000001	1.56	1.56
Plekha4	0.000000	17.53	17.53	Shh	0.000420	2.49	2.49
Plekhb1	0.000000	1.67	1.67	Slamf9	0.000341	0.61	-1.63
Plip	0.001800	0.64	-1.57	Slc16a11	0.000009	1.52	1.52
Plxna2	0.000214	0.58	-1.71	Slc17a8	0.000000	1.89	1.89
Pmaip1	0.002204	0.65	-1.55	Slc24a3	0.000037	3.53	3.53
Pmepa1	0.000323	1.62	1.62	Slit2	0.000181	1.80	1.80
Pmepa1	0.000526	1.56	1.56	Slit3	0.000000	1.83	1.83
Pmp22	0.003731	1.52	1.52	Smad3	0.000166	1.57	1.57
Ppap2a	0.000226	0.47	-2.11	Snta1	0.000001	0.49	-2.03
Ppap2a	0.000001	0.47	-2.11	Snx10	0.000069	1.57	1.57
Ppap2a	0.000000	0.38	-2.66	Snx16	0.000374	2.69	2.69
Ppap2b	0.001931	2.76	2.76	Snx7	0.001131	0.62	-1.61
Ppap2b	0.000091	2.81	2.81	Socs3	0.003840	1.85	1.85
Ppbp	0.001434	1.71	1.71	Sod3	0.000072	2.31	2.31
Ppbp	0.001813	1.94	1.94	Sorcs1	0.000000	2.55	2.55
Ppm2c	0.000696	0.65	-1.53	Sorcs1	0.000000	5.68	5.68
Ppp1r1a	0.000002	0.17	-5.83	Sorcs1	0.000002	1.55	1.55
Ppp3ca	0.000000	2.16	2.16	Sostdc1	0.000002	35.54	35.54
Ppp3ca	0.000026	2.23	2.23	Spon2	0.001100	14.12	14.12
Preip	0.000006	1.66	1.66	Spsb4	0.000001	0.40	-2.48
Prkg1	0.000041	0.34	-2.90	Srp2	0.002500	0.63	-1.58
Prkg1	0.000000	0.40	-2.51	Ssbp2	0.000009	1.52	1.52
Pri2c2	0.001734	1.57	1.57	St3gal5	0.000085	0.55	-1.81
Pros1	0.001808	1.64	1.64	Stc1	0.000171	1.70	1.70
Prss12	0.000004	3.61	3.61	Stc2	0.000039	0.11	-8.82
Prss12	0.000005	3.16	3.16	Stmn4	0.000256	0.60	-1.67

11. Appendix I: Differentially expressed transcripts

Differentially expressed transcripts due to forskolin	Mean Ratio	Fold Change
Column ID	p-value	(20 vs. 0)
Stmn4	0.000060	0.61
Sv2b	0.001656	0.55
Svep1	0.001823	2.53
Syn1	0.000052	1.71
Syn1	0.001779	1.58
Synpo	0.000129	1.53
Tbc1d7	0.001003	1.77
Tcap	0.000035	0.33
Tcap	0.000752	0.55
Tcf3	0.000008	1.51
Tctn3	0.000012	1.54
Tctn3	0.000000	2.05
Tgfbr3	0.000000	3.72
Tgfbr3	0.002110	1.50
Tgm2	0.000025	0.48
Thbd	0.000091	3.59
Thbs1	0.000005	0.50
Thsd4	0.000024	0.47
Tia1	0.000302	1.51
Tmem100	0.000338	1.89

12. Appendix II: Curriculum Vitae

Personal information

Name: Daniela Yolanda Schmid
 Email: daniela.schmid@unibas.ch
 Tel: +41 76 506 5582
 Date of Birth: 16th September 1983
 Place of Origin: Ramsen (SH), Switzerland
 Nationality: Switzerland
 Languages: German (native), English (professional), French (fluent)



Experience

2009-present **Teaching and supervision of Master and PhD students** at the dept. of biomedicine, University Hospital Basel, Switzerland
 02/2008-present **Research assistant**, neurobiology lab at the dept. of biomedicine, University Hospital Basel, Switzerland
 03/2004-10/2005 **Temporary employee at the animal husbandry** (rodents, monkey, dogs and pigs), dept. of discovery research - animal husbandry, F.Hoffmann - La Roche Ltd Basel, Switzerland
 03/2003-09/2003 **Salesperson** at Ochsner Sport, Basel, Switzerland
 2000-2007 **Swimming coach** for children and youth

Education

02/2008-08/2013 **PhD in neurobiology** at the dept. of biomedicine, University Hospital of Basel, Switzerland (Supervision: Prof. Dr. N. Schaeren-Wiemers) *“Functional role of the overexpression of the myelin and lymphocyte protein MAL in Schwann cells”*
 2008-present **FELASA (Federation for Laboratory Animal Science Association) Cat. B;** Institut für Labortierkunde, University of Zurich, Switzerland
 10/2006-01/2008 **Master of Science in molecular biology;** practical master’s thesis in neurobiology at the University of Basel, Switzerland „The influence of the myelin and lymphocyte protein MAL on *Schwann cell differentiation*”
 10/2003-09/2006 **Bachelor of Science in biology, major in molecular biology**
 Biozentrum, University of Basel, Switzerland
 1999-2002 **Matura typus C (mathematics);** high school Gymnasium Oberwil (BL), Switzerland

Expertise and Techniques

Project planning, data analysis and evaluation**Animal Work:**

- Education: FELASA category B (mouse, rat, guinea pig, rabbit)
- Experience with mouse and rat models of the peripheral neuropathy Charcot-Marie-Tooth Disease 1A (CMT1A)
- Routine handling
- Screening, organization of breeding and maintenance, analysis of transgenic mice and rats

Standard Cell Culture:

- Culturing of standard cell lines (NIH 3T3, CHO) and immortalized Schwann cell line (S16)
- Retroviral infection, immunohistochemical and morphological analysis, gene expression analysis

Primary Cell Culture:

- Establishment of stimulation assays on primary cultures
- Primary mouse Schwann cell cultures
- Primary rat Schwann cell cultures
- Myelinating mouse Schwann cell / dorsal root ganglion cocultures
- Myelinating rat Schwann cell / dorsal root ganglion cocultures
- Retroviral infection, immunohistochemical and morphological analysis, gene expression analysis
- Highly elaborated dissection skills (embryonic, newborn and adult mice and rats)

Retroviral Infection:

- Generation of retroviral constructs
- Culturing and transfection of the Phoenix_{Eco} helper cell line
- Infection of cell lines and primary cells

Molecular Biology:

- Molecular cloning including database searches, subcloning, sequencing
- Cloning of fusion protein constructs (GFP, mCherry) for retroviral and lentiviral transfections, including construct design
- Cloning of DIG-incorporated riboprobes for in situ hybridization
- Quantitative RT-PCR (LightCycler[®] Carousel-Based System, Roche, 7500 Fast Real-time PCR System, Applied Biosystems and ViiA7 Real-time PCR System, Applied Biosystems) including RNA isolation, cDNA synthesis, data analysis

Biochemistry:

- Immunohistochemistry on tissue sections and cell cultures
- In situ hybridization on tissue sections

Whole Genome Expression Analysis:

- Assistance in analysis and interpretation of microarray data analysis (Partek Genomic Suites and Database for Annotation, Visualization and Integrated Discovery (DAVID Bioinformatics Resources))

Microscopy:

- Brightfield and epifluorescence microscopy
- Confocal microscopy (LSM 510, Zeis; LSM710, Zeis; A1, Nikon)

Software for data analysis and illustration:

- Microsoft Excel (advanced formulae)
- Adobe Illustrator, Graphpad Prism
- Partek Genomics Suite, Ingenuity Pathway Analysis (IPA) software
- Adobe Photoshop, ImageJ

Manuscripts

Buser A.M.*, **D. Schmid***, F. Kern*, B. Erne*, T. Lazzati and N. Schaeren-Wiemers. 2009. The myelin protein MAL affects peripheral nerve myelination: a new player influencing p75 neurotrophin receptor expression. *European Journal of Neuroscience*. Vol. 29, pp. 2276–2290, 2009 (*: equal authorship)

Kinter J., T. Lazzati, **D. Schmid**, T. Zeis, B. Erne, R. Lutzelschwab, A.J. Steck, D. Pareyson, E. Peles and N. Schaeren-Wiemers. 2013. An essential role of MAG in mediating axon-myelin attachment in Charcot-Marie-Tooth 1A disease. *Neurobiology of disease*. 49:221-231

Schmid D., T. Zeis, M. Sobrio and N. Schaeren-Wiemers. 2013. MAL overexpression leads to disturbed gene expression of components influencing the cytoskeleton organization and Schwann cell differentiation. *Manuscript submitted*

Schmid D., T. Zeis and N. Schaeren-Wiemers. 2013. Transcriptional regulation induced by cAMP elevation in mouse Schwann cells. *Manuscript in preparation*; submission planned for June 2013

Scientific oral presentation

Schmid D., N. Schaeren-Wiemers. PhD Retreat of the Biozentrum Basel, Fribourg, Switzerland. May 26-27, 2011. “Does the Myelin and Lymphocyte protein MAL play a functional role in intracellular Schwann cell signaling?”

Selected scientific presentations

Schmid D., T. Zeis, M. Sobrio, N. Schaeren-Wiemers. Gordon Research Conference on Myelin, Barga, Lucca, Italy. April 29 – May 04, 2012. “What is the functional role of the myelin and lymphocyte protein MAL in intracellular Schwann cell signaling?”

Schmid D., N. Schaeren-Wiemers. 10th Biennial ISN Satellite Meeting on Myelin Biology, Kolymvari, Crete, Greece. August 24-28, 2011. “Which is the functional role of the myelin and lymphocyte protein MAL in intracellular Schwann cell signaling”

Schmid D., N. Schaeren-Wiemers. Swiss Society of Neuroscience, Basel, Switzerland. March 26, 2011. “Does the myelin and lymphocyte protein MAL play a functional role in intracellular Schwann cell signaling?”

Schmid D., N. Schaeren-Wiemers. Current Topics in Myelin Research, Kassel, Germany. March 10-12, 2011. “Does the myelin and lymphocyte protein MAL play a functional role in intracellular Schwann cell signaling?”

Schmid D., N. Schaeren-Wiemers. Swiss Society of Neuroscience, Lausanne, Switzerland. March 12-13, 2010. “Does the myelin and lymphocyte protein MAL play a functional role in intracellular Schwann cell signaling?”

Schmid D., N. Schaeren-Wiemers. 9th European Meeting on Glial Cells in Health and Disease, Paris, France. September 8-12, 2009. March 12-13, 2010. “Does the myelin and lymphocyte protein MAL play a functional role in intracellular Schwann cell signaling?”

Schmid D., N. Schaeren-Wiemers. Swiss Society of Neuroscience, Fribourg, Switzerland. March 14, 2009. “The functional role of the raft protein MAL in Schwann cells”

Schmid D., A.M. Buser, B. Erne, F. Kern, N. Schaeren-Wiemers. 6th Federation of European Neuroscience (FENS) Congress, Geneva, Switzerland. July 12-16, 2008. “The functional role of the raft protein MAL in Schwann cells”

Schmid D., B. Erne, F. Kern, A.M. Buser, N. Schaeren-Wiemers. 8th European Meeting on Glial Cells in Health and Disease, London, England. September 4-8, 2007. “The functional role of the raft protein MAL in the peripheral myelin development”

Schmid D., B. Erne, F. Kern, N. Schaeren-Wiemers. Swiss Society of Neuroscience, Bern, Switzerland. March 9-10, 2007. “The functional role of the raft protein MAL in the peripheral nerve development”